MRI Characterisation of the Lumbar Spine in Lower Trunk Rotation

A thesis submitted in fulfilment of the requirement for the degree of Doctor of Philosophy

By

Baida Ajeal Badir AL-Omairi

B.Sc., M.Sc.

School of Engineering - Cardiff University

UK

January 2019

DECLARATION AND STATEMENTS

DECLARATION

This work has not been submitted in substance for any other degree or award at this or any other university or place of learning, nor is being submitted concurrently in candidature for any degree or other award.

Signed:  Baida Al-Omairi Date: **06/06/2019**

STATEMENT 1

This thesis is being submitted in partial fulfilment of the requirements for the degree of Doctor of Philosophy (PhD).

Signed:  Baida Al-Omairi Date: **06/06/2019**

STATEMENT 2

This thesis is the result of my own independent work/investigation, except where otherwise stated, and the thesis has not been edited by a third party beyond what is permitted by Cardiff University's Policy on the Use of Third Party Editors by Research Degree Students. Other sources are acknowledged by explicit references. The views expressed are my own.

Signed:  Baida Al-Omairi Date: **06/06/2019**

STATEMENT 3

I hereby give consent for my thesis, if accepted, to be available online in the University's Open Access repository and for inter-library loan, and for the title and summary to be made available to outside organisations.

Signed:  Baida Al-Omairi Date: **06/06/2019**

ABSTRACT

Statistical data indicates that the percentage of prevalence of spine-related pain is considered to be high, and even up to 84%. The spinal manipulation technique, which is based on applying external forces to the shoulder and pelvis to twist the human spine can decrease lower back pain. Better understanding of the biomechanical behaviour of the normal lumbar spine during each rotational position of the lower trunk will provide valuable translational information to guide better physiotherapy in the future. It will also provide normal variant data that will help healthcare professionals and specialist in artificial spine implants to understand certain aspects of spinal pain. Therefore, this study proposes an MRI study of the lumbar spine during different lower-trunk rotational positions to investigate their effect on the normal spine structures with consideration of the shoulder and pelvis girdles' motion.

To control the angle of the lower-trunk rotation, an MRI holder and an adaptive goniometer have been developed to position the subject and obtain accurate pelvis angle of rotation during the scan. Before starting the MRI scan, the position of the subject on the MRI holder was checked by calculating specific parameters. Standard supine and four lower-trunk rotational positions with unrestricted left and right shoulder movements were performed. T2 Sagittal, T2 coronal and T2 Axial 3D acquisition cuts were performed for the lumbar spine with a 1.5-T MRI scanner. The MR images were collected from volunteers and analysed using Image J software depending on the determination of particular anatomical landmarks and image processing techniques.

The results show that there is a significant difference between the position of the right and left scapula during lower trunk rotation, while there is no significant relation between the angle of rotation of L5 and the rotational angle of the posterior superior iliac spines relative to the horizontal plane in three tested sections of the sacroiliac joints. In addition, there is no significant difference in the angle of rotation of the examined sections of the sacroiliac joints during different rotational positions of the lower trunk. The effect of different lower trunk rotational positions on the angle of rotation of the lower lumbar segment and spinal canal depth was measured and it was found that the second rotational lower trunk rotational position caused the highest relative motion of the lower lumbar vertebra, while the first lower trunk rotational position caused the highest rotational torque between L5 and L3. In addition, the mean

difference in the spinal canal depth increased significantly following the degree of the applied lower trunk rotational position. Lower trunk rotation caused morphologic changes in the intervertebral discs and intervertebral foramens at L3-L4, L4-L5, and L5-S1 levels. However, the significant change in the area, width and height of the intervertebral foramen and disc depended on the rotational positions of the lower trunk. A strong anatomical relationship was indicated between the posterior height of the intervertebral disc at both sides and the foraminal height. Finally, the degree of the lateral bending was the greatest at the L4-L5 level. The mean differences between the left and right superior articular processes according to their orientation angle and gapping distance at the L3-L4 level were higher than those of the other tested levels, while the L5 level recorded the lowest values. However, the mean differences did not achieve significant effects.

These results may provide baseline information to enable the development of artificial implants of the right and left lumbar facet joints according to changes in lower trunk rotational positions. They can also help to explain the treatment benefits of manipulation therapy in spinal conditions.

DEDICATION

To the memory of my dear father

ACKNOWLEDGEMENTS

I am grateful to Allah, the Prophet Muhammad and Ahl al-Bayt (the peace and blessings of Allah be upon them) for giving me the strength and the ability to attain this goal.

I would like to express my sincere gratitude to my supervisors Dr Michael J. H. McCarthy and Dr Xin Yang for their continuous support during my PhD study, and for their patience, motivation and immense knowledge.

I would like to thank my supervisor Prof Leonard Derek Nokes for providing me with necessary information and direction.

I am grateful to the staff in the Cardiff Bay Hospital and Trauma Clinic at the University Hospital of Wales for their assistance during this project.

I deeply appreciate the financial support of my sponsor, the Iraqi Ministry of Higher Education and Scientific Research, the Iraqi Cultural Attaché in London, the Welsh Arthritis Research Network and Globus Medical, Inc. Without their support and immediate help, this work would not have been achievable.

I would like to give special thanks to my family members, colleagues and friends who supported me during my study.

Baida AL-Omairi

2019

TABLE OF CONTENTS

LIST OF FIGURES

LIST OF TABLES

Chapter 1

Introduction

1.1 Motivation

Statistical data indicates that the percentage of prevalence of spine-related pain is considered to be high, and even up to 84% (Allegri et al. 2016). Consequently, many back-pain patients seek medical attention. The direct healthcare costs of back pain in the UK was estimated at £2.1 billion in 2008. It has also been reported that people with back pain attend 13 million doctor visits and 50 million chiropractor visits annually. Accordingly, a high percentage of these patients will settle with manipulation therapy, which is often used to treat low back pain (NG59 2017; Maniadakis and Gray 2000). The spinal manipulation technique, which based on applying external forces to the shoulder and pelvis to twist the human spine, can decrease lower back pain by reducing disc bulging, and freeing adhesions around a prolapsed disc or facet joint (Herzog 2010; Shekelle et al. 2019; Koes et al. 1996). The mechanical effects of the twisting forces of the spinal manipulation may have dramatic effects on the spine structures and the surrounding soft tissues (Assendelft et al. 1996; Pickar 2002; Ernst and Assendelft 1998).

A better understanding of the biomechanical behaviour of the normal lumbar spine during each rotational position will provide valuable translational information for guiding better physiotherapy in the future. It will also provide a normal variant data that will help healthcare professionals and specialists in artificial spine implants to understand certain aspects of spinal pain. Consequently, this study proposes a magnetic resonance imaging (MRI) study of the lumbar spine during different lower trunk rotational positions to investigate their effect on the normal spine structures, with consideration of the shoulder and pelvis girdles' motion.

It has been suggested that the coordination patterns between the upper and lower body should be considered to obtain optimal functional performance because the range of motion of the shoulder and pelvis are crucial factors to continue a flexible dynamic trunk motion (Park et al. 2012).

The scapula is considered to be a connecting platform that controls and distributes the largest percentage of kinetic energy and force from the trunk and lower extremities to the upper extremities. Several techniques have been introduced to evaluate scapular positioning during static and dynamic posture (Nijs et al. 2007; Hoard et al. 2013; Struyf

et al. 2014). However, the only variable method that is currently available involves the use of a tape measure, and is only capable of measuring the scapula kinematics during the lower trunk rotation using the technique that was introduced by previous studies. Therefore, the findings of this study will help therapists to consider the pattern of motion and position of the scapula during spinal manipulation because the position of the right and left scapula can provide a baseline information about the degree of rotation of the lower trunk.

The rotational angle of the trunk in different positions is affected by the position of the pelvis. Previous studies have used several techniques and devices to control the pelvises of subjects during spine rotation to ensure reproducibility (Rogers et al. 2002;Fujii et al. 2007). While these methods have passively rotated the subject's pelvis, controlled and maintained active lower trunk rotation has not yet been introduced. A novel MRI holder in parallel with a modified goniometer can be used in an accurate vitro device to measure and control different dynamic lower trunk rotations. An MRI holder can also prevent motion artefacts during long term positioning.

The functional link between pelvis and spine has been analysed by the previous researchers, who defined this link as pelvic incidence, which represents the sum of two positional parameters: sacral slope and pelvic tilt. In this definition, the pelvic incidence is tightly correlated with the degree of lumbar lordosis (Tardieu et al. 2017; Ike et al. 2018; Ghasemi et al. 2016). Other researchers have shown that the lumbo-sacro-pelvic structure plays an important role in determining the shear and compressive forces applied on the anterior and posterior elements of the lumbar vertebral column. These researchers analysed the relationship between the lumbar, sacral and pelvic structures as the sacral angle and sacral curvature. While many researchers have stated that the fifth lumbar vertebrae with the pelvis and lower trunk will rotate in a clockwise direction, the upper trunk and shoulders rotate in an anti-clockwise direction when the spine bends laterally and forward when clockwise torque is applied (Gracovetsky and Farfan 1986; LaFiandra et al. 2002; Montgomery 2008). However, it seems that these studies did not take the difference in the rotational degree between the pelvis and the fifth lumbar vertebrae into account. Based on the previously mentioned studies, the current study will introduce a new definition of the relationship between the spine and the pelvis as the relation between the rotational angle of the last lumbar vertebra (L5)

and the rotational angle of the posterior superior iliac spines in three anatomical sections related to the horizon during lower trunk rotational positions using a new technique depending on using the pixel intensity values.

Pain arising from the sacroiliac joint has been reported to account for more than 20% of lower back pain and may be implicated to some extent in more than 50% of patients with lower back pain. This makes the motion of the sacroiliac joint an area of significant clinical research(Cramer and Darby 2005). Although many studies have calculated the translational and rotational motions of the sacroiliac joint during different body positions (Frigerio et al. 1974; Jacob and Kissling 1995; Egund et al. 1978; Sturesson et al. 1999; Sturesson et al. 2000; Adhia et al. 2016; Saunders 2013), the study of the sacroiliac joint motion as the quantification of the angle of rotation of the sacrum compared to ilium in three selected sections depends on using a mask filter and particular landmarks. The findings of these measurements may explain the effects of manipulation therapy, which targets the L5-S1 level and may also provide information about the amount of the mobility of the different sections of the sacroiliac joint in each rotational position of the lower trunk.

Many studies have reported the important relationship between the causes of lower back pain and the mechanical behaviour of the spine. Meanwhile, several studies have focused on the increased risk of lower back pain and the loads acting on the spinal structures in different body positions (Shin et al. 2013; Wong et al. 2017; Adams and Hutton 1981; Videman and Nurminen 2004; Stokes and Iatridis 2004; Natarajan et al. 2008). While the previously mentioned studies introduced the spine function during various dynamic motions or static postures, the knowledge on the degree of the dynamic rotation, the relative motion of the individual lumbar vertebrae and the rotational torque between L3 and L5vertebral levels during each rotational position of the human spine, and in turn their effect on the spinal canal depth, are all still unclear. However, this knowledge is critical for understanding the potential adverse effect of each rotational position of the spine.

Altered vertebral motion has been widely assumed to be a biomechanical factor causing spinal pathology. Many studies have been conducted to calculate the vertebral rotational degree and the range of motion while applying a flexion-extension, bending and axial

rotation torque, with or without load, using techniques such as radiography, ultrasound and MRI, and according to different landmarks (Nash and Moe 1969; Weiss 1995; Cerny et al. 2014; Chi et al. 2006; Aaro and Dahlborn 1981; Ho et al. 1993; Pearcy and Tibrewal 1984; Alqhtani et al. 2016; Chung et al. 2000; Haughton et al. 2002). However, the researchers who used the radiographic methods did not take the risk of radiation exposure into account. In addition, they found difficulty to determine the same landmarks during the maximum vertebral rotation and their methods had a percentage of error because they required many landmarks to be recognised. Meanwhile, using ultrasound to measure the vertebral angle is only valid for the prone position and cannot be used during spine and rotated positions.

In turn, the researchers who used MRI to determine the rotational degree of the lumbar vertebra have either used landmarks that cannot be said as an accurate enough or did not consider the fact that the determination of rotational angle of the lumbar vertebrae using MRI is difficult because the same landmarks of the right and left vertebra cannot be accurately observed on the same axial MRI images because the muscle tendons and ligamentum flavum attachments at both sides prevent the precise localisation of the tip of the transverse and spinous processes and pedicle points. Consequently, this study will introduce a new method of measurements, which is simple, safe (i.e., does not expose the subjects to ionizing radiation) and accurate enough to determine the anatomical landmarks of both sides of each individual vertebra (which tend to appear separately in each slice of MRI as a result of the rotation). This study will also introduce a new, highly accurate, and simple technique to measure the relative motion of the lumbar vertebra.

Many researchers have mentioned the anatomical relationship between the spinal cord compression and spinal canal size during many physiological body actions (White and Panjabi 1990; Lim et al. 2017; Abbas et al. 2010; Ahmad et al. 2011; Marawar et al. 2016). The conclusion of these studies demonstrated that during extension or rotation, the spinal canal and dural sac size decreased and this causes a compression of the nerve roots as a result of the constriction of the cauda equine. Many approaches have been used to quantify the spinal canal and dural sac dimensions (Inufusa et al. 1996; Chung et al. 2000; Cuchanski et al. 2011; Griffith et al. 2016; Amadou et al. 2017; Monier et al. 2017; Yuan et al. 2016) . However, these approaches have found only limited application in physiological loaded and unloaded flexion and extension in unhealthy

subjects. They either provided little information about the effect of different rotational positions on the spinal canal depth or the dural sac position. Only one study has shown the effect of a minimum degree of rotation on the morphology of the spinal canal when the shoulder motion was restricted. Consequently, in the present study, a new method of measurement was used to quantify the amount of compression of the dural sac at two depths of the spinal canal, and according to each rotational position of the spine.

Many studies have reported the association between the applied dynamic axial torque, the mechanism of disc failure, narrowing of the intervertebral foramen and lower back pain (Jensen 1980; White and Panjabi 1990; Argoubi and Shirazi-Adl 1996; Leone et al. 2007; Lu et al. 1996; Costi et al. 2007; Roaf 1960). While these studies have dramatically improved the knowledge on the function of the intervertebral foramen and intervertebral disc during different human trunk activities, determination of the effect of three voluntary lower trunk rotational positions on the intervertebral foramen and disc dimensions and on the degree of the lateral bending have not yet been fully investigated. This may also explain the treatment benefits of the different positions of the spinal manipulative therapy.

Many researchers have shown that the intervertebral disc joints and ligaments are more resistive to compression, destruction, flexion and extension, but are very vulnerable to rotation and horizontal shearing forces. In this condition, the intervertebral disc damage is directly proportional to the applied torque (Roaf 1960; Lu et al. 1996).

Several studies have measured the posterior and anterior disc height of the intervertebral disc by using the visible landmarks on the upper and lower vertebral bodies, and also end plates borders (Lao et al. 2016; Zhou et al. 2000; Tunset et al. 2013). However, the visibility of those landmarks will not be clear enough in a condition of a rotated vertebra, which makes it difficult to distinguish between the borders of the deformed vertebral bodies and end plates.

A few studies have introduced methods to calculate the cross-sectional area of the intervertebral disc depending on using the calculation of the anterior and posterior disc heights or depending on measuring the signal intensity values percentage using T1- and T2-weighted MRI images (Fredericson et al. 2002; Tunset et al. 2013; Bailey et al. 2018). However, these methods were indicated as have a low accuracy or the authors

did not measure the cross- sectional area of the intervertebral disc in mm^2 due to the difficulty to separate the borders of the intervertebral disc from the adjacent structures, such as the longitudinal ligaments.

Finally, from the previously reviewed papers, two studies were found that measured the width of the intervertebral disc. However, these studies used techniques that may not be reliable enough to measure the changing in the sagittal width of the right and left sides of the intervertebral disc.

The present study summarises that it is possible to measure the posterior and anterior disc height of the rotated vertebrae, calculate the cross-sectional area of the right and left side of the sagittal inter-vertebral disc in mm^2 and measure the width of two sides of the intervertebral disc by taking average measurements of two sagittal MRI images using a synchronization tool and a particular saturated pixel percentage with a determined magnification power. This method is safe, reliable and has a high accuracy. The details of the determined landmarks and the procedure are given in Chapter Four.

The anatomical relationship between the intervertebral foramen and spinal nerve compression during many human spine actions has been explained by a large number authors (Fujiwara et al. 2001; Senoo et al. 2014; Panjabi et al. 1983; Inufusa et al. 1996; Zhong et al. 2015). Some of those authors have reported that the axial rotation caused dramatic changes in the lumbar intervertebral foramen dimensions, while others have concluded that extension and lateral bending are the most critical reasons to change the space available for the spinal nerve and, thus, cause nerve root compression. The nerve root is more likely to be subject to injury by mechanical forces (compression) during its path through the intervertebral foramen. These mechanical forces depend upon the effective space available within the intervertebral foramen.

Many studies have investigated the foraminal dimensions (Panjabi et al. 1983; Mayoux-Benhamou et al. 1989; Inufusa et al. 1996; Schmid et al. 1999; Cinotti et al. 2002; Torun et al. 2006; Senoo et al. 2014; Fujiwara et al. 2001) . Most of these studies used computed tomography and cadaveric samples, in which the subjects exposed to ionization radiation and some of the soft tissues were isolated or intersected. Although other studies used MRI to obtain their measurement, they did not take into account that the same landmarks will not be appear obviously for all vertebral segments due to the variations in the rotational degrees of the spine. Accordingly, the present study presents

a safe method with a new orientation of measurements that take into account the natural physiological movements considering the presence of the disc and soft tissues. It will also overcome the variation in the appearance of the same landmarks in each vertebral segment and each rotational position due to the fact that each vertebra rotates with its unique rotational degree.

The interaction between axial torque (axial rotation) and lateral bending rotation (lateral bending moment) can be considered as a basis of the postural coupling. When the lumbar spine is under axial torque, the lumbo sacral region undergoes a combination of axial torque and lateral bending (Oxland et al. 1992; Grassmann et al. 1998).

Many methods have been developed to measure the degree of lateral bending. However, some of these methods of measurement expose the subjects to ionizing radiation, while others have used either methods of measurements that associated with an error or methods that were unsuitable for non-standing postures (Fujii et al. 2007; Pearcy and Tibrewal 1984; Barnes et al. 2009; Ebert et al. 2014; Been et al. 2011).

The present study introduces a simple but highly reliable and safe method that uses a particular saturated pixel percentage with a determined magnification power to measure the lateral bending degree of each individual vertebrae. However, the determination of the landmarks was modified from a technique used by one of the previous researchers, who used computed tomography.

Some studies have shown that the articular facet joints were more likely to be damaged within a less determined amount of axial rotation than that required to affect the intervertebral disc. Meanwhile, many previous studies have focused on the facet joint orientation as a pre-existing morphological factor in degenerative spondylolisthesis. (Adams and Hutton 1981; Kelsey et al. 1984; Shirazi-Adl et al. 1986; Criswell 2013).

The facet joints can primarily share the load in compression, extension and torsion of the lumbar spine and protect the disc against torsion. Therefore, it is proposed that a more sagittal orientation of the facet joint promotes anterior gliding by reducing resistance to anterior shear forces. However, studying the orientation angle of the right and left superior articular processes and the mean differences between the orientations of these processes at each individual lumbar segment during different dynamic lower trunk rotational positions may help artificial facet replacement specialists (Serhan et al.

2007; Kapandji 1974; Ahmed et al. 1990; Van Schaik et al. 1997; Masharawi et al. 2004) .

A review of the literature reveals that many studies have measured the orientation angle of the articular facets, and calculated the gaping distance between the superior and inferior articular facets (Farfan and Sullivan 1967; Noren et al. 1991;Panjabi et al. 1993; Tulsi and Hermanis 1993; Boden et al. 1996; Masharawi et al. 2004; Kozanek et al. 2009; Chadha et al. 2013; Wang et al. 2015; Cramer et al. 2000). However, the present study will present a safe and more accurate method that uses natural physiological movements and considers the angle of rotation of the intervertebral disc. It can also differentiate the solid compact bone of the articular process from the soft tissues, such as the capsular ligaments. As a result of the effect of the torsion, these ligaments tend to prevent the accurate determination of the anteroposterior boarders of the articular processes. The quantification of the degree of the orientation of the articular processes and the gapping distance between two articular processes of the normal facet during different rotational positions of the spine will help to successfully design an artificial facet.

Many methods have been used to diagnose low back pain, such as computed tomography and conventional X-ray. However, these methods have several disadvantages, such as exposing the patient to the risk of the ionizing radiation. In contrast, MRI has been proven to be a safe and effective three-dimensional method to diagnose lumbar spine, such as disc herniation and spinal stenosis.

1.2 Aim

The aim of this project is to investigate the effect of different lower trunk rotational positions on the lumbar spine by using MRI. This will help to understand the biomechanical behaviour of the normal lumbar spine structures during rotation, while given to consideration to the actions of the shoulder and pelvic girdles. In addition, this will provide valuable translational information for guiding better physiotherapy and for artificial spine implant specialists.

1.3 Hypotheses

- There will be a significant difference between the position of the right and left scapula during lower trunk rotation.
- The pelvis angle of rotation will be accurately controlled using a reliable an adaptive goniometer and MRI holder.
- There will be a significant difference between the rotational angle of the left and right posterior superior iliac spines and the rotational angle of the last lumbar spine during all performed lower trunk rotational positions.
- The first lower trunk rotation (mean L5 angle (88^0)) will cause significant and maximum mean differences between the rotational angles of the selected sections of the sacrum and also between the rotational angles of the selected sections of ilium.
- Rotating the spines of healthy subjects with three rotational positions (R1, R2, and R3) with (mean L5 angle: 88^0, 66^0, and 45^0) will help to understand the effect of each rotational position of the spinal manipulation on the lumbar spine structures, and shoulder and pelvic girdles.
- Lower trunk rotation with mean L5 angle (88^0) will cause higher relative vertebral motion at each lower lumbar segments (L3, L4, and L5) compared to the second and third rotational position (mean L5 angle: 88^0, 660, and 45^0, respectively)).
- The first rotational position of the lower trunk (mean L5 angle: 88^0) will result in the maximum rotational torque between L3 and L5 vertebral levels.
- L4 vertebra will rotate with higher relative motion than L3 and L5 vertebrae.
- The maximum mean difference in the spinal canal depth at L3, L4 and L5 lumbar segments will result in the first lower trunk rotation position with mean L5 angle (88^0).
- The intervertebral disc dimensions of each lower spinal segment will be more affected by applying the first active lower trunk rotational position (mean L5 angle (88^0).
- The intervertebral disc dimensions at L4-L5 level will be more affected by applying lower trunk rotation.

- The intervertebral foraminal dimensions of each lower spinal segments will be more affected by applying the first active lower trunk rotational position (mean L5 angle (88^0).
- The intervertebral foraminal dimensions at L4-L5 level will be more affected by applying lower trunk rotation.
- The lateral bending angle will be the greatest with the first rotational position of the lower trunk (mean L5 angle: 88^0).
- The mean differences between the orientation angle of the right and the left superior articular processes at each individual lower lumbar segments will be the highest at the first rotational position of the lower trunk (mean L5 angle: 88^0).
- The mean difference between the orientation angle of the right and the left superior articular processes and the amount of the gapping between two articular processes of the normal facet will be the highest at the L4-L5 level.
- The cross-sectional area of the opening of the left articular will be the greatest at the first rotational position of the lower trunk (mean L5 angle:88^0).
- The degree of the facet orientation and the amount of the gapping between two articular processes of the normal facet during each lower trunk rotational position will help to develop a successful design for an artificial facet.
- MRI will be an effective method to three dimensionally show the lumbar spine and sacroiliac joint structures.

1.4 Objectives

- Define a new method to control the angle of rotation of the lower trunk depending on the consideration motions of the shoulder and pelvis.
- Define a modified method to measure the scapula's motion during lower trunk rotational positions.
- Construct an adaptive goniometer and a novel MRI holder to measure and fix the subject's pelvis during a long MRI scan.
- Define a suitable MRI protocol to determine particular parameters in the lumbar spine and sacroiliac joints.
- Define suitable software to analyse the MRI images and calculate the selected parameters.

- Define a reliable statistical analysis package to test the significant effect of the lower trunk rotational positions on the shoulder, pelvis, and spinal structures.
- Define a new method to investigate the accuracy of the measurements of the adaptive goniometer and also the efficiency of the novel MRI holder to control the pelvic angle of rotation.
- Investigate a new method to evaluate the difference between the rotational angle of the right and left posterior superior iliac spines and the rotational angle of the last lumbar vertebrae (L5).
- Define a new method to measure the angle of rotation of the sacrum and ilium.
- Define a new method to quantify the angle of rotation of the lower lumbar vertebrae.
- Investigate a new technique to evaluate the relative range of motion of the lower lumbar vertebrae.
- Evaluate a new approach to investigate the difference in the spinal canal depth.
- Define a modified method to measure the intervertebral disc dimensions of the lower lumbar segments.
- Investigate a modified technique to measure the intervertebral foramen dimensions of the lower lumbar segments.
- Define a modified technique to quantify the lateral bending angle of each lower lumbar intervertebral segment.
- Evaluate a modified approach to measure the orientation angle of the right and left superior articular processes.
- Define a new method to calculate the cross-sectional area of the gapping distance between the superior and inferior articular processes.

1.5 Thesis Outline

This thesis is structured as follows:

Chapter 1: This chapter highlights the motivation of the research, aim and objectives, and it describes the structure of the thesis.

Chapter 2: This chapter presents a review of the background information including:

- Prevalence of spine-related pain
- The spinal manipulation concept.
- The relationship between the shoulder and the pelvic girdles and the last lumbar vertebrae:
    - The scapula bone,
    - The pelvis,
    - The sacrum,
    - The sacroiliac joint.
- The anatomy of the lumbar spine:
    - Vertebral column,
    - The vertebral canal,
    - The pedicles,
    - The intervertebral disc,
    - The intervertebral foramen,
    - The articular facets.
- Magnetic resonance imaging (MRI):
    - The basic principles of the MRI,
    - Determination of tissue contrast in MRI,
    - Slice selection position and thickness,
    - Pulse sequences,
    - Spatial resolution and K-space,
    - Signal to noise ratio(SNR),
    - MRI artefacts,
    - Limitations of MRI.
- Summary

Chapter 3: This chapter reviews background information relevant to the previous studies and methods concerning:

- The biomechanics of spinal manipulation,
- The relationship between the shoulder and pelvis girdles and the last lumbar vertebrae during lower trunk rotation:
    - The role of scapula in lower trunk rotation,

  - The relationship between the rotational angle of the right and left posterior superior iliac spines and the rotational angle of the last lumbar vertebrae,
  - The relationship between the right and left sacroiliac joint during lower trunk rotation,
  - Controlling and measuring the pelvis rotational angle.

- The biomechanics of the rotation of the lumbar spine:
  - Biomechanics of the rotation of the lumbar vertebrae,
  - Biomechanics of the lumbar spinal cord during rotation, and according to the central spinal canal diameter and the dural sac position,
  - Biomechanics of the lumbar intervertebral disc during different lower trunk movements,
  - Biomechanics of the lumbar intervertebral foramen during different spine positions,
  - The relation between coupled motion and the amount of applied torque,
  - The role of facet orientation during trunk rotation and in designing the artificial facet.

- The role of magnetic resonance (MRI) in diagnosis of the lumbar spine and sacroiliac joint disorders,
- Summary.

Chapter 4: This chapter will provide details on the experimental work, including:

- Experiment Design,
- Subject Positioning,
- Controlling the lower trunk rotational angle:
  - Measuring the scapula position during lower trunk rotation,
  - Measuring and controlling the pelvic rotational angle using an adaptive goniometer and the MRI holder,

- ❖ Designing and manufacturing of the adaptive goniometer,
- ❖ Designing and manufacturing of the MRI Holder.
- ❖ Determination of the rotational angle of the pelvis using an adaptive goniometer and a novel MRI holder,

- Subject positioning measurements,
- MR equipment, protocol and scans of the subjects,
- Image analysis and data collection,
- Quantification of the lumbar and pelvis parameters using MRI,
- Statistical analysis,
- Summary.

Chapter 5: This chapter will explain the effects of different lower trunk rotational positions on following parameters:

- Controlling the rotational angle of the lower trunk depending on the relation between the shoulder and pelvic girdles and the last lumbar vertebrae:
  - o Measuring the scapula position during lower trunk rotation,
  - o Measuring the pelvic rotational angle using an adaptive goniometer and MRI,
  - o The relation between the posterior superior iliac spines and the last lumbar vertebrae during lower trunk rotation,
  - o The relation between the right and left sacroiliac joints according to three anatomical sections and during lower trunk rotation.

- Effect of lower trunk rotation on the lower lumbar spine structures:
  - o The angle of rotation of the lower lumbar spine vertebrae and the difference in the spinal canal depth during lower trunk rotation,

- Effect of Trunk Rotation on the Dimensions of the Lumbar Intervertebral Discs and Neural Foramens: An In vivo MRI study,
- The degree of lateral bending during lower trunk rotation,
- The orientation angle of the left and right superior articular processes and the cross-sectional area of the gapping between the superior and inferior articular processes during lower trunk rotation.

Chapter 6: This chapter discusses and summarises the research.

Chapter 7: This chapter draws the conclusions, and describes the limitations, contributions and makes a number of recommendations for future work.

Appendix A: This appendix describes the low back and shoulder pain questionnaires.

Appendix B: This appendix describes the tables of the results.

Chapter 2

Background

2.1 Introduction

This chapter will provide the necessary background information relating to the percentage of lower back pain prevalence. In addition, the concept of spinal manipulation will be described. The relationship between the shoulder and pelvic girdles, and the last lumbar vertebrae will be provided. The anatomy of the shoulder and pelvis girdles will be reviewed. The anatomy of the lumbar spine structures will be described. In addition, the basic information about the artificial facet joint will be reviewed. Finally, given that this thesis is primarily concerned with data analysis of images obtained through MRI, the basic principles of MRI and a detailed description of the properties of images acquired by MRI will be provided.

2.2 Prevalence of Spine-Related Pain

Statistical data indicates that the percentage of prevalence of spine-related pain is considered to be high, and even up to 84% (Allegri et al. 2016). According to the incidence of back pain among different countries, more than two-thirds of adults will suffer from lower back pain symptoms at some time during their life live in industrialised countries. This is in comparison to 44–54% of 30–50 year-olds in Sweden and Denmark (Leboeuf-Y et al. 1996; Jarvik and Deyo 2002; Brinjikji et al. 2015). According to NICE Guidance (NG59 2017), the direct healthcare costs of all back pain in the UK was estimated at 2.1 billion pounds in 2008 and 10.7 billion pounds in 1998. Roughly 582,595 inpatient and outpatient day cases for manipulations, injection and other surgical procedures were reported between 1994 and 1995 in the UK (Maniadakis and Gray 2000). Moreover, it has been reported that people with back pain attend 13 million doctor visits and 50 million chiropractor visits annually (Nazari 2007). Consequently, manipulative therapy is often used to treat low back pain.

2.3 Spinal manipulation concept

Spinal manipulations are defined as mechanical efforts in which the clinicians exert a force of specific magnitude in a controlled direction to target the spine. Spinal manipulation techniques can be divided into long-lever spinal manipulation and short-lever (high-velocity) spinal adjustment. Long-lever manipulation depends on using specific parts of the body—such as femur, shoulder, head or pelvis—to manipulate the

human spine. Meanwhile, high-velocity manipulation is more closely identified with chiropractic practice than other treatment modalities. In this type of manipulation, the force magnitudes and the rates of force application are high and a specific contact point of vertebrae is used to affect the vertebral joints (Herzog 2010; Shekelle et al. 2019). Consequently, manipulation therapy is based on applying rotational forces on the spine, depending on using shoulder and pelvis to targeting the lumbar spine structures.

2.4 The Relation between the Shoulder and Pelvis Girdles and the Last Lumbar Vertebrae during Lower Trunk Rotation

The global trunk rotation or the segmental rotation of the thoracic spine, lumbar spine and pelvis within the trunk itself can be referred to as trunk rotation (spinal rotation). Anatomical terms, such as the shoulder and upper trunk rotation, were first used by golf researchers to describe the turning movement of the chest on the pelvis. For example, the rotating action of the pelvis during a golf swing has been described to define hip rotation (Montgomery 2016). In general, rotation can be referred to as a movement around a longitudinal axis in a transverse plane for all bones of the body, except for the scapula and clavicle. The femur rotates about a mechanical axis, while in the other extremities rotation occurs about the anatomical axis.

2.4.1 The Scapulae Bone

In the ideal alignment, the side view line of a reference passes midway through the shoulder joint. However, the arm and shoulder positions are governed by the position of the scapulae bone and the upper back. Therefore, when the scapulae introduce a faulty position, a shoulder joint injury can occur. Anatomically, the scapula bone, which rests on the posterior side of the thorax, has a triangular shape. The slightly concave anterior aspect of the scapular bone can easily glide along the convex posterior rib cage, while the humerus bone can articulate with the scapula by the slightly concave oval-shaped glenoid fossa. The supra-spinatous and infra-spinatous fossa are formed when the scapular spine divides the posterior aspect of the scapula into two parts. From the most superior-lateral aspect of the scapula, the acromion process is projected to form a functional roof over the humeru’s head. In contrast, the coracoid process. In contrast, the coracoid process is projected from the anterior surface of the scapula, which is the

site of muscle and ligament attachments (Figure 2-1) (Kendall et al. 2005; Mansfield and Neumann 2014).

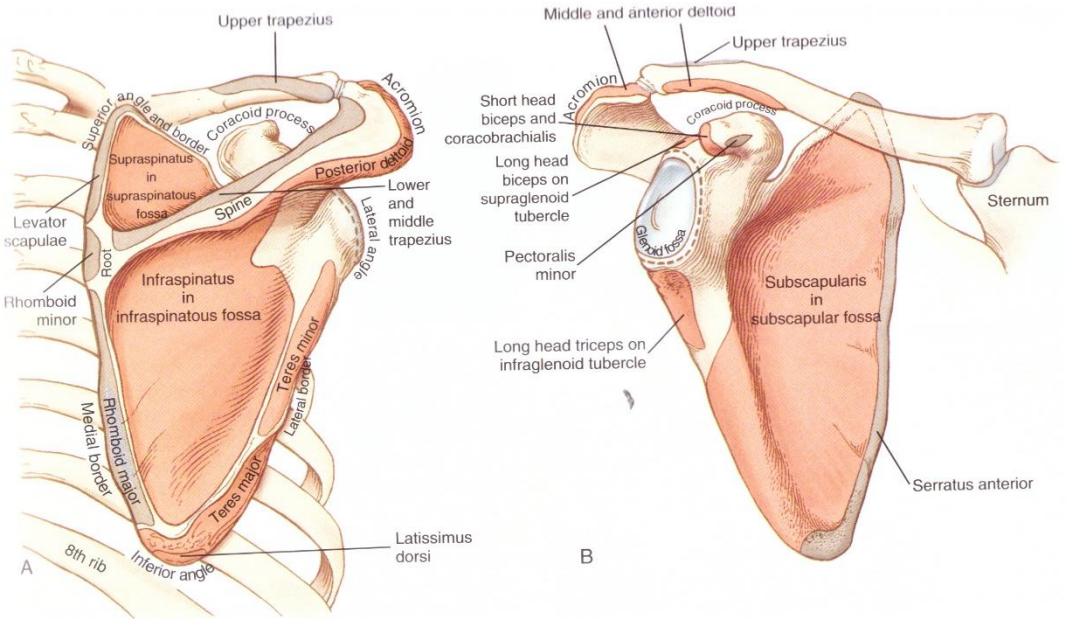

Figure 2-1: The anterior and posterior surfaces of the scapula bone (after Mansfield and Neumann 2014)

The scapula provides a steady base for normal function of the gleno-humeral joint. While the scapula thoracic joint stability is dependent on the coordinated activity of the surrounding muscles structures. For example, for efficient glenohumeral movement to occur, it is essential for the scapular muscles to position the glenoid (Paine and Voight 2013). Generally, for optimal upper-extremity function to occur, it is very important to correctly position the scapula when carrying out various daily activities. The scapula shows different patterns of movements, such as posterior or anterior tilting, upward or downward rotation and internal or external rotation, and also complex motions of anterior translation and internal rotation (scapular protraction) and a combined motion of posterior translation with external rotation (scapular retraction) (Struyf et al. 2014). Meanwhile, the scapular retraction produces a steady base for tasks that require reaching, pushing or pulling (Forthomme et al. 2008).

2.4.2 The Pelvis

The pelvic girdle can be considered as a protective structure for the abdomen and lower pelvis organs. The pelvis also dynamically provides a bony connection between the

vertebral column and the lower limbs. The pelvic girdle is constituted of two innominate, the sacrum, one or two fused bones (coccyx) and two femora, and also the sacro-iliac joint, sacrococcygeal, the pubic symphysis and hip joints (Figure 2-2) (Lee 2004).

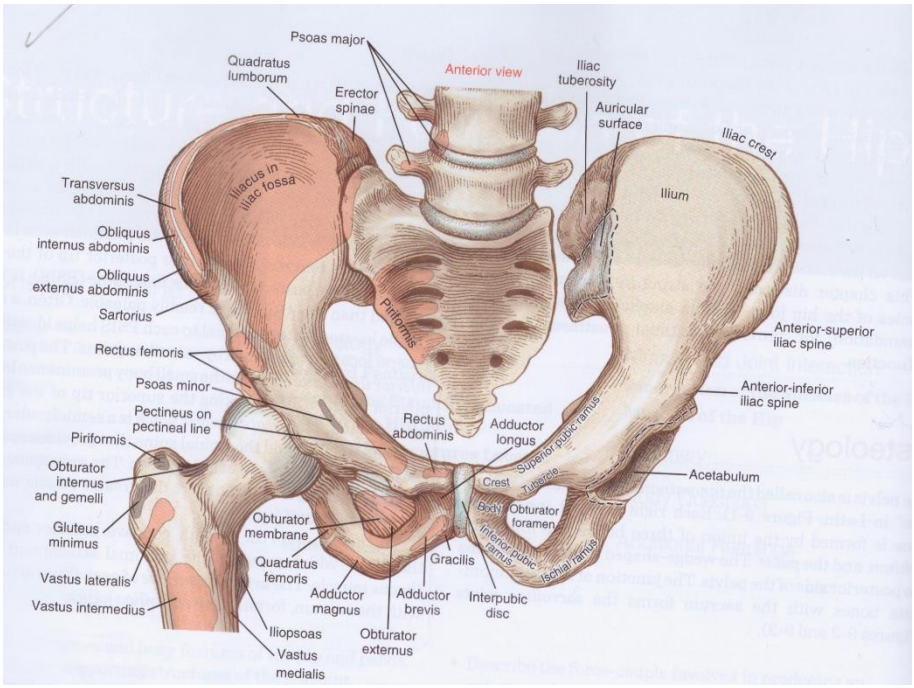

Figure 2-2: Anterior view of pelvis, sacrum and right proximal femur (after Mansfield and Neumann 2014)

The sacrum is clinically defined as an arrangement of five fused vertebral segments. The subsequent decrease in the size of these sacral segments exhibits the sacrum's triangular shape. The apex of the sacrum constitutes the smallest inferior surface facet to allow articulation with a small disc that is located between the sacrum and the coccyx. In contrast, the sacral base is defined as the widest superior surface of the sacrum. In comparison to the vertebral bodies of the spine, the sacral base has a large body. This sacral base body is different in size from left to right, and from front to back (Figure 2-3 and Figure 2-4).

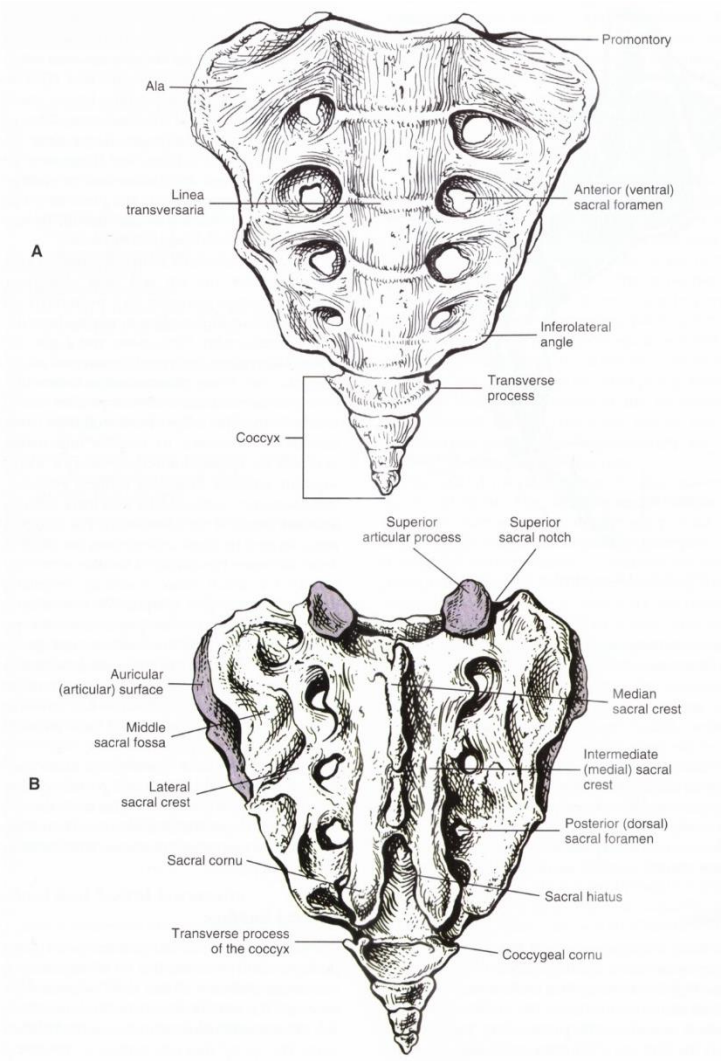

Figure 2-3: A: anterior view of the sacrum, B: posterior view of the sacrum (after Cramer and Darby 2005)

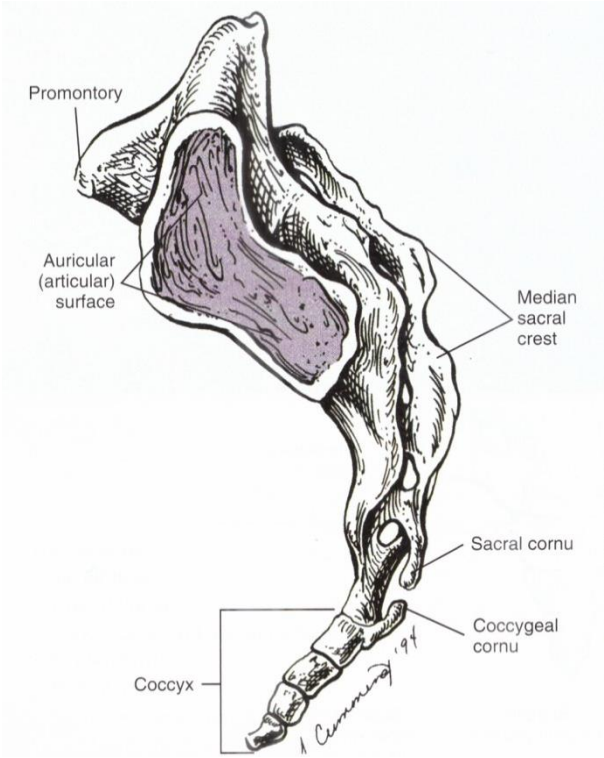

Figure 2-4: Lateral view of the sacrum (after Cramer and Darby 2005)

The anterior rim of the sacral body is recognised as the promontory. The vertebral foramen of the first sacral segment is triangular and constitutes the opening of the sacral canal. At the opening of the sacral canal, the cauda equine continues inferiorly and within the subarachnoid space. The arachnoid mater and dura mater end at the level of the S2 spinous tubercle. The sacral roots, which leave below this level, must exist through the inferior aspect of the arachnoid and dura to extend inferiorly through the sacral canal. These roots form a spinal nerve after receiving the dural root sleeve and they then leave the sacral intervertebral foramen. In contrast, the pedicles of the first sacral segment are small and extend to the left and right laminae, while the laminae convene posteriorly to constitute the spinous tubercle.

The sacrum has three surfaces. First, the transverse processes of the five sacral segments continue to extend laterally and unite with the costal parts of the same segments to shape the large left and right sacral alae (lateral sacral masses or lateral surface). The lateral surface includes the auricular surface in which the auricular surface of the ilium articulates. The shape of the sacral auricular surface is defined as posteriorly concave and continues across the lateral aspects of three of the five sacral levels. In general, there are several elevations and depressions within the area enclosed by the concavity

of the auricular surface, which serves as the connection bony landmarks for the ligaments that support the sacroiliac joint posteriorly. Anatomically, the lateral surface of the sacrum curvature is orientated medially and is thinner from anterior to posterior. The left and right articular processes are extended superiorly from the posterior surface of the sacral base, and face posteriorly and slightly medially.

The plane in which these processes lie differs significantly. More specifically, the orientation of these processes varies between almost a coronal plane to nearly a sagittal plane, which is considered to be asymmetrical in orientation (tropism). For example, one process is more coronally oriented and the other process is shown as more sagittally oriented. This type of tropism can be defined on standard anterior-posterior X-ray films. Moreover, the inferior articular facets of the L5 vertebra articulate with articular facets on the posterior surfaces of the superior articular processes of these processes. The zygapophysial (z) joints formed by these articulations are more planar than those between the two adjacent lumbar vertebrae, and they usually are much more coronally oriented than the lumbar Z joints. However, the orientation of the lumbosacral Z joints differs in the same way as that of the superior articular processes due to the wide variation of the plane in which these processes are located (Cramer and Darby 2005; Peretz et al. 1998; Bogduk 2005).

The left and right superior sacral notches are located lateral to the superior articular facets. These notches are defined as the pathway of the left and right posterior main divisions of the L5 spinal nerve. The second sacral surface (ventral surface) exhibits eight anterior sacral foramina, which are extended posteriorly and medially within the sacral intervertebral foramens (posterior foramens). Meanwhile, the sacral intervertebral foramens are extended within the more medially situated sacral canal. These sacral foraminas serve as an anatomical exit to the major arteries and nerves (Figure 2-5).

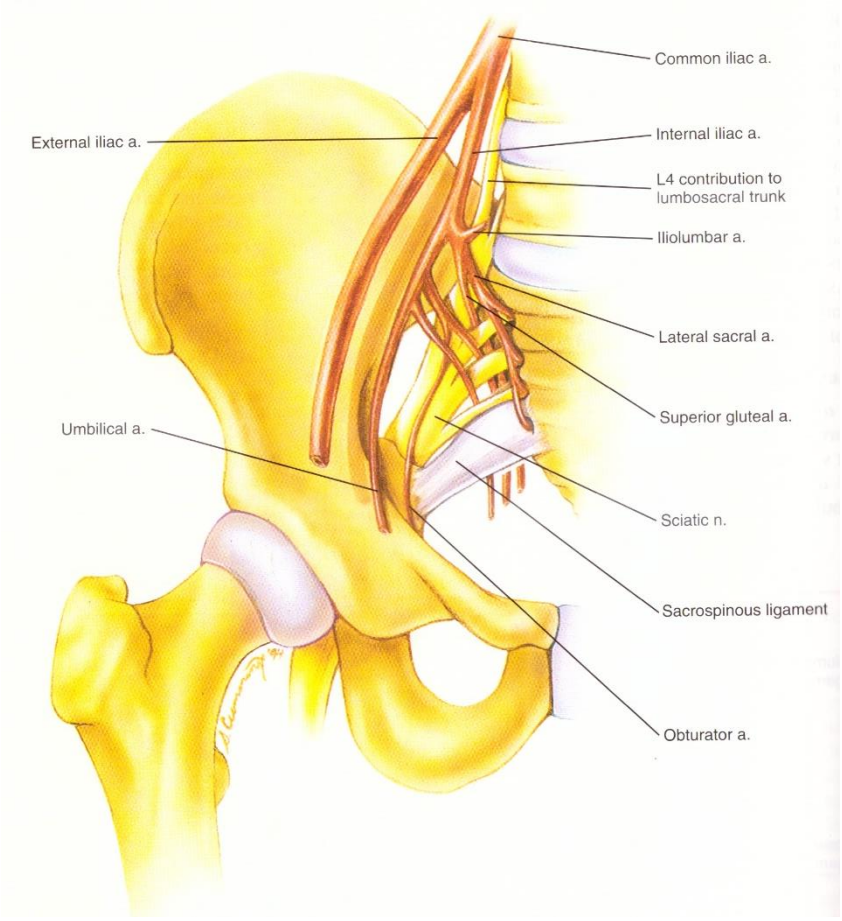

Figure 2-5: The arteries and nerves with the sacral foramena (after Cramer and Darby 2005)

The third sacral surface is called the dorsal surface and it has an irregular shape. The median, intermediate (left and right) and lateral (left and right) sacral crests are located on the posterior surface of the sacrum. Correspondingly, these crests are similar to the spinous processes, articular processes and the transverse processes of the rest of the spine.

Four spinous tubercles are fused with one another and constitute the median sacral crest, which composes the posterior border of the sacral canal. Each sacral tubercle is shaped by the fusion of the left and right laminae of the sacral vertebral segments. The left and right intermediate or medial sacral crests are situated medially to the posterior sacral foramina. These crests are constituted by four fused articular tubercles on each side of the sacrum. The left and right fifth articular tubercles continue inferiorly. The sacral cornuas constitute the left and right inferior borders of the sacral hiatus. In contrast, the left and right lateral sacral crests are located laterally to the dorsal sacral foramina.

The sacrum is concaved anteriorly and, together with the thoracic region, can form a kyphotic curvature to increase the size of bony body cavities. In the normal position of the sacrum, the base of the sacrum is located anteriorly relative to its apex. However, in this case, the sacral curve is positioned anteriorly and inferiorly. The patterns of upright posture, supine sleeping posture and the action of the levator ani muscle are responsible for an increased sacral curve in humans (Abitbol 1989; Ebraheim et al. 2003; Cramer and Darby 2005; Bogduk 2005).

2.4.2.1 The Sacroiliac Joint

Before a clinician makes a diagnosis and carries out treatment for low back pain, the unique anatomical structure of the sacroiliac joint must be taken into account. The sacroiliac joint is considered to be the largest axial joint in the human body, with a mean surface area of 17.5 cm^2. The sacroiliac joint can be described as an articulation between two auricular surfaces of the sacrum and ilium. Recently, this joint has been defined as a typical synovial joint. However, the shape of the auricular surfaces of the sacroiliac joint has been a point of debate for some time. Some authors pointed out that auricular articulation was shaped like an L, while others defined it as a C shape. Generally, different orientations of the articular surface regions of the sacroiliac joint can be seen on MRI and CT images at a transverse plane as a result of their superior and inferior limbs orientations (Figure 2-6). (Cramer and Darby 2005; Cohen 2005).

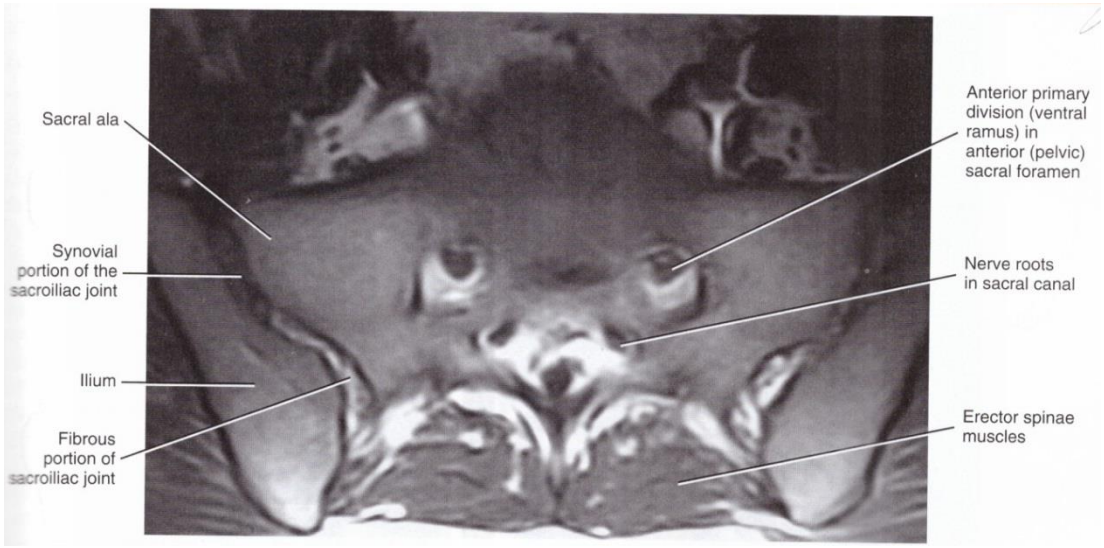

Figure 2-6: Sacroiliac joint orientation in MRI (after Cramer and Darby 2005)

The articular capsule covers the anterior aspect of the sacroiliac joint. In contrast, the interosseous sacroiliac ligament lines the posterior aspect of the sacroiliac joint because the posterior joint surface has no articular capsule (Figure 2-7, Figure 2-8 and Figure 2-9) (Cramer and Darby 2005).

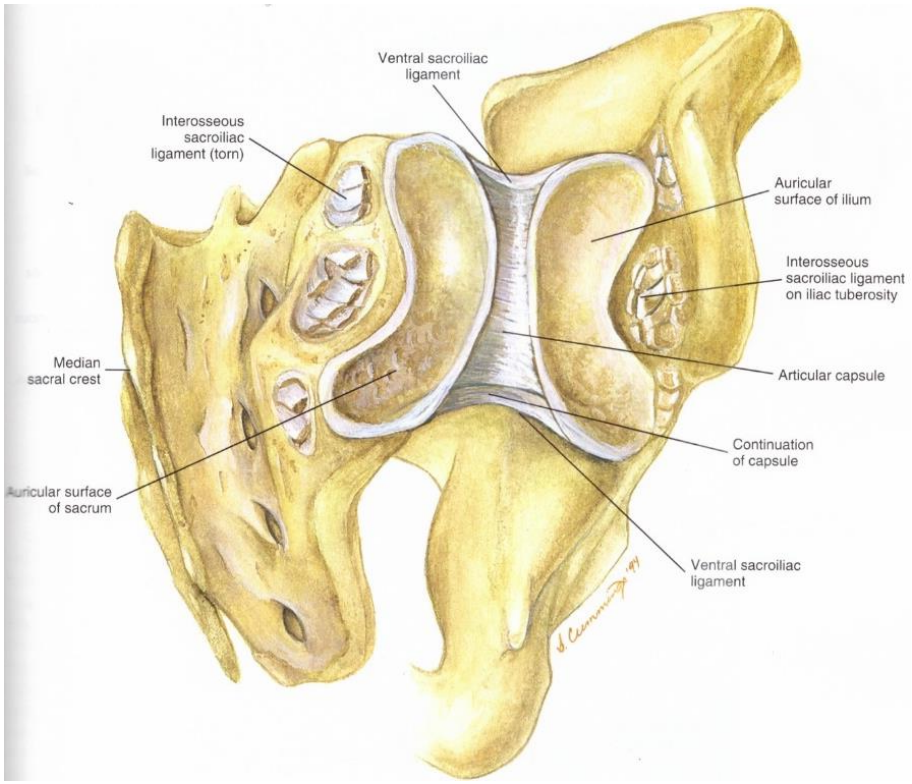

Figure 2-7: Posterior view of an opened right sacroiliac joint (after Cramer and Darby 2005)

The cartilage that lines the auricular surface of the sacrum varies in its histologic properties from that of the auricular surface of the ilium because the auricular sacral surface is covered by hyaline cartilage, while the ilium surface is lined by fibrocartilage. The hyaline cartilage of the sacral surface is thicker and larger than that of the ilium surface and it is round in shape. Pairs of chondrocytes are distributed in columns parallel to the articular surface. However, in later life, the sacral cartilage degenerates and can even become fibrous (Sashin 1930; Bowen and Cassidy 1980).

Superior, middle and inferior sacral fossae are located in the region of the sacrum within the posterior concavity of the sacroiliac joint. The middle fossa is considered to be the axis of the sacroiliac rotation in which the iliac ridge moves circularly in the sacral longitudinal groove (sacral groove) (Figure 2-10).

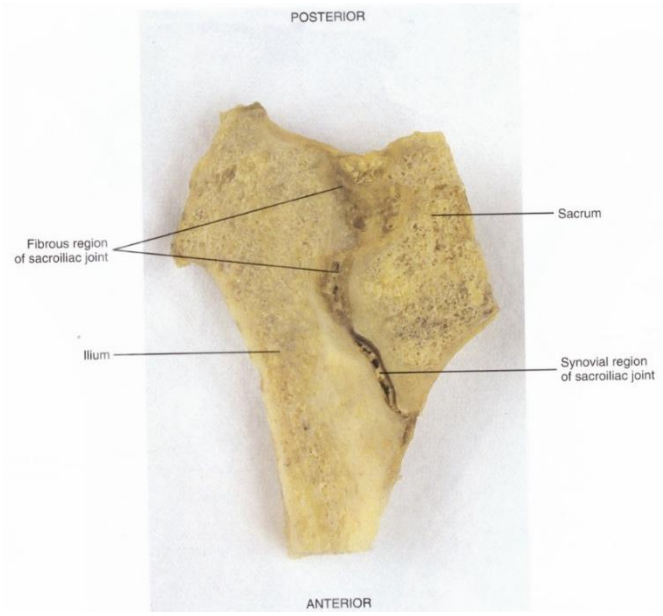

Figure 2-8: The synovial and the fibrous portions of the sacroiliac joint (after Cramer and Darby 2005)

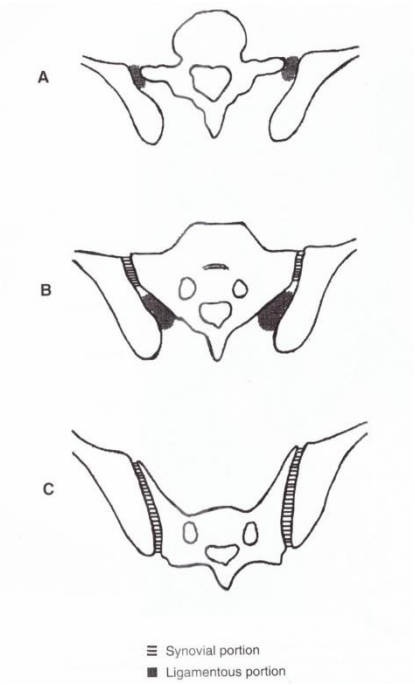

Figure 2-9: A: upper, B: middle, C: lower portions of the sacroiliac joint (after (Parnianpour et al. 1988)

The sacral groove runs from the superior aspect to the inferior aspect of the sacral articular surface. The sacral tuberosity constitutes the posterior rim of this groove, while the inferior end of the iliac ridge constitutes the posterior inferior iliac spine. Therefore, the sacral groove and the iliac ridge, together with a series of interlocking elevations and depressions, maintain sacroiliac joint stability and movement (Figure 2-10) (Bakland and Hansen 1984; Cramer and Darby 2005).

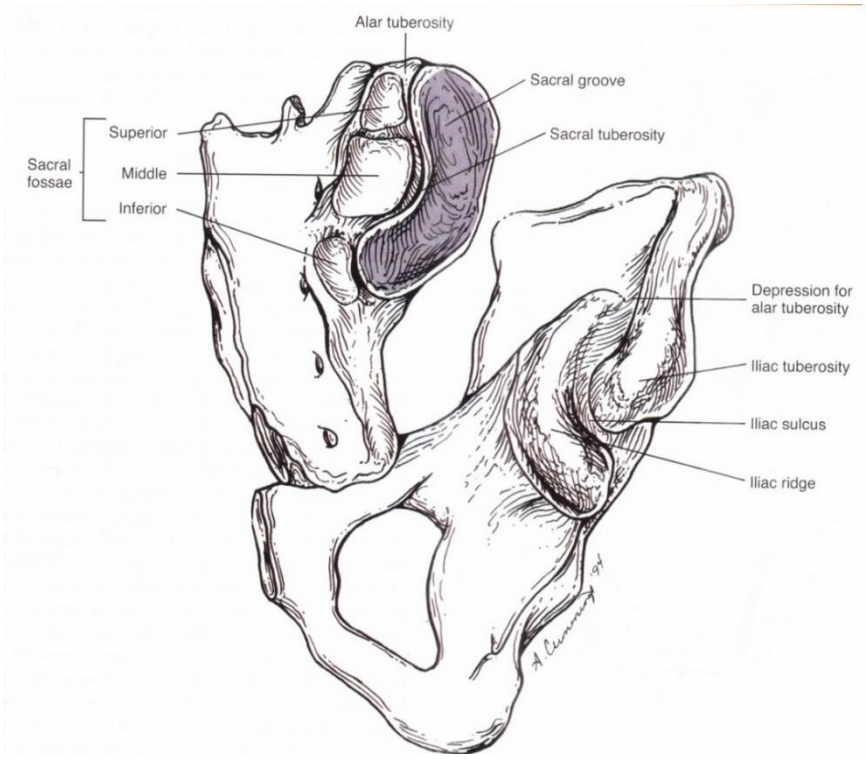

Figure 2-10: The elevations and depressions associated with the sacroiliac joint (after Cramer and Darby 2005)

(Lee 2004) considered that there are three ways to protect the sacroiliac joint from compression forces and bending movements loads. The first is related to the wedge shape of the sacroiliac joint in the anteroposterior and vertical planes. The second is that the irregular shape of the articular cartilage of the sacroiliac joint can enhance stabilisation of the sacroiliac joint. The third is that a frontal dissection through the sacroiliac joint reveals cartilage-covered bony extensions protruding into the joint (ridges and grooves).

The anatomical structure of the sacroiliac joint is more likely to move passively because it has a very small range of motion, which is executed by the muscle action. Meanwhile, the sacroiliac joint functions as a stress relieving joint. For example, during gait, this phenomenon indicates that the sacroiliac joint is positioned in the pelvic ring toward the side, which is under the maximum torsional stress to absorb the twisting forces which are initiated by lower limb movements into the sacroiliac joint ligaments. Three articular areas of the sacroiliac joint should be noticed in adult sacro-iliac dysfunction. The first is the iliac elevation and sacral depression in the upper third of the joint; the second is iliac depression and sacral elevation in the middle third; and the third is iliac elevation and sacral depression in the lower third of the sacroiliac joint (Figure 2-11) (Schafer 1987).

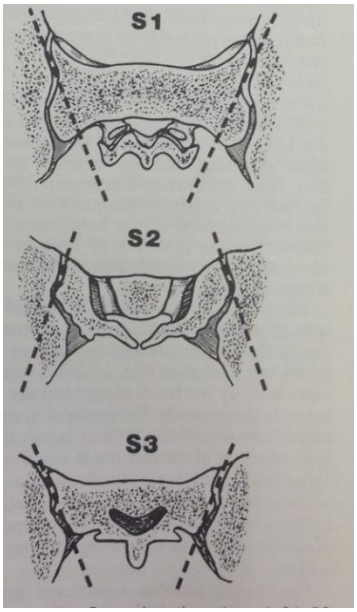

Figure 2-11: The various planes of the sacroiliac joint articulation (after Schafer 1987)

2.4.3 The Lumbar Spine Anatomy

The spine has three complex and fundamental biomechanical functions. First, it provides the mechanical linkage between the upper and lower extremities by transferring the weight, resulting in bending movements of the head and trunk, with any weights being lifted by the pelvic girdle. Second, it allows a mobile connection between these three different body parts. The third and most important function is that it protects

the delicate spinal cord from potentially damaging forces produced by both physiological movements and trauma.

2.4.3.1 Vertebral Column

The functional spinal unit is composed of the vertebrae, which articulate with each other in a controlled manner via a complex of levers, pivots (facets and discs), passive restraints (ligaments) and activations (muscles) (White and Panjabi 1990).

The movable lumbar spine has a normal lordosis curve and is composed of five vertebrae. The upper lumber vertebrae articulate with the rigid, kyphotic thoracic region and the lower lumbar vertebrae with the rigid, kyphotic sacrococcygeal region (Figure 2-12) (Storm et al. 2002).

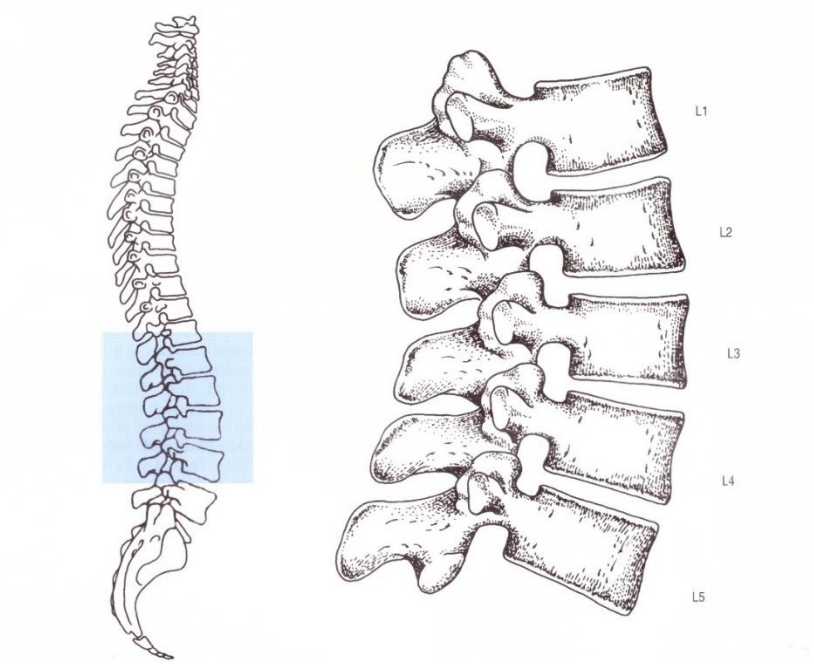

Figure 2-12: The movable lumbar spine (the blue shaded region) relating to the entire vertebral column (after Bogduk 2005)

A lumbar vertebra has an irregular shaped bone structure, which consists of a vertebral body, two pedicles, facet joints and spinous processes. The vertebral body is the anterior component of the vertebrae and its function is load bearing, while the articular, accessory, mammillary, spinous and transverse processes and the laminae are the posterior parts of the vertebrae. These processes work as the attachments for the muscles, which act directly on the lumbar spine (Figure 2-13).

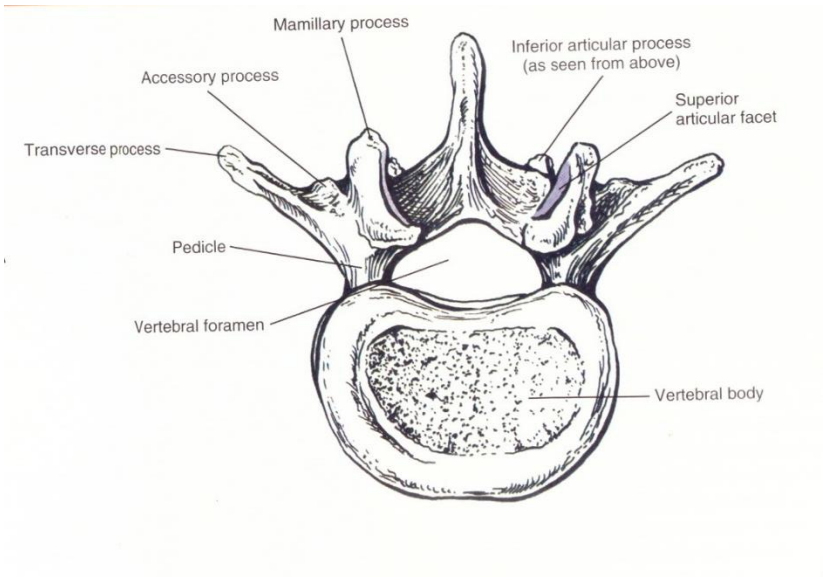

Figure 2-13: A superior view of the typical lumbar vertebrae and the position of the pedicle and vertebral body (after Cramer and Darby 2005).

2.4.3.2 The lumbar vertebral canal

The lumbar vertebral canal is formed by the alignment of the five lumbar vertebra. The posterior surfaces of the lumbar vertebra, discs and the posterior longitudinal ligament constitute the anterior wall of this canal, while the lamina and the ligamentum flavum form the posterior wall of the canal. The delicate spinal cord is enclosed within the hard structure of the spinal canal. The conus medullaris of the spinal cord ends at the level of the first lumbar vertebrae. The cauda equina is located inferior to this lumbar vertebral level. The spinal canal itself is covered with dural mater, arachnoid, and subarachnoid space (Figure 2-14). Collectively, these enclosed structures by the spinal canal are called the thecal or dural sac. Abnormal stretching forces on the conus medullaris and the lower lumbar spinal cord segments can cause low back pain.

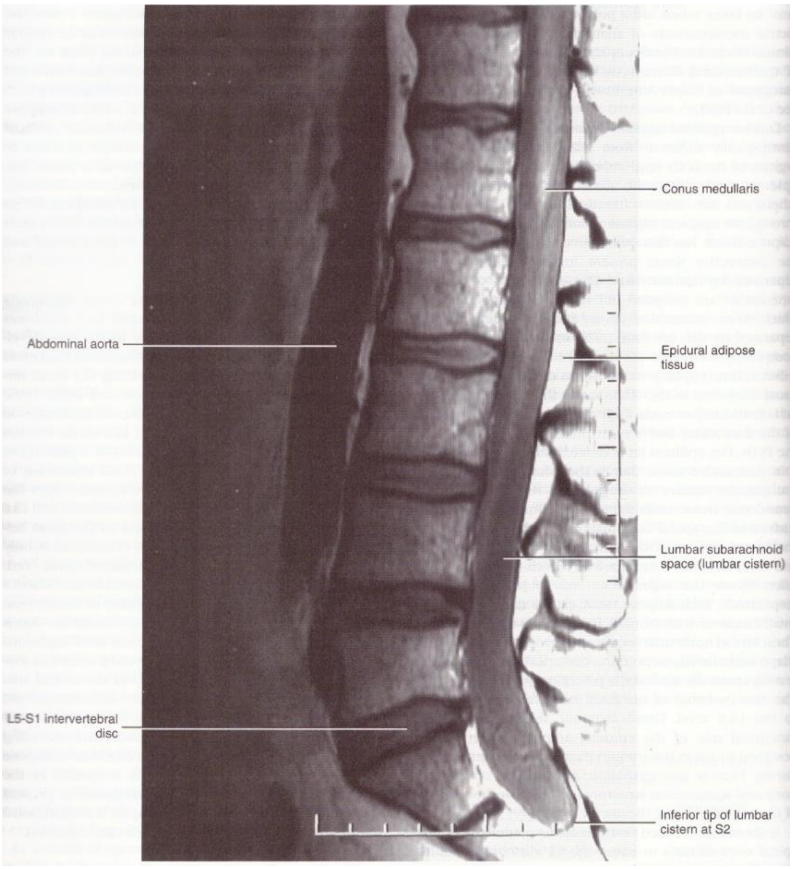

Figure 2-14: Midsagittal plane magnetic resonance imaging scan of the lumbar region shows the spinal canal and dural sac components (after Cramer and Darby 2005)

2.4.3.3 The Pedicles

The vertebral arch has several unique structures (pedicles, lamina, and superior articular, inferior articular, transverse and spinous processes). The pedicles are short, thick and rounded in shape, which creates the narrow anterior portions of the vertebral arch and attaches to the posterior and lateral aspects of the vertebral body. The pedicles with the vertebral body and the laminae constitute the bony protective structure (spinal canal) for the spinal cord. Because the pedicles are smaller than the vertebral bodies, a groove, or vertebral notch, is formed above and below the pedicles (superior and inferior vertebral notches).

The lumbar vertebra has a superior vertebral notch that is less distinct than that of the cervical region, while the inferior vertebral notch is considered to be prominent. In turn, the pedicles of the lumbar spine are short and strong, and their attachments are lower

on the vertebral bodies than the pedicles of the thoracic region but higher than those of the cervical region. The size of the pedicles can vary among individuals of different ethnic backgrounds. For example, the length of the pedicles of individuals of East Indian descent is less than that of Caucasians. In this condition, the trabecular pattern of the L4 and L5 pedicles seems to indicate that most loads placed on these vertebrae may be transferred from the vertebral bodies to the region of the posterior arch, specifically to the pars interarticulans.

The trabecular architecture of the lumbar vertebral bodies is ideal for the loads placed on the spine during axial compression and, because their centre being located between the vertebral body and the posterior elements, the pedicles serve as the force and moment transformer to the vertebral body (White and Panjabi 1990; Bogduk 2005; Cramer and Darby 2005; Nazari 2007).

2.4.3.4 The Intervertebral Disc

The intervertebral disc composes the anterior articulation section between two vertebral bodies and constitutes 20–30% of the entire height of the vertebral column. In the company of the facet joints, it provides load pathways within a motion segment, while allowing movements of the spinal column. Its principal responsibility is to react to all compression forces to which the spine is subjected. The structures that supply the disc with these unique properties are the three inert-dependent arrangements (i.e. the nucleus pulpous, the annulus fibrosis and the cartilaginous end-plates).

The nucleus pulpous, which is composed of a gelatinous muco-protein and muco-polysaccharide, is centrally located between the cartilaginous end-plate and is embedded by the annulus fibrosus. The water content inside the nucleus ranges from 85–90%, which decreases in later years. As the normal nucleus has a preload mechanism (the pressure inside the centre of the normal nucleus is not equal to zero), the disc possesses a great ability to resist compressive forces. The nucleus pulpous in the cervical and lumber spine segments is characterised by a greater size and swelling ability than other spine regions.

The outer zone of the disc contains concentric arranged laminated bands, which are called the annulus fibres. The inner region of these fibres connects with the cartilaginous

end-plates, while its boundaries attach directly into the osseous tissue of the vertebral body by Sharpe's fibres. With respect to the disc, these fibres intersect with each other diagonally at nearly ± 30 degrees and as a result of their oblique alteration orientation, the annulus fibrosus can resist the movements in all directions. The anterior region of the annulus is characterised by more abundant and denser fibres than the posterior one, whereas the parallel alignment of the posterior and the posterior-lateral fibres is greater than the anterior fibres (Figure 2-15) (Jensen 1980; White and Panjabi 1990; Nazari 2007). The annulus, which encapsulates the radial bulge of the nucleus pulposus, has two functions: first, to allow the consistent distribution and transfer of compressive loads between the vertebral bodies; and second, to permit distending and rotation to facilitating joint mobility. These functions are made possible by its unique, microstructural composition, which provides both compressive and tensile forces (Smith and Fazzalari 2009). The nucleus and annulus are separated from the adjacent vertebral bodies by a cartilaginous end-plate, which consists of hyaline cartilage (White and Panjabi 1990). This structure serves as a nourishing passage to the intervertebral disc and it has a deflection ability when sufficient axial loads are transmitted between the intervertebral disc and the vertebral body (Nazari 2007).

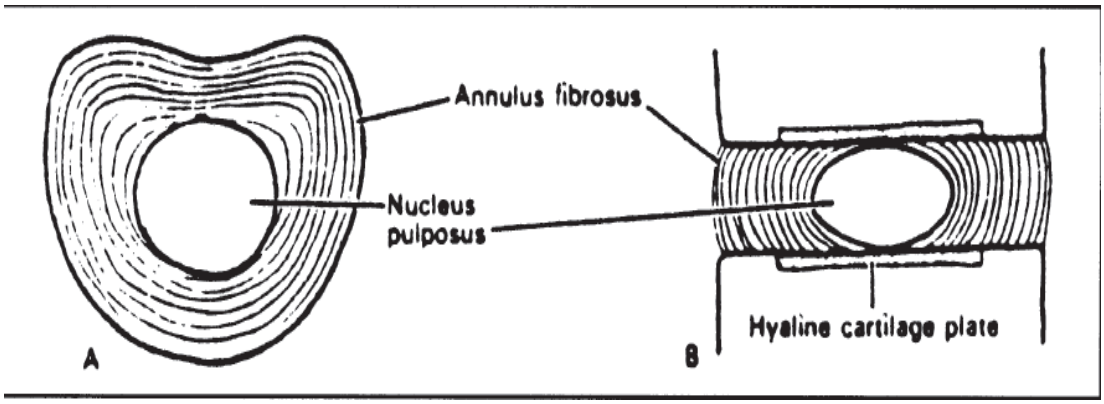

Figure 2-15: Disc components (after Jensen 1980).

2.4.3.5 The Lumbar Intervertebral Foramen

The lumbar intervertebral foramen has a similar shape to an inverted teardrop and it constitutes a passageway that joins with the spinal canal. The intervertebral foramen (IVF) is bordered superiorly and inferiorly by the pedicles of the contiguous vertebrae: the postero-inferior margin of the superior vertebral body, the intervertebral disc, the postero-superior vertebral notch of the inferior vertebral body anteriorly, and the

ligamentum flavum and superior and inferior articular facet posteriorly (Figure 2-16) (Inufusa et al. 1996; Senoo et al. 2014).

It is generally accepted that one of the causes of clinical nerve compression is the narrowing of the foraminal spinal canal (Cuchanski et al. 2011). Compression of the nerve roots depends upon the effective space available within the IVF, accounting for the soft tissue within the canal and the decreased size of the canal due to both degenerative and physiological movements by vertebrae. In comparison with a peripheral nerve, the spinal nerve has a less abundant epineurium, no branching fasciculi and poor lymphatic drainage. This illustrates that the nerve root is more subject to injury by mechanical forces (compression during its path through the intervertebral foramen) (White and Panjabi 1990). The normal values of the foraminal dimensions (height, width, cross-sectional area) have been reported by many researchers who used techniques such as cadaveric, CT, MRI, cryomicrotome and callipers. These studies reported that the intervertebral foramina height during neutral position ranged from 15.9 to 23.4mm and the cross-sectional area varied from 115 to 140.5mm^2. In addition, the foraminal width of more than 4mm was included as a normal value (Inufusa et al. 1996; Smidt et al.1997; Fujiwara et al. 2001; Cinotti et al. 2002; Al-Hadidi et al. 2001; Cramer et al. 2003; Torun et al. 2006; Senoo et al. 2014). However, (Hasegawa et al. 1995), mentioned that a foraminal height less than 14.31 and 17.68mm at L5-S1 and L3–L4, respectively, and can be recorded as a critical sign of foraminal stenosis.

Figure 2-16: The intervertebral foramen (after (Cramer and Darby 2005)

2.4.3.6 The Articular Facet

The facet joints compose the posterior articulation between two articulated vertebrae and are located between the superior and inferior articulating processes (Nazari 2007). (Jaumard et al. 2011) stated that at each spinal segment, there is a pair of facet joints that are positioned on the posterior-lateral aspects of each motion segment and extend from the cervical to the lumbar spine (Figure 2-17). The complex mechanical performance of the facet joints is dependent on the responses imposed by the whole spine responses via its relationship to the intervertebral disc, its anatomical orientation and its own mechanical behaviour.

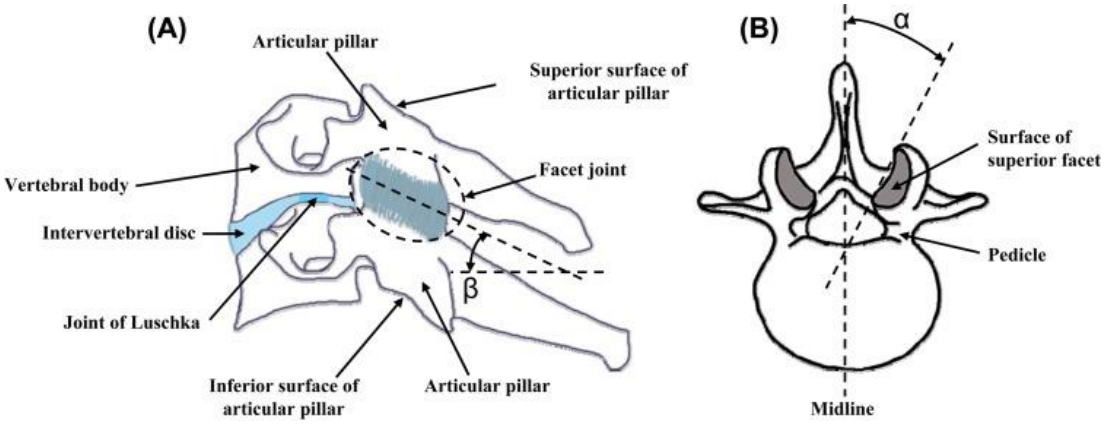

Figure 2-17: Lateral view of a cervical (A) and axial view of a lumbar (B) vertebra showing the overall anatomy and the facet joints, articulations and orientation relative to its angle with each of the axial planes (β) and the sagittal plane (α) (after Jaumard et al. 2011).

Clinically, the articular facets can vary both in the shape of their articular surfaces and in the general orientation they face (Figure 2-18). The articular facets may appear flat or planer or may be curved in the transverse plane. The curvature may be slightly different from a flat plane or may be more pronounced (Figure 2-19).

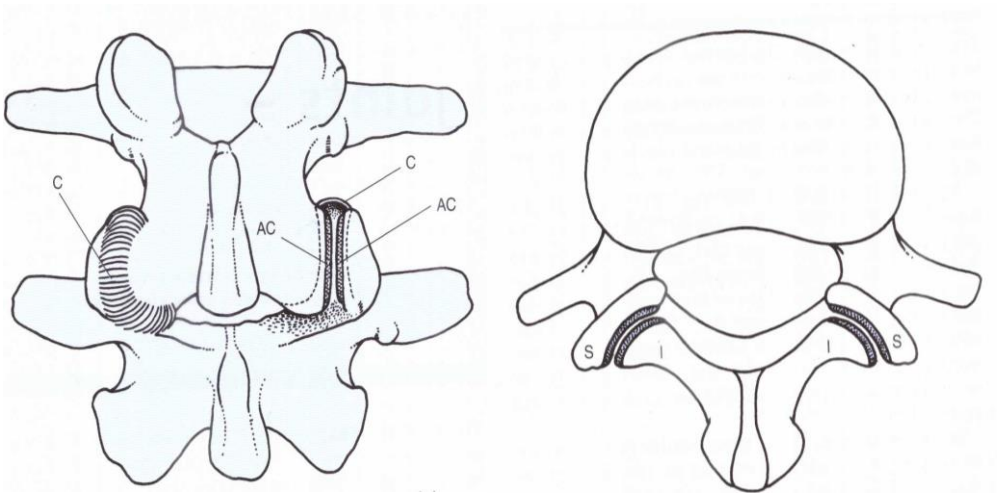

Figure 2-18: A posterior view of the L3-L4 zygapophysial joints (right figure); a top view of the L3-L4 zygapophysial joint showing the curved facet in the transverse plane (left figure) (after Bogduk 2005).

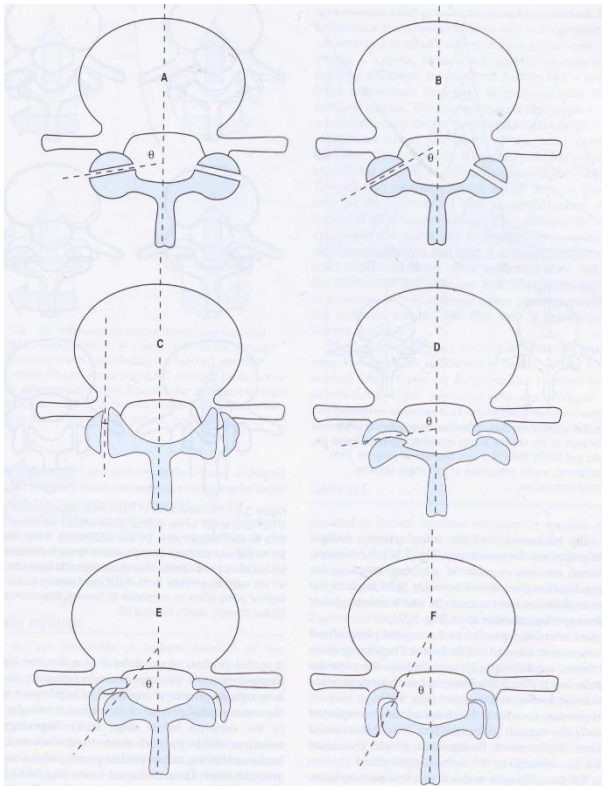

Figure 2-19: The variations of the orientation and curvature of the lumbar zygapophysial joints (A, B, C) flat joints, (D and E) curved joints, (F) J-shaped joints (after Bogduk 2005).

The mechanics of the flat lumbar zygapohysial joints can be summarised by Figure 2-20. A flat joint at 60° to the sagittal plane provides resistance to both forward

displacement (A) and rotation (B). A flat joint at 90° to the sagittal plane strongly resists forward displacement (C), but during rotation (D), the inferior articular facet can glance off the superior articular facet. A flat joint parallel to the sagittal plane offers no resistance to forwarding displacement (E) but actively resists rotation (F).

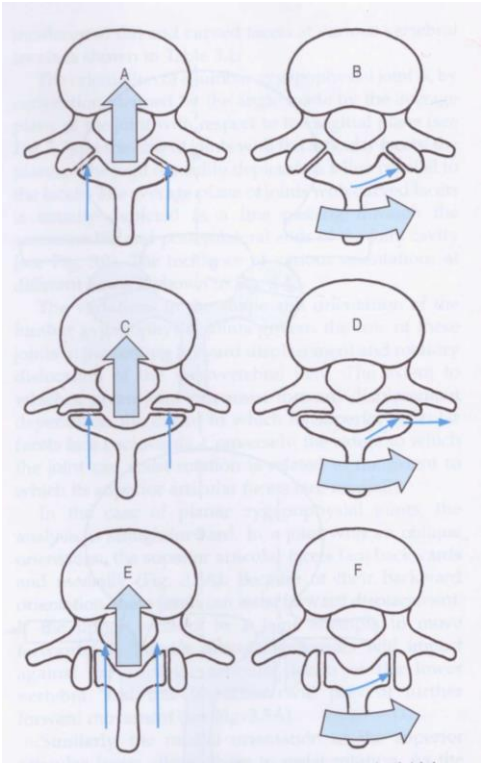

Figure 2-20: The mechanics of the flat lumbar zygapophysial joint (after Bogduk 2005)

The mechanics of the curved lumbar zygapophysial joints are shown in Figure 2-21. (A): C-shaped joints have a wide anteromedial portion which faces backwards (indicated by the bracket), and this portion resists forward displacement. (B): J-shaped joints have a narrower anteromedial portion (bracket) that, nonetheless, resists forward displacement. (C, D) Both C- and J- shaped joints resist rotation, as their entire articular surface impacts (Bogduk 2005).

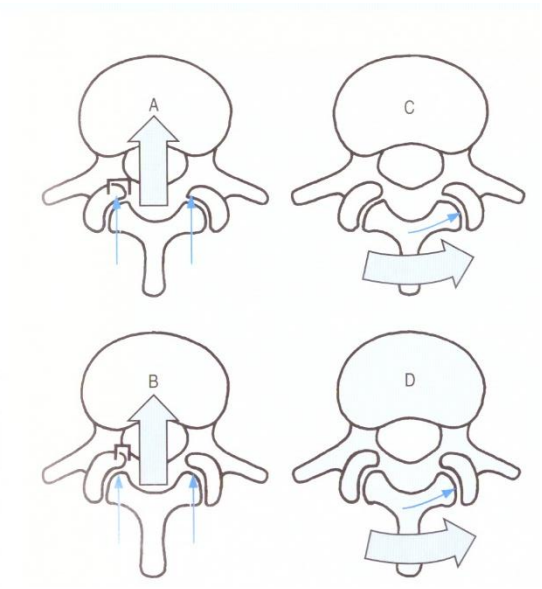

Figure 2-21: The mechanism of a curved lumbar zygapophysial joint (after Bogduk 2005).

Facet orientation can be defined as the angle of the facet joint in the transverse view relative to the coronal plane (Boden et al. 1996). Many previous studies have focused on facet joint orientation as a pre-existing morphological factor in degenerative spondylolisthesis. The facet joints primarily can share the load in compression, extension and torsion of the lumbar spine and protect the disc against torsion. It is, therefore, proposed that a more sagittal orientation of the facet joint promotes anterior gliding by reducing resistance to anterior shear forces (Kalichman et al. 2009; Toyone et al. 2009).

Facet joint tropism is an asymmetry between the left and right facet joint angles, with one joint having a more sagittal orientation than the other. This was proposed to increase the risk of degenerative diseases in the corresponding disc, such as disc herniation and rotational instability of the spinal segment. However, categorical facet tropism has been defined as the difference from 6º to 15º (Boden et al. 1996; Kalichman et al. 2009; Do et al. 2011; Chadha et al. 2013).

Asymmetry of facets (tropism), especially if it is marked, is a subject of intense interest because it has the potential to markedly alter the biomechanics of lumbar spinal movements and precipitate early degenerative changes, either in the joint or adjacent intervertebral discs contributing to back pain (Kim et al. 2013).

(Farfan and Sullivan 1967) first reported that the asymmetry of the facet joints is correlated with the development of disc herniation because the coronally facing facet

joint offers little resistance to intervertebral shear force. This means that the rotation occurs towards the side of the more coronally facing facet joint, which possibly leads to additional torsional stress on the annulus fibrosus. However, this hypothesis, also the role of the sagittal or coronal orientation of the articular facet on the side of the disc herniation, have been considered as a point of argument by numerous researchers (Adams and Hutton 1981; Krnrsi and Lesur 1985; Park et al. 2001; Noren et al. 1991; Boden et al. 1996; Ishihara et al. 1997; Ko and Park 1997; Masharawi et al. 2004; Chadha et al. 2013).

The cartilage of the normal lumbar zygapophysial joints has no specific features. Generally, the articular cartilage covers the facets of the superior and inferior articular processes and assumes the same concave or convex curvature as the underlying facet (Figure 2-22). To enable the normal motion in a healthy spine, these cartilage surfaces afford a low-friction interface (Bogduk 2005; Jaumard et al. 2011).

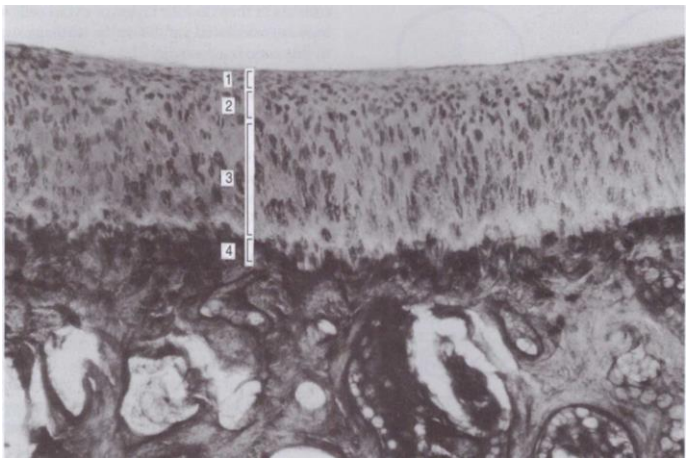

Figure 2-22: A histological section of the lumbar zygapophysial joint cartilage showing the four zones of cartilage: 1, superficial zone; 2, transitional zone; 3, radial zone; 4, calcified zone (after Bogduk 2005).

(Bogduk 2005) stated that each lumbar zygapophysial joint is encircled by a fibrous capsule all over its dorsal, superior and inferior boundaries. The posterior capsule is fibrous and connects to the inferior articular process. Its other end attaches to the superior articular process and the boundary of the articular cartilage capsule. In contrast, the ligamentum flavum constitutes the anterior capsule (Figure 2-23).

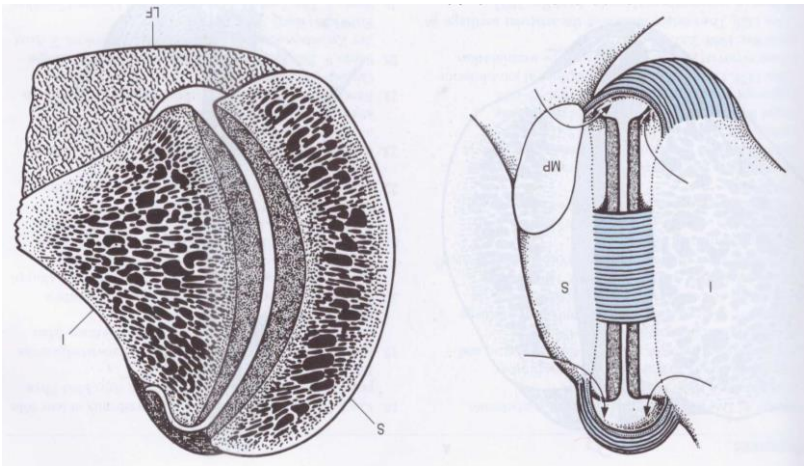

Figure 2-23: A transverse section through a lumbar zygapophysial joint showing: I: inferior articular process; S: superior articular process; LF: Ligamentum flavum (after Bogduk 2005).

2.5 Magnetic Resonance Imaging (MRI)

2.5.1 The Basic Principle of MRI

There are three reasons why MRI uses the magnetic properties of the hydrogen nucleus (H1) to produce images of the body. First, the hydrogen nucleus is the most abundant isotope of hydrogen. Second, its spin value is ½. Lastly, the response from the hydrogen nucleus (^{1}H) to an applied magnetic field is one of the largest found in nature. The human body is composed of water (H_2O) and the methylene and methyl groups of fat molecules (CH_2, CH_3), both of which contain hydrogen.

The protons are oriented randomly if the magnetic field is absent (Figure 2-24 A), while if an external magnetic field is applied (Bo), the protons will align towards this magnetic field. Thus, the tissue sample now possesses a net magnetisation vector (Mo) parallel to Bo (Figure 2-24 B). Mz and Mt are the two vectors which are split from Mo. At this time, Mz is parallel to Bo and Mt is perpendicular to Bo.

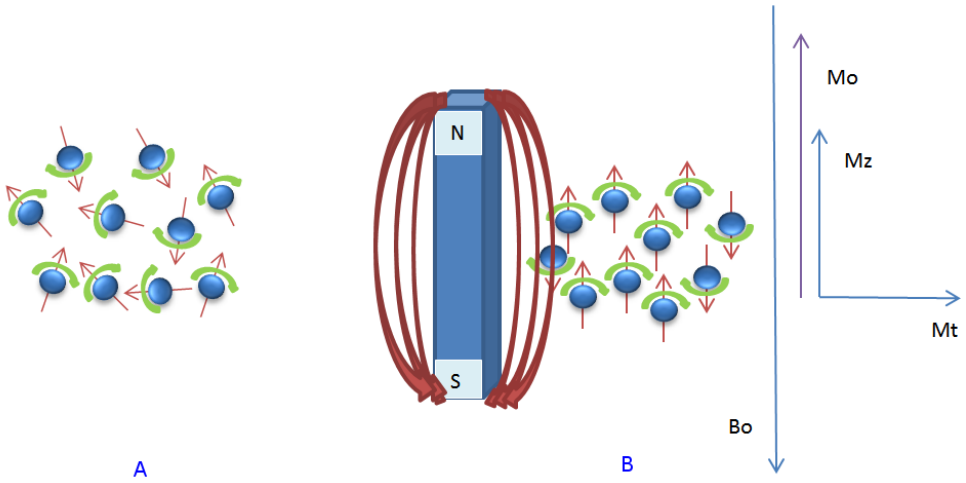

Figure 2-24: A: Randomly orientation of the collection of protons in the absence of an external magnetic field, B: Collection of protons rotate about an external magnetic field Bo and Mo, with its two components (Mz and Mt)(after Mendieta 2016).

At this stage, the collection of protons that are located in the low energy state are pointing north, and the protons in the high energy state are pointing south. Because the number of protons in the low energy state is greater than that of the high energy state group, the sample now possesses a net magnetisation vector (Mo). At this point, the Larmor equation can be interpreted as the frequency at which the proton precesses around an external magnetic field:

$$w_o = \gamma B_o \qquad (1.1)$$

Where w_o is the angular precessional frequency, which can be expressed in radians per second or Hertz: γ is the gyromagnetic ratio, which is a proportionally constant fixed for a specific nucleus: and B_o is the strength of the external magnetic field given in tesla (T).

Magnetic field strength varies according to the purpose required for the scan. For example, for clinical use, the magnetic field strength is in the range of 0.1T to 3T, while for research purposes, the systems use up to 9T or 12T. However, 1.5T and 3T are commonly recommended for medical imaging (Mendieta 2016).

(Rathnayaka Mudiyanselage 2011)demonstrated that the magnetic field strength of 3T can cause an increase in signal-to-noise ratio and spatial and temporal resolution.

To generate a readable signal, which is generated in the receiving coil (RF coil), the magnetisation has to be flipped to the transverse (X - Y) plane and a given tissue sample must be exposed to a radio frequency (RF) pulse along the x-axis, perpendicular (90º $pulse$) to the main magnetic field. With the introduction of the new magnetic field (RF), the protons will precess along the x axis instead of precessing in the Z plane. Now, the precessional frequency is:

$$w_1 = \gamma B_1 \qquad (1.2)$$

where B_1 is the magnetic field associated with the radiofrequency pulse.

The T1 (longitudinal relaxation time) can be obtained when the radio frequency wave (t = 0) is shut off and the Mz starts to recover. At the same time, Mt(Mxy) starts to decay. At this point, the exponential rate constant of decay is called transverse relaxation time T2.

These two processes occur separately, as T2 decays 5 to 10 times more rapidly than T1 recovers. The values of T1 and T2 can be different according to the large variations between tissue types (Hashemi et al. 2010; Rathnayaka Mudiyanselage 2011; Mendieta 2016).

2.5.2 Determination of Tissue Contrast in MRI

The differences between T1, T2 and the proton density of the tissue serve as the basis for the image contrast. At this point, other scan parameters: TR (repetition time) and TE (echo delay time) can be selected to manipulate the contrast. The repetition time is the time interval between pulses of 90° and time to echo is the short period elapsed after applying the RF pulse. TR and TE are intimately connected to T1 and T2, but T1 and T2 are parameters defined by the tissue being imaged, contrary to TE and TR, which are times that can be controlled by the operator to create images contrasted on T1 or T2.

When short times (TR) are selected, the images are called T2-weighted images. T2-weighted images can be obtained from modulating T2 contrast by changing echo time (TE). Meanwhile, the proton density weighted images can be acquired by determining the proton density of the tissue. The proton density parameter governs both characteristic T1 (recovery) and T2 (decay).

2.5.3 Slice Selection Position and Thickness

Gradient coils are used to achieve spatial discrimination from the signal received. However, at this stage, the magnetic field becomes weaker at the feet but gradually increases through the rest of the body. The three linear mutually perpendicular gradients used for slice selection, frequency or readout and phase encoding are Gx, Gy and Gz. When a magnetic field gradient is applied on top of existing main field (Bo in x, y, or z directions, the spins at different locations along the gradient experience slightly different magnetic fields. Thus, a specific location along the body or gradient will precess at a specific Larmor frequency, which is given by the following equation:

$$v_r = \gamma(B_0 + G.r) \qquad (1.3)$$

Where $v_r$the spin frequency at a specific location (r), Bo is the uniform magnetic field, γ is the gyromagnetic ratio, and G is the gradient vector with amplitude and direction.

By using these gradient coils, if a single frequency (RF) is applied to the subject, then the information from a determined line of the body will be received, but the width of this line will be very thin. Consequently, the bandwidth technique is used in which a range of frequencies obtain a slice with a reliable thickness (Mendieta 2016).

2.5.4 Pulse Sequences

A pulse sequence compresses a number of instructions to the hardware for switching on and off the RF pulses and gradient pulses and keeping timings between them to acquire a desirable contrasted image by manipulating the relevant parameters: (TR, TE and FA (flip angle)). Along TR and short TE, the sequence is called proton density –weighted, a short TR and short TE sequence is called T1- weighted, while a long TR and long TE sequence is called T2-weighted. The two commonly pulse sequences used in MR imaging are the Spin Echo Sequences and Gradient Echo Sequences, which are mostly used for clinical imaging because both of these sequences can produce T1- and T2-weighted images (Rathnayaka Mudiyanselage 2011; Mendieta 2016).

2.5.5 Spatial Resolution and K-Space

Spatial resolution is defined by the voxel size (three-dimensional object). Therefore, the resolution of the slices depends on many factors, including matrix size, the field of view and slice thickness. The matrix is used to produce the raw data. The raw data contains all the information necessary to reconstruct an image. Each time that a sequence is repeated, a full line in the frequency-encode is acquired (256 or 512 points). Therefore, the phase encode is changed for each repetition, resulting in each line having a different position. Consequently, the k-space (Fourier space) will be filled by this data line by line, which is strongly dependent on the strength of the three gradients coils (Gx, Gy and Gz) (Mendieta 2016).

Information regarding the borders and contours of the image and the detail of the structures can be provided by the periphery rows of the raw data matrix, while the low spatial frequencies (the centrally located rows) describe the general information of the image(Moratal et al. 2008).

The K-space can be described as the space covered by the phase and frequency encoding data. This is sampled by the receiver coil and stored as a function of time. Every point in the raw data matrix contains part of the information for the complete image. In other words, each slice contains the whole set of MR images, which possess its own K-space.

The centre line of the K-space will contain the information of the phase encoding from the weakest gradients and thus, the most signal and outer line of the K-space originates from the largest gradients and therefore, it has the least signal.

2.5.6 Signal to Noise Ratio (SNR)

Image quality can be reduced by the random variation in the pixel intensity values (image noise). The radiofrequency may result from many factors, such as the tissue being scanned (such as human body thermal mass), fluorescent lights and the electronic monitoring equipment (Mendieta 2016).

The signal-to-noise ratio (SNR) is important because it can determine the image quality in an MRI system. According to Equations (1.4) and (1.5), the intrinsic SNR is approximately proportional to the strength of the main magnetic field, voxel size

(sampling larger surface), the square root of the total sampling time, field of view, slice thickness, receiver bandwidth per pixel, flip angle and T1, T2, TR and TE:

$$SNR_{SE} \propto B_O V \sqrt{\frac{N_{PE} N_{PA} N_{AV}}{BW}} \left(1 - e^{-\frac{TR}{T_1}}\right) e^{-\frac{TE}{T_2}} \quad (1.4)$$

$$SNR_{GER} \propto B_O V \sqrt{\frac{N_{PE} N_{PA} N_{AV}}{BW}} \frac{\sin(\theta)\left(1-e^{-\frac{TR}{T_1}}\right)}{\left(1-e^{-\frac{TR}{T_1}}\cos(\theta)\right)} e^{-\frac{TE}{T_2}} \quad (1.5)$$

where SNR_{SE} is the signal-to-noise ratio for the spin echo sequence, SNR_{GE} is the signal-to-noise ratio for the gradient echo sequence, Bo is the constant magnetic field, V is the voxel volume, N_{PE} is the number of acquired phase encode lines, N_{PA} is the number of acquired partitions or frequency lines, N_{AV} is the slice number, BW is the receiver bandwidth per pixel, $T_1$is the longitudinal relaxation time, T_2 is the transverse relaxation time, and θ is the flip angle (Merkle and Dale 2006; Rohrer et al. 2005; Rathnayaka Mudiyanselage 2011).

2.5.7 MRI Artefacts

Artefacts can be defined as a region of the tissue being scanned that have signals that do not correspond to the actual tissue at the location. The first type of MRI artefacts are motion artefacts, which can occur as a result of breathing, blood flow in the vessels, respiration and heartbeat. Longer scanning times can cause random moving of the body's parts, such as muscle contraction, which is initiated from nerve excitation and can be seen in the final image stack. Therefore, motion artefacts can occur as a result of the miss-registration of pixels along the phase-encoding direction (Erasmus et al. 2004). Thus, the protocol used and the length of movement of the scanned structure can determine the nature and the extent of the artefacts.

Designing MRI protocols to synchronise data acquisition is the optimal solution to minimise these periodic movements (breathing, blood flow). However, using the same

technique could find it difficult to eliminate the motion artefacts that are generated from the body's movements.

The second type of artefacts are called magnetic susceptibility difference artefacts and are initiated when two adjacent tissues have different magnetic susceptibility properties, such as the cortical bone and tissue. Thus, when scanning a region with these two different anatomical types of tissues, a significant change in the local magnetic field will cause a noticeable signal loss (Rathnayaka Mudiyanselage 2011).

Consequently, in the present study, an MRI holder will be used to fix the subjects' movements during scanning.

2.5.8 Limitations of MRI

MRI is considered to be safe and healthy subjects can be scanned without being exposed to ionisation radiation. However, MRI has number of limitations.

The most important is the longer scanning time, which can cause motion artefacts. The second limitation is that the images of certain anatomical regions in the human body can appear with a poor contrast due to the presence of different soft tissue types, such as muscles, ligaments, joint capsules and cartilage. The third limitation concerns the non-uniformity of the external magnetic field (Figure 2-25). Thus, the signal of the MRI images tends to distort towards the ends of the magnetic field. Finally, the limited accessibility to MRI scanners due to their considerable cost and workload is problematic (Rathnayaka Mudiyanselage K 2011).

In the present study, these limitations can cause difficulties in recognising the tip of the transverse process of the lumbar vertebrae, the anterior-posterior surfaces of the articular facets and the articulated surfaces of the sacroiliac joint, also the differentiation between the anterior border of the disc and the surrounding muscular structures. Therefore, several landmarks will be obtained to measure the determined parameters.

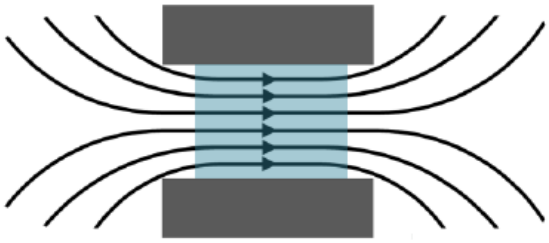

Figure 2-25: The non- uniformity of the magnetic field (the blue shaded region shows the uniform region) (after Rathnayaka Mudiyanselage 2011)

2.6 Summary

Statistical data indicates that the percentage of prevalence of spine-related pain is considered to be high and even up to 84%. Spinal manipulations are considered to be mechanical efforts in which the clinicians using shoulder and pelvis girdles of the individuals to exert a twisting force of specific magnitude in a controlled direction to target the spine.

Anatomically, there is very strong relationship between the human spine's flexibility and the action of both shoulder and pelvic girdles. For optimal upper extremity function to occur, it is very important to correctly position the scapula when carrying out various daily activities. Therefore, when the scapulae introduce a faulty position, shoulder joint injury can occur. The acromion process is projected from the most superior-lateral aspect of the scapula to form a functional roof over the head of the humerus.

The pelvis dynamically provides a bony connection between the vertebral column and the lower limbs. Before a clinician makes a diagnosis and carries out pain treatment for low back pain, the unique anatomical structure of the sacroiliac joint must be taken into account.

The sacroiliac joint can be described as an articulation between two auricular surfaces of the sacrum and ilium. The sacroiliac joint is positioned in the pelvic ring toward the side, which is under the maximum torsional stress to absorb the twisting forces that are initiated by lower limb movements into the sacroiliac joint ligaments.

Consequently, before treating the human spine disorders it is important to understand the anatomy and functions of its structures. The spine has three complex and fundamental biomechanical functions. First, it provides the mechanical linkage between the upper and lower extremities by transferring the weight, resulting in bending movements of the head and trunk, with any weights being lifted by the pelvic girdle. Second, it allows a mobile connection between these three different body parts. The third and most important function is that it protects the delicate spinal cord from potentially damaging forces produced by both physiological movements and trauma.

The functional spinal unit is composed of the vertebrae, which articulate with each other in a controlled manner via a complex of levers, pivots (facets and discs), passive restraints (ligaments) and activations (muscles).

The vertebral body is the anterior component of the vertebrae and its function is load bearing. The lumbar vertebral canal is formed by the alignment of the five lumbar vertebra.

The intervertebral disc composes the anterior articulation section between two vertebral bodies and constitutes 20-30% of the entire height of the vertebral column. In the company of the facet joints, it provides load pathways within a motion segment, while allowing movements of the spinal column. In addition, its principal responsibility is to react to all compression forces to which the spine is subjected.

The lumbar intervertebral foramen has a similar shape to an inverted teardrop and it constitutes a passageway that joins with the spinal canal. The intervertebral foramen (IVF) is bordered superiorly and inferiorly by the pedicles of the contiguous vertebrae: the postero-inferior margin of the superior vertebral body, the intervertebral disc, the postero-superior vertebral notch of the inferior vertebral body anteriorly, and the ligamentum flavum and superior and inferior articular facet posteriorly

The facet joints compose the posterior articulation between two articulated vertebrae and are located between the superior and inferior articulating processes. At each spinal segment, there is a pair of facet joints which are positioned on the posterior-lateral aspects of each motion segment and extend from the cervical to the lumbar spine. The complex mechanical performance of the facet joints is dependent on the responses imposed by the whole spine responses via its relationship to the intervertebral disc, its anatomical orientation and its own mechanical behaviour.

MRI is considered to be safe and healthy subjects can be scanned without being exposed to ionisation radiation. However, MRI has number of limitations. The most important is the longer scanning time, which can cause motion artefacts. The second limitation is that the images of certain anatomical regions in the human body can appear with a poor contrast due to the presence of different soft tissue types, such as muscles, ligaments, joint capsules and cartilage.

Chapter 3

Literature Review

3.1 Introduction

This chapter will describe the biomechanics of the spinal manipulation technique, the biomechanics of the shoulder and sacroiliac joint and the lumbar spine structures during different trunk activities, particularly during rotational positions. Consequently, a wide range of studies have been reviewed.

3.2 The Biomechanics of Spinal Manipulation

Spinal manipulation requires the action of an externally applied force upon one or both vertebrae of a chosen spinal motion segment. The biomechanics of spinal manipulation can be divided into external and associated internal forces. External forces are represented by chiropractors which vary dramatically between clinicians and depending on the location of treatment application. Meanwhile, the internal forces that are produced by the spinal manipulation are the stresses and strains forces. However these internal forces are strongly involved with short-lever (high-velocity) spinal adjustment (Herzog 2010; Shekelle et al. 2019).

During spinal manipulation, only the most posterior features of the vertebrae are close to the skin's surface. In this condition, the forces applied at the skin's surface at the target spinal region must pass through substantial superficial tissue. In lumbar spine manipulation, to create rotational torque, the majority of force has to be applied indirectly to the vertebrae, via the remote body segments such as the pelvis and thigh. This means that any direct spinal manipulation technique requires that the patient be orientated in such a way that force is applied perpendicular to the overlying skin surface to act upon the vertebrae beneath. The body weight of the clinician should be used during the manipulation technique and the patient must be orientated in such a way that the point of contact at the skin surface is horizontal and that the clinicians centre of mass is aligned directly above (Evans 2010) (Figure 3-1)

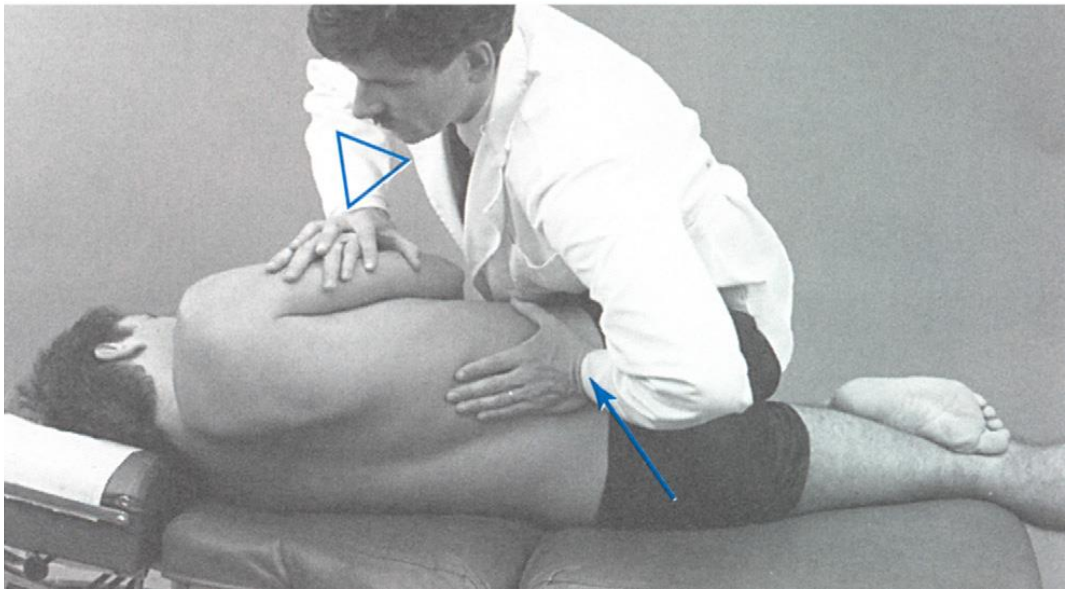

Figure 3-1: Side- posture rotational lumbar manipulation (after Evans 2010).

Therefore, it seems that the lumbar spine manipulation depends on creating a passive rotational torque of the spine by applying two opposing externally forces on the shoulder and pelvic girdles. This passively rotated position can relive low back pain by reducing disc bulging, freeing adhesions around the prolapsed disc or facet joint (Shekelle et al. 2019; Koes 1996). Conversely, lumbar spine manipulation can lead to serious complications of the involved spinal segments such as disc herniation, mechanical changes of the intervertebral foramen and quada equine syndrome (Assendelft et al. 1996; Pickar 2002; Ernst and Assendelft 1998).

Consequently, the relationship between the upper and lower body should be considered to obtain optimal functional performance of the spine, given that the range of motion of the shoulder and pelvis are crucial factors to continue a flexible dynamic trunk motion.

Meanwhile, a better understanding of the biomechanical behaviour of the lumbar spine during different lower trunk rotational positions of healthy subjects will provide valuable translational information for guiding therapies in the future.

The current study introduces a hypothesis that rotating the spines of healthy subjects with three rotational positions (R1, R2, and R3) with mean pelvic angles of 90^{o}, 68.6^{o} and 43^{o} will help us to understand the effect of each rotational position of the spinal manipulation on the lumbar spine structures, and the shoulder and pelvic girdles.

3.3 Controlling the rotational angle of the lower trunk depending on the relation between the shoulder and pelvic girdles and the last lumbar vertebrae

It has been suggested that the coordination patterns between the upper and lower body should be considered in order to obtain optimal functional performance, as the range of motion of the shoulder and pelvis are crucial factors to continue a flexible dynamic trunk motion.

(Gracovetsky and Farfan 1986; LaFiandra et al. 2002; Montgomery 2008; Park et al. 2012) introduced a pattern of lumbar spine motion as a result of muscular actions during gait analysis. Although these studies concerned the analysis of gait, their results indicated that the amount of axial torque could occur when the lumbar spine exhibited a coupling phenomenon. Moreover, the amount of torque can be increased if the facet orientation is directed in a proper manner. In this phenomenon, the spine bends laterally and forward as a result of the clockwise torque. As a consequence, the lumbar lordotic curve will decrease. Therefore, the fifth lumbar spine with the pelvis and lower trunk will rotate in a clockwise direction, while the upper trunk and shoulders rotate in an anti-clockwise direction. In this literature, the role of the scapula, L5, posterior superior iliac spines and the sacroiliac joints rotational angle has been taken into account in response to the lower trunk rotation in healthy subjects.

3.3.1 The Role of the Scapula in Lower Trunk Rotation

The scapula is considered to be the connecting platform to control and distribute the largest per cent of kinetic energy and force from the trunk and lower extremities to the upper extremities. This complicated role of the scapula into the shoulder actions can be offered as an important reason for therapists to take into account the pattern of motion and position of the scapula in terms of shoulder injuries (Forthomme et al. 2008).

Several techniques for evaluating scapular positioning are described in this scientific literature. Some of these studies measured the static scapular positioning as the distance between the posterior border of the acromion and the examined table by using callipers, an inclinometer tape measure and an infrared motion capture system (Nijs et al. 2007; Hoard et al. 2013; Struyf et al. 2014).

In contrast, (Karduna et al. 2000) used Euler angle sequences method by placing three receivers on the thorax at the level of T3, humerus and scapula during sitting position. (Weiser et al. 1999) mounted five fresh-frozen cadaveric gleno-humeral joints on a custom translation device in order to evaluate the effect of simulated scapular protraction on anterior glenohumeral translation. (Lewis et al. 2002)used the skin surface palpitation technique to determine six points on the scapular spine, the acromion and the inferior angle of the scapula using red-topped metal pin markers. Other researchers have measured the scapular positioning at different degrees of shoulder movement using various methods, such as attaching a transmitter to the sternum, acromion and humerus and the middle aspect of the clavicle bone (Nagai et al. 2013) or using 3D measuring methods with a magnetic tracking device and radiographic protocol or using only an ejector magnetic tracking (Karduna et al. 2000; Berthonnaud et al. 2005; Myers et al. 2005; Borich et al. 2006; Scibek and Carcia 2014). (Von Eisenhart-Rothe et al. 2002) used an open magnetic imaging and 3D post-processing technique to assess shoulder instability in non-traumatic and traumatic subjects.

However, the only variable method for the current study involved using a tape measure, as it was only capable of measuring the scapula kinematics during the lower trunk rotation using the technique of (Nijs et al. 2007). To evaluate the hypothesis that there will be significant difference between the position of the right and left scapula during lower trunk rotation, the distances between the posterior borders of the acromion processes and the shoulder board of the MRI holder will be measured using a tape measure during three actively lower trunk rotational positions.

3.3.2 Measuring and controlling the pelvic rotational angle

The rotational angle of the trunk during different positions is affected by pelvis position. Two studies used different techniques and devices to control the trunk rotation of subjects as reproducibly as possible depending on controlling the pelvis rotational angle. (Rogers et al. 2002)used a rotating table in which the patient was positioned with the head and thorax on the longer part of the table, while the hip was placed on the shorter part of the table. (Fujii et al. 2007)used a different technique depending on a rotating device consisting of many angled pelvic holders (15°, 30°, 45° and maximum). However, these techniques were valid to produce only 8° of passively trunk rotation in

the case of techniques introduced by (Rogers et al. 2002), while the (Fujii et al. 2007) technique was designed to rotate the subjects' trunks passively.

On the other hand, (Sprigle et al. 2003; Prushansky et al. 2008; Preece et al. 2008) used goniometers, digital inclinometer and palmeters to measure pelvic tilt by determining both anterior superior iliac spine and posterior superior iliac spine positions. (Alsancak et al. 1998)used a plurimeter and callipers to determine the pelvic tilt on the horizontal and sagittal plane by placing the callipers on a line drawn which joined the right and left posterior superior iliac spines. However, these devices could not be used in supine and rotation positions.

As the current study will be based on the three actively lower trunk rotational positions with accurately controlled angle of rotation of each lower trunk rotational position, the current study will use a novel lower trunk holder (MRI holder) and a modified goniometer. A modified goniometer and a novel lower trunk holder (MRI holder) will be used to obtain and maintain the accurate measurements of the lower trunk rotational angle depending on controlling and measuring the pelvis angle of rotation. In such way that the modified goniometer will be used to measure the rotational angle of the right and left posterior superior iliac spines while the novel lower trunk holder will be used to fix the pelvic to maintain the performed active angle of rotation. In addition the novel lower trunk holder (MRI holder) will be used to prevent the motion artifacts during long MRI scan as a result of fixing the subjects pelvic during MRI.

To evaluate the hypothesis that the pelvis angle of rotation depending on measuring the rotational angle of the right and left posterior superior iliac spine relative to the horizon will be accurately controlled by using a reliable an adaptive goniometer and MRI holder, the measurements of the angle of rotation of the right and left posterior superior iliac spines relative to the horizon by using the adaptive goniometer will be compared to those will obtain by using MRI at three sections of the ilium (3.4.2).

3.3.3 The relation between the right and left posterior superior iliac spines and the last lumbar vertebrae during trunk rotation

The position of the spine, pelvis, and hip balances the mass of the trunk above it, and the mobility of these articulations allows for coordinated motion during activities such as moving from standing to sitting or bending forward at the waist.

The functional linkage between pelvis and spine has been translated by many researchers. Some of those researchers defined this linkage as pelvic incidence which represents the sum of two positional parameters, sacral slope and pelvic tilt. In this definition, the pelvic incidence is tightly correlated with the degree of lumbar lordosis (Tardieu et al. 2017; Ike et al. 2018).

The pelvic incidence was defined as an angle formed by a line from femoral head to the centre of the S1 end plate and a line tangent to the S1 end plate. In turn, sacral slope defined as the angle between the horizontal and the sacral plate. While, pelvic tilt angle was drawn by the angle between the vertical and the line through the midpoint of the sacral plate to femoral heads axis (Lavignolle et al. 1983).

Other researchers showed that lumbo-sacro-pelvic structure plays an important role in determining the shear and compressive forces applied on the anterior (vertebral body and intervertebral discs) and posterior (facet joints) elements of the lumbar vertebral column. Those researchers analysed the relation between the lumbar, sacral and pelvic structures as the sacral angle and sacral curvature. The sacral angle was defined as a straight line along the superior margin of the sacrum, drawn to meet the horizontal line. While sacral curvature represented by the angle between the first and the last sacral vertebrae (Ghasemi et al. 2016).

On the other hand, as mentioned in 3.4, (Gracovetsky and Farfan 1986; LaFiandra et al. 2002; Montgomery 2008; Park et al. 2012) stated that the fifth lumbar vertebrae with the pelvis and lower trunk will rotate in a clockwise direction, while the upper trunk and shoulders rotate in an anti-clockwise direction when the spine bends laterally and forward when clockwise torque is applied. However, it seems that these studies did not take into account the difference in the rotational degree between the pelvis and the fifth lumbar vertebrae. Based on the previously mentioned studies, the current study will introduce a new definition of the relation between the spine and the pelvic as the relation between the rotational angle of the last lumbar vertebra (L5) and the rotational angle of the posterior superior iliac spines in three anatomical sections related to the horizon during lower trunk rotational positions.

To investigate the hypothesis that there will be a significant difference between the rotational angle of the left and right posterior superior iliac spines and the rotational angle of the last lumbar spine during all performed lower trunk rotational positions, the

rotational angle of the left and right posterior superior iliac spines in three sections relative to the horizontal plane will be measured using a new technique by determining the lowest attached points of the erector spinae muscle tendons to the posterior superior iliac spines depending on using the pixel intensity values between 091-094 per cent. While the rotational angle of the last lumbar vertebrae (L5) will be measured at the convex posterior disc margins relative to the horizontal plane.

The coordination between the trunk, the shoulder and pelvis movements are very important in understanding rehabilitation strategies for lower back pain. Nonetheless, no study has yet examined the position of the scapula (as the position of bilateral posterior borders of the acromion processes) and the motions of the posterior superior iliac spines related to the L5 angular motion during different rotational positions of the lower trunk.

3.3.4 The relation between the right and left sacroiliac joints during lower trunk rotation

The relation between low back pain and sacroiliac dysfunction has been mentioned for many decades by researchers. It has been reported that the pain related to the sacroiliac joint can cause more than 20% of the lower trunk pain. This indicates that the sacroiliac joint movement is an area of significant clinical importance (Cramer and Darby 2005).

The sacroiliac joint has been reported as having a three-dimensional rotating and translating motions along three axes with a central point that lies between the right and left posterior superior iliac spines. The transverse axis accounts for sacral rotation in the sagittal plane. In this movement, the transverse axis passes through the posterior superior iliac spine. In turn, the longitudinal axis accounts for the sacral rotation in the transverse plane. For sacral rotation to occur in the coronal plane, the sagittal axis passes antero-posterior midway between two points represented by the right and left anterior superior iliac spines (Goode et al. 2008).

The translational and rotational motions of the sacroiliac joint have been reported to be varied in values between investigators according to the different used methods.

In order to calculate three-dimensional sacroiliac joint rotational and translational motions, (Frigerio et al. 1974; Jacob and Kissling 1995; Egund et al. 1978;Sturesson et al. 1999; Sturesson et al. 2000) all used the Roentgen Stero-Photogrammetric analysis.

The findings of these studies reported that the sacro-iliac joint has a small amount of movement (2°). Despite these studies determined several points on the superior, medial and inferior parts of the ilium. In addition, they used markers on the left and right ilium and sacrum during different positions of the trunk, these studies did not achieve a high precise measurements.

Similar findings have been concluded by (Smidt et al. 1995; Adhia et al. 2016)who used a high accuracy method (3-D digitizing technique). These studies offered the lowest levels of error in the measurement.

The sacroiliac joint motion was measured by many researchers using different techniques, (Smidt et al. 1997) evaluated the degree of sacroiliac joint motion during full flexion and extension of the hip joint using the long levers of the cadavers' lower limbs in order to load maximum stress to the sacroiliac joint. Despite the fact that this study proved that the extreme hip positions can cause the sacroiliac joint to move with an average range between 3° to 17°, the use of un-embalmed cadaver and long lever torque to incorporate movements might have caused a decrease in the active pelvic stabilities.

(Barakatt et al. 1996) reported similar observations of the sacroiliac joint motion with about 22 to 36° degrees in young gymnasts and non-gymnasts during standing, modified standing, modified sitting and half kneeling positions. This study obtained the measurement of the oblique sagittal and transverse angle of the inclination of the right and left innominate from the method used by (Smidt et al. 1995) depending on the position of two lines relative to the sagittal and horizontal plans and on different postures. The first line was connecting the right posterior superior iliac spine and right anterior superior iliac spine. While the second line connected the left posterior superior iliac spine and left anterior superior iliac spine. In this study, the reported higher values of motion of the sacroiliac joint than other studies previously carried out could be related to the subjects' half-knee position during measurements. In addition, the degree of pelvic motion was not accurately obtained because the lower back and hip were not adequately controlled.

While, (Adhia et al. 2016) used a technique introduced by (Smidt et al. 1995) for defining a plane through the right and left posterior superior iliac spines and the anterior superior iliac spines to show the innominate rotation about Y-axis and to calculate the

transverse plane innominate angles from the respective posterior superior iliac spine and the innominate vector using a particular formula.

(Frigerio et al. 1974)used an equation and a purely mathematical analysis to express the differences in the rotational and translational angles of the innominate according to different body positions. In contrast, (Jacob et al. 1995)used a calibration method depending on a helical axis of motion, which consisted of two vertical panels together with a horizontal one. Which represented the zx, yz, and xy planes of a Cartesian coordinate system.

(Saunders 2013) used CT scans to measure the inclination angles of the ilium relative to the sacrum by placing three lines: the first line was placed down the medial surface of the ilium (along the ligamentous component)while the second line was positioned along the lateral surface of the sacrum(the synovial component). The reference line placed along the lowest points in the dorsal sacral lamina. Although this study was consistent with previous studies relating to the minute amount of the inclination of the sacroiliac joint, it might be considered more reliable for the measurements of the sacro-iliac joint motion of animals.

On the other hand, (Wilder et al. 1980; Ehara et al. 1988) introduced another type of sacro-iliac joint motion, which can be interpreted as a rotatory movement along an axis that passes longitudinally through the iliac ridge of the sacroiliac joint. The results of these studies indicated that although the iliac ridge may move the only 2 mm, the distance between the two antero- superior iliac spines increases or decreases by as much as l0 mm.

To date, no previous study has clarified in vivo kinematic changes in the sacroiliac joint at three anatomical sections of the sacrum and ilium with respect to three lower trunk rotation positions. This approach will explain how each section of the right and left ilium moves relative to the other sections and relative to the sacrum and vice versa during each lower trunk rotational position.

To investigate the hypothesis that the first lower trunk rotation (mean pelvis angle 900) will cause the significant and maximum mean differences between the rotational angles of the selected sections of the sacrum, as well as, between the rotational angles of the selected sections of ilium, three consecutive slices or sections of the sacrum and ilium

will be used to quantify the rotational angle of each section relative to the horizon depending on using un sharp mask filter and by localizing specific points on the wedges of the right and left sacrum and by determination superior and inferior points on the surface of the ilium.

3.4 Biomechanics of the Rotation of the Lumbar Spine

Vertebral segments of the human spine are known to function synergistically to maintain the stability of the human body. Altered vertebral motion has been widely assumed to be a biomechanical factor causing spinal pathology (Shin et al. 2013). Consequently, numerous studies have been conducted to understand spinal biomechanics depending on applying different body positions and methods(Wong et al. 2017; Mawston and Boocock 2012; Dolan et al. 1994; McGill 1997; Videman and Nurminen 2004; Stokes and Iatridis 2004).

3.4.1 The Biomechanics of the Rotation of the Lumbar Vertebrae

In defining rotation, the anterior surface of the vertebral body is used rather than the elements of the posterior arch. For example, when T3 rotates to the right in relation to T4, its anterior surface turns to the right and the spinous process deviates to the left. The anatomical planes of movement are divided into the sagittal, coronal and horizontal planes. When considering the rotation of the bone in three dimensions, all the points throughout the bone can be grouped into individual planes that lie parallel to the direction of motion. In each plane, the points move around a centre situated in that plane. Whenever all the centres of all the planes are lined up, they result in a straight line that forms what is known as the axis of rotation of the bone. The location of the axis of rotation is not an intrinsic characteristic of the bone that moves about it but it is a property of the forces act on the bone. Therefore, different forces will generate different axes of rotation. Backwards or forward rotations are defined as movements within the sagittal plane, while side bending is considered as rotation in the coronal plane, and twisting is defined as rotation in the horizontal plane. A sideways gliding movement over the horizontal plane would be considered as a horizontal translation, while movements up or down are described as coronal translation (Figure 3-2).

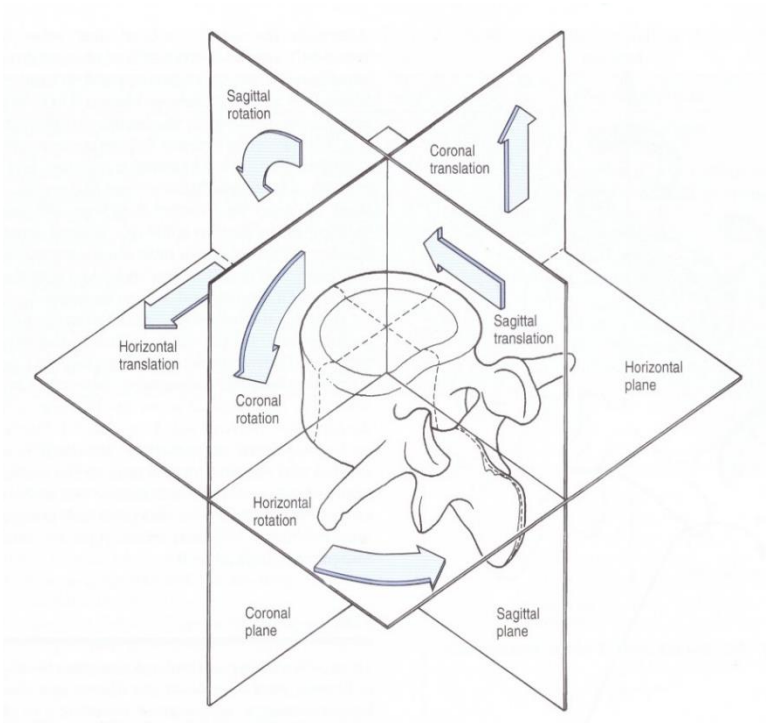

Figure 3-2: Anatomical system (planes and directions of motion) (after Bogduk 2005)

The vertebral motion can be described as a rotation around an axis and translates along an axis with the body movements within one of the cardinal planes. The ability to rotate around an axis and translate along an axis results in six degrees of freedom for each vertebra. Therefore, vertebral motion can be defined as having an overturning movement (rotation around an axis and/or translation along an axis).

Translation happens when a single net force acts on a bone and results in all points in this bone to move in parallel, in the same direction, and to the same extent. In this condition the force that tends to result in translation is known as shear force (Figure 3-3).

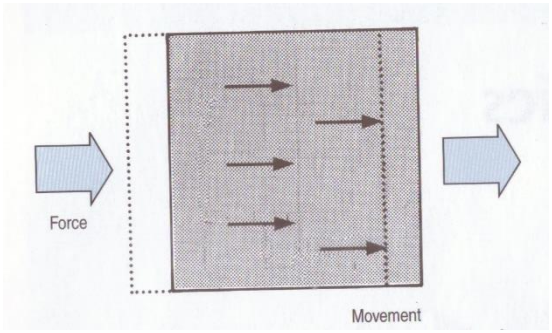

Figure 3-3: Translation motion (after Bogduk 2005)

In contrast, when all the points on a bone moving in parallel and around a curved path which is centred on some fixed point, rotation will be generated . In this condition, these points move in the same direction, but to various extents, depending on their radial distance from the fixed point (the centre of rotation) (Figure 3-4). In other words, during rotation, the points in any plane of a body move around a centre located in that plane. The axis of rotation is a line formed by these centres. Therefore, rotation around the y-axis with the translatory movement can be described as a vertebral rotation, depending on the vertebral segment involved.

Rotation in the spine happens when two unaligned forces act in opposite directions on various parts of the bones, forming what is called a force couple. The net force that results in the rotation is referred to as the torque. Torque can occur under many circumstances, such as two opposing forces, the effect of muscular actions and ligamentous resistance, or it may be the result of gravity action being opposed by either muscular action or ligamentous resistance.

In contrast, the rotation is always a component of side bending (coupled motion), with the exception of the atlanto-axial joint. Coupled motion is defined as the rotation or translation of a vertebral body about or along one axis that is consistently associated with rotation or translation about a second axis.

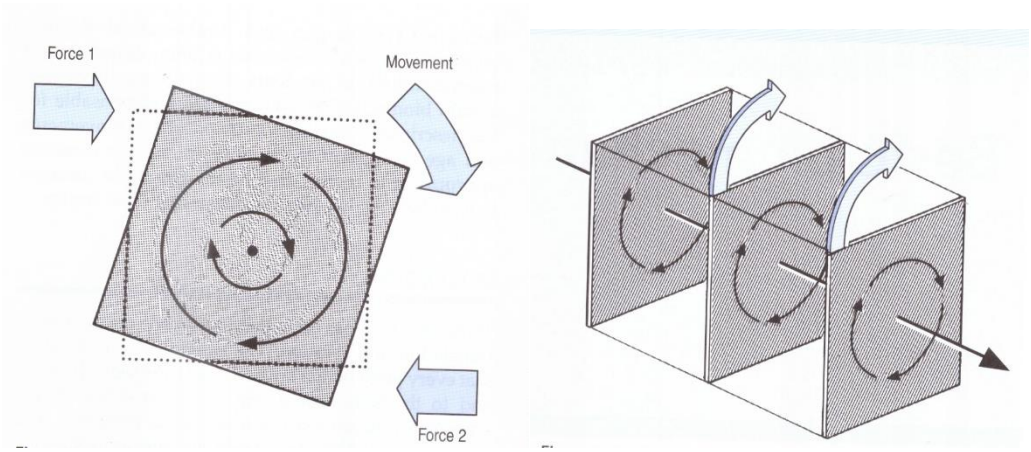

Figure 3-4: Rotation definition (after Bogduk 2005)

Coupling of the spinal motion is derived from the kinematics of the individual vertebrae, the anterior-posterior curvature and the connecting ligaments of the spine (Bogduk

2005; DeStefano 2017). The direction of the coupled rotation in the various areas of a side bent spine is still controversial. Therefore an understanding of the vertebral anatomy and spine biomechanics is crucial in understanding coupling mechanics and vertebral dysfunction.

Several scholars have attempted to measure the axial rotations of the lumbar vertebrae. Early studies measured the vertebral rotation depending on the pedicle position by using radiographic methods (Nash and Moe 1969; Weiss 1995). Despite the fact that these methods are considered to be the most used by many clinicians, they are not accurate enough to determine the precise angle of rotation. In contrast, the Cobb method measures the angle of rotation by determining the spinous process of the vertebra. However, this method may be inappropriate for defining the spinous process on real X-ray film (Cerny et al. 2014). In this study, Cerny et al. (2014)used an antero-posterior projection of a conventional X-ray based on the geometric shape of the vertebrae and their dimensional characterisation (vertebral body width and height). The angle of rotation was measured by comparing the locations of the pedicle shadows and vertebral body using a pencil, ruler and protractor. However, the authors stated that this method was applicable for values of rotation up to 30°.

Based on the comparison between the results of the angle of rotation obtained by CT images and that collected from X-ray film, (Chi et al. 2006) presented a new method to measure the angle of rotation by recognising the projection of a vertebral body and pedicle in a transverse plane. This method has a limitation in terms of defining the concave pedicle shadow when the rotation exceeds 35^0.

Axial rotation has been determined as the angle between the line joining the most posterior points of two pedicles and the vertical plane or as the angle between the vertical plane and junction point of the inner surface of the right and left laminae. Meanwhile, other researchers have calculated the angle of vertebral rotation as the angle between a straight line through the posterior central aspect of the vertebral foramen and the middle of the vertebral body and the sagittal plane (Aaro and Dahlborn 1981; Ho et al. 1993; (Krismer et al. 1996; Göçen et al. 1999). Furthermore, (Drerup 1985) developed a method by selecting vertebral module parameters depending on the position of the pedicles in relation to the vertebral body.

However, these methods of measurements used computed tomography, which can expose the patient to radiation and requires many landmarks to be recognised.

(Suzuki et al. 1989) used ultrasound to measure the angle of rotation by outlining the laminae and the spinous process of the vertebra. In this method of measurement, the transverse processes and the lamina are displayed on screen and transducer is inclined until the image of the lamina becomes horizontal on the screen, the inclination of the transducer is then the rotation of the lamina. Although this method proved to be safe and easy to follow up for the prognosis of patients with idiopathic scoliosis, this method can only be used in the prone position and it cannot be used to evaluate the angle of rotation during spine position.

The assessment of rotation of the lumbar spinal segments using MRI is a safe method of measurement. For example, (Birchall et al. 1997) measured the vertebral rotation at the endplates level in idiopathic scoliosis subjects using a T2-weighted sagittal MRI of the thoracic spine depending on selection of three datum points , the first is located at the junction of the inner surfaces of the two laminas. The other two points are located on each inner surface of the lamina as a close as possible to the pedicle. In this method, the degree of axial rotation is calculated by drawing a line bisecting this angle and comparing it with a vertical line drawn perpendicular to the scanner table. The accuracy of this method depends on a reference to a neutrally rotated vertebra. In addition, this study did not take into account the muscle tendons and ligamentum flavum attachments when obtaining the localisation of the three datum points. (Haughton et al. 2002) developed a radiographic technique to measure axial rotation based on the measurement of rotation from axial MRI images using an automated programme to choose the midline on the dorsal aspect of the vertebral body and then using a pixel shift program. However, this method needs the vertical reference line to be set in the thorax region.

(Chung et al. 2000)calculated the angle of vertebral rotation as the angle between the horizon and a line connecting both convex posterior margins of the intervertebral level. However, the application of this method with a maximum lower trunk rotation is limited because the convex margin of the disc cannot be defined as an obvious landmark.

(Janssen et al. 2010)studied the standing upright and supine rotational positions in comparison to the quadrupedal position in healthy subjects using MRI. The vertebral

rotation was determined as the angle between two axes: the first axis was the longitudinal axis of the vertebra and the second axis was the mid-sagittal axis of the trunk. In this technique, the first axis was defined as the line that connects between the line passing through the centre of the spinal canal and the determined centre of the anterior part of the vertebral body, while the line that connects the centre of the spinal canal and the centre of the sternum at the T8 level was called the mid sagittal axis. The authors in this study used anatomical landmarks that were present in the thoracic region.

Each vertebra has its unique relative motion as responding to the whole spine rotation. Measuring the lumbar range of motion (relative motion) is typically performed using sensors, markers, a three-dimensional radiographic technique, voxel-based registration method using MRI, and stereo photogrammetry (Alqhtani et al. 2016; Pearcy and Tibrewal 1984; Panjabi et al. 1994; Fujii et al. 2007).

Some of these methods are limited because they expose the subjects to ionisation radiation. Meanwhile, others used in vitro landmarks, which provided an estimate of lumbar range of motion. The limitation of applying the voxel-based registration method to measure the relative vertebral motion is that the degree of trunk rotation was measured on the absolute spatial coordinate system using volume registration of the sacrum.

Determination of rotational angle of the lumbar vertebrae using MRI is difficult because the same landmarks of the right and left vertebra parameters cannot be observed on the same axial MRI images. In addition, the muscle tendons and ligamentum flavum attachments at both sides prevent the precise localisation of the tip of the transverse and spinous processes and pedicle points. Consequently, the present study used a synchronisation technique and depended on the adjustment of histogram intensity values to determine the same landmarks on each selected cut of the MRI.

This new measurement method of measurements is simple, safe (e.g. did not expose the subjects to ionising radiation) and accurate enough to determine the anatomical landmarks of both sides of each individual vertebra which tend to appear separately in each slice of MRI as a result of the rotation.

The present study will measure the degree of vertebral rotation ,the rotational torque between L3 and L5vertebral levels and the range of vertebral motion(relative

motion)during neutral position (N) and three actively lower trunk rotational positions (R1, R2, and R3) at two levels of each lumbar vertebra by using three-dimensional T2 MRI images to evaluate the hypothesis that the first lower trunk rotational position (mean pelvic angle 90^0) will result in the maximum rotational torque between L3 and L5 vertebral levels, higher relative motion at each lower lumbar segment and maximum mean difference in the spinal canal depth.

3.4.2 Biomechanics of the Spinal Cord During trunk movements and According to the Central Spinal Canal Diameter and the Dural Sac Position

Many studies have reported the biomechanical behaviours of the spinal cord and the cauda quina under applied stress, and also the change in spinal canal size according to the different positions of the lumbar spine. For example, (White and Panjabi 1990), found that during flexion, the spinal cord first unfolds, with minimum increase in its tension, followed by some elastic deformity near the full flexion of spine. Meanwhile, during extension, the spinal cord first folds with a minimum decrease in tension, followed by some elastic compression. Hypertrophy of ligamentum flavum, disc bulge and osteophyte cause abnormal internal spinal cord stress. In this condition, two forces—compression, and tension and moment bending—act on the spinal cord as a result of the applied load. The compression forces result in compress stress that decreases in magnitude away from the point of the impingement cord, in addition to the shear stress that has maximum values in the middle of the cord. The resulting stresses are all tensile and are uniformly distributed across the cross-section of the cord. The bending moment results in tensile stresses on the convex and compressive stress on the concave side of the bent spinal cord. The magnitude of these stresses is highest on the surfaces and decreases to zero in the middle.

(Inufusa et al. 1996) reported that flexion, extension and lateral bending cause alterations in the length of the spinal canal. In addition, the cross-sectional area experiences change with the physiological flexion and extension as a consequence of tissue bulge (disc and ligamentum flavum). Accordingly, the mid-sagittal diameter of the spinal canal is reduced by 2mm. A significant decrease of the central canal area and

subarticular diameter can be seen when the lumbar spine moves from flexion to extension.

(Chung et al. 2000) measured the possible mechanism of the changing posture on the morphological behaviour of the spinal canal and dural sac during neutral, flexed, extended and rotation positions. They concluded that during extension or rotation, the spinal canal size decreased as a result of the increasing thickness of the ligamentum flavum. The posterior margin of the intervertebral disc, approximated to the facet joint, shows no change in the shape and size of the disc. This may explain the posture-dependent symptom of spinal stenosis. In addition, this study demonstrates that the anatomical relationship of the ligamentum flavum, intervertebral disc and spinal canal might be changed significantly during rotational and flexion-extension movements of the spine in a living subject.

The same observation was reported by (Alyas et al. 2008) who showed that the inward plugin of the ligamentum flavum and posterior disc plugin in the extension lead to a narrowing of the central canal by reducing the anterior posterior diameter of the canal. This study reported that weight and muscle activation causes a reduction in the disc height, which starts as a small increase in the anterior disc height and a reduction in the posterior disc height in the upright position. This results in the decrease in the size of the canal. In contrast, (Schmid et al. 1999) reported that the minor disc bulges during extension , which may decrease the cross-sectional area of the spinal canal significantly. This conclusion stems from the fact that the large proportion of the spinal canal border is formed by the disc. (Weishaupt et al. 2000) demonstrated that there were significant changes in the cross-sectional areas of the dural sac as a result of the supine and seated extension positions. (Tunset et al. 2013) indicated that the dural sac size and the intervertebral disc have a direct anatomical and mechanical relationship. In particular, a lumber disc herniation will cause the disc to take space in the spinal canal.

(Willén et al. 1997) reported that the changing of posture from supine to standing results in a considerable narrowing of the spinal canal in patients with sciatica or neurogenic claudication. This study pointed out that the cross-sectional area of the dural sac decreases in at least one site during axial compression in slight extension and increases in forwarding flexion because extension causes a compression of the nerve roots, while flexion reduces the constriction and root compression. The authors of this study stated that the most significant factor affecting the dimensions of the canal was the disc axial

compression. These results conducted that the constriction of the cauda equina to a size less than 75mm2 at L3-L4 will affect the normal function of the nerve roots.

(Saifuddin et al. 2003) indicated that the reductions in the sagittal dimensions of the spinal canal and dural sac cross-sectional area in healthy subjects imaged in supine positions with extension and rotation increased the thickness of the ligamentum flavum. Meanwhile, imaging in the erect extended position reduced the central canal dimensions, particularly at the degenerate disc level. This study demonstrated that axial loading with extension in supine position causes a decrease in the dural sac section area, which is most commonly seen at L4-L5. (Cuchanski et al. 2011) found that the occlusion per cent of the spinal canal is dependent on the amount and direction of the dynamic applied load on the intervertebral disc.

Therefore, the central canal's parameters, such as the cross-section area and diameter, are very important factors to permit the normal functions of the canal contents (spinal cord, cauda equine, meninges and vessels) and any decrease in the normal canal size might cause lower back pain (Tacar et al. 2003; Lim et al. 2017; Abbas et al. 2010; Ahmad et al. 2011; Marawar et al. 2016).

The proposed normal values of the cross-sectional area of the central spinal canal at the lumbar region are more than 146.5 mm^2 and less than 215 mm^2 (Gouzien et al. 1990; Inufusa et al. 1996; Ahmad et al. 2011; Miao et al. 2013).

In contrast, a midsagittal diameter that is less than 12 mm reflects a pathological condition. The normal values of the transverse and the antero- posterior diameters of the spinal canal (from L1 to S1 levels) range between 22.4 mm and 33.2 mm and 13 mm and 25 mm, respectively (Tacar et al. 2003; Ahmad et al. 2011).

Several anatomical studies have emphasised the measurements of the mid sagittal diameter and the depth of the spinal canal as a line connecting two points: the posterior border of the mid-disc and the point where the margins of the laminae intersect at the midline of the spinous process (Inufusa et al. 1996; Chung et al. 2000; Cuchanski et al. 2011; Ahmad et al. 2011; Griffith et al. 2016; Amadou et al. 2017). Others have determined the antero-posterior diameter of the spinal canal on the mid portion of the vertebral body or in a plane perpendicular to the longitudinal axis of the spine and at pedicle levels (multi- planar reconstruction on viewing mode) (Gouzien et al. 1990; Kim et al. 2013; Monier et al. 2017). (Yuan et al. 2016) used a system of five grades to

evaluate the anteroposterior diameter of the spinal canal to investigate lumbar central canal stenosis. In contrast, the transverse diameter of the central canal has been calculated by (Tacar et al. 2003)as the minimum distance between the medial surfaces of the pedicles.

Previous studies have analysed the close relationship between the dural sac cross-sectional area inside the spinal canal and the lower back pain (Ogikubo et al. 2007; Iwahashi et al. 2016; Lim et al. 2017). In addition, (Inufusa et al. 1996) proposed that the cross-sectional area of the dural sac can be considered as an indicator for lumbar central spinal canal stenosis.

The critical size of the cross-sectional area of the dural sac has been a topic of debate for many researchers. Early research proposed that the minimum values of the cross-sectional area of the dural sac ranged from 87-100 mm2 (Gouzien et al. 1990; Inufusa et al. 1996) proposed that the minimum values of the cross-sectional area of the dural sac ranged from 87-100 mm^2. However, more recent studies have stated that values of less than 70 mm2 indicate critical stenosis (Marawar et al. 2016).

Several methods have been used to measure the dural sac diameter. For example, (Knirsch et al. 2005) measured the dural sac diameter as the longest distance between the posterior border of the vertebral body and the anterior border of the spinous process. (Amadou et al. 2017) measured the antero-posterior and the transverse diameters of the dural sac as the distance between the anterior border and the posterior border and the distance between the right and the left border of the dural sac, respectively.

Several methods have been conducted to evaluate the spinal canal size and the dural sac area according to age changes, different populations and in different states of loading and postures in normal or pathological spine conditions based on cadaveric samples, CT, MR, semi-automated computerised methods, Vernier callipers and measuring scales (Gouzien et al. 1990; Inufusa et al. 1996; Chung et al. 2000; Saifuddin et al. 2003; Tacar et al. 2003; Knirsch et al. 2005; Hughes et al. 2015; Hansson et al. 2009; Ahmad et al. 2011; Kim et al. 2013; Yuan et al. 2016; Monier et al. 2017; Marawar et al. 2016; Kanno et al. 2016; Iwahashi et al. 2016; Griffith et al. 2016; Amadou et al. 2017).

These approaches have found only limited application in physiological loaded and unloaded flexion and extension in unhealthy subjects. For example, they provided little information about the effect of different rotational positions on the spinal canal depth or the dural sac position. Only one study has shown the effect of a minimum degree of rotation on the morphology of the spinal canal when the shoulder motion was restricted.

In the present study, the difference in the spinal canal depth was calculated between two slices of MRI of individual lumbar vertebrae and according to different voluntary rotational positions (R1, R2, and R3) to evaluate the hypothesis that the maximum mean difference in the spinal canal depth at L3, L4 and L5 lumbar segments will result in the first lower trunk rotation position with mean pelvis angle (90°). These two slices of MRI represented the most left and right sides of the spinal canal. This new approach offers the promise of leading to quantify the amount of compression of the dural sac at two depths of the spinal canal and according to each rotational position of the spine by calculating the length of the line that connects the end of the dural sac at the first cut of MRI which showed the obvious left transverse process, and the end of the dural sac at the second cut of MRI, which showed the obvious right transverse process.

3.4.3 Biomechanics of the Lumbar Intervertebral Disc during Different Trunk Activities

When a load is applied to a physical structure, it causes either a longitudinal strain (change in unit length) or angular stress deformation (internal force per unit area). The ratio of the change in stress to the change in the strain in the direction of the load identifies the elastic modulus of the structure (Young's modulus) (Figure 3-5). If a material has large elastic modules, it requires greater stress to produce a given strain than material with a small one. Normal and shear stresses can be produced from the applied load. Tension and compression are examples of normal stress and both are collinear forces, but these forces act in different positions: the former tends to separate, while the latter has a tendency to push together. The directly applied load produces either compression or tension stress, while indirectly applied force at an angle to the axis of the structure causes bending or torsion stresses.

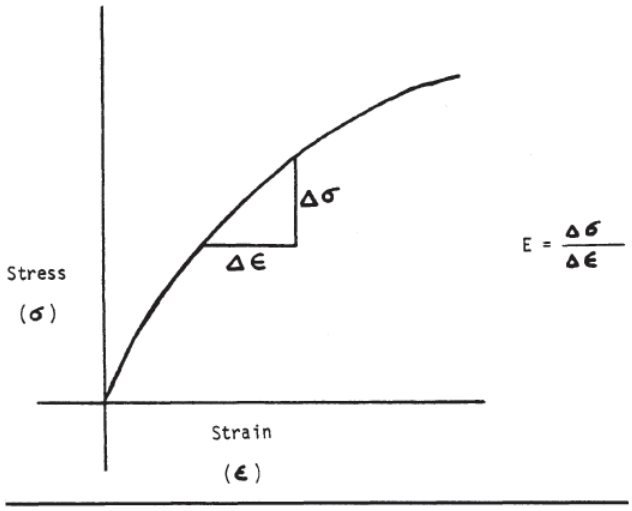

Figure 3-5: The elastic modulus of the structure (after Jensen 1980)

When a straight structure undergoes a load, all areas experience the same torque (i.e. the load on the structure applied in a multiaxial situation). Meanwhile, in a curved structure, the load is applied at a point away from the neutral axis and is indirectly supported. Consequently, both torque and bending are produced. In the spine, an externally applied weight generates stress and strains on the vertebral body or disc or both. Because the disc has a lesser elastic module than the vertebral body, strains can be generated easily with a greater effect in the disc in which the resultant forces must distribute. When the stresses at a point exceed the strength of the tissue at that point, the tissue fails.

It is essential to differentiate between the load applied to the disc as a structure and the stress made within the disc components. For example, when a human stands in a neutral posture, the disc is subjected to a compression load while its nucleus is exposed to a tensile stress. The compressive load is distributed from one vertebral endplate to the other through the nucleus pulposus and the annulus fibrous (Figure 3-6). The nucleus serves as a gelatinous mass due to its water content. When a load is applied, this material produces a pressure within the nucleus that pushes the compressive stress to the surrounding structures in all directions away from the centre of the nucleus.

The compression load also produces complex stresses within the annular ring. The inner layers of the annulus are subjected to small compressive stress, which is transferred to other vertebrae by the fluid pressure of the nucleus, while in the outer layers, stress is tensile because of the presence of the obliquely arranged fibres at ± 30.

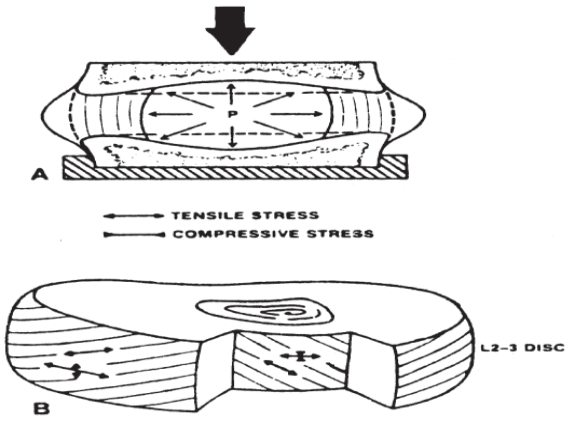

Figure 3-6: Compression load in a healthy disc. A: the pressure inside the nucleus pushes the disc annulus and the two end- plates outwards. B: in the outer layers of the annulus, the stresses are larger than in the inner layers (after Jensen 1980).

Disc malfunctioning occurs when the nucleus loses its preloading mechanism, and when there is a decrease in the elasticity of the annulus fibres and degeneration in the cartilage of the endplate (Jensen 1980; White and Panjabi 1990).

(Kulak et al. 1976) reported that when the nucleus decreases its water content, this leads to a loss of its properties. In this condition, the disc behaviour changes from an internally pressurized thick-walled tube with considerable tensile hoop stress to a thick ring under axial compression with a very little tensile hoop stress as a result of the absence of a nucleus-annulus interaction. This indicates that the nucleus has a remarkable effect on sustaining the compressive axial loads—if the nucleus is absent, the calculated disc stiffness tends to decrease by a factor of two.

While (Argoubi and Shirazi-Adl 1996)results was in line with (Kulak et al. 1976). , they added that the loading on the annulus fibres and the facet joints would be greater when the fluid inside the nucleus is lost, which indicates the creep behaviour of the motion segments. In other words, the normal path way of the fluid diffusion will be transferred to the central portions of the vertebral endplates rather than through the surrounding fibres.

Many authors have tried to define the disc behaviour during many body activities with or without load. (Jensen 1980) stated that bending alone involves simultaneous tension and compression, and also some shear stresses at different locations on the disc.

Bending in forwarding flexion, lateral flexion or extension of the spine results in tensile stress on the convex side of the annulus and compressive stress on the concave side. In this condition, the side of the annulus under tension stretches, while the side under compression bulges. When undergoing bending, a disc structure will have maximum stress at the outer surface (Figure 3-8). Similarly, (Natarajan et al. 2008) concluded that the activity that combined lifting with lateral bending caused the highest risk to the disc structures as a result of the largest translations and rotational motions of the disc.

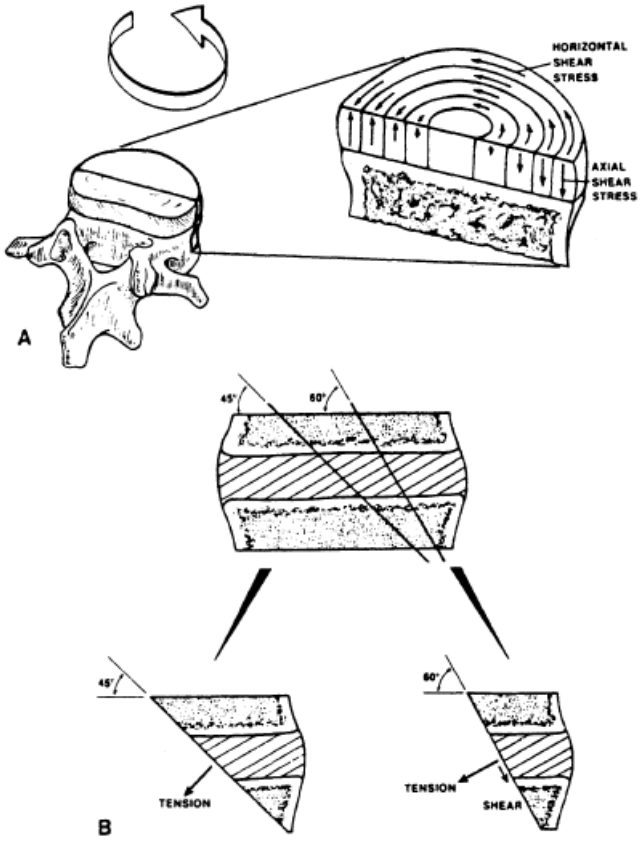

Figure 3-7: Torsion load on the disc causes tension and shear stress. A: shear stress results from the application of a torsion load, B: normal stress is present at 45 degrees to the disc plane and both normal and shear stress at 60 degrees to the disc plane (after Jensen 1980)

In the vertebral column, this means that the outer peripheral surfaces of the annulus will be subjected to the highest tensile stresses on the convex side and the highest compressive stresses on the concave side. In turn, (Leone et al. 2007) stated that rotation and lateral bending may be coupled to each other. The stress on the disc is, thus, a combination of tension, compression and shear. In detail, torsion stress in the spine

comes from twisting or rotating on the long axis. The motion of one vertebra on another produces both tensile and shear stresses in the annulus. The shear stresses take place in the horizontal plane about the rotational axis. Because the annulus fibres cross at oblique angles to the horizontal plane, torsion results in tensile stresses in the fibres that resist rotation. However, shear stresses exist perpendicular to the annulus fibre direction.

Given that the bond between parallel fibres is relatively weak, these shear stresses may cause failure in the annulus (Figure 3-7). The peripheral surface structures of the annulus are subjected to the largest stresses and subsequently, develop the greatest strains. The magnitude of the strain is proportional to the distance from the peripheral annulus to the axis of rotation. In the disc, this stress is maximal at the posterolateral angles of the annulus where there is already a structural weakness. Thus, combinations of movements, such as twisting, bending and bending with rotation, will result in increasing stresses and strains on the disc, especially with a superimposed load. These stresses alone can account for disc injury—in the presence of any disc degeneration, the stresses are only magnified(Jensen 1980).

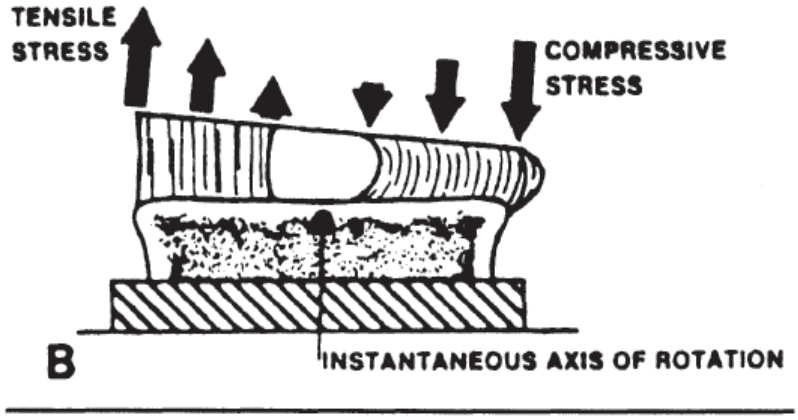

Figure 3-8: Tensile and compression stresses in the disc during bending (after Jensen 1980)

The previous studies defined the mechanism of the disc injury during movement. (Adams and Dolan 1995) stated that the vertebral end-plates bulge into the vertebral bodies as a reaction to the hydrostatic pressure in the nucleus pulposus as a result of

disc compression. At the same time, the inner and middle annulus act directly against the compression and the disc bulges radially outwards (Figure 3-9). Meanwhile, in a full flexion, outer annulus provides most of disc resistance during bending and torsion. While, (Lu et al. 1996)demonstrated that the inner posterior annulus fibres presented maximum tensile stress under applied combined compression, bending and twisting.

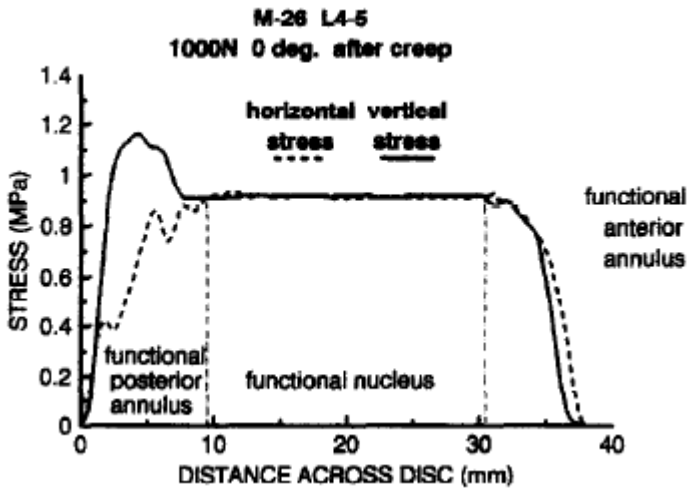

Figure 3-9: The inner and middle annulus act directly against the disc compression and the disc bulges radially outwards (after Adams and Dolan 1995)

(Roaf 1960) reported that, as vertical pressure increases, there is a very slight bulge of the annulus, but no alteration in the shape of the nucleus pulposus. The major distortion is a bulge of the vertebral end-plate. In this condition, the annular bulge occurs when the two vertebrae move closer to each other (diminution of disc space).

This study illustrated that the intervertebral disc joints and ligaments are more resistive to compression, destruction, flexion and extension, but are very vulnerable to the rotation and horizontal shearing forces.

(Hindle et al. 1989) reported that the torque is unimportant in disc damage mechanism because the rotational angles that might cause the damage to the annular fibres cannot be achieved due to the effective role of the compression zygapophysial joint. Therefore, torsion could produce annular damage in a two-stage process. First, repeated torsional trauma could be expected to lead to the thinning of the articular cartilage, giving rise to a greater ability of a joint to twist. This combined with other types of loading or extra

rotation available, and when acting in combination with flexion, may be sufficient to cause annular damage. The conclusion of this study was that the lumbar spine had a greater rotational capacity in a flexed posture than when erect, which implies that torsion may be a cause of injury to the intervertebra1 disc when combined with flexion.

(White and Panjabi 1990) showed that the disc bulge occurs in the mid-disc plane when the functional spinal unit is subjected to simultaneous compression and lateral bending. This disc bulge occurs most in the lateral and posterolateral direction on the concave side of the lateral bend and this value increases more than two times in the case of disc degeneration.

According to the previous illustrations, the posterior lateral regions of the disc could be the structure that is most likely to be subjected to the risk of the injury. While anterior lumbar disc herniation may cause pain and symptoms, this condition happens rarely. Other annular tears are present by early adulthood and are associated with the long-term development of disc degeneration and herniation (Costi et al. 2007).

This result is in agreement with (Argoubi and Shirazi-Adl 1996) who stated that the posterior disc plugging decreases when the period of applied coupled flexion and rotation increases, while the anterior and lateral portions of the disc plugs increase subsequently.

In the present study, the lower trunk was rotated with three different rotational positions (R1, R2 and R3) to investigate the effect of these rotational positions on the intervertebral disc cross-sectional area, width, and posterior and anterior disc height.

Several studies have demonstrated the measurement of the intervertebral disc height and width.

For example, many researchers agreed to use the sagittal MRI to measure the disc height as a line connecting the corners of the upper and lower vertebral bodies or using points on the upper and lower endplates, such as (Lao et al. 2016; Zhou et al. 2000; Tunset et al. 2013; Mahato 2011; Lewis and Fowler 2009; Kimura et al. 2001; Yamaguchi et al. 2011; Miao et al. 2013). While, (Chung et al. 2000) measured the disc height at two regions of the axial MRI, the sagittal and mid-sagittal of the intervertebral disc. The right and left sagittal diameter of the disc was defined as lines drawn from the convex posterior margin to the anterior margin of the intervertebral disc. The mid- sagittal

diameter was measured as a line connecting the anterior and posterior borders of the disc at the mid disc.

Other authors used different methods, (Hong et al. 2010) measured the central intervertebral disc space of each lumbar segment using MRI as the ratio of disc space distance to the length of the upper margin of the lower lumbar vertebrae in the area connecting the central portion of the lower margin of the upper lumbar vertebrae and the central portion of the upper margin of the lower lumbar vertebra. The anterior disc space was measured in the area connecting the tip of the anterior margin of the vertebral body, while the posterior disc distance was calculated in the area connecting the tip of the posterior margin of the vertebral body.

The posterior disc bulge was measured by (Fredericson et al. 2002) as a length of the line drawn from the most posterior edge of the disc to a line drawn connecting the two posterior edges of the endplates.

However these studies used the same landmarks to measure the posterior and anterior disc height (corners of the vertebral bodies or the borders of the end plates). In addition, their methods of measurements did not take into account the deformation of the vertebral bodies that occur during spine rotational positions.

(Tunset et al. 2013) introduced a method to calculate the cross sectional area of the anterior and posterior intervertebral disc height by selecting sagittal T2 images from the visible right and left pedicles. However, the authors stated that the accuracy of the image analysis may decrease as a result of using high magnification levels (1100% -1200%).

(Bailey et al. 2018) calculated the cross sectional area of the intervertebral disc depending on quantification of the signal intensity values percentage using T1- and T2-weighted MRI images. However, the change in the cross sectional area of the intervertebral disc was measured in percentage.

Consequently, the calculation of the cross-sectional area of the right and left side of the sagittal intervertebral disc in mm^2 has not yet been obtained yet, which illustrates the difficulty of separating the borders of the intervertebral dis from the adjacent structures.

From the previously reviewed papers, two studies were found that measured the width of the intervertebral disc (mid-coronal diameter) using the axial MRI, the disc width

was identified as the maximal transverse diameter of the disc. (Chung et al. 2000). In addition, width of each individual disc was calculated as a ratio which was represented as the mean value between the left-right width in the upper and lower endplate by using 3-D reconstructions of all vertebrae and intervertebral discs from T4 to L5 from CT scans using 3-D endplate vectors (Chen et al. 2017). However, measuring the changing in the sagittal width of the right and left sides of the intervertebral disc separately to indicate the effect of the rotation on theses sides has not yet been achieved.

The current study believes that it is possible to use a safe and suitable techniques of measuring the posterior and anterior disc height of the rotated vertebrae, the calculation of the cross-sectional area of the right and left side of the sagittal intervertebral disc in mm2 and measuring width of two sides of the intervertebral disc by taking average measurements of two sagittal MRI images depending on using a synchronisation tool and using a particular saturated pixel percentage with a determined magnification power(see Chapter 4).

In this technique, the posterior disc height is measured as the length of a line connecting the nearest two points that are located on the far right side of the lower and upper end plate. While the anterior disc height is measured as the length of a line connecting two farthest points that lie on the far left side of the lower and upper end plates. In the current study, these landmarks are determined to quantify the minim posterior disc height and the maximum anterior disc height during spine rotation.

In turn using this new technique, the cross-sectional area of the disc can be outlined manually after using particular saturated pixel percentage with a determined magnification power to differentiate between the disc borders and the adjacent structure such as the longitudinal ligaments. In addition, the disc width is measured as the line connecting the most anterior and most posterior points of the outlined cross-sectional area of the intervertebral disc.

Three active lower trunk rotational positions of healthy subjects will be used to test the hypothesis that the intervertebral disc dimensions of each spinal segments will be affected more by applying the first active lower trunk rotational position (with mean pelvis angle 90°).

3.4.4 Biomechanics of the Lumbar Intervertebral Foramen during Different Spine Positions

The daily physiological movements of the lumbar spine cause continuous changes in the morphology of the intervertebral foramen (Fujiwara et al. 2001). Therefore, the effect of different spine positions on the intervertebral foramen has been investigated by many researchers.

During supine position, (Senoo et al. 2014) compared the foraminal height and width according to gender, age and lumbar level of healthy subjects. Their results demonstrated that during the neutral position, the foraminal width at lower lumbar levels was significantly smaller than that at the upper levels. (Cramer et al. 2003; Torun et al. 2006) added that there were no differences between left and right intervertebral foramens and their dimensions were almost similar.

(Panjabi et al. 1983) found that flexion motion increased the foramen area of the non-degenerate and degenerated specimens by 30% and 20% respectively, while in extension, the foramen closed by nearly 20%, for both specimens. In addition, this study illustrated that there was a reduction in the foramen height of 6% as a result of extension movement. Similarly, (Inufusa et al. 1996) found that extension produced a significant decrease in all foraminal dimensions. These findings were confirmed by (Mayoux-Benhamou et al. 1989; Schmid et al. 1999; Zhong et al. 2015). However, (Zhong et al. 2015) reported that the lumbar intervertebral foramen area and width decreased with lumbar extension at all lumbar segments except at L5-S1.

Through axial rotation, the foramen underwent complicated changes on the side of rotation. The infero-posterior borders of the cephalad vertebral body and the upper half of the disc closed the intervertebral foramen. At the same time, the upper portion of the pars articularis of the cephalad lamina and upper half of the ligamentum flavum bulged posteriorly. These changes resulted in a 5.7% reduction in the cross-sectional area of the foramen. On the opposite side of rotation, the cross-sectional area of the foramen increased by about 6.5%

The intervertebral foramen might vary from level to level and from individual to individual. These anatomical differences resulted in various changes to the intervertebral foramen dimensions during axial rotation. Meanwhile, the left lateral bending opened the right intervertebral foramen by about 4% and the right lateral bending closed the right intervertebral foramens by about 2% (Panjabi et al. 1983; Fujiwara et al. 2001).

The normal values of the foraminal dimensions (height, width, cross-sectional area) have been reported by many researchers who used techniques, such as cadaveric, CT, MRI, cryomicrotome technique and callipers. These studies reported that the intervertebral foramina height during neutral position ranged from 15.9 mm to 23.4 mm, while the cross-sectional area varied from 115 to 140.5 mm^2. In contrast, the foraminal width of more than 4 mm was included as the normal value (Inufusa et al. 1996; Schmid et al. 1999; Fujiwara et al. 2001; Cinotti et al. 2002; Al-Hadidi et al. 2001; Cramer et al. 2003; Torun et al. 2006; Senoo et al. 2014). However, (Hasegawa et al. 1995) mentioned that a foraminal height of less than 14.31 mm and 17.68 mm at L5-S1 and L3-L4 can be recorded as critical signs of foraminal stenosis.

To investigate the foraminal dimensions, only three studies have determined the foraminal cross-sectional area. (Schmid et al. 1999)measured the intervertebral foramen area as the region outlined by the spine structures that constitute the intervertebral foramen (pedicle, ligamentum flavum, posterior vertebral body and the posterior edge of the intervertebral disc) using parasagittal MRI images. Meanwhile, (Panjabi et al. 1983; Inufusa et al. 1996) used a computer digitizer and mathematical model to analyse the CT images and photographs of the thinly sectioned functional spinal unit from their specimens.

Several studies have measured the height of the foramen as the distance connecting the inferior and the superior surfaces of the upper and lower pedicles (Panjabi et al. 1983; Mayoux-Benhamou et al. 1989; Inufusa et al. 1996; Schmid et al. 1999; Cinotti et al. 2002; Cramer et al. 2003; Torun et al. 2006).

In contrast, the width of the intervertebral foramen has been a point of conflict for many researchers. (Senoo et al. 2014) calculated the foraminal width as the narrowest area between the postero-inferior corner of the upper vertebral body and the nearest point that is located on the nearest border line. In contrast, (Inufusa et al. 1996; Fujiwara et

al. 2001; Cinotti et al. 2002) divided the foraminal width into three types: superior, minimum and inferior width. However, (Cinotti et al. 2002) defined these types of foramen widths as follows: the superior foramenal width was measured below the inferior surface of the superior pedicle, while the lower foramen width showed the narrowest diameter of the intervertebral foramen. The distance between the posterior annulus of the disc and the lower vertebral endplate was indicated as the pedicle length.

Most of the previous studies used computed tomography and cadaveric samples in which the subjects exposed into ionisation radiation and some of the soft tissues were isolated or intersected. Others used MRI to obtain their measurement but these studies did not take into account that the same landmarks will not be appear obviously for all vertebral segments and at each rotational degree of the spine. Accordingly, the present study presented a safe method with a new orientation of measurements that take into account the natural physiological movements with the consideration of the presence of the disc and soft tissues to overcome the variation in the appearance of the same landmarks in each vertebral segment and each rotational position, due to the fact that each vertebra rotates with its unique rotational degree. Therefore, depending on using a determined saturated pixel percentage, the values of the intervertebral foramen dimensions (cross-sectional area, width, height) were taken as the average for two consecutive slices which showed the apparent nerve root, pedicles of the two articulated vertebrae, the most posterior- lateral point of the lower endplate of the upper vertebra and the obvious tip of the superior facet (see chapter 4).

Accordingly, three active lower trunk rotational positions of healthy subjects will be used to test the hypothesis that the intervertebral foramen dimensions of each lower spinal segment will be more affected by applying the first active lower trunk rotational position (with mean pelvis angle 90°).

3.4.5 The Relationship between the Coupled Motion and the Amount of Applied Torque

Postural and structure coupling are the types of rotational coupling in the spine. Various orientations of the vertebrae of the lumbar spine (lordosis) can be defined as postural coupling. In contrast, the physical characteristic of the joint (structural coupling) under an applied external load forces this joint to move in directions other than that of the applied load (coupled motion). The interaction between axial torque (axial rotation) and

lateral bending rotation (lateral bending moment) can be considered as a basis of the postural coupling. When the lumbar spine is under axial torque, the lumbosacral region undergoes a combination of axial torque and lateral bending. The lateral bending moment will cause lateral rotation (coupled motion under the externally applied axial torque). When the lumbar spine is under lateral bending moment, the lumbosacral joint would be subjected to both lateral bending and axial torque. The axial rotation caused by the local axial torque is called coupled motion. (Figure 3-10) (Oxland et al. 1992).

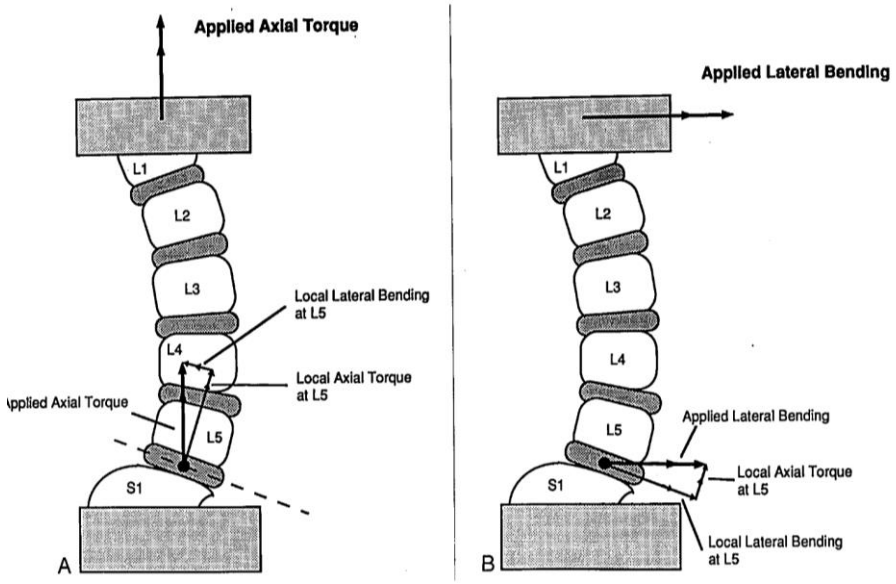

Figure 3-10: The lumbosacral region undergoes a combination of local left axial torque and left lateral bending moment at L5-S1 when the spine is subjected to left axial torque (A). An applied right lateral bending moment is resolved into the local right lateral bending moment and left axial torque at L5-S1 (B) (after Oxland et al. 1992).

Coupled phenomena and the direction of the spinal segments during spine rotation with or without applied load were taken into account during the lumbar spine studies. The coupled lateral rotation of the two most caudal lumber segments is in the same direction as the applied torque, while at the cephalic levels, the coupled lateral rotation is in the opposite direction (Grassmann et al. 1998). The coupled lateral flexion of lumbar spine segments (L1-L2 to L4-L5) was in the opposite direction of the trunk rotation. Meanwhile, coupled lateral bending was in the same direction of rotation at T1-L1 and L5-S1 levels (Fujii et al. 2007).

Many methods have been used to evaluate the degree of the lateral bending such as automatically superimposing a segmented 3D MRI, three-dimensional radiographic technique, stereo photogrammetry, camera three-dimensional motion analysis system, a wooden rule, strain gages on a thin stainless steel beam (Fujii et al. 2007; Pearcy and Tibrewal 1984; Barnes et al. 2009; Ebert et al. 2014; Donatell et al. 2005, Been et al. 2011). However, some of these studies used methods of measurement that exposed the subjects to ionising radiation, while others used either methods of measurements that an associated with error or were unsuitable for non-standing postures. The present study introduced simple but highly reliable and safe method using a particular saturated pixel percentage with a determined magnification power to measure the lateral bending degree of each individual vertebrae which is based on the landmarks that was used by (Been et al. 2011).

The present study used mid-sagittal MRI to measure the lateral bending angle as the angle between two lines which are parallel to the inferior and superior endplates of the two consecutive endplates. Three voluntary rotational positions of the lower trunk(R1,R2 and R3) were obtained without restriction of the shoulder movements to evaluate the hypothesis that the lateral bending angle will be the greatest with the first rotational position of the lower trunk(pelvic at 90^{0}).

3.4.6 The Role of the Facet Orientation in Trunk Rotation and in Designing the Artificial Facet

The role of axial torque and facet orientation in intervertebral disc injuries and lower back pain is a controversial element of many studies. Previous studies have indicated that disc failure and degeneration can occur only under torsion forces and the facet joints play a protective role (Farfan and Sullivan 1967; Farfan et al. 1970). However, these studies had no final conclusion.

For example, (Adams and Hutton 1980; Adams and Hutton 1981; Kelsey et al. 1984; Shirazi-Adl et al. 1986; Shirazi-Adl 1989) all suggested contrary views, indicating that the torsion alone or without any applied lifting activities cannot cause disc injury. They showed that the apophyseal joint was the first structure that resisted the compression and torsion forces of the lumbar spine.

In a limited number of single motion segment studies (Ueno and Liu 1987; Shirazi-Adl 1991), the significant role of the facet joint in axial torque has been confirmed. These studies concluded that the facet could endure 10-40 % of the applied torsion forces depending on the gap distance between the superior and inferior articular facets and on which segment that the load was applied. However, (Shirazi-Adl 1994)stated that the gap distance might be affected by the condition of the cartilaginous layer of the articular surface of facet joints.

Similarly, (Criswell 2013) stated that the posterior elements of the spinal segments (the facet joint) has the role in restricting the spinal motion. For example, in the lower thoracic region, axial rotation had an increase in motion of 40 % after posterior elements were removed.

Accordingly, when a tear occurs in capsular ligaments and the volume increases due to hypertrophy, the facets begin to move medially and exhibit tropism. These changes reduce vertebral foramina volume, and ultimately cause anatomic and dynamic foraminal stenosis. The nerve root in each involved foramen becomes compressed by surrounding degenerative tissues.

In this condition, the facets have been identified as a source of pain. With facet degeneration, it is also common to experience disc degeneration at that level. As the disc's degeneration progresses, the stresses are increased at the facets which propagates the degeneration at the facet location.

Many attempts have been made to replace degenerated facet joints and one of these solutions was the artificial facet (Ozer et al. 2015; Criswell 2013).

Artificial facet replacement is indicated for back and leg pain caused by lumbar stenosis with advanced facet disease requiring destabilizing facetectomy for adequate decompression. Stenosis resulting from grade one degenerative spondylolisthesis represents an ideal indication for artificial facet replacement.

Artificial facets are robust biomechanical devices that are intended to replace the facets and the posterior elements in the lumbar spine. In contradistinction to posterior dynamic stabilisation devices, artificial facets are intended to be a stand-alone, motion-preserving alternative to standard lumbar fusion (Figure 3-11).

Figure 3-11: ACADIA (Globus Medical) facet replacement system (after Coric 2014)

Generally, many different designs for an artificial facet have been introduced, such as ACADIA (Globus Medical) and TOPS (Premia Spine), the ACADIA facet replacement system is a titanium pedicle screw–based system with bilateral articulating elements that mimic native facets. While, the TOPS artificial facet is a pedicle screw–based system that consists of a single titanium articulating post covered by a cushioning polyurethane layer covered by a polyurethane boot (Coric 2014).

Meanwhile, facet joint replacement devices can be used to replace painful facet joints, restore stability, and/or to retain a failed disc or nucleus prosthesis without losing motion, does not fully restore joint functionality. Therefore, any facet replacement device will require a significant amount of controlled clinical studies before being brought to market. Therefore, in case of artificial facet implants, the artificial facet would have to mate with the natural articular process mechanical properties.

In general, the major factors that lead to success or failure of arthroplasty are the size of the joint surface (stress at the joint surface), the degree and extent of multiplanar motion and/or load transfer through the device or joint, the strength and size of the anchor points, long-term performance (Serhan et al. 2007).

Based on the degree and extent of multiplanar motion and the gapping distance between two articular processes of the normal facet, it has been suggested that the facet angulation can result in a rotational coupling phenomenon in the lumbar spine. In turn, facet orientation is associated with the degree of rotation along the different body axes at each individual motion segment (Kapandji 1974; Ahmed et al. 1990; Van Schaik et al. 1997).

(Masharawi et al. 2004) mentioned that regardless of which axes in which the lumbar segment motion is involved, a complex multiplanar movement can occur. This could explain the mechanism of rotational movement in the lumbar spine, which depends on the more angulated left facet.

Finite element, cadaveric, MRI and CT models, instrumented spatial linkage methods, modified protractors, micro scribes and three-dimensional apparatus have all been used to evaluate the orientation and the tropism angle of the lumbar facet, depending on the reference lines. The reference lines used can be classified as a mid-sagittal line which passes through the intervertebral disc and divides the spinous into equal halves or as a transverse and a coronal plane. The reference line of the right and left facet was defined as a line connecting two endpoints on the articular facets (Farfan and Sullivan 1967; Noren et al. 1991; Panjabi et al. 1993; Tulsi and Hermanis 1993; Boden et al. 1996; Masharawi et al. 2004; Kozanek et al. 2009). However, (Kozanek et al. 2009) measured the transverse facet angle as the angle between the line of the facet width projected onto the transverse plane of the vertebra and the antero-posterior axis of the vertebrae. However, to reduce the time of the radiation exposure, this study did not evaluate the in vivo instantaneous positions of the lumbar vertebrae during dynamic motion of the body. In addition, the L5 segment was not involved as a result of the limited field of view.

On other hand, based on both techniques, which were defined by (Farfan and Sullivan 1967; Boden et al. 1996), (Chadha et al. 2013;Wang et al. 2015) introduced a different technique to measure the facet tropism angle as being located between the line which is drawn between the two margins of the superior articular facet and a mid-sagittal line, which passes through the intervertebral disc centre and the centre of the base of the spinous process.

A review of the literature reveals that only one study has measured the gaping distance between the superior and inferior articular facets. (Cramer et al. 2000) measured the gaping distance of the articular joint as the linear distance from the centre of the facet joint passing from the inferior to the superior articular processes.

The difference between these previous methods of measurements and the present study is that the present method will present safe, healthy volunteer with natural physiological movements with the consideration of the angle of rotation of the intervertebral disc. It

will also take differences between the solid compact bone of the articular process and the soft tissues, such as the capsular ligaments, into account. These. As these ligaments tend to prevent the accurate determination of the antero-posterior boarders of the articular processes as a result of the effect of the torsion (Chapter 4).

Three voluntary lower trunk rotational positions will be performed to evaluate the hypothesis that the mean differences between the orientations angle of the right and the left superior articular processes at each individual lower lumbar segment will be the highest at the first rotational position of the lower trunk (mean pelvis angle (90°). It will also be used to test the hypothesis that the cross-sectional area of the opening of the left articular facets at each individual lower lumbar segment will be the highest at the first rotational position of the lower trunk (mean pelvis angle: 90°).

Quantification of the effect of the three voluntary lower trunk rotational positions on the orientation angle of the left and right lower lumbar superior articular processes and on the amount of change in the cross sectional area of the lumbar spine facet opening will be evaluated using 3D T2 MRI images and adjusting the image contrast.

The current study will address the hypothesis that providing highly accurate data of the degree of orientation of the articular processes and the gapping distance between two articular processes of the normal facet during lower trunk rotation will help to successfully design an artificial facet.

3.5 The role of MRI in the Diagnosis of Lumbar Spine and Sacroiliac Joint Disorders

Although traditional imaging techniques (i.e. conventional x-rays and computed tomography) have been used to diagnose lower back pain (Aaro and Dahlborn 1981; Krismer 2002; Göçen et al. 1999; Cerny et al. 2014), these methods have their shortcomings. Conventional X-rays and computer tomography expose the patient to ionising radiation. Additionally, there is a limited contrast between structures provided by these imaging techniques. Meanwhile, artificial enhancement techniques (contrast agent injections) may be required to provide low or high radiographic density, such as iodinated fluids. In addition, three-dimensional reconstruction and analysis of bony

structures cannot be achieved by conventional X-rays, as it is a two-dimensional imaging modality.

In contrast, MRI provides higher soft tissue resolution and, therefore, is often used in the diagnosis of lumbar spine conditions, such as disc herniation and spinal stenosis (Mendieta 2016).

For example, (Hall and Robinson 2004) examined the ability of MRI to diagnose locked facets in a series of six patients with traumatic cervical spine fractures. Plain films, computed tomography and magnetic resonance scanning were carried out immediately following injury. The results concluded that magnetic resonance proved to be equally effective in diagnosing unilateral and bilateral locked facets, and demonstrated the disruption of the posterior longitudinal ligament with clarity. (McRobbie et al. 2003) reported that spine imaging is an important application of MRI because of the high prevalence of back pain and the possibility of herniated discs, discitis or trauma.

To maximise the SNR in spine imaging, a surface coil is placed directly over the portion of the spine to be imaged. Because the spine is typically divided into cervical, thoracic and lumbar regions, surfaces coils are available that are optimised for each of those territories. Phased array coils that have multiple elements are also available, which can be used to cover the entire spine.

Regarding the use of sagittal T1-weighted sequences, sagittal T2-weighted images and axial images, (McRobbie et al. 2003) reported that it is essential to image the spine with a sagittal T1-weighted sequence in order to evaluate the bone marrow and for a high SNR assessment of the anatomy. In contrast, sagittal T2-weighted imaging is used to assess the hydration of the intervertebral discs and to help characterise any pathology detected. Finally, axial images through each disc are important to better assess the extent of any disc herniation and to look for compression of nerve roots.

(Ishii et al. 2004) demonstrated in vivo intervertebral coupled motions of the upper cervical spine by using three dimensional MRI. Voxel-based registration was obtained to segment three-dimensional MRIs of each vertebra in the neutral position and superimpose over images taken at other positions.

To highlight the appearance of the rotated atlanto-axial joint on MRI and computed tomography, (Roche et al. 2002) found that the computed tomography showed the atlanto-axial rotation in one direction, while MRI demonstrated the movement of the

articular surfaces of the first cervical vertebrae on the second one in multiple directions. Similarly, (Jaumard et al. 2014) determined whether there is any difference in facet joint architecture between symptomatic and asymptomatic subjects with the head in each neutral and pain-eliciting rotation using MRI. These authors demonstrated that the MRI showed that facet joint space thickness and volume were smaller in the symptomatic subjects than in the asymptomatic subjects.

(Shin et al. 2013) investigated in vivo characteristic motion patterns of the human lumbar spine during a dynamic axial rotation. Specifically, the contribution of each motion segment to the lumbar axial rotation and the coupled bending of the vertebrae during the dynamic axial rotation using MRI.

(Fujii et al. 2007) developed a novel 3D analysing system for the relative motions of individual lumbar vertebrae using (three-dimensional MRI) during trunk rotation.

Consequently, T2 sagittal and T2 axial three-dimensional acquisition cuts will be used to investigate the hypothesis that MRI will be the effective method to show the changes in the lumbar spine and sacroiliac joints structures in three dimensions during lower trunk rotation.

3.6 Summary

Understanding the biomedical and biomechanical conditions of the lumbar spine and the performance of the shoulder and pelvis girdles during different lower-trunk rotational positions of healthy subjects will help improve the manipulative therapy in the future to reduce the financial burden. The biomechanics of the spinal manipulation can be divided into the external and the associated internal forces. The external forces are represented by chiropractors, which vary dramatically between clinicians and depending on the location of treatment application. Meanwhile, the internal forces that are produced by the spinal manipulation are stress and strain forces. Accordingly, lumbar spine manipulation is considered to be a type of a rotational torque. This passively rotated position of the spine can either reduce low back pain or may cause adverse effects.

It has been suggested that the coordination patterns between the upper and lower body should be considered to obtain optimal functional performance because the range of

motion of the shoulder and pelvis are crucial factors to continue a flexible dynamic trunk motion.

Many studies have measured the scapula's position during many body activities. However, the only variable method for the current study involved using a tape measure, because it is the only method that is able to measure the scapula's kinematics during lower-trunk rotation.

Previous studies have used many different techniques and devices to control and measure the pelvic rotational angle of subjects, while making it as reproducible as possible. However, these devices could not be used in supine and actively lower-trunk rotational positions. Given that the current study will be based on the three actively lower-trunk rotational positions with accurately controlled angle of rotation, it will use a novel lower trunk holder (MRI holder) and a modified goniometer.

The position of the spine, pelvis, and hip balances the mass of the trunk above it and the mobility of these articulations allows for coordinated motion during activities, such as moving from standing to sitting or bending forward at the waist. Accordingly, several studies defined the relation between the spine and pelvis depended on using many measurements and landmarks. However, these studies did not take into account the difference in the rotational degree between the pelvis and the fifth lumbar vertebrae. Based on the previous studies, the current study will introduce a new definition of the relationship between the spine and the pelvic depending on the relation between the last lumbar vertebrae and three sections of the posterior superior iliac spines during lower-trunk rotational positions.

The sacroiliac joint has been reported as having three-dimensional rotating and translating motions along three axes, with a central point that lies between the right and left-posterior superior iliac spines. Although several studies have tried to calculate sacroiliac joint rotational and translational motions, they did not achieve highly precise measurements or active pelvic stabilities. To date, no study has been able to accurately clarify the in vivo kinematic changes in the sacroiliac joint mobility at three anatomical sections of the sacrum and ilium with respect to three lower-trunk rotation positions. This approach will explain how each section of the right and left ilium moves relative

to the other sections and relative to the sacrum, and vice versa, during each lower-trunk rotational position.

Many studies have been conducted to understand spinal structures biomechanics during different trunk positions and methods, and also to measure the vertebral rotational degree, the relative motion and the rotational torque between L3 and L5vertebral levels. However, some of these previously mentioned methods have critical limitations, such as exposing the subjects to ionisation radiation, while other studies used in vitro landmarks that provided an estimate of lumbar range of motion that required determination of many landmarks. No study has given attention to the fact that the muscle tendons and ligamentum flavum attachments at both sides of the vertebrae prevent the precise localisation of the tip of the transverse and the anatomical points on the spinous processes and pedicle. Consequently, the present study will use simple, safe (did not expose the subjects to ionising radiation), and more accurate method to overcome these difficulties in the determinations of particular landmarks.

Many previous studies have aimed to describe the close relationship between the spinal canal and dural sac dimensions and the lower back pain. In addition, several anatomical studies have emphasised the measurements of the spinal canal and dural sac dimensions. However, these studies did not take into account the measurement of the difference of depth of the spinal canal depending on dural sac position at the two sides of the lumbar vertebrae during different rotational positions.

The corners of the vertebral bodies or the borders of the endplates have previously been used to measure the height of the intervertebral dis. However, these studies did not take into account the deformation of the vertebral bodies that occur during spine rotational positions, which require more than one slice of MRI to recognise. In addition, due to the difficulty to separate the borders of the intervertebral dis from the adjacent structures such as the longitudinal ligaments, the cross-sectional area of the intervertebral disc in mm2 has not been measured. Moreover, from the previously reviewed papers, only two studies found that measured the width of the intervertebral disc. However, these studies used techniques may not be reliable to measure the changing in the sagittal width of the

right and left sides of the intervertebral disc. Accordingly, the current study, will use a safe, reliable and highly accurate method to measure the disc dimensions during spine rotation.

Most of the previous studies investigated the foraminal dimensions based on radiographic techniques, which exposed the subjects to ionisation radiation, or used cadaveric samples in which some of the soft tissues were isolated or intersected. Although other studies have used MRI to obtain their measurement, they did not take the variation in the appearance of the same landmarks in each vertebral segment and each rotational position into account due to the fact that each vertebra rotates with its unique rotational degree. Accordingly, the present study will present a safe method with a new orientation of measurements that take into account the natural physiological movements, giving consideration to the presence of the disc and soft tissues and the same landmarks.

The degree of lateral bending has been evaluated by using many methods. Some of these studies used methods of measurement that exposed the subjects to ionising radiation, while others used either methods of measurements that an associated with error or were unsuitable for supine and rotated position. The present study will introduce a simple but highly reliable and safe method to measure the lateral bending degree of each individual vertebrae depending on the same landmarks that have been used by one of the previous studies.

Many studies have been carried out on measuring the orientation angle of the articular facets and on calculating the gaping distance between the superior and inferior articular facets. The difference between the measurements of these previously studies and the present study is that the present study will present a safer and more accurate method using natural physiological movements and giving consideration to the angle of rotation of the intervertebral disc. It will also take into account the differentiation of the solid compact bone of the articular process from the soft tissues, such as the capsular ligaments. As a result of the effect of the torsion, these ligaments tend to prevent the accurate determination of the antero-posterior boarders of the articular processes. The

quantification of the degree of the orientation of the articular processes and the gapping distance between two articular processes of the normal facet during different rotational positions of the spine will help to develop a successful design for an artificial facet.

Finally, MRI has been proven to be an effective method to diagnose low back disorders, in such way that the spinal structure can be shown clearly. Therefore, the current study will use T2 sagittal and T2 axial three-dimensional acquisition cuts of MRI to show the changes in the lumbar spine and sacroiliac joints structures in three dimensions during lower-trunk rotation.

Chapter 4

Materials and Methodologies

4.1 Introduction

This chapter will introduce the experimental methods, the development of the technique and the required materials. The position of the scapula will be measured according to the position of the right and left posterior borders of the acromion processes using a tape. An adaptive goniometer and an MRI holder have been developed to position the subject to obtain the accurate pelvis angle of rotation during the scan. An MRI protocol has been identified to meet the requirement of delivering quantified data from the lumbar spine and sacroiliac joints structures. The MRIs have been collected from volunteers and analysed using Image J software. The statistical analysis has been carried out in SPSS (version 23, IBM Corp.).

4.2 Inclusion and Exclusion Criteria

Ethical approval was obtained from the University Ethics Committee at the School of Engineering. All volunteers provided written consent before participation in the study. The volunteers were invited to participate in the study. They were interviewed and evaluated according to the inclusion and exclusion criteria. Table 4-1 shows the inclusion criteria of the participants. The exclusion criteria included degenerative disc disease, any disc pathology, and any spinal deformity or pathology as assessed by the Consultant Spinal Surgeon and the Consultant Musculoskeletal Radiologist

Table 4-1: The participants' inclusion criteria

Gender	Health status	Age	Body mass index	Pelvis circumference(cm)	
		Mean ±SD	Mean ±SD	Mean ±SD	ICC
Male	Healthy	24.9±2.5	23±1.5	89.6±3.7	.87(.85-.90)

The body mass index was plotted according to the measurements of the height and weight of the participants. The height and weight of the volunteers were confirmed using a height and weight scale. The pelvic circumferences of the volunteers were obtained in cm using a measuring tape. Each subject also completed rotation MRI questionnaire and shoulder pain questionnaire (Appendix A). The questionnaires

included the neck, shoulder, arm, leg and back pain and disability scales. Any subject who obtained the best healthy back, neck and shoulder qualified for the scan.

After the questionnaires, the subjects who completed lower back and shoulder pain questionnaires (Appendix A) with the full healthy score were asked to position themselves on the MRI holder mimicking the low trunk rotation position during the scan for 30 minutes to check whether they could maintain the scan position with a pain-free back (Appendix A). Those subjects who felt generally comfortable were informed of the scanning procedure in writing and given a consent form to sign if they were happy to continue with the study.

4.3 Subject Positioning

The subject was positioned at neutral and rotation positions during the study. The neutral position involved the subject lying supine with their hands leaving on both sides of the body. During the rotation position, the subject was instructed to flex their left knee. Consequently, the subject's right knee was slightly flexed. Then, the subject's left pelvis rotated to the right to reach the side position. The left leg was forced towards the centre of the body fulcrum as shown in Figure 4-1.

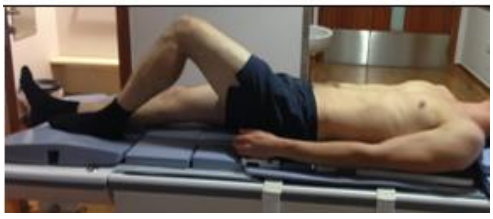

Figure 4-1: Start of rotation

4.4 Controlling the Lower Trunk Rotational Angle

As previously mentioned in the literature review, the range of motion of the shoulder and pelvis are crucial factors to continue a flexible dynamic trunk motion. The lower trunk rotational angle will be controlled depending on determination the right and left scapula positions, and on measuring and controlling the pelvis rotational angle.

4.4.1 Measuring the Scapula's Position During Lower Trunk Rotation

The position of the right and left scapula was determined according to the position of the right and left posterior borders of the acromion processes. The position of the right and left posterior borders of the acromion processes were measured as the distance between the posterior border of the acromion process and the shoulder board of the MRI holder using a tape (Nijs et al. 2007) as shown in Figure 4-2. The bony prominences of the right and left posterior borders of the acromion processes were confirmed by palpating fingers and according to the suggestion by (Cael 2010), who stated that the palpation of the acromion process was done by located the clavicle and palpated its most lateral edge, then palpated laterally and posteriorly onto the rounded point of the shoulder, which is formed by the acromion.

Figure 4-2: The measurement of the distance between the posterior border of the acromion process and the shoulder board using a tape.

4.4.2 Measuring and Controlling the Pelvic Rotational Angle using an Adaptive Goniometer and the MRI Holder

To position the volunteer properly and quantitatively during the scan with a determined angle of low back rotation, the pelvic rotational angle was measured and controlled using an adaptive goniometer and a novel MR holder. The adaptive goniometer and the novel MR holder have been designed and manufactured in the mechanical workshops of the School of Engineering, Cardiff University.

A- Designing and manufacturing the adaptive goniometer

An adaptive goniometer was used to quantify the degree of low trunk rotation depending on measuring the pelvis rotational angle. This goniometer was adapted from the universal goniometer. Solid Works software (2018) was used to design the adaptive goniometer. The goniometer can stand on a reference bar, with a dial installed on the goniometer to read the angle between the measuring bar and the reference bar. There is a screw at the centre, which can hold the measuring bar for reading, as shown in Figure 4-3. Figure 4-4 shows the final version of an adaptive goniometer that was manufactured using the laser sintering technique.

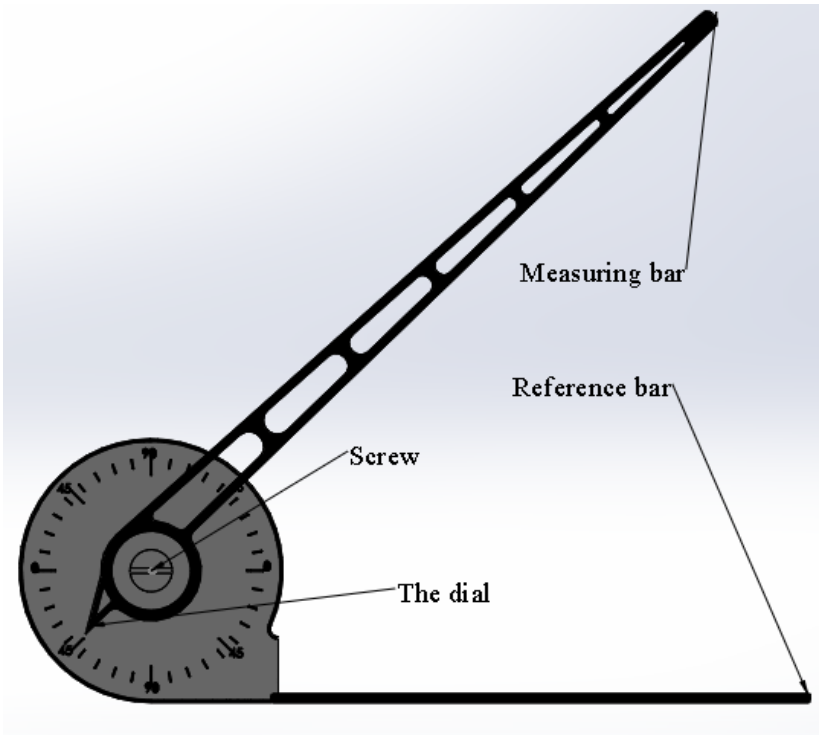

Figure 4-3: Diagram of the adaptive goniometer

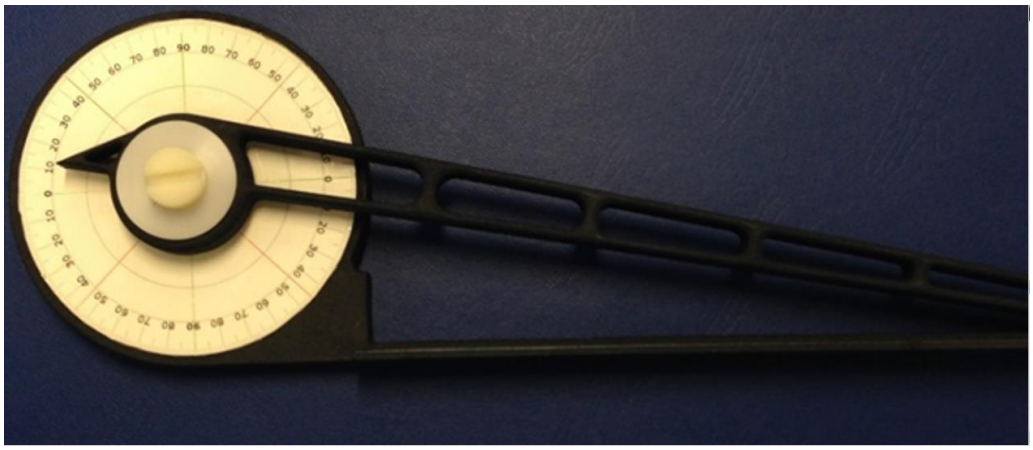

Figure 4-4: The final version of the adaptive goniometer

B- Designing and manufacturing the MRI Holder

There are four aspects that highlight the biomechanical importance and function of the novel MRI holder:

1. Holding and fixing the volunteer's pelvis to maintain the controlled angle allows reproducibility. In detail, the MRI holder was used to fix and maintain the volunteer's pelvis angle of rotation which was measured by the adaptive goniometer (4.3).
2. Maintaining a comfortable, good body-balanced position during a long period of time for the MRI scan using a curved shaped cushion and fixators. This good body-balanced position could participate in preventing motion artefacts in the MRI.
3. The MRI holder can be used to position both the left and right sides of the human pelvis.
4. To suit the need of easy fabrication and MR compatibility, nylon has been used to make the MRI holder. Nylon has excellent surface resolution and low humidity absorption.

Because the MRI holder will be used inside the MRI scanner, the dimensions of the MRI holder were subject to the size of the MRI bore of the scanner and body coil, the parameters follow:

- The diameter of the bore of the MRI scanner =60 cm,
- The width of the body coil (table top) =39cm,

- Edge of the body coil to the edge of the bore = 8 cm,
- Body coil to the top of the bore (strip lights) = 39 cm.

The MRI holder has been designed in the mechanical workshops of the School of Engineering, Cardiff University using Solid Works software (2018).The MRI holder consisted of two parts made up of the shoulder board, pelvis board and the pelvis support. The pelvis support was bolted perpendicularly to the pelvis board using adjustable pins (Figure 4-5). The MRI holder was manufactured using selective laser sintering. Selective laser sintering is an additive layer manufacturing technique which allows low-volume rapid prototyping of irregular shapes on a rigid material. Finally, packed foam has been fixed to the holder apparatus and added to the final version of the MRI holder (Figure 4-6).

The MRI holder was used in such way that the subject was positioned with the shoulder and the upper trunk placed on the shoulder board, while the lower trunk and hip were placed on the pelvis board (Figure 4-9).

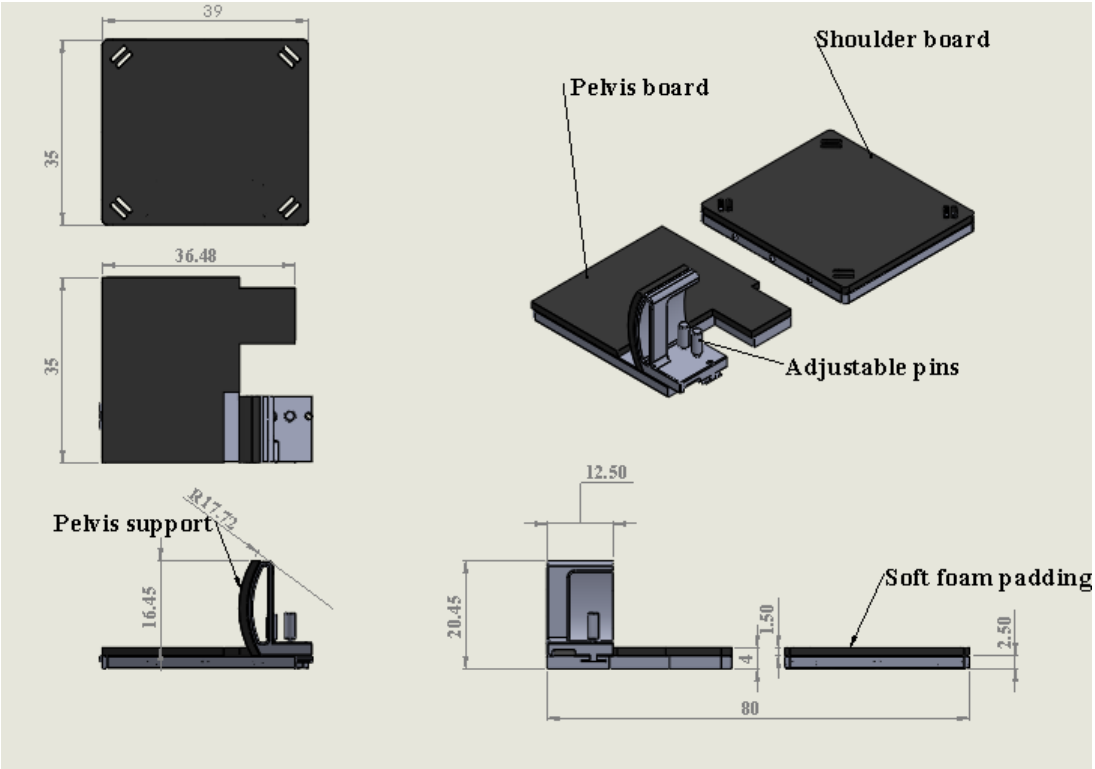

Figure 4-5: The MRI holder consisting of the pelvis board, pelvis support and shoulder board.

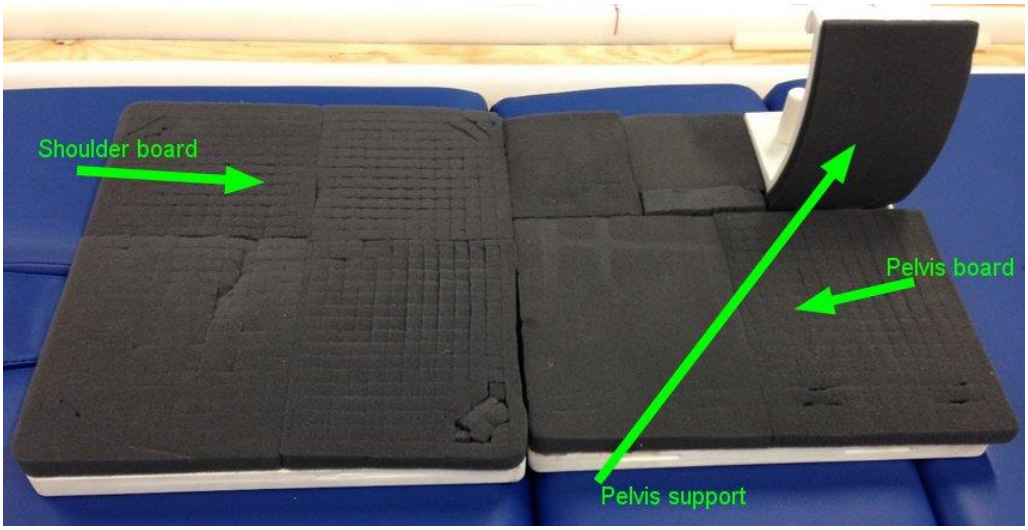

Figure 4-6: The final version of the MRI holder. The pelvis support is fixed on the pelvis board, while the shoulder board is separated from the pelvis board.

C- Determination of the rotational angle of the pelvis using an adaptive goniometer and a novel MRI holder.

First, the pelvis support of the pelvis board was removed to permit free actively rotation of the subjects. The rotational angle of the pelvis was measured according to the location of the right and left posterior superior iliac spines and relative to the horizontal plane by using the modified goniometer (Figure 4-7). In detail, the bony prominences of the right and left posterior superior iliac spines was determined a according to the suggestion by (Cael 2010), who stated that the localisation of the posterior superior iliac spine can be done by locating the iliac crest with the fingers and followed the crest posteriorly onto the posterior superior iliac spine-the most prominent projection is just lateral to the sacrum. After measuring the pelvis rotational angle, the pelvis support was inserted into the pelvis board through the slide portion and fixed using pins in such a position that the superior medial edge of the pelvis support was fixed and aligned with the level of the coccygeal cornu to maintain the free rotation of the L5-S1 level (Figure 4-8). Figure 4-8 shows the actions of the shoulder and pelvic during lower trunk rotation.

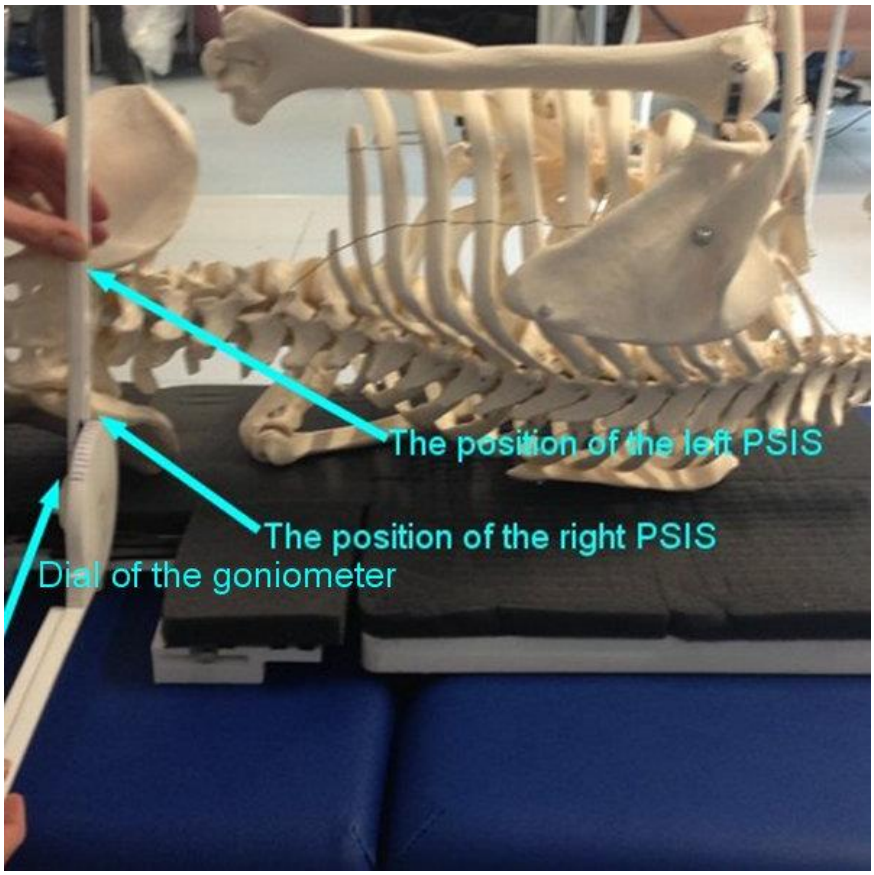

Figure 4-7: Determination of the pelvic angle of rotation depending on the position of the right and left posterior superior iliac spines and relative to the horizontal plane

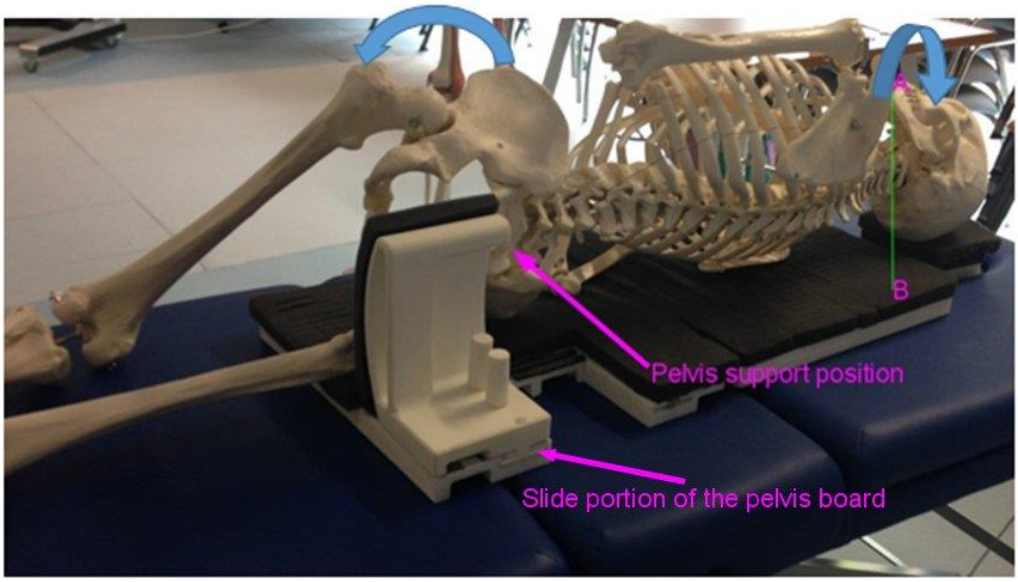

Figure 4-8: Shows the fixing of the pelvis support into the pelvis board. As well as the actions of the shoulder and the pelvic during lower trunk rotation; the right arrow shows the line of shoulder action, the left arrow shows the line of pelvis action.

4.4.3 Subject Positioning Measurements

Before starting the MRI scan, the position of the subjects on the MRI holder was checked by using the previously mentioned measurements of the scapula position and the pelvic rotational angle (Sections 4.4.1 and 4.4.2). The distance between the posterior borders of the right and left acromion processes and the shoulder board of the MRI holder (scapula position) were repeated three times. The distances measurements were taken for neutral, first rotation, second rotation and third rotational positions ($\boldsymbol{n1}, \boldsymbol{r1}$, $\boldsymbol{r2}$, and $\boldsymbol{r3}$) and for left and right scapula($\boldsymbol{DL\ and\ \ DR}$).

In addition, the measurements of the rotational angle of the right and left posterior superior iliac spines (pelvis rotational angle) were done three times. The pelvis rotational angle measurements ($\boldsymbol{A_{r1}\ and\ A_{r2}}$)were taken only for the first (mean 90^0.7) and second (mean 65.5^0) rotational positions

The pelvis rotational angle for the neutral and third rotational position (mean 43 ^{o}) was not measured using the adaptive goniometer because there was a difficulty to position the measuring arm of the adaptive goniometer with the right and left posterior superior iliac spines.

Therefore, the third pelvis rotational angle (mean 43 ^{o}) was checked depending only on the position of the right and left scapula and later this angle of pelvis rotation (mean 43^o) was confirmed by using MRI (5.4), as shown in Table 4-2 and Figure 4-9 .

All of these measurements were done for the second, third and fourth groups of the MRI scans. The first group of MRI scan performed the lower trunk rotation with using a foam pad to hold the subject still during the MRI acquisition (Figure 4-10).

Table 4-2: Subject positioning measurements

Parameters	**Neutral**	**Rotation (90^0.7)**	**Rotation (65.5^0)**	**Rotation (43^0)**
Distance between the left-posterior border of the acromion process and the shoulder board	$\boldsymbol{DL_n}$	$\boldsymbol{DL_{r1}}$	$\boldsymbol{DL_{r2}}$	$\boldsymbol{DL_{r3}}$
Distance between the right-posterior border of the acromion process and the shoulder board	$\boldsymbol{DR_n}$	$\boldsymbol{DR_{r1}}$	$\boldsymbol{DR_{r2}}$	$\boldsymbol{DR_{r3}}$
Angle between the left and right posterior superior iliac spines and the horizon		$\boldsymbol{A_{r1}}$	$\boldsymbol{A_{r2}}$	

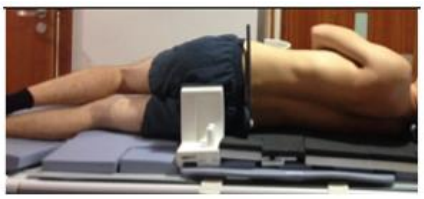

First rotational position (Mean pelvic angle using goniometer (90^0.7))

Second rotational position

(Mean pelvis angle using goniometer (65.5^0))

Third rotational position

(Mean pelvic angle (43^0))

(Depending on scapula position and MRI)

Figure 4-9: Subject rotation at various positions assisted by the MRI holder

Figure 4-10: First rotational position without using MRI holder

4.5 MRI Equipment, Protocol and Scans of the Subjects

4.5.1 MR Equipment

The experiments were performed with a 1.5-T MRI scanner (Signa HDxt Imager; GE Medical Systems, USA) located at Cardiff Bay Hospital to scan each subject, as seen in Figure 4-11.

The GE HDxt 1.5 Tesla is an advanced type of GE Signa HD series of 1.5T MRI scanner. This MRI machine consists of a homogeneous 1.5T magnet that produces a

field of view of 48 cm using sixteen channels of resonant frequencies. The bore size of the Signa HDxt Imager can offer safety and comfort for the patient (60 cm). The GE HDxt has 8- channel body array coils. These high definition coils use a parallel imaging technique, which offers 48 cm converges and good visualisation. Therefore, in this MRI scanner, high signal-to-noise ratio and closer radio frequency pulses to the region of interest can be obtained (University of Nottingham 2018).

Figure 4-11: Scan of the subject using GE medical system device in Cardiff Bay Hospital

4.5.2 MRI Protocol

T1- and T2-weighted images were both obtained for providing different and complementary information of the same subject. In comparing sagittal T2 with sagittal T1, sagittal T2 can better visualise the spinal cord, cauda equine nerve roots, intervertebral foramen and epidural fat tissue. In contrast, sagittal T1 is good at detecting degenerative endplate changes and differences between osteophytes and disc material with or without posterior disc protrusion.

Axial T2 is preferred in detecting the nerve roots in relation to the disc structure. In turn, the three-dimensional MRI can adjust and acquire thin slices with a high signal-to-noise ratio, which provides detailed morphologic data and observations from multiple directions (Van Goethem 2010; Takashima et al. 2016).

The MRI Protocol of the current study was developed by the Consultant Spinal Surgeon and the Consultant Musculoskeletal Radiologist at the University Hospital of Wales. The MRI Protocol divided into:

1- Performing standard supine MRI lumbar spine T2 sagittal, T2 coronal and T2 Axial 3D cuts acquisition (30 minutes) using a built-in body coil positioned about 5 cm above the iliac crest to centre the region of interest to the bore of the magnet and to include the conus medullaris and the sacrum within the field of view. The MRI holder was used to hold the subject in position.
2- Performing four lower trunk rotational positions with unrestricted left and right shoulder movements. T2 Sagittal, T2 coronal and T2 Axial 3D cuts acquisition (30 minutes) using a body coil, holder and beanbag to minimise motion artefact.

The MRI acquisition parameters were obtained as follows:

1- Four signals were acquired.
2- 3D T2- weighted images:
   A- Fast spin-echo images [2000/ 60 (TR/ET)],
   B- The field of view was 230,
   C- The image matrix 288 X224,
   D- The slice thickness was 1mm,
3- Sagittal T2 weighted images,
   A- The image matrix 488 X224.
   B- The field of view was 320.
   C- The slice thickness was 4mm.
   D- Fast spin-echo images [6580/9680 (TR/ET)].

4.5.3 MRI Scans of Different Positions

A total of 27 healthy male volunteers aged (24.9 ± 2.5), BMI (23 ± 1.5) with no previous back problems or interventions were scanned for 30 minutes to obtain T2 sagittal, T2 coronal and T2 axial 3D cuts in a neutral position. Four subjects were diagnosed as not having well-hydrated lower lumbar intervertebral discs. Two subjects were excluded from the data because the images had noise and motion artefacts. The remaining scanned subjects (21subjects) were divided into four groups:

1. The first scanned group (seven volunteers) were scanned for 30 minutes (T2 sagittal, T2 coronal, T2 Axial 3D cuts). This scanned group performed lower trunk rotational angle (mean 88^0) without using the MRI holder.
2. The second scanned group (five volunteers) were scanned for 30 minutes (T2 sagittal, T2 coronal and T2 Axial 3D cuts) for the first rotational positions using the MRI holder (mean 87.5^0).
3. The third scanned group (five volunteers) were scanned for 30 minutes (T2 sagittal, T2 coronal and T2 Axial cuts 3D) for the third rotational position using the MRI holder (mean 66^0).
4. The fourth scanned group (four volunteers) were scanned for 30 minutes (T2 sagittal, T2 coronal and T2 Axial 3D cuts) for the fourth rotational positions using the MRI holder (mean 44.9^0).

The difference in the numbers of the MRI scanned groups (second, third, and fourth) could be related to the excluded number of the subjects (six volunteers) because the excluded subjects were planned to perform the first (with using MRI holder), second and third rotational positions (Figure 4-12).

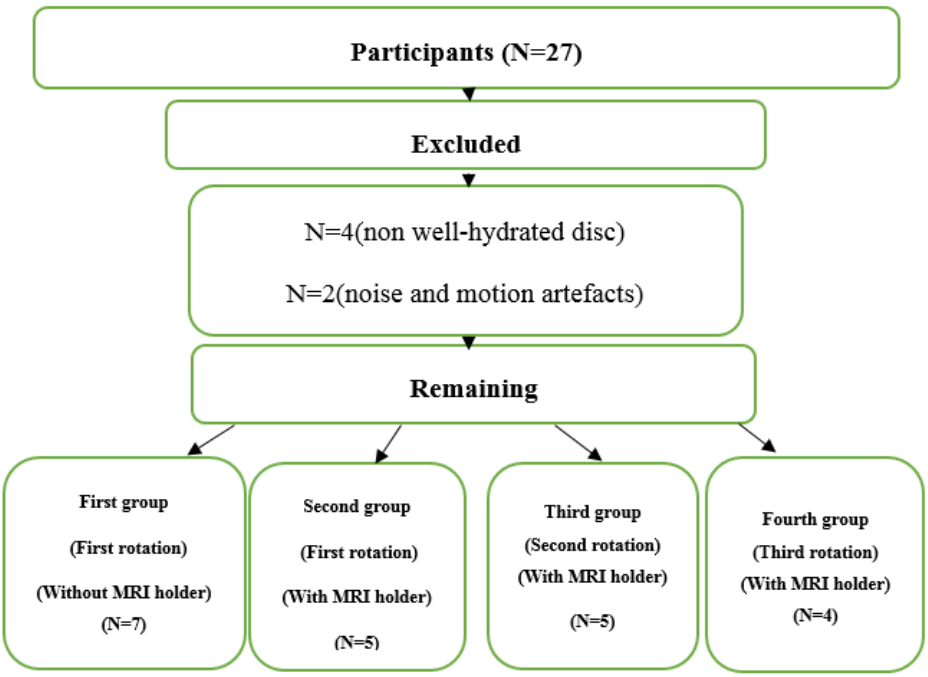

Figure 4-12: MRI scans at different positions

4.6 Image Analysis and Data Collection

4.6.1 Image Analysis Using Image J Software.

MRI data was saved in a DICOM format and transferred to Image J software (V1.49P; National Institutes of Health, Bethesda, USA). There are several advantages of using an MRI formatted using DICOM:

1- The MRI can be directly obtained from imaging equipment and Picture Archiving and Communication System (PACS) storage without any intermediate steps.
2- Valuable information can be included and stored through the DICOM headers, such as scan parameters (TR, field of view, slice thickness). Later, these MRIs formatted in DICOM can be used in image analyses and error checking (Barboriak et al. 2005).

Image J is open source software that is written in Java. This version was developed by the National Institutes of Health (Collins 2007; Schneider et al. 2012). Image J was designed with the developed macros and plug-ins, which can be download to the Image J folder, and recordable macros. It can acquire, display, edit, analyse, process, save and print 8-bit colour and grayscale, 16-bit integer and 32-bit floating point images.

Regarding the MRI images of the human spine, Image J can highlight ambiguous details in an image to carry out all analysis and processing functions that operate at any magnification factor (Rasband and Ferreira 2012).

Many studies have computed their results using Image J as reliable image processing software. (Liu et al. 2006) measured the facet joint articulation overlap in the sagittal plane, (Mendieta 2016) applied the segmentation technique to filter lumbar MRI images, while (Meakin et al. 2008) measured the total and inter-segmental lordosis angles. The images magnified by 300% and were contrast-enhanced using histogram equalisation and normalisation. In addition, (Fazey et al. 2010) identified and marked the corners of each vertebral body from L1 to L5, while (Fortin et al. 2017) obtained the paraspinal muscle composition measurements by using a manual thresholding technique in NIH Image J software. In the present study, the lumbar spine and pelvis parameters were analysed using Image J software.

4.6.2 Pre-processing Techniques

As mentioned in the literature review, images with poor contrast between soft tissue structures and bone can affect the precise localisation of the anatomical landmarks, particularly the muscle tendons and ligamentum flavum attachments. In addition, the anatomical landmarks on both sides of the lumbar vertebrae cannot be observed on the same axial cut of the MRI images, such as the left and right tips of the transverse processes, as a result of vertebral rotation. Therefore, it was necessary to consider pre-processing the MRI images in order to obtain precise measurements of the selected landmarks.

The pixel size on the image was determined according to the reference scale on the MRI image, as shown in Figure 4-13. Contrast enhancement was obtained to equalise the histogram by using contrast stretching with a saturating pixel percentage of 70. Then, the area of interest was outlined using a freehand selection tool to update the contrast of the entire image and to obtain the obvious landmarks (Figure 4-14).

An unsharp mask filter with a radius of 4 pixels and mask weight of 0.6 was selected to overcome the low signal-to-noise ratio in the MRI images. This technique can subtract the blurred image and rescale it to maintain the same contrast of the large structures in the same original image, such as the sacroiliac region.

Figure 4-13: Determination of the pixel size

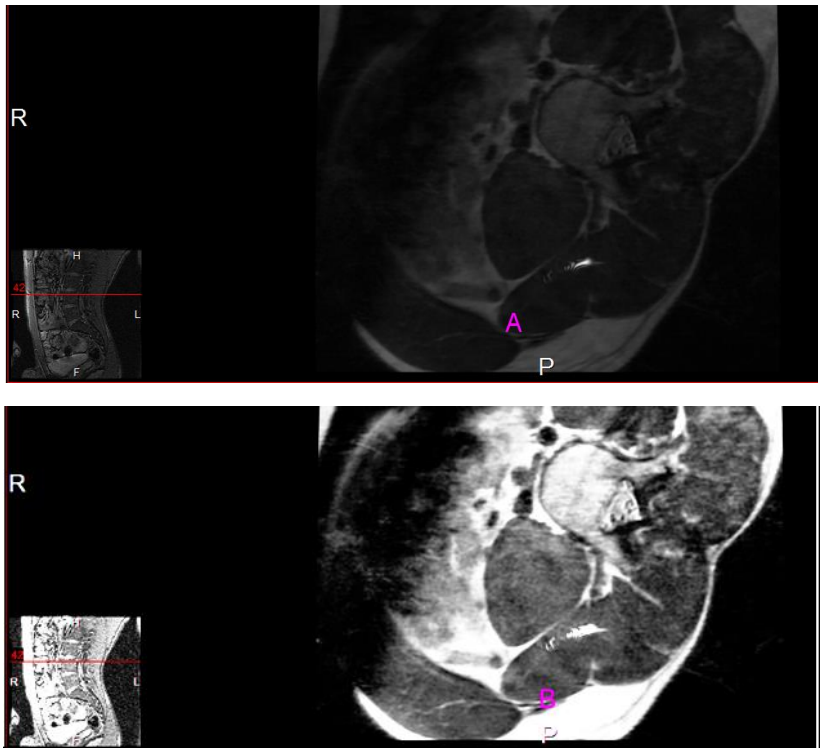

Figure 4-14: The original (A) and the contrast-enhanced image (B)

4.6.3 Quantification of the Sacroiliac Joints and Lumbar Parameters Using MRI

The following parameters were measured for each subject in each performed position from the analysed image. Definitions of the measured parameters and the methods of their measurement are detailed in the following subsections.

A. The relation between the right and left posterior superior iliac spines and the last lumbar vertebrae and the relation between the left and right sacroiliac joints during lower trunk rotation.

The effect of the first trunk rotational position (first group) on the right and left-posterior superior iliac spines and the last lumbar vertebrae and the relation between the left and right sacroiliac joints were not obtained because most of the MRI did not include the sacroiliac joints.

In addition, because images artefacts were present, the data for three volunteers were excluded. T2 Axial 3D images cuts of four healthy males (group 2), four healthy males (group 3), four healthy males (group 4) and three healthy males (group four) were taken

to determine the relation between the posterior superior iliac spines and the L5 vertebrae, the left and right sacroiliac joints, relative to the horizon and according to four positions of the lower trunk. In the present study, three consecutive cuts were selected that showed three sections of the left and right sacroiliac joints. The first cut was obtained at the level of the sacral ala which included the lower part of the L5 – S1 disc. The second cut was measured at the level of S1- S2 vertebrae, while the third cut was obtained at S2-S3 level. An unsharp mask filter with a radius of 4 pixels and the mask weight of 0.6 was selected to clarify the borders of the sacroiliac joints. The measurement of the angle of the rotation of the L5 vertebra according to the horizontal plane was mentioned in Section 4.6.3 (C). A new technique was used to measure the angle between the right and left posterior superior iliac spines and the horizon by determining the lowest attached points of the erector spinae muscle tendons to the posterior superior iliac spines depending on using the pixel intensity values between 091- 094 %. This method proved to be highly accurate as the Intra-rater reliability was checked by repeated measurements (three times) (the Intraclass Correlation Coefficients ranged between 0.95 -1).

The rotational angle of the left and right sacrum relative to the horizon obtained by localising specific points on the wedges of the right and left sacrum, while the most superior and inferior points on the prominent surfaces of the ilium were determined to calculate the angles between the horizon and the superior and inferior borders of the ilium. Figure 4-15 showed the clarification of the selected landmarks for the measurements of the rotational angle of the L5, the right and left posterior superior iliac spines, and the sacrum and ilium.

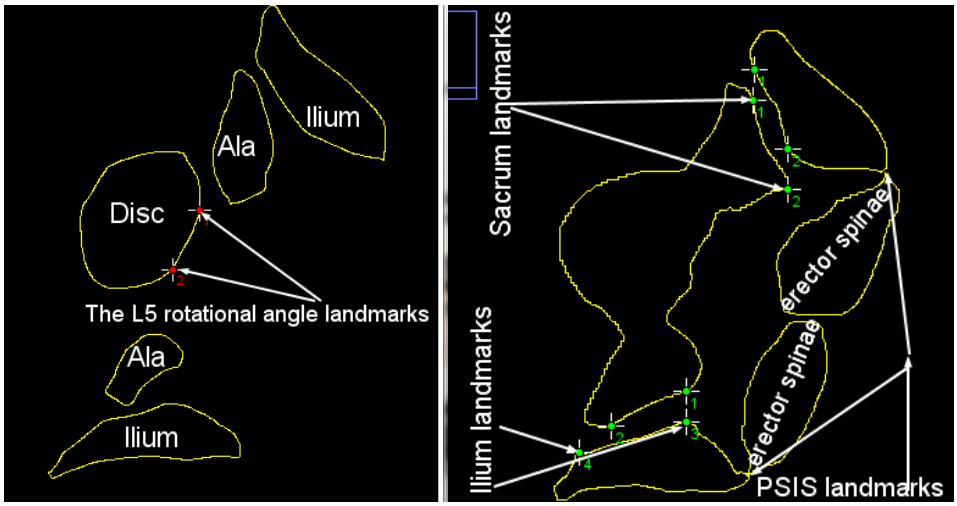

Figure 4-15: Determination of the anatomical landmarks

Figure 4-16 and Figure 4-17 showed the measurements of the rotational angle of the L5, the right and left posterior superior iliac spines, and the sacrum and ilium at three anatomical sections. Intra-rater reliability was checked by repeated measurements (three times) (the Intraclass Correlation Coefficients ranged between 0.99 -1).

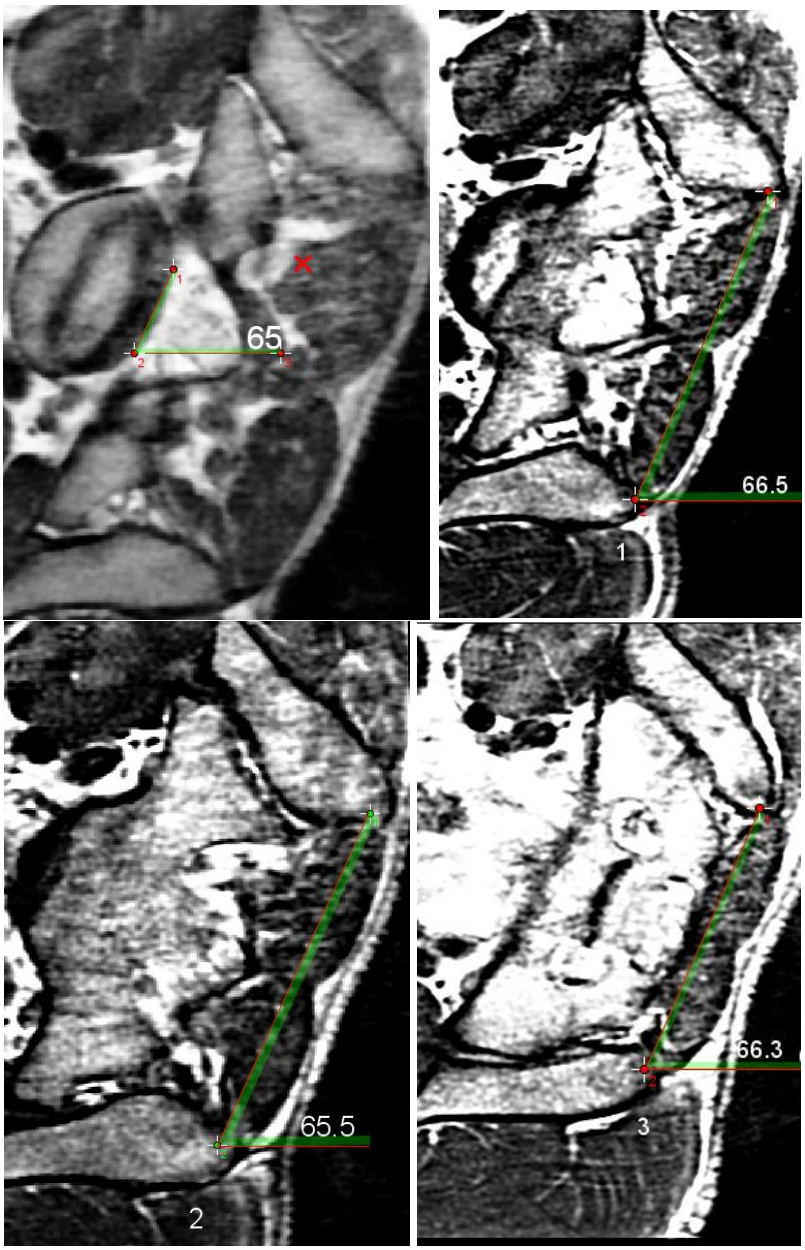

Figure 4-16: The angle between L5 and horizon (the upper left image), 1, 2, 3 images show the angle between the left and right posterior superior iliac spines at three sections.

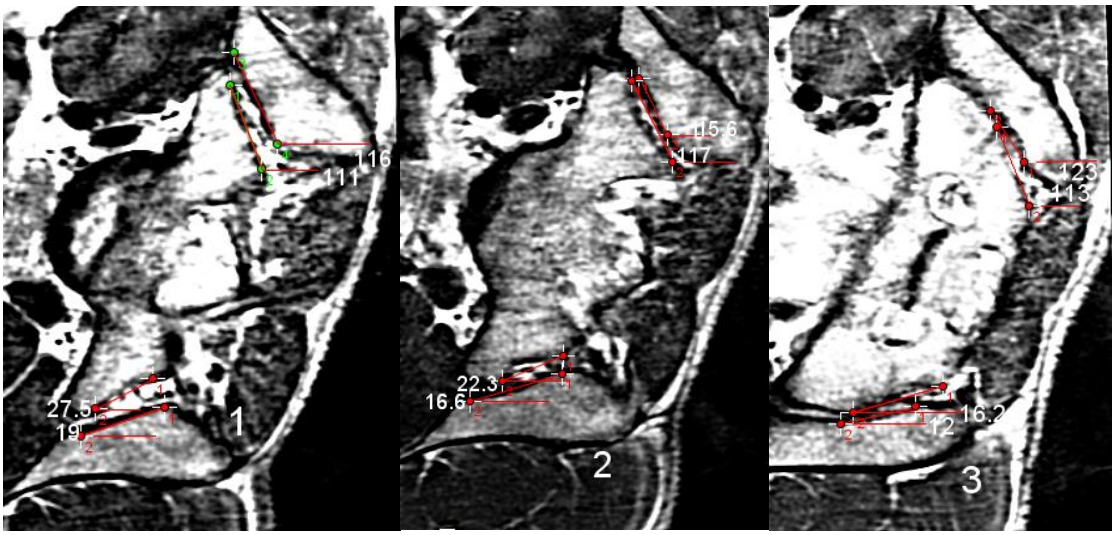

Figure 4-17: 1, 2, 3 images show the angle between the sacrum and the horizon and the angle between the ilium and the horizon according to three sections and two sides.

B. The angle of rotation of the lower lumbar spine vertebrae and the difference in the spinal canal depth during lower trunk rotation

The angle of rotation of the lower lumbar vertebrae (L3, L4, L5) relative to the horizontal plane during five different positions of the lower trunk was measured using T2 axial 3D image cuts of seven healthy males (group 1), five healthy males (group 2), five healthy males (group 3), and four healthy males (group 4).

The present study used a novel method to merge two selected cuts of T2 Axial cuts 3D acquisition. Synchronisation technique and the adjustment of histogram intensity values were used to merge two particular landmarks (left and right side) in one slice which are usually present separately in two cuts of MRI. A synchronisation tool from the Image J package was used to locate two anatomical landmarks at each selected cut by synchronising a mouse motion and input between multiple windows. The first cut was made at the end of the pedicle (the most posterior point) and parallel to the upper-end plate which showed the first obvious point of the left transverse process. At this cut, the angle of rotation was represented by the intersection of two lines: the first line was represented by the horizon, while the second line was drawn between two anatomical points. The first point was represented by the attachment of the left pedicle with the left superior articular process and the second point was represented by the attachment of the

right pedicle with the right superior articular process. In contrast, the second cut was made at the middle of the pedicle and parallel to the upper end plate, which showed the last right apparent point of the transverse process. At this cut, the angle of rotation was calculated between the horizon and two anatomical points: the first point was represented by the base of the left pedicle, while the second point was represented by the base of the right pedicle. The green shaded lines were plotted to clarify the thin lines of the angle tool, as shown in Figure 4-18 and Figure 4-19. The Intra-rater reliability was checked by repeated measurements (three times) (the Intraclass Correlation Coefficients ranged 0.93-1).

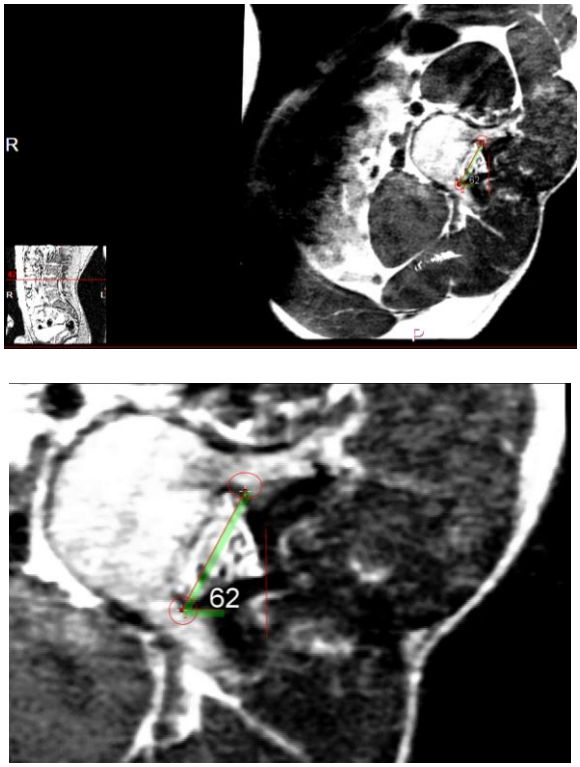

Figure 4-18: The top image shows the first selected cut and the determined anatomical points at L4 vertebrae in the third rotational position (R3). The bottom image shows the magnified version from the above one (300%).

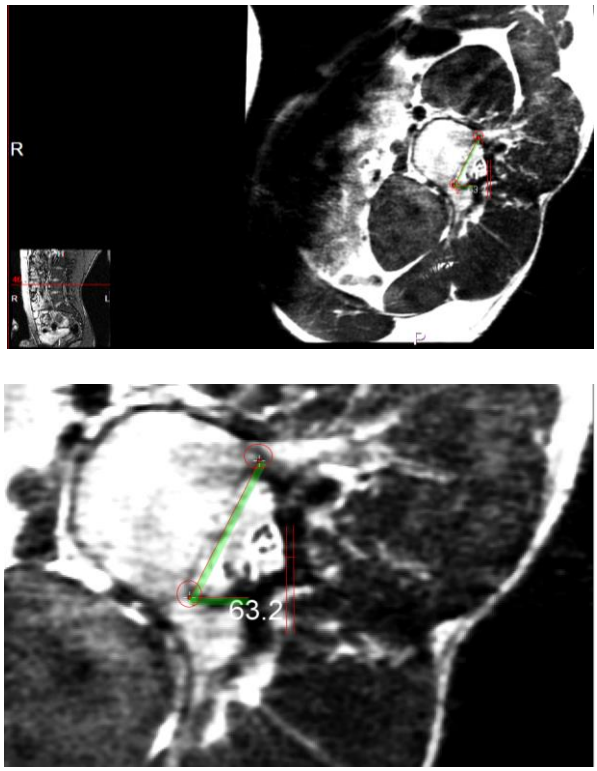

Figure 4-19: The top image shows the second selected cut and the determined anatomical points at L4 vertebrae in the third rotational position (R3). The bottom image shows the magnified version from the above one (300%).

The amount of compression of the dural sac at two depths of the spinal canal and according to each rotational position of the spine was quantified as the difference in the spinal canal depth between two selected cuts of MRI. The difference in the spinal canal depth between the first and second selected cuts was calculated by marking two freehand lines. The first line was plotted at the end of the spinal canal at the first selected cut, while the second line fitted with the end of the spinal canal at the second tested slice. The connecting line between these two lines represented the difference in the spinal canal depth and calculated in mm (Figure 4-18 and Figure 4-19). The Intra-rater reliability was checked by repeated measurements (three times) (the Intraclass Correlation Coefficients ranged 0.95- 1).

C. Effect of Trunk Rotation on the Dimensions of the Lumbar Intervertebral Discs and Neural Foramens: An In vivo MRI study.

The data for six volunteers were excluded because image artefacts were present. To determine the effect of two rotational positions of the lower trunk on the intervertebral

foramen and intervertebral disc, sagittal T2 weighted MRI of seven healthy males (group 1), four healthy males (group 2), and four healthy males (group 3) were taken.

Because there was a variation of angle of rotation according to the rotational positions (R1, R2 and R3) of each group and each subject, the area, width and height of the intervertebral foramen and disc were obtained by calculating the average of the measurements of two consecutive slices that showed the apparent nerve root, pedicles of the two articulated vertebrae, the most posterior- lateral point of the lower endplate of the upper vertebra and the obvious tip of the superior facet. A synchronisation tool and a particular saturated pixel percentage with a specific magnification power for each structure (disc and foramen) were used to obtain highly accurate measurements as these approaches can show the intervertebral disc and foramen morphology between numbers of MRI cuts more easily.

The measurements of the area, width, and height of the intervertebral disc were taken from the same cut as the foraminal measurements. The differentiation between the disc material and the adjacent longitudinal ligaments was a challenge. Therefore, a saturated pixel percentage of 70 with a magnification power of 600 % were found to be the most effective values to separate the outlines of the disc properly. The cross sectional area of the intervertebral disc was measured by outlining the borders of the disc using the freehand selection tool.

The posterior disc height was determined as the line connecting most nearest two points located on the right side of the lower and upper-end plate of two consecutive vertebrae, while the anterior disc height was calculated as the line connecting the most farthest two points positioned on the left side of the lower and the upper-end plate of two consecutive vertebrae. The intervertebral disc width was measured as the line connecting the most anterior and most posterior points on the outlined intervertebral disc area. Some examples are shown in Figure 4-22 and Figure 4-23.

The present study modified the technique obtained by Punjabi et al., 1983 to measure the height and width of the left and right intervertebral foramen according to the apparent selected landmarks of two slices of MRI which included: nerve root, pedicles of the two articulated vertebrae (1&2), the most posterior- lateral point of the lower endplate of the upper vertebra (3) and the obvious tip of the superior facet (4) (Figure

4-20 and Figure 4-21). This technique was used for each lower lumbar segment (L3-L4, L4-L5 and L5-S1). The cross-sectional area of the intervertebral foramen was measured in mm^2 by manually outlying the foramen boundaries using freehand selection tool. The freehand lines tool was selected to measure the height and width of the intervertebral foramen (Figure 4-22 and Figure 4-23).

Intra-rater reliability was checked by repeated measurements (three times). The Intraclass Correlation Coefficients ranged between 0.93 and 1.

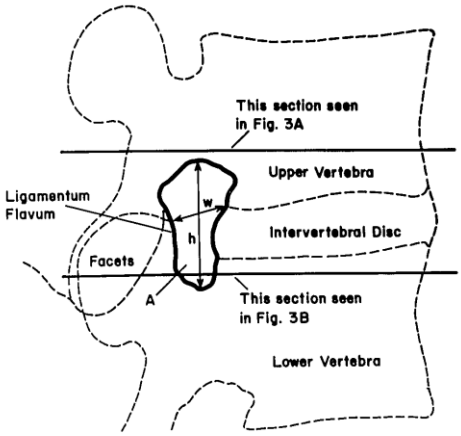

Figure 4-20: A, h, w shows the area, height and width of the vertebral foramen (after Punjabi et al, 1983)

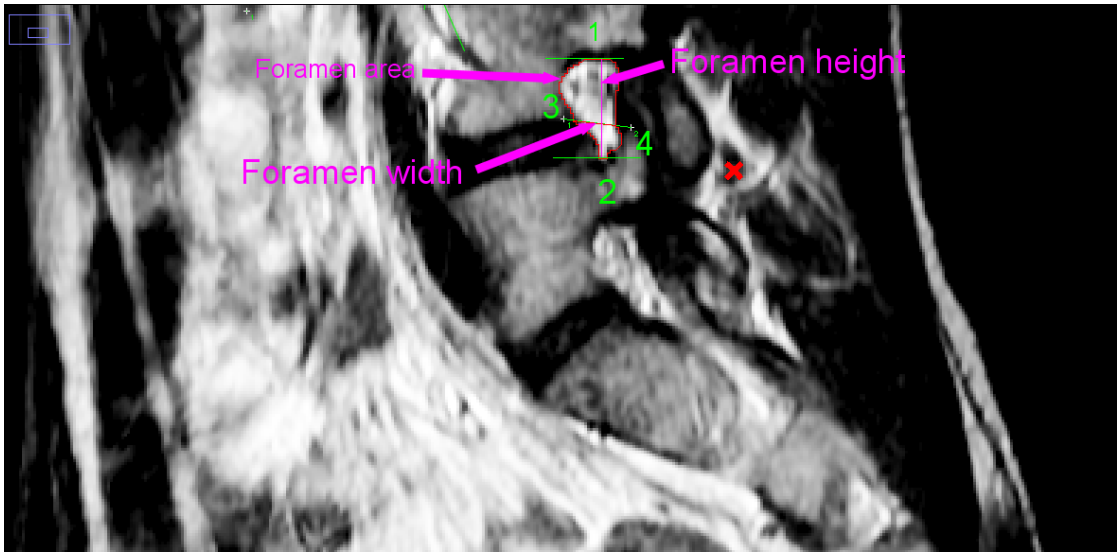

Figure 4-21: The selected landmarks for the width and height measurements of intervertebral foramen

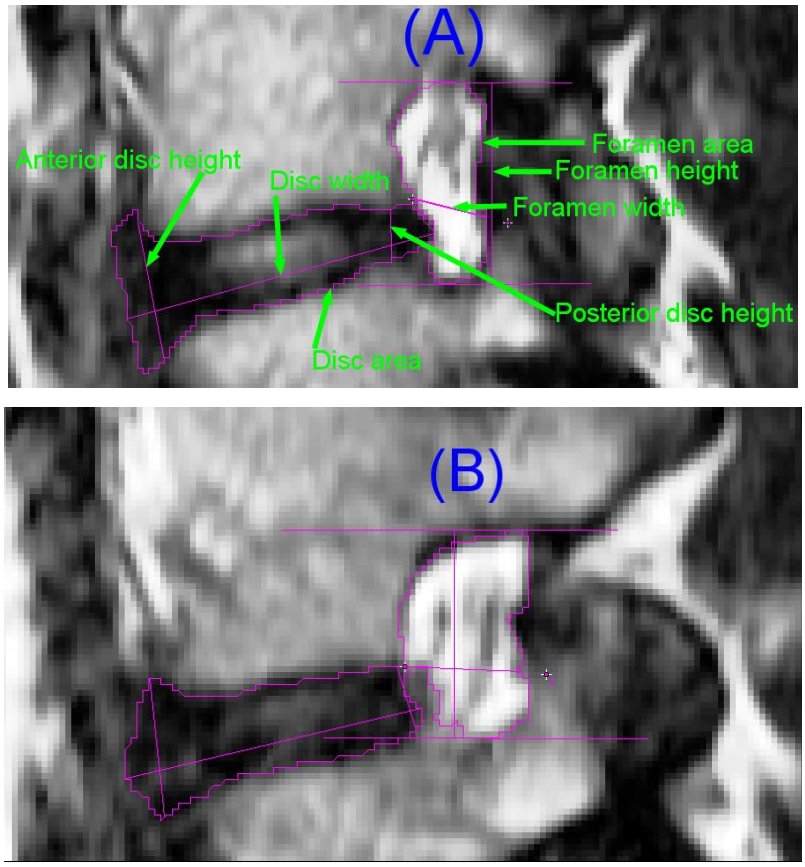

Figure 4-22: The measurements of the area, width and height of the left disc and foramen at L4-L5 level during neutral position in two selected slices (A and B).

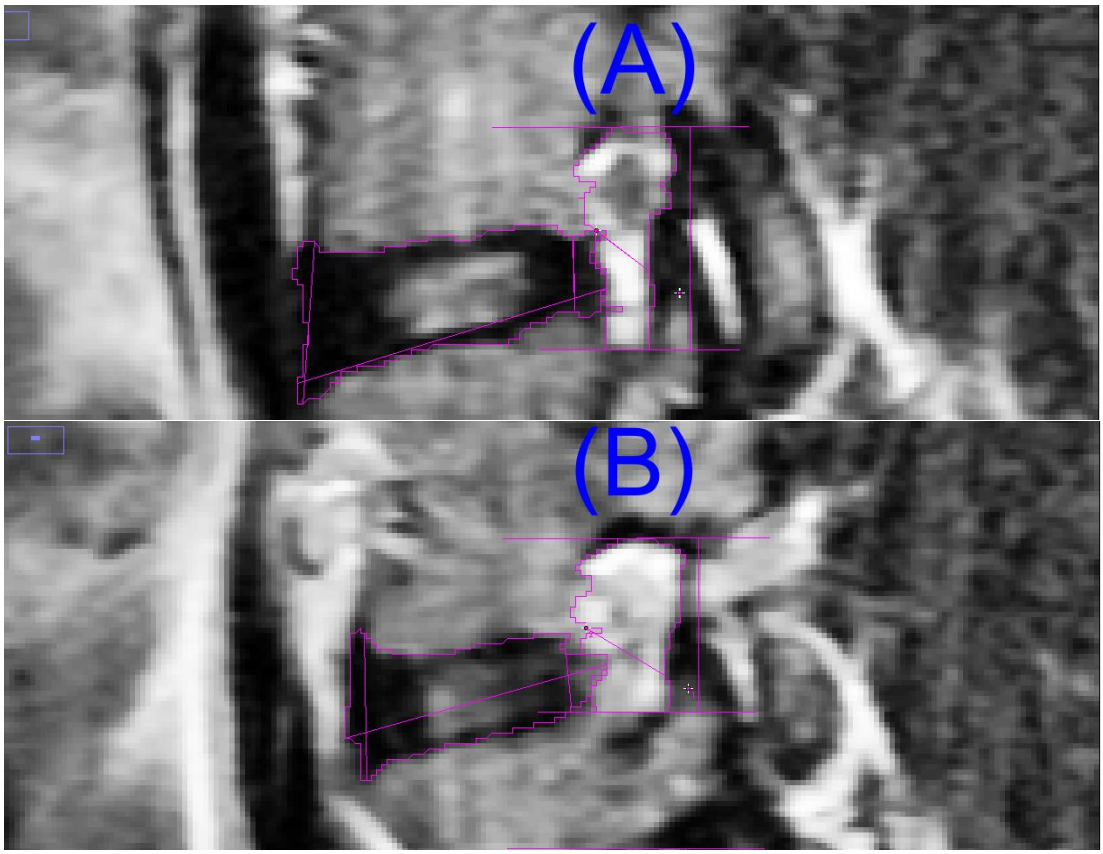

Figure 4-23: The measurements of the area, width and height of the left intervertebral disc and foramen at L4-L5 level during third rotational position (R3) in two selected slices (A and B).

D. The degree of lateral bending during lower trunk rotation

The data for six volunteers were excluded because image artefacts were present. To determine the effect of two rotational positions of the lower trunk on the degree of lateral bending during lower trunk rotation, sagittal T2 weighted MRI of seven healthy males (group 1), four healthy males (group 2), and four healthy males (group 3) were taken.

The lateral bending degree of each individual vertebrae was measured manually using the angle tool by selecting the mid-sagittal MRI and using a saturated pixel percentage of 70 with a magnification power of 300 %. This technique is based on the landmarks technique that was used by Been et al., 2011, which measured the lateral bending angle as the angle between two lines: the first line was fixed and parallel to the inferior

endplate of the superior vertebra and the second line was parallel to the superior endplate of the inferior vertebra, as shown in Figure 4-24.

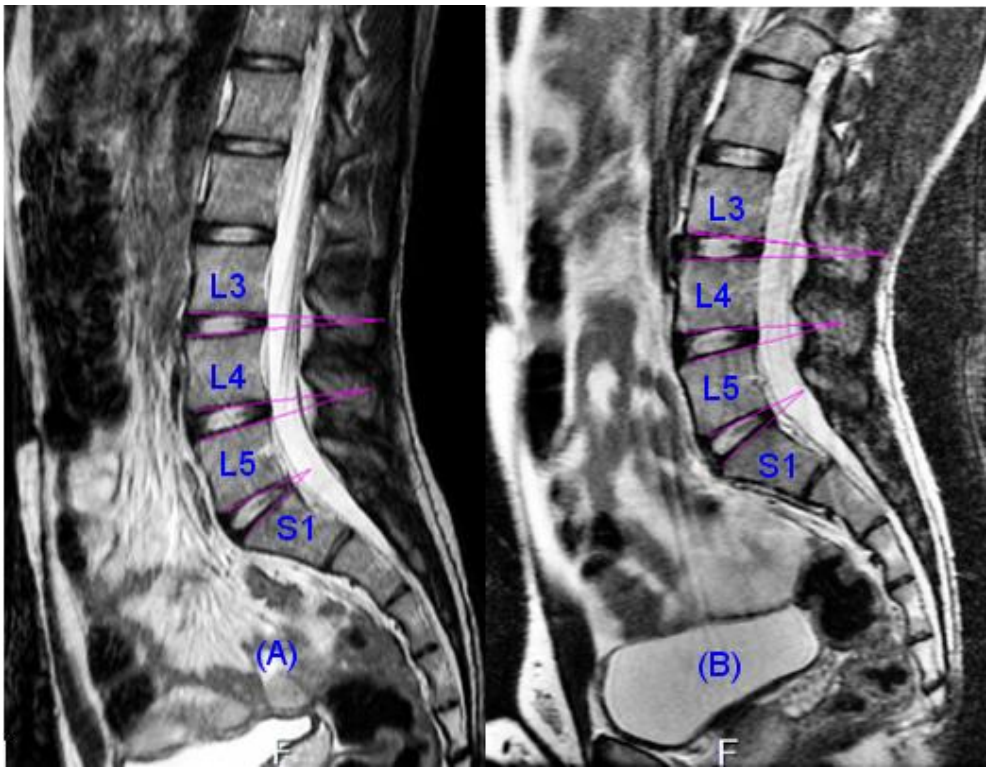

Figure 4-24: The measurements of the lateral bending at L3-L4, L4-L5 and L5-S1 lumbar levels during neutral (A) and third rotational positions (B)

E. The orientation angle of the left and right superior articular processes and the cross-sectional area of the gapping between the superior and inferior articular processes during lower trunk rotation.

The data for six volunteers were excluded because image artefacts were present. The effect of lower trunk rotation on the orientation of the superior articular process of the lower lumbar vertebrae relative to the intervertebral disc rotational angle, and on the cross-sectional area of the gapping between the superior and inferior articular processes were evaluated by using T2 axial cuts of three-dimensional images of five healthy males (group1), three healthy males (group 2), four healthy males (group3), and three healthy males (group 4). In the present study, a modified technique from Boden et al. (1996) was employed (Figure 4-25).

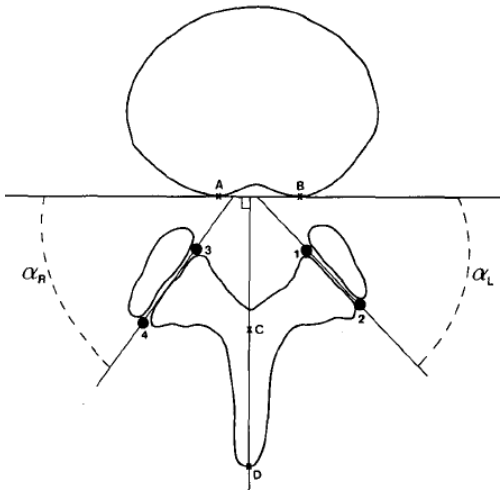

Figure 4-25: The technique used by (Boden et al. 1996), the disc reference line was defined by AB: the posterior aspect of the disc space or by a line drawn a perpendicular to the spinous process (C and D). The facet line was defined by two points were then used to define the margins of the left (1 and 2) and the right (3 and 4) facet joint. The angles αL and αR represent the left and right facet angles (Cited from Boden et al., 1996).

The modified technique was used to distinguish between the antero-posterior borders of the left and right superior articular processes, the ligamentum flavum and the capsular ligaments. In this technique, the synchronisation window tool was used to merge three consecutive cuts of the MRI. The first selected cut was made at the mid intervertebral disc and the second cut selected at the end of the disc (near the upper-end plate). In contrast, the third slice was obtained at the level of the upper end plate. Two fixed points were determined on the antero-posterior borders of the left and right superior articular processes at all selected slices. The first point was closest to the most depressed point of the dural sac, while the second point was at the end point of the superior border near the facet gapping (the most distal point of the superior articular process). The angle of rotation of the intervertebral disc was calculated at the second selected cut and pointed out by the left and right convex posterior disc margins and the horizon. The orientation angle of the left and right superior articular processes was obtained relative to the rotational angle of the intervertebral disc by using angle tool in Image J software as shown in Figure 4-26, Figure 4-27 and Figure 4-28. The measurements of the angle of the rotation at the at L5-S1 intervertebral disc level and the orientation angle of the superior articular process level were measured at the third selected cut because the third

cut showed the nearest point to the end of the disc befor the apperance of the endplate level. The Intra-rater reliability was checked by repeated measurements(three times). The Intraclass Correlation Coefficients ranged between 0.95 and 1.

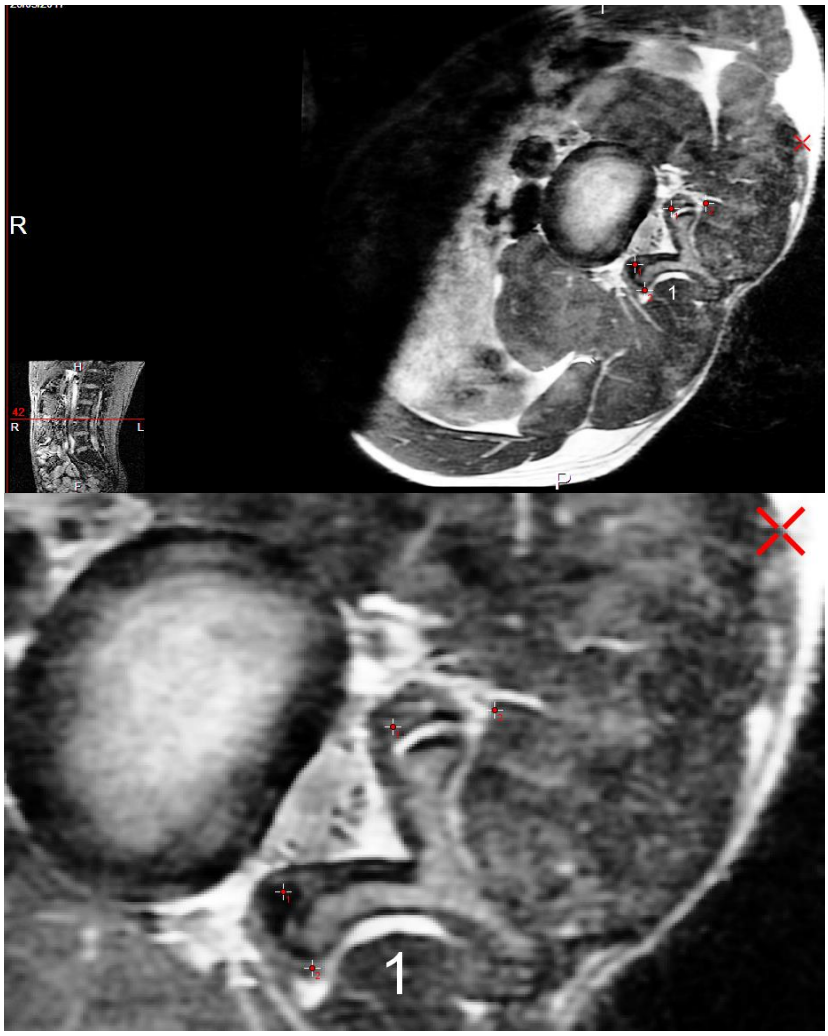

Figure 4-26: The top image shows the orientation of the left and right superior articular processes at the L3 level and the first selected cut. The bottom image shows the magnified version from the above one (300%).

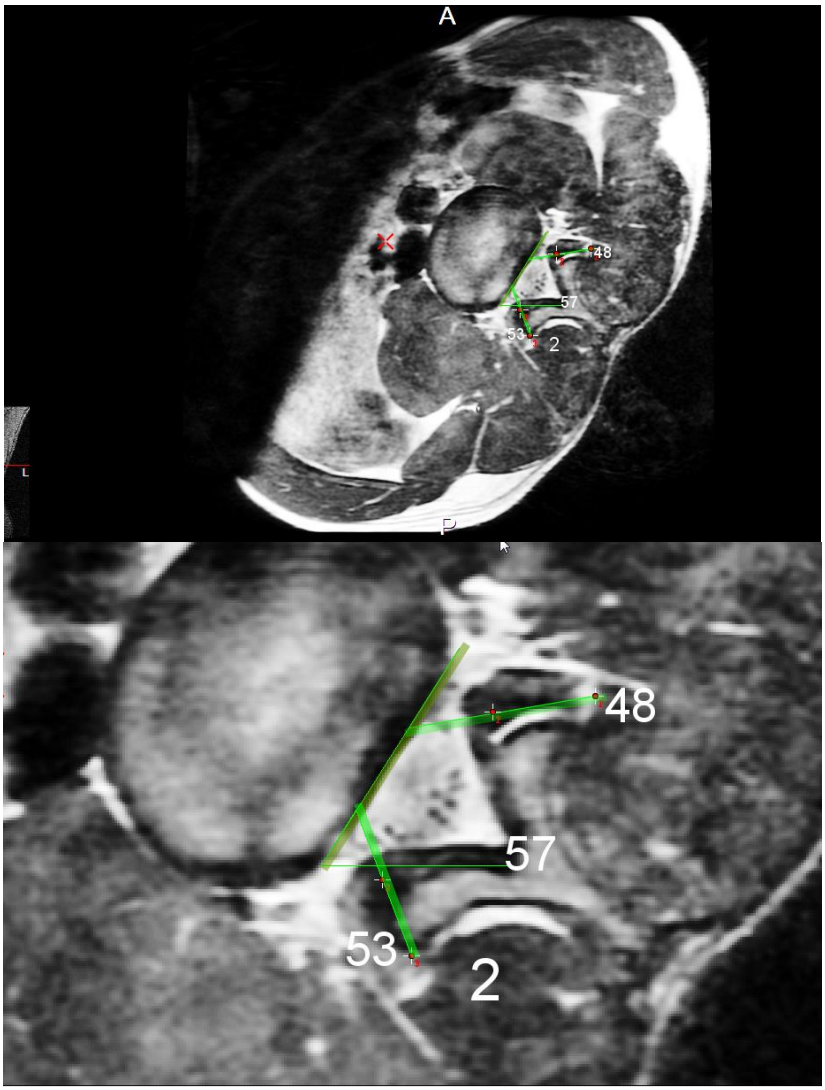

Figure 4-27: The top image shows the rotational angle of the intervertebral discs at L3 level , the orientation angle of the left and right superior articular processes at the second tested cut. The bottom image shows the magnified version of the above one (300%).

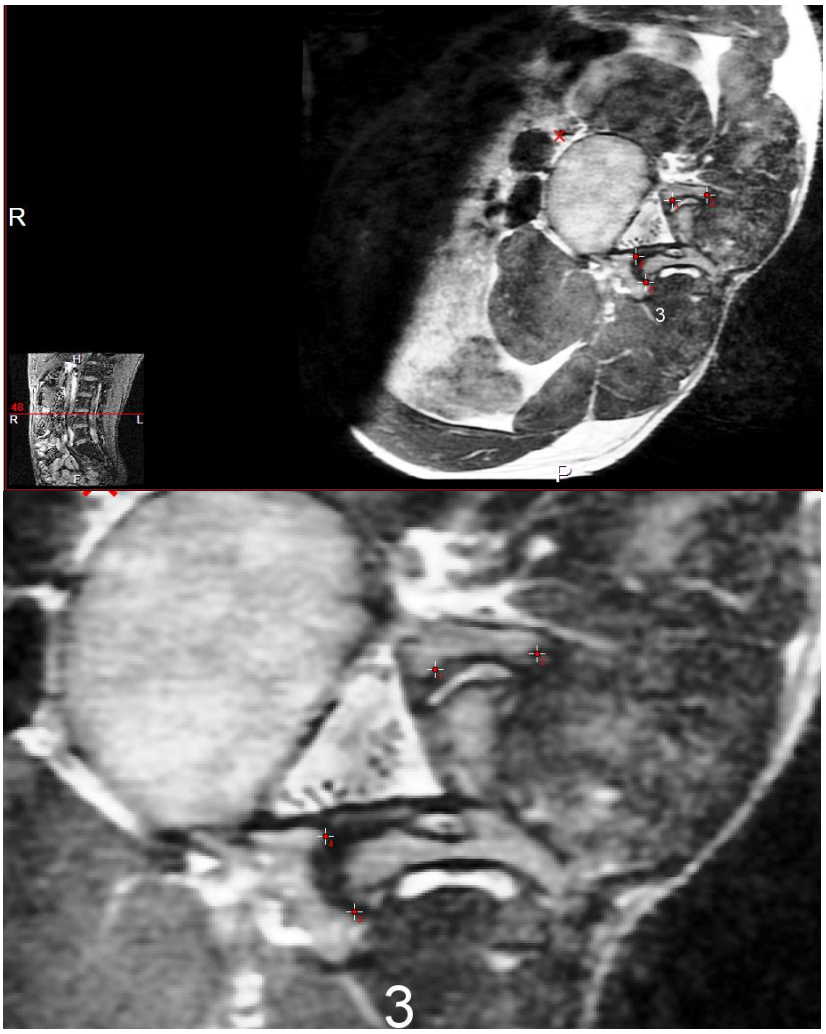

Figure 4-28: The top image shows the orientation of the left and right superior articular processes at the L3 level and the third selected cut. The bottom image shows the magnified version of the above one (300%).

The cross-sectional area of the gapping between the superior and inferior articular processes was obtained in mm^2 by adjusting the image brightness/contrast to 160 %, then the MR images were magnified 1200%. The boundaries of the gapping between the superior and inferior articular processes were drawn between the ligamentum flavum anteriorly and the joint capsule posteriorly, and between the superior and inferior articular processes using the freehand selection tool, as shown in Figure 4-29. The Intra-rater reliability was checked by repeated measurements (three times). The Intraclass Correlation Coefficients ranged between 0.97 and 1.

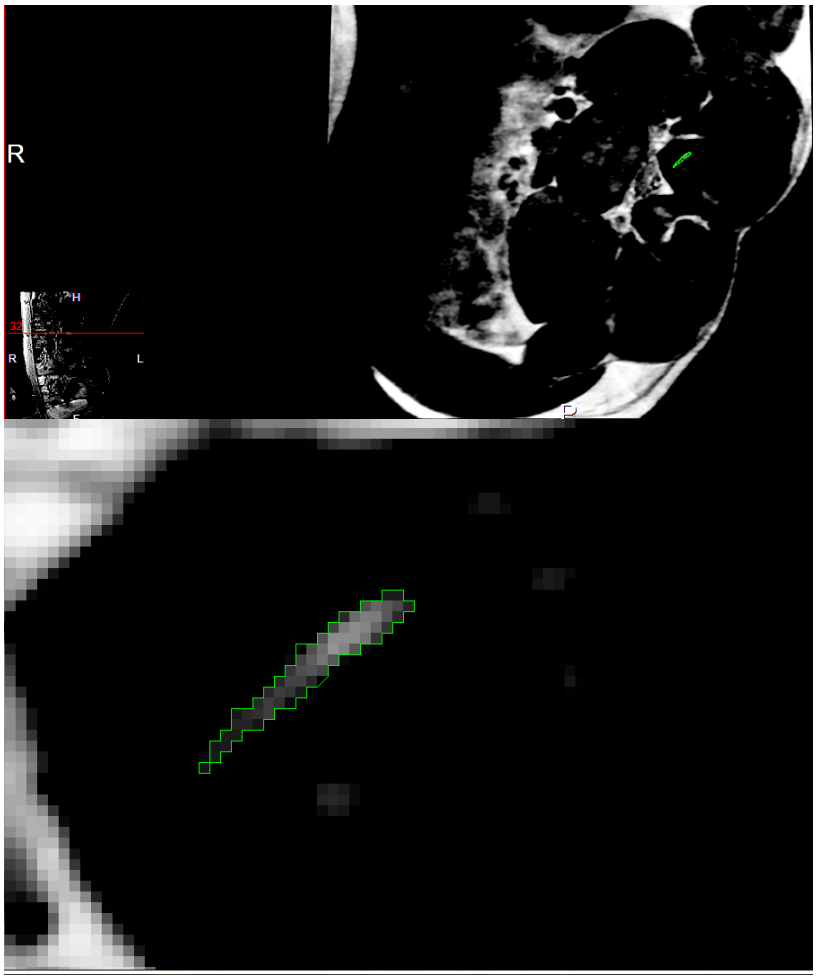

Figure 4-29: The measurement of the cross-sectional area of the opening distance between the superior and inferior articular processes using enhancing contrast technique after using a magnification power of 1200%((The bottom image shows the magnified version of the top image).

4.7 Statistical Analysis

The mean differences and P- values for the angle of vertebral rotation, the difference in the spinal canal depth, the facet orientation angle and the gapping distance, the relation between the rotational angle of the L5 and the rotational angle of the posterior superior iliac spines, and the relation between sacrum and sacrum according three sections were all obtained using MANCOVA and MANOVA.

Student's t-test was obtained to evaluate the mean differences and P- values of the intervertebral foramen, intervertebral disc and lateral bending parameters.

A matched paired t-test was used to evaluate the mean differences values and P- values of the distance between the posterior border of the acromion processes and the shoulder board of the MRI.

P-values and mean differences between the measurements from the MRI and the modified goniometer were obtained using analysis of variance (equality of means).

4.8 Summary

The performance of the shoulder and pelvis girdles are considered to be crucial factors that are necessary to continue flexible dynamic trunk motion. Accordingly, the lower-trunk rotational angle has been measured and controlled depending on determination the right and left scapula positions and on measuring and controlling the pelvis rotational angle by using a tap, adaptive goniometer and MRI holder.

A total of 21 healthy male volunteers aged (24.9 ± 2.5), BMI (23 ± 1.5) with no previous back problems or interventions were scanned for 30 minutes to obtain T2 sagittal, T2 coronal and T2 axial three-dimensional cuts in neutral position and for 30 minutes for each one of the three lower-trunk rotational positions. Exclusion criteria included degenerative disc disease, any disc pathology and any spinal deformity or pathology as assessed by the Consultant Spinal Surgeon and the Consultant Musculoskeletal Radiologist. Ethical approval was obtained from the University Ethics Committee in the School of Engineering. All volunteers provided written consent before participation in the study.

MRI data was saved in a DICOM format and transferred to Image J software (V1.49P; National Institutes of Health, Bethesda, USA). A synchronisation tool was used to merge more than one cut of the MRI. The pixel size on the image was determined according to the reference scale on the MRI image. Contrast enhancement was obtained to equalise the histogram by using contrast stretching with a saturating pixel percentage of 70, as well as, a determined magnification power was used. An unsharp mask filter with a radius of 4 pixels and mask weight of 0.6 was selected to overcome the low signal-to-noise ratio in the MRI images. These processing and analysis procedures were applied on the MRI using the Image J to obtain the obvious landmarks for the measurements of the following parameters:

1- The angle of rotation of the lower lumbar vertebrae.
2- The difference in the spinal canal depth.
3- The intervertebral disc and foramen dimensions.
4- The lateral bending angle of the lower lumbar vertebrae.
5- The orientation angle of the superior articular processes.
6- The gapping distance between the superior and inferior articular processes.
7- The rotational angle of the L5 vertebrae.
8- The rotational angle of the posterior superior iliac spines at three anatomical sections.
9- The rotational angle of the sacrum and ilium at three anatomical sections.

Intra-rater reliability was checked by repeated measurements. The Intraclass Correlation Coefficients ranged between 93 and 1. Statistical analysis has been carried out in SPSS (version 23, IBM Corp.).

Chapter 5

Results

5.1 Introduction

The coordination patterns between the upper and lower body should be considered to obtain optimal functional performance, because the range of motion of the shoulder and pelvis are crucial factors to continue a flexible dynamic trunk motion. In this chapter, based on the determination of the shoulder and pelvic girdles motions during different trunk positions, the lower trunk rotational angle was controlled to obtain the effect of different lower trunk rotational positions on the lumbar spine anatomical structures. Figure 5-1 shows the quantified shoulder, pelvis and spine structures.

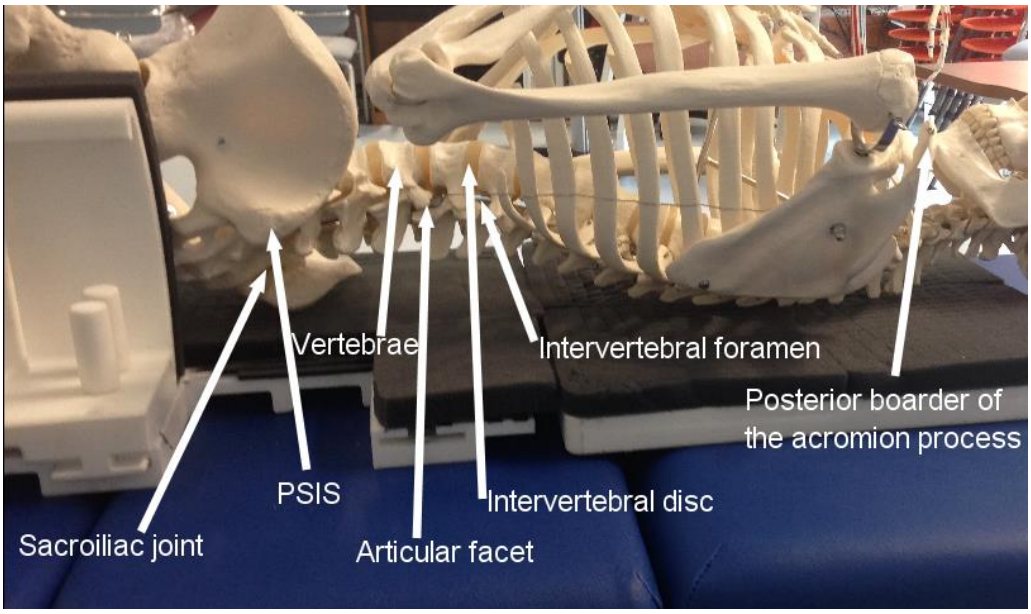

Figure 5-1: The measured parameters of the spine, shoulder and pelvis girdles

To obtain the scapula position during different lower trunk positions, the distance between the posterior border of the acromion processes and the shoulder board was obtained using tape and according to four lower trunk positions.

T2 Axial cuts 3D images and the modified goniometer readings have been selected to control the pelvic rotational angle depending on the same anatomical landmarks.

T2 Axial cuts 3D images of the sacroiliac joint have been divided into three sections in order to identify the relation between the rotational angle of the right and left

posterior superior spines and the rotational angle of the L5 vertebrae relative to the horizontal plane, and according to four lower trunk positions.

The rotational angle of the left and right sacrum and ilium was measured relative to the horizontal plane and according to three sections and four lower trunk positions using T2 Axial cuts

3D images.

Meanwhile, T2 Axial cuts 3D images have been used to measure the rotation angle of the vertebrae, the spinal canal depth and the orientation angle of the left and right superior articular processes, in addition to the relating gapping distance of the left and right facets of the lower lumbar spine.

The area, width and height of the intervertebral foramen and the intervertebral disc have been obtained using a T2 sagittal MRI. The lateral bending angle of each two consecutive lower lumbar vertebrae has been calculated by selecting a mid-sagittal MRI.

The statistical analysis was obtained using SPSS (version 23, IBM Corp.). The mean values were found to be normally distributed as checked by the Shapiro-Wilk test ($p > 0.05$). Therefore, the mean differences and P- values for the angle of vertebral rotation, the difference in the spinal canal depth, the facet orientation angle and the gapping distance, the relation between the rotational angle of the L5 and the rotational angle of the posterior superior iliac spines, and the relation between sacrum and sacrum according to three sections were obtained using MANCOVA and MANOVA.

A Student's t-test was used to evaluate the mean differences and P- values of the intervertebral foramen, intervertebral disc and lateral bending parameters.

Meanwhile, a matched paired t-test was used to evaluate the mean differences values and P- values of the distance between the posterior border of the acromion processes and the shoulder board of the MRI.

P-values and mean differences between the measurements obtained by using MRI and the modified goniometer were obtained using analysis of variance (Equality of Means).

Homogeneity of variance was assessed using Levene's test. The Intra-rater reliability was checked by repeated measurements (three times) using Intraclass Correlation Coefficients tests. The Intraclass Correlation Coefficients tests showed excellent results. Therefore, the following parameters were measured three times by the same observer and the mean values of the three measurements were then used in this study.

5.2 Controlling the Rotational Angle of the Lower Trunk Depending on the Relationship between the Shoulder and Pelvic Girdles and the Last Lumbar Vertebrae

5.2.1 Measuring the Scapula's Position during lower trunk rotation

In the present study, the scapula's position was measured as the distance between the posterior borders of the acromion processes and the shoulder board of the MRI holder during different lower trunk rotational positions.

Table 5-1 illustrates the mean value (M) of the distance between the right posterior border of the acromion process and the shoulder board of the MRI, and between the left posterior border of the acromion process and the shoulder board of the MRI holder in each rotational position of the lower trunk, unit of value (cm), standard error (SE) and the intraclass correlation coefficient percentage (ICC) of three consecutive measurements in four healthy males (Group2), four healthy males (Group 3), and three healthy males (Group 4).

Table 5-1: The distance between the posterior borders of the acromion processes and the shoulder board of the MRI holder according to different lower trunk positions

Group	Position	LPAD(cm) (M ± SE)	ICC	RPAD(cm)(M ± SE)	ICC
2	1(N) n=4	7.1 ± .4	89(.87-.93)	6.6 ±. .2	90(.87-.92)
	2(R1) n=4	19.2 ± .4	90(.85-.90)	.7 ± .4	89(.86-.91)
3	1(N) n=4	7 ± .3	90(.90-.93)	6.6 ±. .3	92(.89-.93)
	2(R2) n=4	14.7± .4	91(.89-.90)	3.2 ± .4	90(.80-.90)
4	1(N) n=3	6.8 ± .4	87(.87-.92)	6.5± .2	85(.87-.91)
	2(R3) n=3	11 ±. .5	87(.85-.90)	5± .5	85(.89-.93)

LPAD: left posterior acromion process distance, RPAD: right posterior acromion process distance, M: mean, SE: standard error, N: neutral, R1: first rotation, R2: second rotation, R3: third rotation, ICC: intraclass correlation coefficient.

The results indicated that the mean values of the distance of the left: right posterior acromion processes and the MRI holder were 19.2:7.5 cm, 14.7:3.2 cm, and 11:5 cm for the first, second, and third lower trunk rotational positions, respectively (Figure 5-2).

The distance between the right posterior border of the acromion process and the shoulder board of the MRI, and between the left posterior border of the acromion process and the shoulder board of the MRI holder altered significantly ($p < 0.005$) in response to the neutral and three lower trunk rotation positions (Table 5-2).

Table 5-2: The distance between the right posterior border of the acromion process and the shoulder board of the MRI, and between the left posterior border of the acromion process and the shoulder board of the MRI holder during

Posterior Border of the Acromion Process and the shoulder board of MRI holder	No.	Descriptive Statics		Matched Paired t-test		
		Mean	SD	t-test	d.f.	P-value
Right side (N+R)	22	4.705	2.394	-4.182	21	0.000
Left side(N+R)	22	11.182	4.958			

N: neutral position, R: rotation position, SD: standard deviation, d.f.: degree of freedom

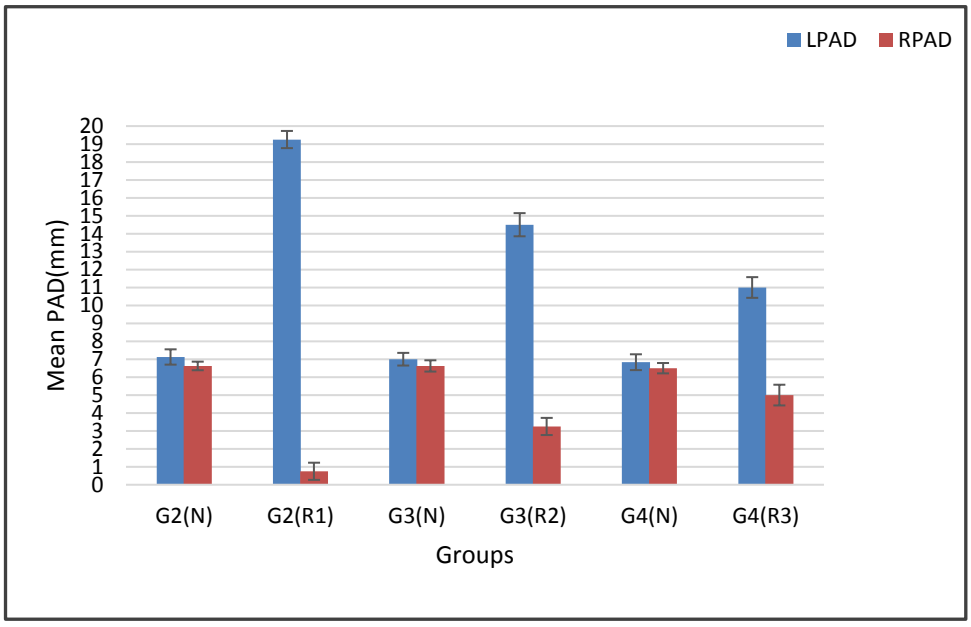

Figure 5-2: The distance between the right (RPAD)and left (LPAD)posterior acromion processes and the shoulder board of the MRI holder during neutral and rotation positions(N and R) in three groups(G2, G3, G4).

5.2.2 Measuring the Pelvic Rotational Angle Using An Adaptive Goniometer and MRI.

The measurements that were obtained to measure the angle between the left and right posterior iliac spines and the horizon using MRI images (Section 5.2.3) were compared with those obtained using the modified goniometer to control the pelvis's angle of rotation during the first and second rotational positions of the lower trunk.

The mean value (M), unit of value(^{0}), standard error (SE), and the intraclass correlation coefficient percentage (ICC) of three consecutive measurements in four healthy males

(Group2) and four healthy males (Group 3) as shown in Table B-1. The mean differences values showed no significant difference, as seen in Table 5-3 and Figure 5-3.

Table 5-3: Comparison between goniometer and MRI measurements of the pelvis rotational angle using right and left posterior superior iliac spines

Groups	Positions	The mean difference of the pelvis rotation measurements between Goniometer and MRI		
		MD1(^{0}) (G-PSIS1)	MD2(^{0}) (G-PSIS2)	MD3(^{0}) (G-PSIS3)
2	(R1) n=4	.5	.2	-.3
3	(R2) n=4	-3.1	-2.1	-2.5

R1: first rotational position, R2: second rotational position, PSISS1: the angle between the left and right posterior iliac spines and the horizontal plane at the level of the ala of the sacrum , PSISS2: the angle between the left and right posterior iliac spines and the horizontal plane at the level of the S1-S2, PSISS3: the angle between the posterior iliac spines and the horizontal plane at the level of the S2-S3, MD1: the mean difference between the goniometer and MRI measurements(PSISS1), MD2: the mean difference between the goniometer and MRI measurements(PSISS2), MD3: the mean difference between the goniometer and MRI measurements(PSISS3) .

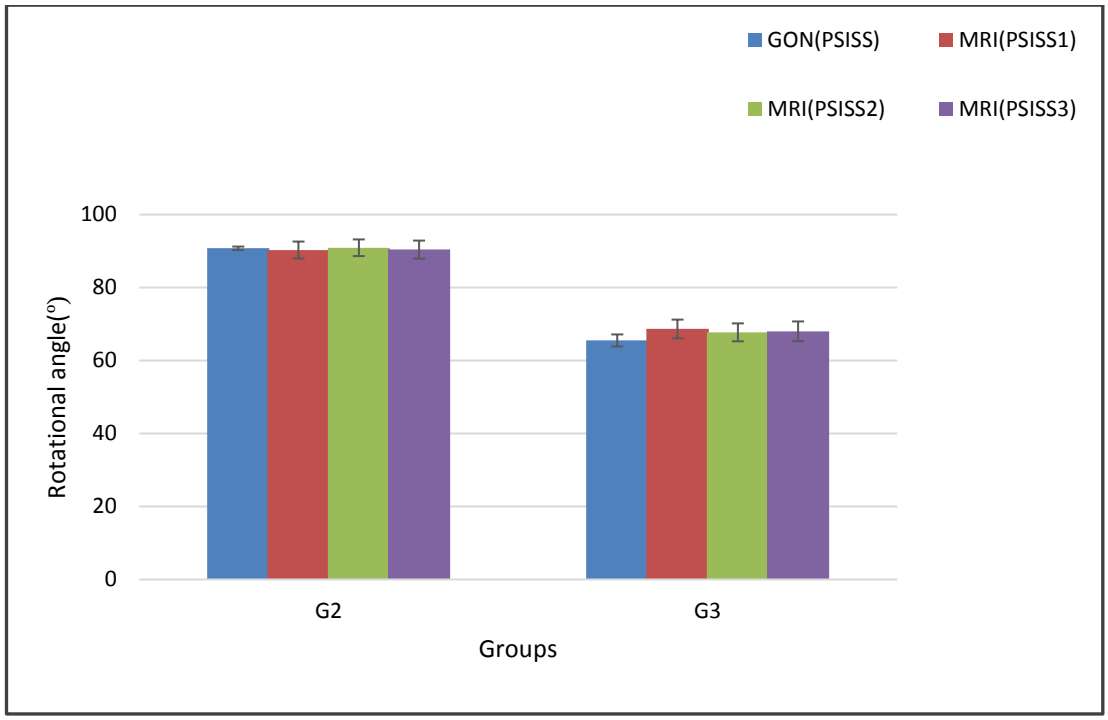

Figure 5-3: Comparison between goniometer(GON) and MRI measurements of the pelvis angle of rotation at three sections of the ilium during first and second rotational positions of the lower trunk in the second and third groups (G2, G3).

5.2.3 The Relationship between the Posterior Superior Iliac Spines and the Last Lumbar Vertebrae during Lower Trunk Rotation

Table 5-4 illustrates the mean of the rotational angle of the right and left posterior iliac spines and the L5 relative to the horizontal plane in each lower trunk position.

The mean value (M), unit of value (^{0}), standard error (SE), mean differences(MD) and the intraclass correlation coefficient percentage (ICC) of three consecutive measurements in four healthy males (Group2), and four healthy males (Group 3), and three healthy males (Group 4).

The mean differences between the angle of rotation of L5 and the rotational angle of the left and right posterior superior iliac spines in three tested sections relative to the horizontal plane was limited to cause a nonsignificant effect. However, the second rotation position of the lower trunk caused the maximum mean differences values compared to the first and third rotation positions, as seen in Figure 5-4.

Table 5-4: The relation between the rotational angle of L5 and the right and left posterior superior iliac spines at three tested anatomical sections(PSISS1, PSISS2, PSISS3)relative to the horizontal plane and according to four lower trunk positions (N, R1, R2, R3)

MD1 (L5A - PSISS11)			MD2 (PSISS1-PSISS2)			MD3 (PSISS2- PSISS3)		
R1 (H)	R2 (H)	R3 (H)	R1 (H)	R2 (H)	R3 (H)	R1 (H)	R2 (H)	R3 (H)
-.7	-1.2	-.5	-.7	.9	.1	.5	-.3	.5

L5A: The angle between the intervertebral disc at L5-S1 level and the horizon, PSISS1: the angle between the left and right posterior iliac spines and the horizontal plane at the level of the ala of the sacrum , PSISS2: the angle between the left and right posterior iliac spines and the horizontal plane at the level of the S1-S2, PSISS3: the angle between the posterior iliac spines and the horizontal plane at the level of the S2-S3, R1: first rotation with using MRI holder, R2: second rotation with using MRI holder, R3: third rotation with using MRI holder , MD1: the mean difference between the rotational angle of L5 angle and PSIS1, MD2: the mean difference between rotational angle of PSISS1 and PSISS2, MD3: the mean difference between the rotational angle of PSISS2 and PSISS3

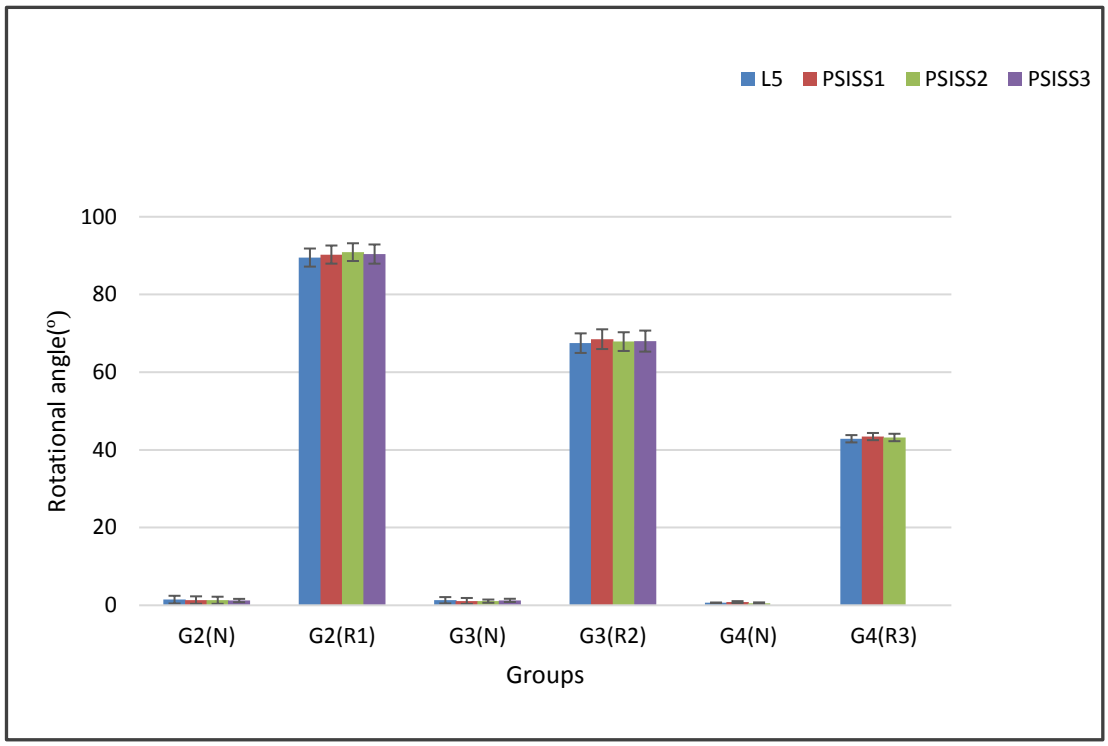

Figure 5-4: The relation between the rotational angle of L5 and the three sections of the posterior superior iliac spines (PSISS1, PSISS2, PSISS3) relative to the horizontal plane during neutral and three lower trunk rotational positions(N, R1,R2,R3) in three groups(G2,G3, G4).

5.2.4 The Relationship between the Right and Left Sacroiliac Joints According to three Anatomical Sections and during Lower Trunk Rotation

Table B-1 and Table B-2 (Appendix B), summarise the mean value (M), unit of value (°), standard error (SE) and the intraclass correlation coefficient percentage (ICC) of three consecutive measurements of the three section of the sacrum and ilium in four healthy males (Group2), four healthy males (Group 3), and three healthy males (Group 4).

The second lower trunk rotation (R2) caused the highest mean differences between the rotational angle of two consecutive sections of the sacrum and between two consecutive sections of the ilium. Meanwhile, the third lower trunk rotation caused the lowest mean differences values in both sacroiliac joints and in all three sections of the sacrum and ilium.

In the second lower trunk rotational position (R2), the highest mean differences of the rotational angles were between the first and second sections (MD1) of the right sacrum, right ilium, and left sacrum(MD1 > MD2). Meanwhile, the mean differences between the second and third sections (MD2) of the left ilium were the greatest (MD2 > MD1).

In contrast, in the first lower trunk rotation, the highest mean differences of the rotational angles were between the first and second sections (MD1) of the right sacrum and left ilium (MD1 > MD2). While, the mean differences between the second and third sections (MD2) of the left sacrum and right ilium were the greatest (MD2 > MD1).

The third lower trunk rotation followed a different behaviour in which the highest mean differences of the rotational angles were between the first and second sections (MD1) for the both right and left sacrum and ilium (MD1 > MD2). However, the mean differences values showed a nonsignificant effect (Table 5-5) and (Figure 5-5, Figure 5-6, Figure 5-7, and Figure 5-8).

Table 5-5: The mean difference of the angle of rotation of the sacrum and ilium between three sections during lower trunk rotation

(LSA1-LRSA2) (MD1)			(LSA2-LSA3) (MD2)			(LIA1-RSA2) (MD1)			(LIA2-LIA3) (MD2)		
R1 (H)	R2 (H)	R3 (H)	R1 (H)	R2 (H)	R3 (H)	R1 (H)	R2 (H)	R3 (H)	R1 (H)	R2 (H)	R3 (H)
-3.8	-10.2	-3.3	-5	0.7	2.3	6.9	5.3	4.5	3.1	-10.5	-2.8
(RSA1-RSA2) (MD1)			(RSA2-RSA3) (MD2)			(RIA1-RSA2) (MD1)			(RSA1-RSA3) (MD2)		
R1 (H)	R2 (H)	R3 (H)	R1 (H)	R2 (H)	R3 (H)	R1 (H)	R2 (H)	R3 (H)	R1 (H)	R2 (H)	R3 (H)
7	8	3.7	4.4	6.9	-2.2	-1.1	5.9	2.3	3.1	5.6	-1.6

RSAS1: the angle between the right sacrum and the horizontal plane at the level of the ala of the sacrum , RSAS2: the angle between right sacrum and the horizontal plane at the level of the S1-S2, RSAS 3: the angle between the right sacrum and the horizontal plane at the level of the S2-S3, RIAS1: the angle between the right ilium and the horizontal plane at the level of the ala of the sacrum , RIAS2: the angle between right ilium and the horizontal plane at the level of the S1-S2, RIAS 3: the angle between the right ilium and the horizontal plane at the level of the S2-S3

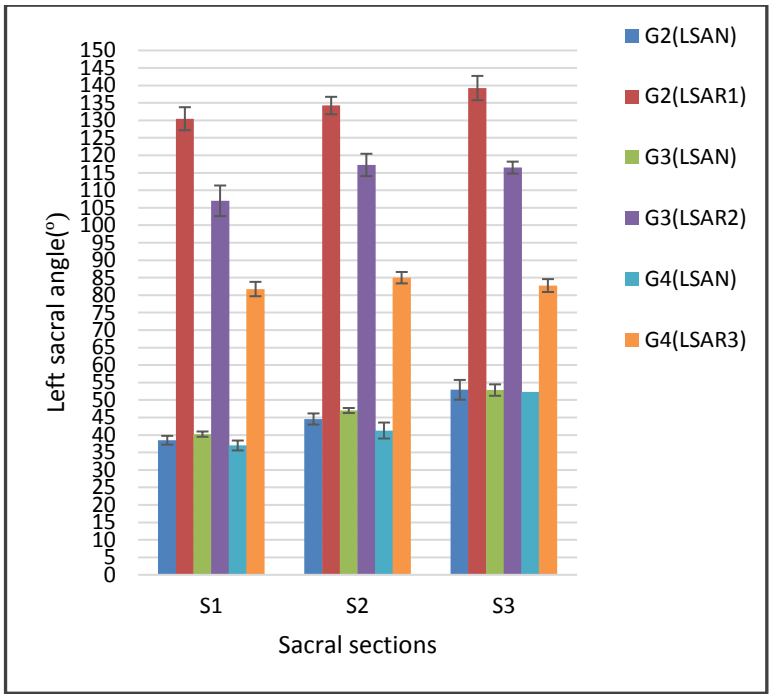

Figure 5-5: The rotational angle of the left sacrum (LSA) relative to the horizontal plane and according to three anatomical sections of the sacrum (S1,S2,S3) and during neutral, first, second, and third rotational positions (N,R1,R2,R3) of the lower trunk in three groups (G2, G3,G4).

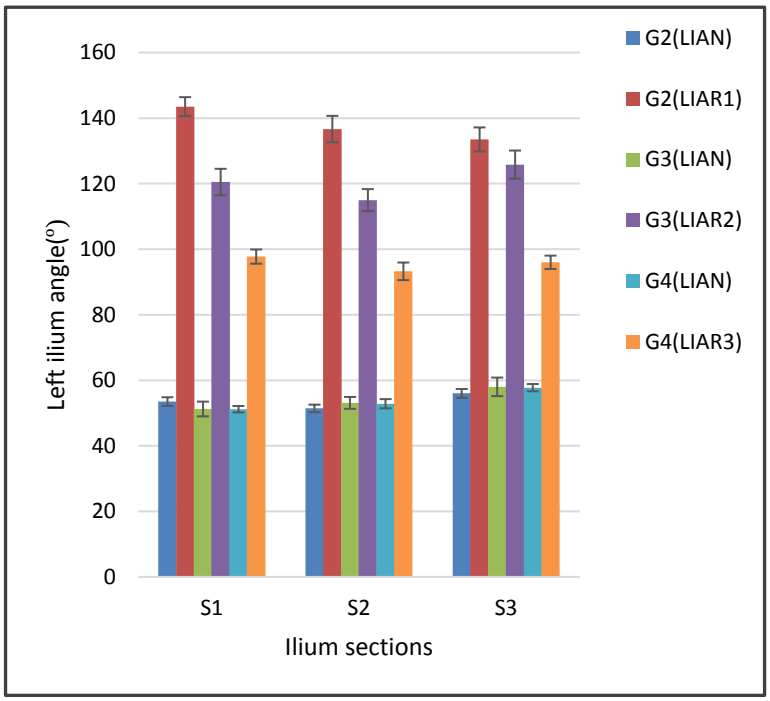

Figure 5-6: The rotational angle of the left ilium (LIA) relative to the horizontal plane and according to three anatomical sections of the sacrum (S1,S2,S3) and during neutral, first, second, and third rotational positions (N,R1,R2,R3) of the lower trunk in three groups (G2, G3,G4).

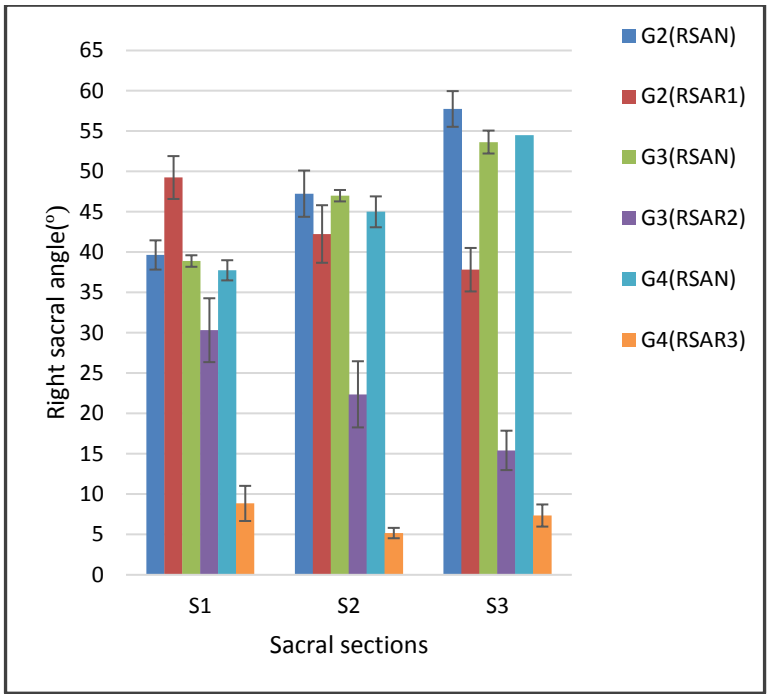

Figure 5-7: The rotational angle of the right sacrum (RSA) relative to the horizontal plane and according to three anatomical sections of the sacrum (S1,S2,S3) and during neutral, first, second, and third rotational positions (N,R1,R2,R3) of the lower trunk in three groups (G2, G3,G4).

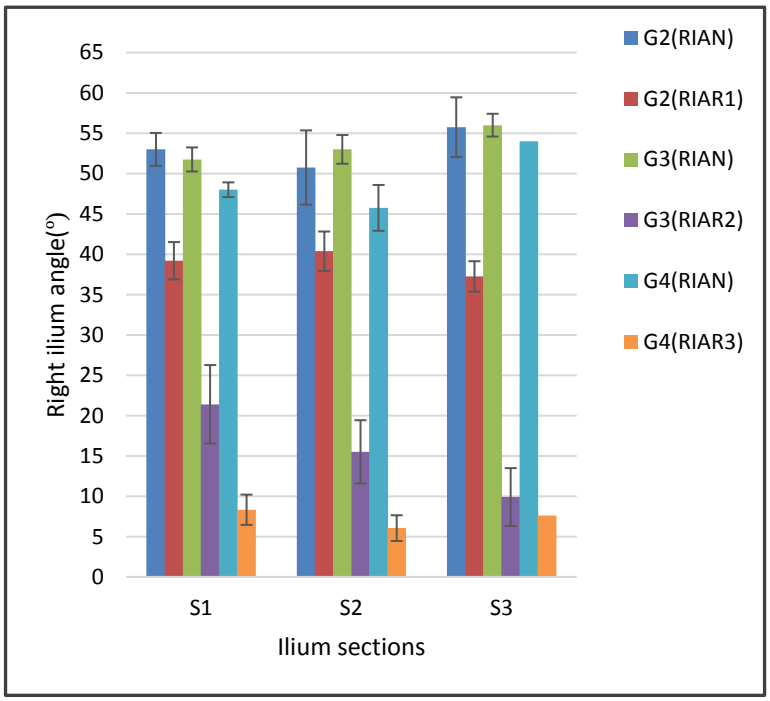

Figure 5-8: The rotational angle of the right ilium (RIA) relative to the horizontal plane and according to three anatomical sections of the sacrum (S1,S2,S3) and during neutral, first, second, and third rotational positions (N,R1,R2,R3) of the lower trunk in three groups (G2, G3,G4).

5.3 Effect of Lower Trunk Rotation on the Lower Lumbar Spine Structures

5.3.1 The Angle of Rotation of the Lower Lumbar Spine Vertebrae and the Difference in the Spinal Canal Depth during Lower Trunk Rotation

Tables B-3 and B-4(Appendix B) summarise the mean value (M), unit of value (°), standard error (SE), mean differences values (MD) and the intraclass correlation coefficient percentage (ICC) of three consecutive measurements in seven healthy males (Group1), five healthy males (Group 2), five healthy males (Group3) and four healthy males (Group 4).

A. The angle of rotation of the lower lumbar vertebrae according to the different lower trunk positions

In the neutral position, the angle of rotation of the lower lumbar vertebrae (L3, L4 and L5) showed relative mean values in all tested groups. However, the first group obtained the highest values.

The degree of vertebral rotation that was calculated at the second selected cut of each lumbar vertebral level was higher than that tested at the first cut. The mean differences between the vertebral rotation at the first cut and the second cut (the relative vertebral motion) did not achieve statistical significances in all examined vertebral levels, positions and groups. However, the second rotational position (mean 66^0) caused the highest relative vertebral motions.

The lower trunk rotation caused the third lumbar vertebrae (L3) to rotate with the lowest degree compared to L4 and L5 vertebrae in all tested groups and positions. However, the first rotational position(second group) (mean 87.5^0) caused the highest mean differences (rotational torque)between the rotational degree of the L5 and L3 vertebrae for the second selected cut as shown in Table 5-6, Table 5-7, Figure 5-9 and Figure 5-10. In addition, the lower trunk rotation caused the L3 vertebra to rotate with higher relative motion than L4 and L5 vertebrae.

Table 5-6: The degree of the individual relative vertebral motion, the rotational torque and the difference in the spinal canal depth during the first lower trunk rotational position for the first and second groups.

Group	Position	IVL	Relative vertebral motion(^{0}) (RA1-RA2)(MD)	Rotational torque(^{0}) (L5-L3)(MD)	Spinal canal depth (mm) (N-R)(MD)
1 (Without MRIH)	1(N) n=7	L3	-.4	-0.5	-1.2*
		L4	-0.8		-1
		L5	-0.2		-.7*
	2(R1) n=7	L3	-1	7.2	
		L4	-.5		
		L5	-.4		
2 (With MRIH)	1(N) n=5	L3	-0.3	0.2	-2.3*
		L4	-0.2		-1.4
		L5	-0.1		-1*
	2(R1) n=5	L3	-1.2	8.9	
		L4	-.7		
		L5	-.5		

IVL: intervertebral level, N: neutral position, R:rotation position, R1: the first rotational position, SCD: spinal canal depth, MRIH: MRI holder, MD: mean difference, RA1: rotational angle at the first cut, RA2: rotational angle at the second cut.

Table 5-7: The degree of the relative vertebral motion, the rotational torque and the difference in the spinal canal depth during the second and third lower trunk rotational positions for the third and fourth groups.

Group	Position	IVL	Relative vertebral motion(^{0}) (RA1-RA2)(MD)	Rotational torque(^{0}) (L5-L3)(MD)	Spinal canal depth (mm) (N-R)(MD)
3 (with MRIH)	1(N) n=7	L3	-.3	0.3	-1.3*
		L4	-.1		-.9
		L5	-.1		-.7*
	2(R2) n = 7	L3	-2	6.2	
		L4	-1.1		
		L5	-.8		
4 (with MRIH)	1(N) n = 5	L3	-.3	0.6	-.7
		L4	-.2		-.4
		L5	-.1		-.2
	2(R3) n = 5	L3	-.8	5.5	
		L4	-.5		
		L5	-.4		

IVL: intervertebral level, N: neutral position, R: rotation position, R2: second rotational position, R3: third rotational position, SCD: spinal canal depth, MRIH: MRI holder, MD: mean difference, RA1: rotational angle at the first slice, RA2: rotational angle at the second slice.

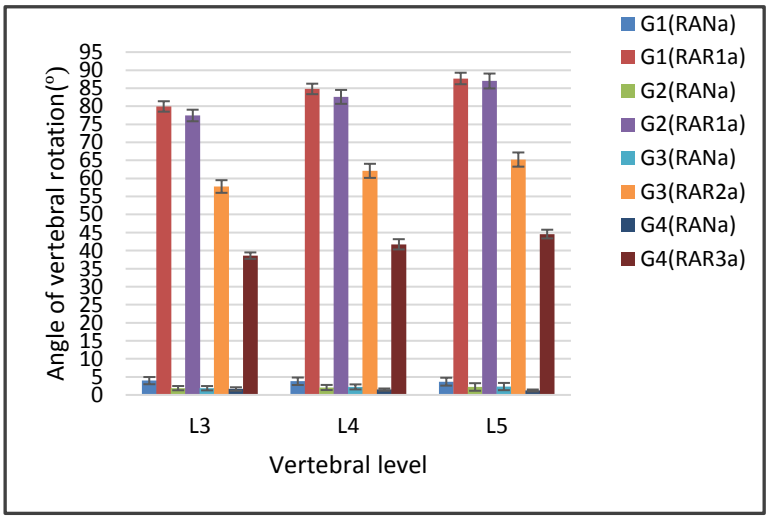

Figure 5-9: Mean degree of rotation at L3, L4 and L5 vertebral levels for the first selected cut during different lower trunk positions: neutral (RAN a), first rotation (RAR1 a), second rotation (RAR2 a), third rotation (RAR3 a) and according to different groups (G1, G2, G3, G4).

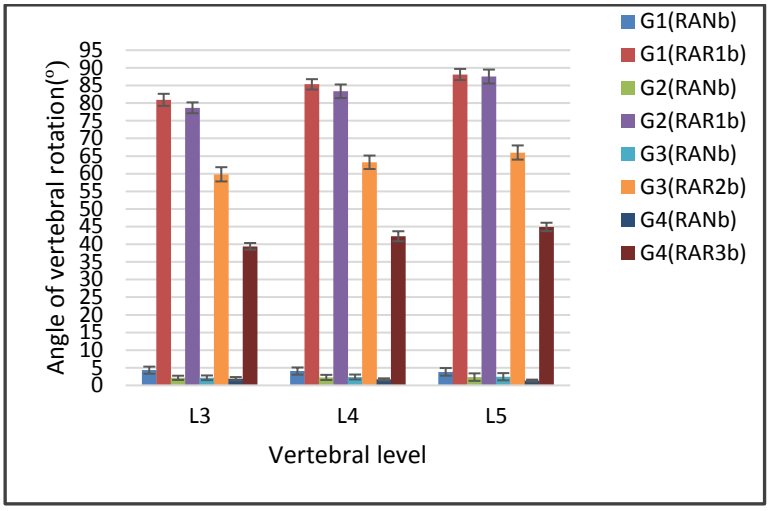

Figure 5-10: Mean degree of rotation at L3, L4 and L5 vertebral levels for the second selected cut during different lower trunk positions: neutral (RAN b), first rotation (RAR1 b), second rotation (RAR2 b), third rotation (RAR3 b) and according to different groups (G1, G2, G3, G4).

B. The difference in the spinal canal depth during lower trunk rotation

The mean differences of the spinal canal depth between the two tested vertebral cuts at each vertebral level increased dramatically following the degree of the applied lower trunk rotational position. However, the data showed that the first and second rotational positions obtained the significant values at L3 and L5 intervertebral levels ($p < 0.05$). In contrast, performing third lower trunk rotation position caused the lowest and nonsignificant mean differences values at all examined lumbar levels, as shown in Table 5-6, Table 5-7 and Figure 5-11.

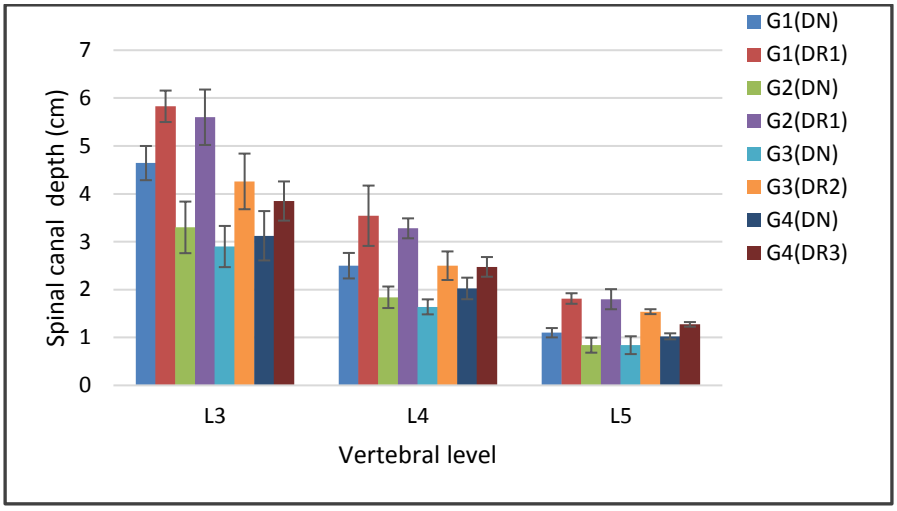

Figure 5-11: Mean differences of the spinal canal depth at L3, L4 and L5 vertebral levels during different lower trunk positions: neutral (DN), first rotation (DR1), second rotation (DR2), third rotation (DR3) and according to different groups (G1, G2, G3, G4).

5.3.2 Effect of Trunk Rotation on the Dimensions of the Lumbar Intervertebral Discs and Neural Foramens: An MRI Study.

The area, width, and height of the left and right intervertebral disc and foramen(IVD and IVF) for neutral position and three left lower trunk rotational positions were calculated using sagittal MRI images. The mean (M) of the calculated variables with their mean standard errors (SE), at the neutral position (N) and three lower trunk rotation positions were given in Tables B-5, B-6, B-7, B-8, B-9, B-10 (Appendix B). The intraclass correlations were measured for the following measurement.

A. The area, width, and height of the right and left sides of the intervertebral disc (IVD)

The mean values of the area, width, and height (posterior and anterior) of the left and right side of the intervertebral disc were found to be normally distributed as checked by the Shapiro-Wilk test ($p > 0.05$). Therefore, Student t-test was performed to statistically evaluate the mean difference (MD) between the neutral and rotation positions (Table 5-8).

Table 5-8: Mean differences values of the intervertebral disc area, width and height between the neutral and three lower trunk rotational positions

IVL Right Side	Area N-R (MD)			Width N-R (MD)			Posterior disc height N-R (MD)			Anterior disc height N-R (MD)		
	R1 (WH)	R1 (H)	R2 (H)	R1 (WH)	R1 (H)	R2 (H)	R1 (WH)	R1 (H)	R2 (H)	R1 (WH)	R1 (H)	R2 (H)
L3-L4	24.2↓	29.8↓	50.2↓	3↓	3.3↓	4.8↓	-0.3↑	-0.7↑	-1.1↑	0.9↓	1	0.7
L4-L5	30.7↓	35↓	61.5↓	3.5↓	3.8↓	7.7↓	0.7↓	1↓	1.2↓	0.6↓	0.7	-0.2
L5-S1	26.4↓	34↓	70*↓	2.8↓	3↓	6.8*↓	0.6↓	0.6↓	1*↑	0.9↓	-0.4	1.2*
IVL Left Side	Area N-R (MD)			Width N-R (MD)			Posterior disc height N-R (MD)			Anterior disc height N-R (MD)		
	R1 (WH)	R1 (H)	R2 (H)	R1 (WH)	R1 (H)	R2 (H)	R1 (WH)	R1 (H)	R2 (H)	R1 (WH)	R1 (H)	R2 (H)
L3-L4	-15↑	-36.5↑	-46.7↑	1↓	0.8↓	-0.2↑	-0.5↑	-0.6↑	-0.9↑	-0.4↑	-1↑	-1.9*↑
L4-L5	-31↑	-66↑	-74*↑	-0.4↑	-0.2↑	-1.3↑	-0.3↑	-0.7↑	-1*↑	-0.6↑	-1.2↑	-2.3*↑
L5-S1	23.1↓	20.3↓	15↓	1.1↓	1↓	0.2↓	0.8↓	0.4↓	0.8↓	-0.6↑	-0.7↑	-1.8*↑

IVL: intervertebral level, N: neutral position, R: rotation position, R1 (WH): first rotation without MRI holder, R1 (H) first rotation with MRI holder, R2 (H): second rotation with MRI holder, MD: mean difference, ↑: increase, ↓: decrease.

1. The change of the area of the intervertebral disc (IVD)

Left lower trunk rotational positions decreased the area of the right side of the sagittal intervertebral disc at L3-L4 and L4-L5 intervertebral levels without significant mean differences values. However, the second rotational position showed the highest values.

In contrast, the area of the left side of the sagittal disc increased at L3-L4 and L4-L5 levels. However, the mean differences values did not achieve significant values except that at L4-L5 level. The mean differences in the increasing and decreasing of the area of both side of the disc at L4-L5 level showed the highest values.

The area of the disc decreased at both sides at L5-S1. However, the left side showed the lowest values, as shown in Figure 5-12.

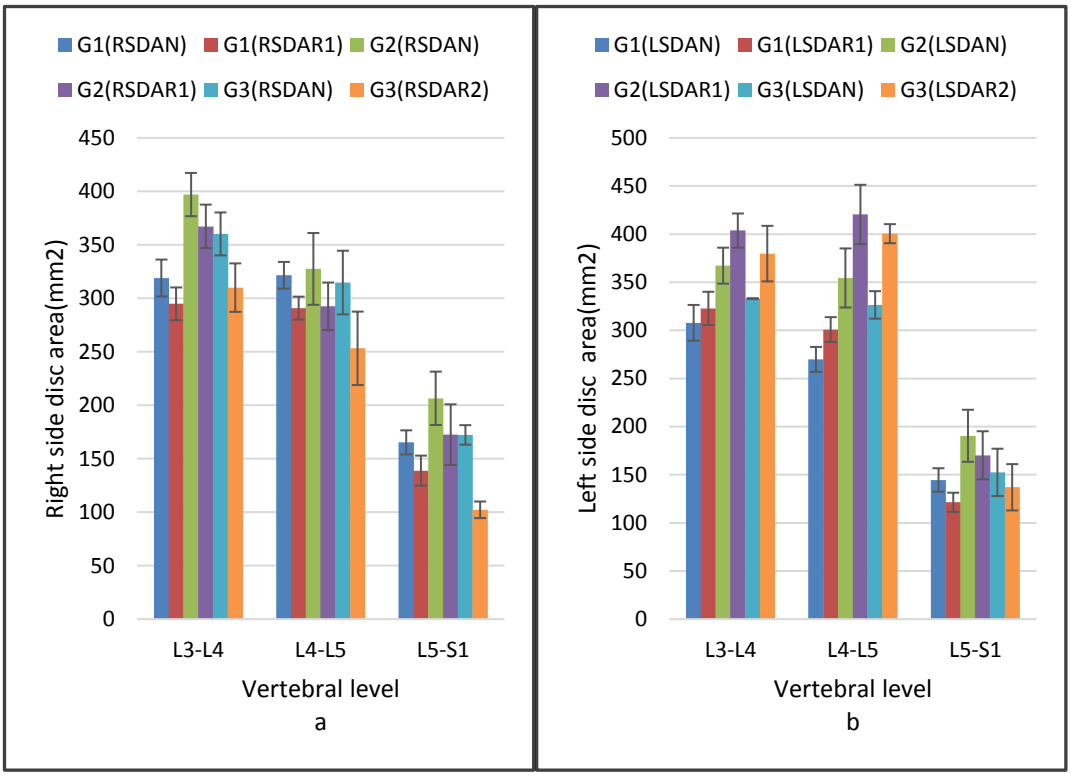

Figure 5-12: The changes of the area of the right(RSDA) and left sides(LSDA) of the intervertebral disc during neutral position (N) compared with rotation (R1and R2) in first group (G1), second group(G2), third group(G3).

2. The change of the width of the intervertebral disc (IVD)

The left lower trunk rotational positions decreased the width of the right and left sides of the intervertebral disc at L3-L4 and L5-S1 levels during the first rotation position. However, the decreasing in the intervertebral disc width at the right side showed the highest mean values.

The L4-L5 intervertebral discs showed different patterns in which the left side width of the disc increased, while the right side decreased.

In contrast, the second rotational position showed the greatest effect on the width of the right and left sides of the intervertebral disc. Therefore, the width of the left sides of the intervertebral disc increased at L3-L4 and L4-L5 levels while the right side width decreased as shown in Figure 5-13. The increasing and decreasing in the width of the

left and right sides of the disc at L4-L5 showed the highest values. However, these changes in the width of the disc did not show any significant differences except of that of the right side of the disc at L5-S1.

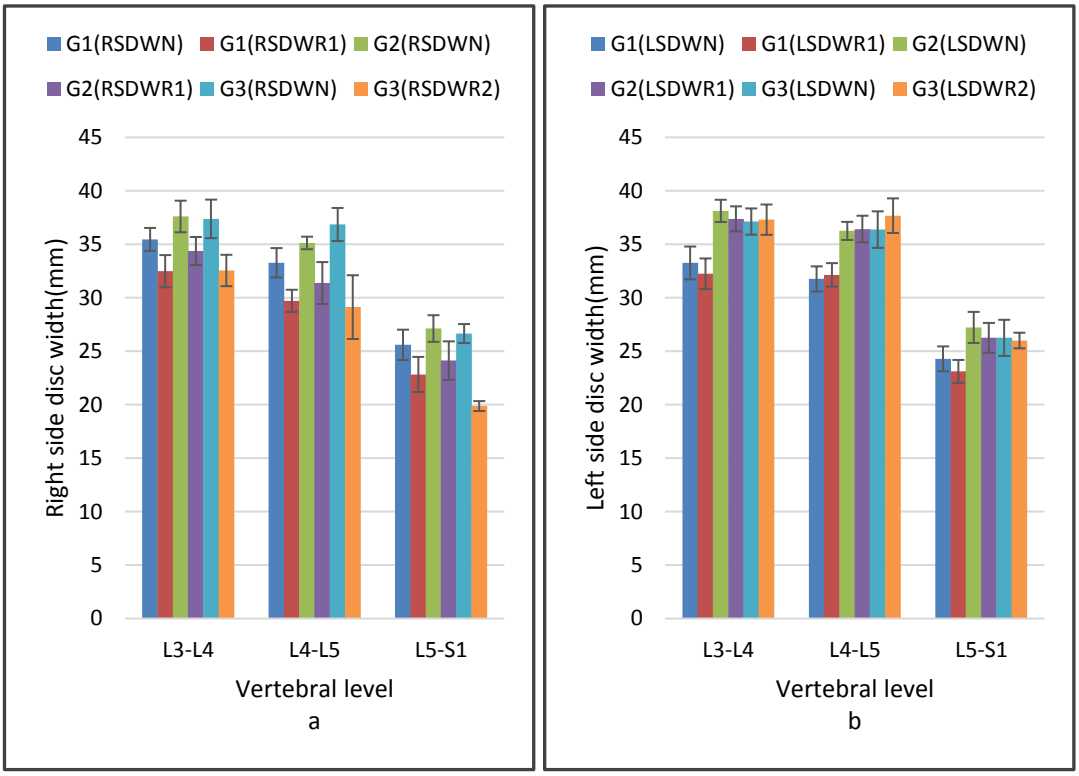

Figure 5-13: The changes of the width of the right (RSDW) and left sides (LSDW) of the intervertebral disc during neutral position (N) compared with rotation (R1and R2) in first group (G1), second group (G2), third group (G3).

3. The change of the posterior height of the intervertebral disc (IVD)

In general, the left rotational positions of the lower trunk increased the posterior disc height of the right and left sides at L3-L4 lumbar segment, while reverse observations found at L5-S1 lumbar segment. However, the mean differences values did not achieve significant P-values, except that of the right side of the L5-S1 level for the second rotational position.

Different observations showed by the intervertebral disc at L4-L5 level in which the posterior disc height of the right side decreased while the posterior height of the left side of the intervertebral disc increased. However, the mean differences values did not

achieve significant P-values, except that of the right side of the L4-L5 level for second rotational position, as shown in Figure 5-14.

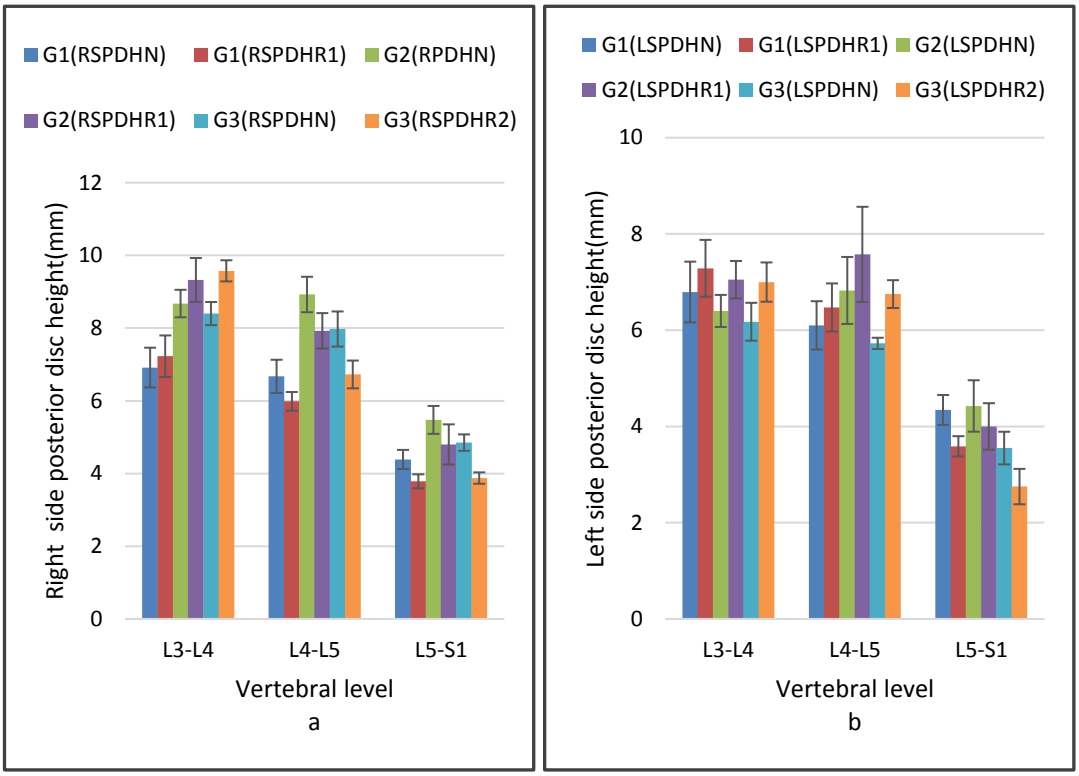

Figure 5-14: The changes of the posterior disc heights of the right side (RSPDH) and left side (SPDLH) during neutral position (N) compared with rotation (R1and R2) in first group (G1), second group (G2), third group (G3).

4. The change of the anterior height of the intervertebral dis (IVD)

The anterior disc height of the left side increased at all lower lumbar segments and left lower trunk rotational positions (R1 and R2). However, the second rotational position caused the significant decreasing of the anterior disc height at all lower lumbar segments.

In contrast, the impact of the left rotation on the anterior disc height at the right side caused reciprocal behaviours. However, the mean differences values did not show significant P-values except that of the L5-S1 level for the second rotational position, as shown in Figure 5-15.

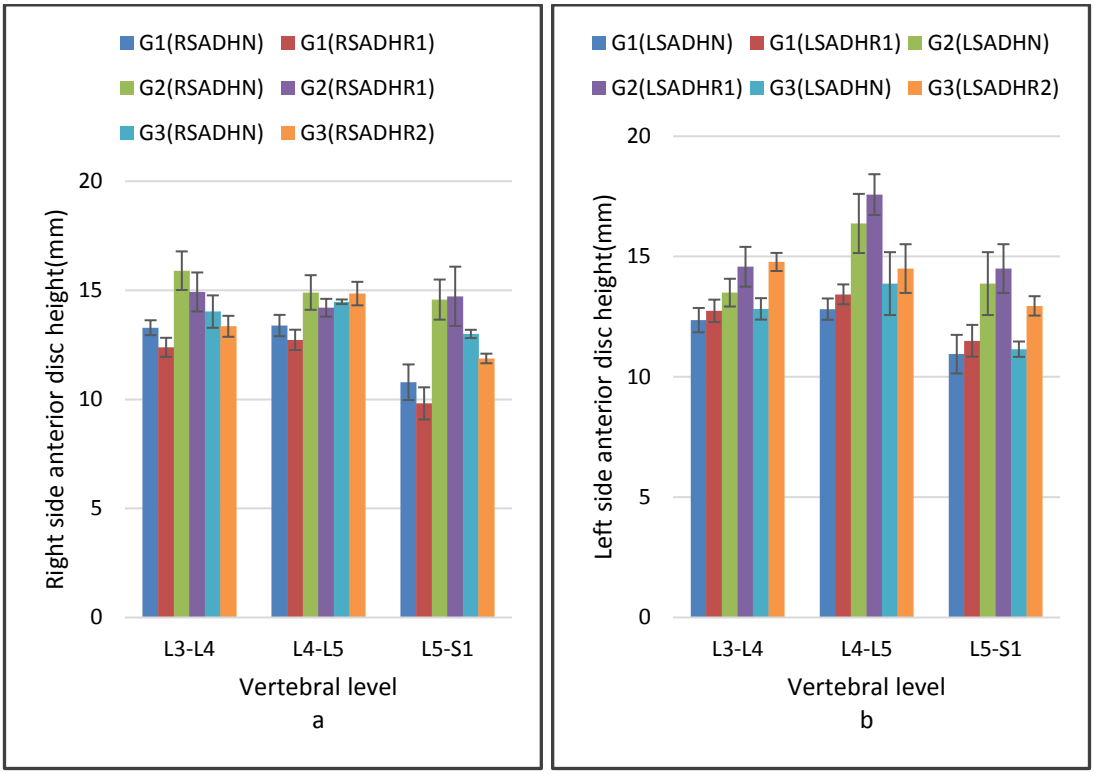

Figure 5-15: The changes of the anterior disc heights of the right side (RSADH) and left side (SADLH) during neutral position (N) compared with rotation (R1and R2) in first group (G1), second group (G2), third group (G3).

B. The area, width, and height of the intervertebral foramen (IVF)

The mean values of the area, width, and height of the left and right intervertebral foramen were found to be normally distributed as checked by the Shapiro-Wilk test ($p > 0.05$). Therefore, Student t-test was performed for statistically evaluating the mean difference (MD) between the neutral and rotation positions (**Table 5-9**).

Table 5-9: Mean differences values of the intervertebral foramenal area, width and height between the neutral and three lower trunk rotational positions

IVL (Right Side)	Area N-R1 (MD)			Width N-R1 (MD)			Height N-R1 (MD)		
	R1 (WH)	R1 (H)	R2 (H)	R1 (WH)	R1 (H)	R2 (H)	R1 (WH)	R1 (H)	R2 (H)
L3-L4	-14*↑	-18*↑	-43.2*↑	-1↑	-1.7*↑	-3.3*↑	-0.6↑	-1.1↑	-1.5↑
L4-L5	-9↑	-16.2*↑	-27.3*↑	-0.7↑	-1↑	-2.3*↑	0.6↑	0.8↑	2.7↑
L5-S1	-5.8↑	-7.7↑	-11.3↑	-1↑	-1.5↑	-2*↑	1↓	1.1↓	1.7↓
IVL (Left Side)	**Area N-R1 (MD)**			**Width N-R1 (MD)**			**Height N-R1 (MD)**		
	R1 (WH)	R1 (H)	R2 (H)	R1 (WH)	R1 (H)	R2 (H)	R1 (WH)	R1 (H)	R2 (H)
L3-L4	13.3*↓	21.5*↓	31.2*↓	1.1*↓	1.9*↓	3.2*↓	-0.2↑	-0.2↑	-0.7*↑
L4-L5	10.2↓	15.5*↓	27.7*↓	1↓	1.2*↓	2.3*↓	1↓	-1.4↓	-1.8*↓
L5-S1	7.4↓	7.2↓	18↓	1↓	1.2↓	2.1*↓	0.7	1.2↓	1.5↓

IVL: intervertebral level, N: neutral position, R: rotation position, R1 (WH): first rotation without MRI holder, R1 (H) first rotation with MRI holder, R2 (H): second rotation with MRI holder, MD: mean difference, ↑: increase, ↓: decrease.

1. The change of the intervertebral foramen (IVF) area

Left lower trunk rotation decreased left foramen areas, and the mean differences MDs were statistically significant at L3-L4 and L4-L5 lumbar segments. In contrast, right foramen areas increased at all tested lumbar levels. The mean differences were found to be significant at L3-L4 and L4-L5 levels ($p < 0.005$). However, the right and left intervertebral foramen area at L3-L4 level affected more by lower trunk rotation than L4-L5 level.

In addition, the second rotational position caused the highest changes in the area of the left and right intervertebral foramen, as shown in Figure 5-16.

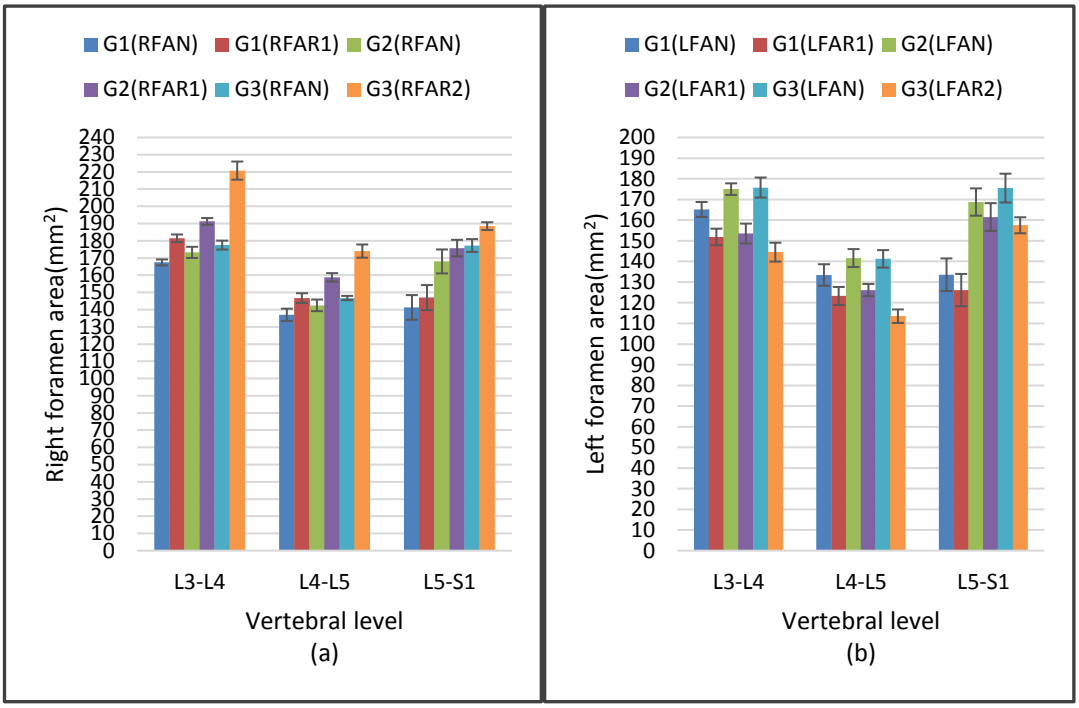

Figure 5-16: The changes of the right (a) and left (b) foramen areas (RFA and LFA)during rotation (R1, R2) compared with neutral position (N) in first group (G1), second group (G2), third group (G3).

2. The change of the intervertebral foramen (IVF) width

Left lower trunk rotation increased the right foraminal width (RFW) at L3-L4, L4-L5 and L5-S1 segments. The mean differences showed significant values at L3-L4 in the first rotational positions, while the second rotational position caused the right foramen width to increase significantly at all lower lumbar levels.

The three rotational positions of the lower trunk caused the left foramen width to decrease at L3-L4, L4-L5 and L5-S1 levels, as shown in Figure 5-17.

However, the mean differences did not show significant values at L4-L5 and L5-S1 levels for the first rotational position (R1WH), while the first rotational position (R1H) did not cause significant decrease in the foraminal width at L5-S1level. However, the second rotational position caused significant decrease in the left foraminal width at all lower lumbar segments.

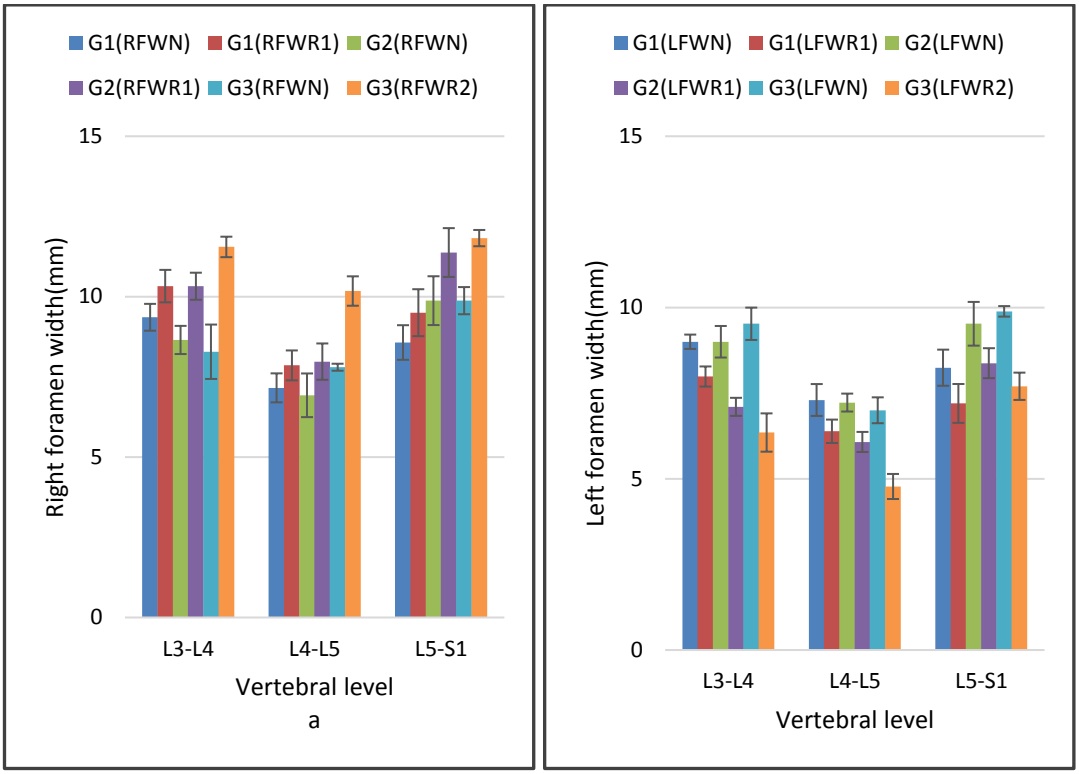

Figure 5-17: The changes of the right (a) and left (b) foramen widths(RFW and LFW)during rotation (R1, R2) compared with neutral position (N) in first group (G1), second group (G2), third group (G3).

3. The change of the intervertebral foramen (IVF) height

First left rotational position without using MRI holder, first and second rotational positions with using MRI holder (R1 (WH), R1 (H) and R2 (H)) caused the right and left foramen height to increase at the L3-L4 level. In contrast, the right and left foraminal height at the L5-S1 level decreased.

The height of the right and left foramen at L4-L5 had different behaviours, the right foraminal height decreased at L4-L5, while left foraminal height increased at L4-L5 as shown in Figure 5-18. However, the mean differences did not show significant values except of that at the left foramen at L3-L4 and L4-L5 for the second rotational position.

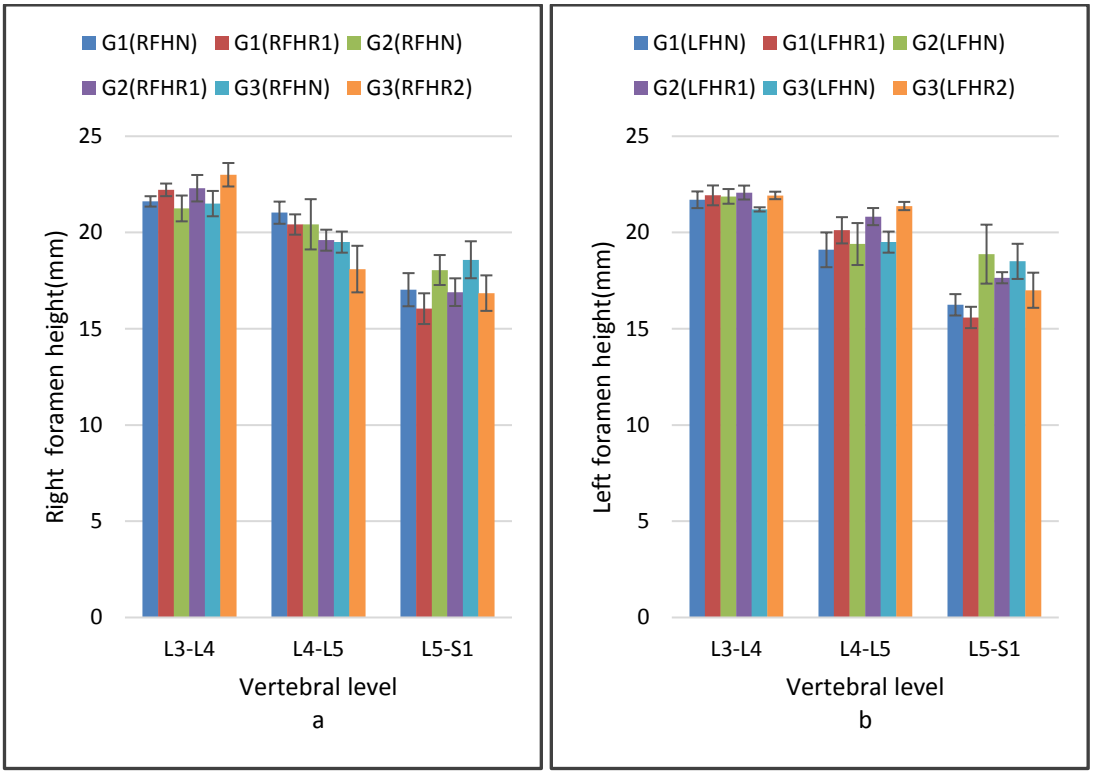

Figure 5-18: The changes of the right (a) and left (b) foramen heights (RFH and LFH) during rotation (R1, R2) compared with neutral position (N) in first group (G1), second group (G2), third group (G3).

5.3.3 The Degree of Lateral Bending During Lower Trunk Rotation

The lateral bending angle of each two consecutive lower lumbar vertebrae for neutral and three rotational positions of the lower trunk was calculated using mid-sagittal MRI images. The mean (M) of the calculated variables with their mean standard errors (SE) and the mean differences (MD) at the neutral position (N) and two lower trunk rotational positions were measured and are given in Table 5-10.

Student t-test was obtained to evaluate the mean differences and P- values of the intervertebral foramen, intervertebral disc parameters.

The lateral bending angle of each two consecutive lower lumbar vertebrae increased according to the applied rotational position. The lateral bending angle at L4-L5 was the highest at all rotational positions. However, the mean differences values were only found to be significant ($p < 0.005$) during the second rotational position as shown in Figure 5-19.

Table 5-10: The degree of the lateral bending of the lower intervertebral segments in neutral and three rotational positions of the lower trunk

IVL	Lateral bending degree		MD
	(M±SE)	ICC	
L3-L4(N)	6.7±.3	.98(.95-.99)	-.9↑
L3-L4(R1) (WH)	7.6±.3	.98(.94-.99)	
L3-L4(N)	6±.4	.99(.97-1)	-1.5↑
L3-L4(R1)(H)	7.5±.5	.99(.97-1)	
L3-L4(N)	5.8± .6	.99(.98-1)	-2.5*↑
L3-L4 (R2)(H)	8.3± .6	.99(.97-1)	
L4-L5 (N)	8.6±.2	.98(.95-.99)	-2.1*↑
L4-L5(R1) (WH)	10.7±.3	.99(.97-.99)	
L4-L5 (N)	8.7±.4	.99(.97-1)	-2.5*↑
L4-L5(R1)(H)	11.2±.5	.99(.97-1)	
L4-L5 (N)	8.6± .4	.98(.94-.99)	-2.9*↑
L4-L5(R2)(H)	11.5± 1	.99(.99-1)	
L5-S1(N)	15.7±.6	.99(.99-1)	.3↑
L5-S1(R1) (WH)	16±.8	.97(.90-.99)	
L5-S1(N)	17.5±1	.99(.99-1)	-1.3↑
L5-S1(R1)(H)	18.8±1	.99(.99-1)	
L5-S1(N)	14.6± 1	.99(.99-1)	-2.2↑
L5-S1(R2)(H)	16.8± 1	.99(.99-1)	

IVL: intervertebral level, N: neutral position, R: rotation position, R1 (WH): first rotation without MRI holder, R1 (H) first rotation with MRI holder, R2 (H): second rotation with MRI holder, M: mean, SE: standards error, ICC: intraclass correlation coefficient, MD: mean difference, ↑: increase, ↓: decrease.

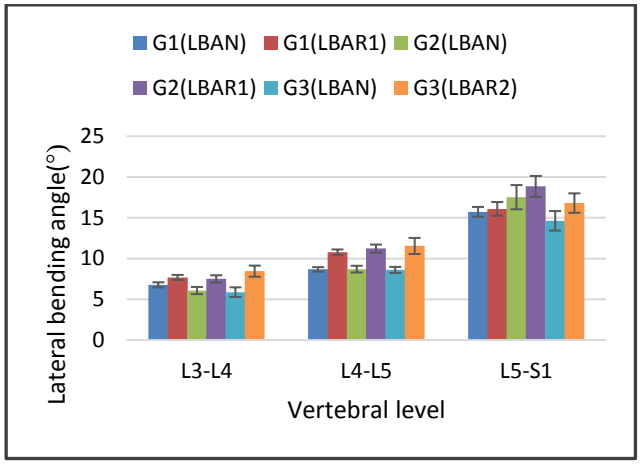

Figure 5-19: The changes of the lateral bending angle during rotation (R1 and R2) compared with neutral position (N) in first group (G1), second group (G2), third group (G3), LBA: lateral bending angle

5.3.4 The Orientation Angle of the Left and Right Superior Articular Processes and the Cross-Sectional Area of the Gapping between the Superior and Inferior Articular Processes during Lower Trunk Rotation.

Appendices B-11 and B-12 summarise the mean value (M), unit of value (°), standard error (SE) and the intraclass correlation coefficient percentage (ICC) of three consecutive measurements of the orientation angle of the left and right superior articular processes and of the cross-sectional area of the gapping between the superior and inferior articular processes during lower trunk rotation were obtained for five healthy males (Group1), three healthy males (Group 2), four healthy males (Group3) and three healthy males (Group 4).

A. Lumbar superior articular processes orientation angle relative to the intervertebral disc rotational angle during lower trunk rotation.

In the neutral position, the results of the analysed data revealed that there was a relative mean difference between the orientation angle of the left and right superior articular processes in all tested lumbar segments and groups, as shown in Appendices B-10 and B-11.

During lower trunk rotation, the mean difference between the orientation angle of the left superior articular process and the right one at L3-L4 vertebral level was the greatest compared to the L2-L3, L4-L5 and L5-S1 intervertebral levels for all tested lower trunk rotational positions. The second rotation position caused the highest mean differences values between the orientation angle of the left and right processes, followed by the first rotation position. However, these mean differences were not significant at all the examined lumbar segments as shown in Table 5-11, Figure 5-20 and Figure 5-21.

Table 5-11:The mean differences between the orientation angle of the left and right superior articular processes of the lower lumbar segments relative to the disc rotational angle and during three lower trunk rotational positions for the first, second, third, and fourth groups

IVL (Right Side)	Rotational angle of the disc(^{0})				RAPA-LAPA(^{0})(MD)			
	R1 (WH)	R1 (H)	R2 (H)	R3 (H)	R1 (WH)	R1 (H)	R2 (H)	R3 (H)
L2-L3	81	80.3	56.4	39.3	-1.4	-2.4	-3.8	-1
L3-L4	83.6	85.3	61.5	40.9	-2.4	-3	-5.2	-2.6
L4-L5	86.4	86.9	65.3	42.2	-1.4	-2.1	-3.7	-1.9
L5-S1	88	88.3	67.4	42.8	-1.3	-2	-2.8	-1.7

IVL: intervertebral level, LSAPOA: left superior articular process orientation angle, RSAPOA: right superior articular process orientation angle, R1 (WH): first rotation without MRI holder, R1 (H) first rotation with MRI holder, R2 (H): second rotation with MRI holder, R3 (H): third rotation with MRI holder.

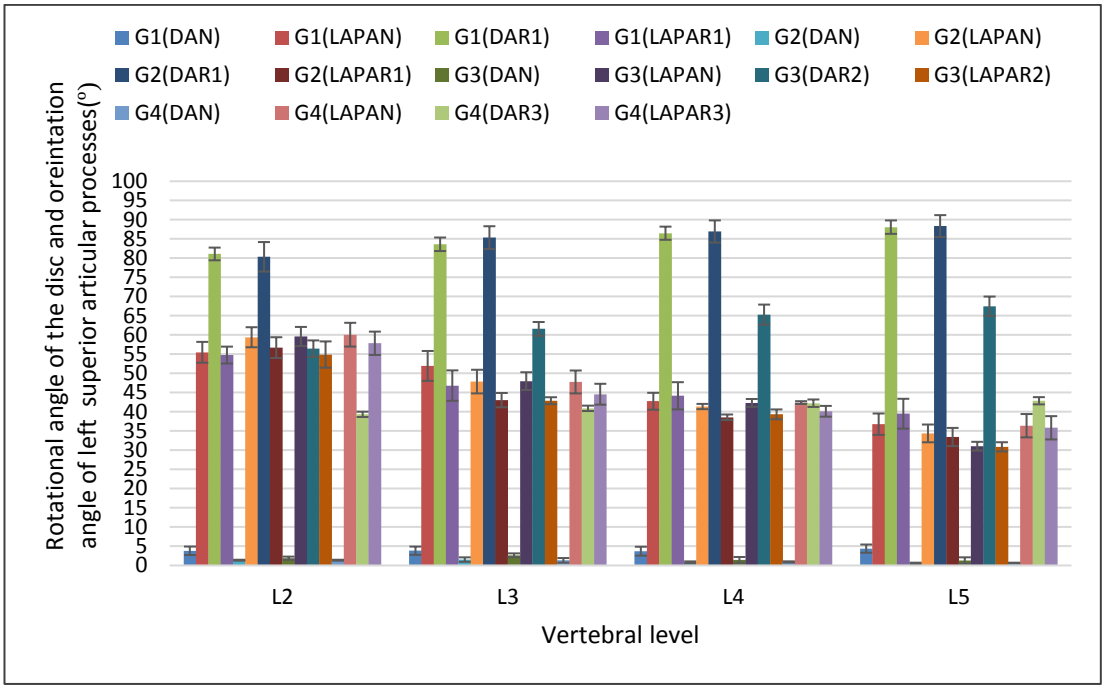

Figure 5-20: Mean rotational angle of the disc (DA) and orientation angle of the left superior articular process (LAPA) at L2, L3, L4, and L5 vertebral levels during rotation (R1,R2,R3) compared with neutral position (N) in first group (G1), second group (G2), third group (G3), and fourth group (G4).

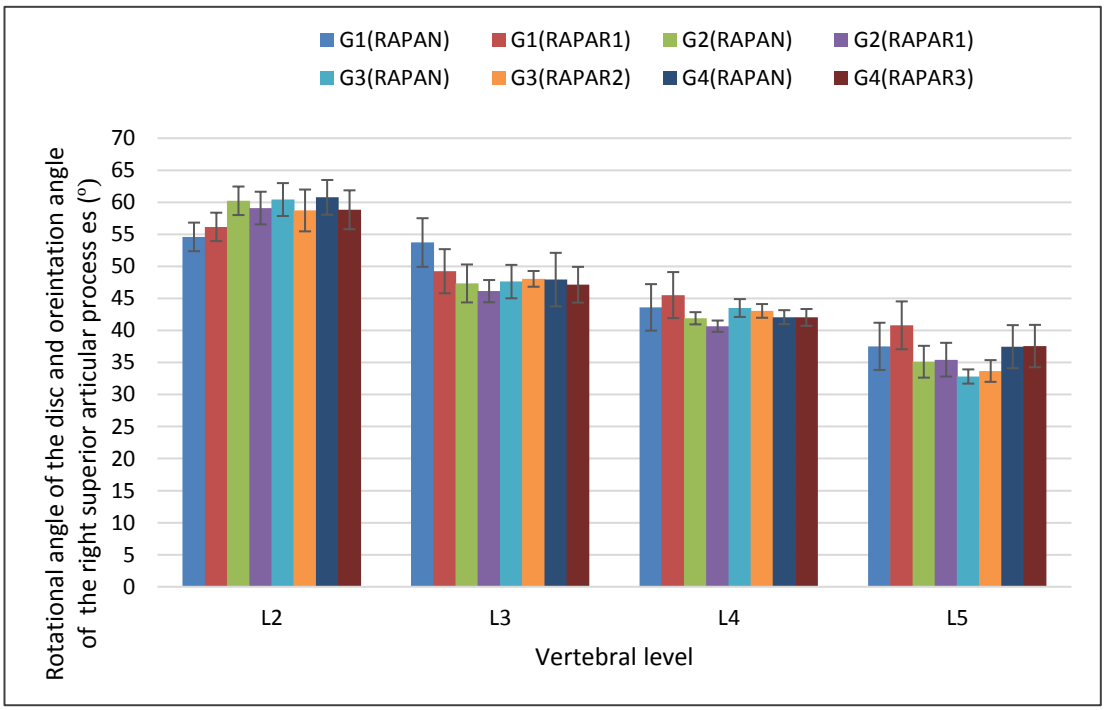

Figure 5-21: Mean orientation angle of the right superior articular process (RAPA) at L2, L3, L4, and L5 vertebral levels during rotation (R1,R2,R3) compared with neutral position (N) in first group (G1), second group (G2), third group (G3), and fourth group (G4).

B. The cross-sectional area of the gapping between the superior and inferior articular processes during different lower trunk rotational positions

Appendices B-11 and B-12 illustrate the means of the cross-sectional area of the gapping between the superior and inferior articular processes of the left and right facets in each of the examined intervertebral levels and positions. The gapping distance of the left articular facets at the L3 level was the greatest followed by facets at the L2 level, while, the left articular facet at the L5 level did not show any opening according to the level that was measured and the contrast value that was used. However, the second rotational position caused 7mm of gapping between the left superior and inferior articular processes at L5-S1 level (Appendices B-11 and B-12).

The data observations showed that the mean differences of the cross-sectional area of the gapping distance of the left articular facets at all tested intervertebral levels significantly increased (< 0.05) when subjects changed positions from neutral to the rotation positions. The second rotational position caused the highest mean differences values (-17.1 mm^2) (Table 5-12).

In contrast, the right facet did not show any gapping between the superior and inferior articular processes, as seen in Figure 5-22.

Table 5-12: Pairwise comparisons for the measurements of the cross-sectional area of the studied left facets according to different positions

Positions	Mean difference	P-value
N-R1(WH)	-5.7	< 0.05
N-R1(H)	-8.9	<0.005
N-R2(H)	-17.1	<0.005
N-R3(H)	-5.3	<0.05

N: neutral position, R1 (WH): first rotation without MRI holder, R1 (H) first rotation with MRI holder, R2 (H): second rotation with MRI holder, R3 (H): third rotation with MRI holder.

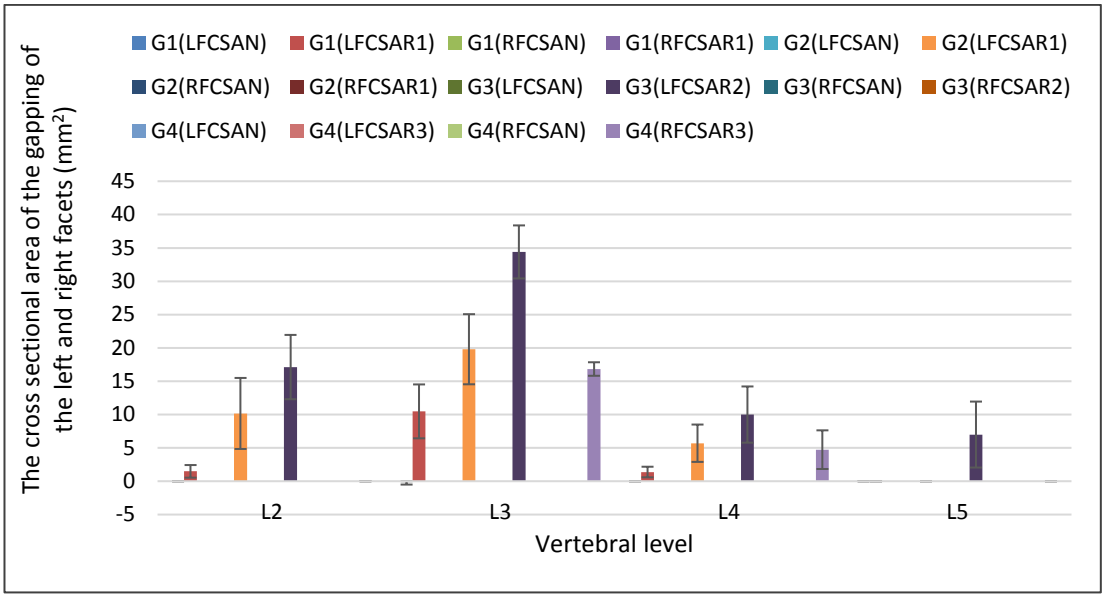

Figure 5-22: The change of the cross- sectional area of the gapping distance of the left (LFCSA) and right (RFCSA) facets at L2, L3, L4, and L5 vertebral levels during rotation (R1,R2,R3) compared with neutral position (N) in first group (G1), second group (G2), third group (G3), and fourth group (G4).

5.4 Summary

The range of motion of the shoulder and pelvis was taken under consideration to control the rotational angle of the lower lumbar spine during different rotational positions.

The right and left posterior boarders of the acromion processes were used to measure the scapula positions during neutral and three lower trunk rotational positions. The results indicate that the left and right acromion processes were positioned significantly according to the degree of the performed lumbar spine rotational position.

To prove the accuracy of the modified goniometer to control the pelvic angle of rotation during the first and second rotational positions of the lower trunk, and also the efficacy of the MRI holder to maintain the measured pelvis angle, the angle between the left and right posterior iliac spines and the horizon was measured using the modified goniometer. The goniometer measurements were then compared with MRI measurement. However, the mean differences values showed no significant difference.

The mean differences between the angle of rotation of L5 and the rotational angle of the left and right posterior superior iliac spines in three tested sections were measured relative to the horizontal plane using MRI and during the first, second, and third lower trunk rotational positions. The results indicate a nonsignificant effect. However, the second rotation position of the lower trunk caused the maximum mean differences values compared to the first and third rotation positions.

The angle of rotation of the three sections of the sacrum and ilium in three lower trunk rotational positions were measured relative to the horizontal plane using MRI. The results show that the second lower trunk rotation (R2) caused the highest mean differences between the rotational angles of two consecutive sections of the sacrum and between two consecutive sections of the ilium. Meanwhile, the third lower trunk rotation caused the lowest mean differences values in both sacroiliac joints and in all three sections of the sacrum and ilium.

The effect of lower trunk rotation on the lower lumbar spine structures was quantified using MRI.

The degree of vertebral rotation was calculated at two consecutive cuts of MRI to measure the relative vertebral motion at each individual lower lumbar segment and to quantify the rotational torque between L5 and L3 lumbar vertebral levels.

The results show that the relative vertebral motion and the degree of the rotational torque did not achieve statistical significances in all examined vertebral levels and lower trunk rotational positions. However, the second rotational position caused the highest relative vertebral motions, while the first rotational position caused the highest rotational torque between the rotational degree of the L5 and L3 vertebrae.

The difference in the spinal canal depth between two tested vertebral cuts at each vertebral level using MRI increased dramatically following the degree of the applied lower trunk rotational position. However, the data showed that the first and second rotational positions obtained the significant values at L3 and L5 intervertebral levels In

contrast, performing third lower trunk rotation position caused the lowest and nonsignificant mean differences values at all examined lumbar levels.

The area, width, and height of the left and right intervertebral disc and foramen for neutral position and three left lower trunk rotational positions were calculated using sagittal MRI images.

The lower trunk rotational positions decreased the area of the right side of the sagittal intervertebral disc at L3-L4 and L4-L5 intervertebral levels, while the area of the left side showed opposite observations. However, the mean differences values did not achieve significant values except that at L4-L5 level. The second rotational position showed the highest values. In contrast, the area of the disc decreased at both sides at L5-S1.

The second lower trunk rotational position showed the greatest effect on the width of the right and left sides of the intervertebral disc, in which, the width of the left sides of the intervertebral disc increased at L3-L4 and L4-L5 levels while the right side width decreased. The increasing and decreasing in the width of the left and right sides of the disc at L4-L5 showed the highest values.

In contrast, the width of the disc at both sides of the L5-S1level decreased according to the lower trunk rotation. However, the right side of the disc width showed significant mean differences values.

In general, the lower trunk rotation increased the posterior disc height of the right and left sides at L3-L4 lumbar segment, while reverse observations were found at the L5-S1 lumbar segment. Different observations showed by the intervertebral disc at the L4-L5 level, in which the posterior disc height of the right side decreased while the posterior height of the left side of the intervertebral disc increased. However, the mean differences values achieved significant P-values only during the second rotational position for the right side of the L4-L5 and L5-S.

The anterior disc height of the left side increased at all lower lumbar segments and left lower trunk rotational positions (R1 and R2). Meanwhile, the anterior disc height of the right side showed reciprocal observations. However, the second rotational position caused the significant decreasing of the anterior disc height at all lower lumbar segments.

The left lower trunk rotation decreased left foramen areas, while, right foramen areas increased at all tested lumbar levels. The mean differences were found to be significant at L3-L4 and L4-L5 levels. However, the right and left intervertebral foramen areas at L3-L4 level affected more by lower trunk rotation than L4-L5 level. In addition, the second rotational position caused the highest changes in the area of the left and right intervertebral foramen.

The right foraminal width increased at the L3-L4, L4-L5 and L5-S1 segments as a result of the left lower trunk rotational positions. While the right foramen showed reciprocal observations. The mean differences for the second rotational position caused the significant values at all lower lumbar levels.

The lower trunk rotational positions caused the right and left foramen height to increase at the L3-L4 level. In contrast, the right and left foraminal height at the L5-S1 level decreased.

In contrast, the height of the right and left foramen at L4-L5 exhibited a different behaviour, the right foraminal height decreased at L4-L5, while left foraminal height increased at L4-L5. However, the mean differences did not show significant values except of that at the left foramen at L3-L4 and L4-L5 for the second rotational position.

The lateral bending angle of each two consecutive lower lumbar vertebrae for neutral and three rotational positions of the lower trunk was calculated using mid-sagittal MRI images.

The lateral bending angle of each two consecutive lower lumbar vertebrae increased according to the applied rotational position. The lateral bending angle at L4-L5 was the highest at all rotational positions. However, the mean differences values were found to be significant only during the second rotational position.

The effect of lower trunk rotation on the orientation of the superior articular process of the lower lumbar vertebrae relative to the intervertebral disc rotational angle, and on the cross-sectional area of the gapping between the superior and inferior articular processes were evaluated by using T2 Axial cuts 3D images. The mean difference between the orientation angle of the left superior articular process and the right one at L3-L4

vertebral level was the greatest compared to the L2-L3, L4-L5 and L5-S1 intervertebral levels for all tested lower trunk rotational positions. The second rotation position caused the highest mean differences values between the orientation angle of the left and right processes, followed by the first rotation position. However, these mean differences were not significant at all the examined lumbar segments.

The data observations showed that the mean differences of the cross-sectional area of the gapping distance of the left articular facets at all tested intervertebral levels significantly increased when the subject changed position from a neutral to the rotation position. However, the second rotational position caused the highest mean difference values.

Chapter 6

Discussion

6.1 Introduction

This study has controlled the lower trunk rotational positions depending on the quantification of the range of motion of the shoulder and pelvis. In turn, the effect of the lower trunk rotational positions on the lower lumbar spine structures was quantified using MRI.

The right and left scapula positions during different lower trunk positions were measured as the distance between the posterior borders of the acromion processes and the shoulder board of the MRI holder.

Meanwhile, the pelvic rotational angle was measured during neutral and different lower trunk rotational positions as the rotational angle of the left and right posterior superior iliac spines relative to the horizon using adaptive goniometer. The measured angle of pelvis rotation was fixed with using MRI holder. The measurements of the pelvis rotational using a modified goniometer were compared with those obtained using MRI images to quantify the efficacy of the modified goniometer and the MRI holder to control the pelvis angle.

The relationship between the posterior superior iliac spines and the L5 vertebrae was obtained during neutral and different lower trunk positions using MRI by measuring the rotational angle of the left and right posterior iliac spines relative to the horizontal plane and compared with that of the L5 level.

Furthermore, the relationship between the rotational angle of the right and left sacroiliac joints relative to the horizontal plane was obtained during neutral and different lower trunk positions and at three anatomical sections of the sacroiliac joint using MRI.

The changes of the spinal structures during different lower trunk rotational positions were investigated to quantify the variation of the angle of rotation of the lower lumbar spine vertebrae and the difference in spinal canal depth, lumbar intervertebral discs and neural foramens dimensions, the lateral bending angle of each two consecutive lower lumbar vertebrae, and the orientation angle of the left and right superior articular processes , as well as, the gaping distance between the superior and inferior articular processes.

6.2 Controlling the Rotational Angle of the Lower Trunk Depending on the Relationship between the Shoulder and Pelvic Girdles and the Last Lumbar Vertebrae

6.2.1 Measuring the scapula position during lower trunk rotation

This study has reported that the distance between the right and left a posterior border of the acromion process and the shoulder board of the MRI holder altered significantly ($p < 0.005$) in response to the degree lower trunk rotation. These results may be explained by (Gracovetsky and Farfan 1986) , who found that an amount of axial torque can occur when the lumbar spine exhibits a coupling phenomenon. In this condition, the amount of the torque can be increased if the facet orientation is directed accurately. In this phenomenon, the spine bends laterally and forward as a result of the clockwise torque effect. Therefore, the lumbar lordotic curve will decrease. This means that the fifth lumbar vertebrae and the pelvis rotate in a clockwise direction, while the upper trunk and shoulders rotate in a counter clockwise direction.

(Nagai et al. 2013) indicated that the trunk rotation affects scapular kinematics and muscle activities in such way that the performance of the upper trapezius and serratus anterior muscles actively increased during the contralateral rotated trunk rotation in healthy subjects.

In addition, (Crommert et al. 2015) indicated that the relationship between trunk muscle activation and the direction of perturbation torque during one and the same arm movements should be considered in order to identify the activation patterns of the trunk muscles.

This study has confirmed the effect of the different trunk rotational positions on the shoulder movements particularly the scapula bone. It has also shown that there will be significant difference between the position of the right and left scapula during lower trunk rotation.

6.2.2 Measuring and controlling the pelvic rotational angle using the modified goniometer, MRI holder and MRI

(Alsancak et al. 1998; Sprigle et al. 2003; Prushansky et al. 2008; Preece et al. 2008) used goniometers, digital inclinometers, and Palmers to measure pelvic parameters, such as pelvic tilt, depending on marking particular landmarks, including the anterior and posterior superior iliac spines. These manual methods were able to find the determined parameters, especially when tested with the reliability test. In the current study, the modified goniometer was designed to provide a simple, accurate means to measure the angle between the posterior superior iliac spines (left and right) and the horizon. In addition, MRI holder was used to fix the measured pelvis angle. A new method was also used to compare the obtained data from the modified goniometer and the MRI images. The results indicated a nonsignificant difference and proved the hypothesis of the efficacy and accuracy of the modified goniometer and the MRI holder to measure and control the pelvis rotational angle.

6.2.3 The relation between the posterior superior iliac spines and the last lumbar vertebrae during lower trunk rotation

The role of the left side rotation on the relation between the angles of rotation of L5 and rotation angle of the left and right posterior superior iliac spines relative to the horizon was deemed to cause a nonsignificant effect. This observation can be explained in two ways. First, the sacrum is a single bone and the angles between L5 and any section of the PSIS must be similar. (Lee 2004) stated that during the final stage of rotation, the left axial rotation generated intra pelvic torsion in which the right innominate rotated anteriorly while the left innominate and the sacrum rotates posteriorly. However, L5 is defined to turn side flex correspondingly with the sacrum motion. In the current study, this might be the second reason why the mean values of the rotational angles showed approximately the same values at all the selected posterior superior iliac spine sections. Consequently, the hypothesis that there will be a significant difference between the rotational angle of the left and right posterior superior iliac spines and the rotational angle of the last lumbar spine during all performed lower trunk rotational positions was rejected.

6.2.4 The relation between the right and left sacroiliac joints according to three anatomical sections and during lower trunk rotation

The current study has shown that the rotational angles of the anatomical selected sections of both right and left sacroiliac joints were varied corresponding to the amount of the left side rotation.

(Barakatt et al. 1996) reported that the sacroiliac joint of young gymnasts and non-gymnasts could move at about 22 to 36 degrees. In a non- weight bearing position study, (Lavignolle et al. 1983) found that the innominate rotated posteriorly by 10-12°, coupled with 6 mm of anterior translation, while the amount of anterior rotation was 2°, coupled with 8mm of anterior translation. (Sturesson et al. 2000) reported in a weight-bearing study that the innominate rotated by 2.5°, coupled with 0.5 to 1.6 mm of translation. (Jacob and Kissling 1995) confirmed the findings of (Sturesson et al. 2000) and they stated that any values higher than 6° of innominate rotation and 2 mm of translation must reflect a pathological condition.

Despite the different positions and techniques that have used to obtain the maximum angle of motion of the sacroiliac joint in these previous mentioned studies, the current study produced a new technique to measure the angle of sacroiliac joint motion according to three sections of the sacroiliac joint, in which, the rotational angle of each section of the sacrum and ilium was measured separately during three rotational positions of the lower trunk. In addition, the mean difference between each two consecutive sections was measured.

The results show that the second lower trunk rotation (R2) caused the highest mean differences between the rotational angles of two consecutive sections of the sacrum and between two consecutive sections of the ilium. Meanwhile, the third lower trunk rotation caused the lowest mean differences values in both sacroiliac joints and in all three sections of the sacrum and ilium. This can be explained by the fact that the second rotational position of the lower trunk may cause the greatest pelvis torsion in which one side of the hip is more rotated than the other.

The three tested sections of the right and left sacrum as well as the ilium followed different behaviours in response to the degree of the lower trunk rotation.

In the second lower trunk rotational position (R2), the highest mean differences of the rotational angles were between the first and second sections (MD1) of the right sacrum,

right ilium, and left sacrum(MD1 > MD2). Meanwhile, the mean differences between the second and third sections (MD2) of the left ilium were the greatest (MD2 > MD1).

In contrast, in the first lower trunk rotation, the highest mean differences of the rotational angles were between the first and second sections (MD1) of the right sacrum and left ilium (MD1 > MD2). While, the mean differences between the second and third sections (MD2) of the left sacrum and right ilium were the greatest (MD2 > MD1).

The third lower trunk rotation followed a different behaviour in which the highest mean differences of the rotational angles were between the first and second sections (MD1) for the both right and left sacrum and ilium (MD1 > MD2). However, the mean differences values showed a nonsignificant effect

(Lee 2004) findings could help to explain these results. Although (Lee 2004) discussed the mechanism of gait, he also stated that a pattern of a physiological gliding movement (anterosuperior) relative to the sacrum could occur when the non-weight bearing innominate rotates posteriorly. The weight bearing innominate glides posteriorly and superiorly depending on the anatomical structures of the articular surfaces of the sacroiliac joint. He proposed that inferiorly and posteriorly patterns of gliding motion are possible concerning the arms of the sacrum when the innominate rotates anteriorly. Furthermore, (Cramer and Darby 2005) stated that the sacroiliac portions are entirely different according to their shapes when studied in the horizontal plane. Therefore, the upper portion and a large section of the middle portion are the ligamentous portions, while the lower portion is a synovial portion. These observations can help to explain the variations in the angle of rotation between the first, second and third sections of the sacroiliac joint during lower trunk rotational positions. Accordingly, the hypothesis which stated that the first lower trunk rotation (mean L5 angle: 88^0) will cause the significant and maximum mean differences between the rotational angles of the selected sections of the sacrum, as well as, between the rotational angles of the selected sections of ilium was rejected.

6.3 Effect of Lower Trunk Rotation on the Lower Lumbar Spine Structures

6.3.1 The angle of rotation of the lower lumbar spine vertebrae and the difference in the spinal canal depth during lower trunk rotation

The degree of vertebral rotation was calculated at two consecutive cuts of MRI to measure the relative vertebral motion at each individual lower lumbar segment and to quantify the rotational torque between L5 and L3 lumbar vertebral levels during neutral and three lower trunk rotational positions.

The data analysis showed that in the neutral position (for the first group), the lower lumbar vertebrae (L3, L4 and L5) recorded degree of rotation in all tested groups. This observation may be associated with the use of pillows under the subject's heads and the position of the MRI coils which caused an elevation of one side of the pelvis relative to the other side. Consequently, in the following MRI scans, the pillows were removed, and the positioning measurements were obtained in order to maintain the subject's neutral position as much as possible.

The degree of vertebral rotation that was calculated at the second selected cut of each lumbar vertebral level was higher than that tested at the first cut. The mean differences (the relative vertebral motion) did not achieve statistical significances in any of the examined vertebral levels, positions and groups. However, the second rotational position (mean 66^0) caused the highest relative vertebral motions. In addition, the lower trunk rotation caused the L3 vertebra to rotate with higher relative motion than L4 and L5 vertebrae.

(Pearcy and Tibrewal 1984) used an in vivo study and found that each lumbar intervertebral level rotated with approximately two degrees. (Panjabi et al. 1994) documented 2.3 º, 1.2 º and 1 º of axial rotation at L3-L4, L4-L5 and L5-S1, respectively by applying loads on the lumbar and lumbosacral spine of cadavers. While (Fujii et al. 2007) concluded that the range of motion in the left axial rotation was 1.5 º,1.9 º, and 1.6 º at L3-L4, L4-L5, and L5-S1 vertebral levels, respectively.

Although the current study conducted the mean differences of the degree of rotation by comparing different landmarks between the two tested vertebral cuts of the same vertebrae, the results indicated that the second lower trunk rotational positions caused L3, L4 and L5 to rotate with a mean difference of -2º, -1.1º and - 0.8º, respectively. These observations are in accordance with (Panjabi et al. 1994).

The mean differences (relative vertebral motion) between the first and second tested cuts for the second rotational position were the highest. This finding can be explained by the fact that the volunteers of the first and second groups (first rotation) started the rotation to reach the side position without exerting the maximum muscular effort in comparison to the third group (second rotation). (Parnianpour et al. 1988; Shirazi-Adl 1994) reported that the coupled axial torque could be generated in individuals with exhausted iso-inertial flexion and extension of the spine in order to compensate for any load perturbations.

The analysed data showed that the lower trunk rotation caused the third lumbar vertebrae (L3) to rotate with the lowest degree compared to L4 and L5 vertebrae in all tested groups and positions. However, the first rotational position (second group) caused the highest mean differences (rotational torque) between the rotational degree of the L5 and L3 vertebrae.

(Bogduk 2005; Lovett 1905) findings may explain this observation. They stated that each segment of the lumbar spine has a dominant movement with regards to the amount of rotational force that produces torsional strain and lateral shear on the individual discs and zygapophyseal joints, the line of the gravity, the musculature activity, and the degree of the lumbar lordotic curvature.

In addition, (Pearcy and Tibrewal 1984; Lovett 1905) showed that the upper lumbar intervertebral levels rotate in the opposite direction to the lower segments during coupled motion of the lumbar spine, while L4-L5 level rotates unpredictably or maybe remained neutral.

Due to its anatomical position, L4-L5 may be exposed to a high rotational movement which may explain the appearance of degenerative changes at this level in comparison

to L3-L4 and L5-S1 levels. In the current study, the L4 level rotation following the L5 segment as a result of its strong connection to the ilia via the ilium ligament.

This result may be explained by the fact that the L4-L5 level was not exposed to high stress due to the greater rotation movement at this level but because of the greater movement from the two opposite rotated segments (L3-L4 and L5-S1). Therefore, manipulative therapy may mainly focus on this level during treatment.

Accordingly, the hypothesis which indicated that the lower trunk rotation with mean L5 angle (88^0) will cause higher relative vertebral motion at each lower lumbar segment (L3, L4, and L5) compared to the second and third rotational position (mean L5 angle: 880, 66^0, and 45^0, respectively) was rejected. In addition, the hypothesis was rejected which stated that the L4 vertebra will rotate with higher relative motion than L3 and L5 vertebrae. While the hypothesis was proved which stated that the first rotational position of the lower trunk (mean L5 angle: 88^0) will result in the maximum rotational torque between L3 and L5 vertebral levels was rejected.

In the present study, the difference in the spinal canal depth between two tested vertebral cuts of individual vertebral level increased dramatically following the degree of the applied lower trunk rotational position. This observation concurs with (Chung et al. 2000), who concluded that the size of the spinal canal and dural sac size decreased in the rotation position as a result of the increase in the ligamentum flavum thickness and the approximation of the posterior margins of the intervertebral disc to the facet joint.

Furthermore,(Cuchanski et al. 2011) concluded that the occlusion per cent of the spinal canal was dependent on the amount and direction of the dynamic applied load on the intervertebral disc.

In contrast, (White and Panjabi 1990) stated that the bending moment results in tensile stresses on the convex side of the spinal cord while the concave side of the cord is exposed to the compressive stress. The magnitude of these stresses is highest on the surfaces and decreases to zero value in the middle.

In the current study, the data showed that the first and second rotational positions obtained the significant values at L3 and L5 intervertebral levels. Meanwhile, performing third lower trunk rotation position caused the lowest and nonsignificant mean differences values at all examined lumbar levels. However, the first rotational position showed the highest mean differences values. This observation could be explained by that the lower trunk rotation which carried out by the third group (second rotation) and fourth groups (third rotation) could be accompanied by flexion or lateral bending which confirmed the results of the aforementioned studies. So, the hypothesis was accepted which stated that the maximum mean difference in the spinal canal depth at L3, L4 and L5 lumbar segments will result by the first lower trunk rotation position with mean L5 angle (88^0).

6.3.2 Effect of Trunk Rotation on the Dimensions of the Lumbar Intervertebral Discs and Neural Foramens: An MRI study

As anticipated, the left lower trunk rotation changed the left and right side dimensions of the intervertebral disc.

In detail, lower trunk rotational positions decreased the area of the right side of the sagittal intervertebral disc at L3-L4 and L4-L5 intervertebral levels, while the area of the left side showed opposite observations. However, the mean differences values did not achieve significant values except that at L4-L5 level. In contrast, the area of the disc decreased at both sides at L5-S1.

The left lower trunk rotational positions caused changes in the width of the right and left sides of the intervertebral disc, in which, the width of the left sides of the intervertebral disc increased at L3-L4 and L4-L5 levels while the right side width decreased. The increasing and decreasing in the width of the left and right sides of the disc at L4-L5 showed the highest values. In contrast, the width of the disc at both sides of the L5-S1level decreased according to the lower trunk rotation.

The findings of the present study are in line with those (Pearcy and Tibrewal 1984) who reported that each intervertebral lumbar spine level had a degree of axial rotation nearly 0 - 2° as a result of the facet orientation and left axial rotation showed higher degrees

of the motion at L3-L4 and L4-L5 lumbar intervertebral levels while L5-S1 showed opposite records.

The current study has also indicated that the area and width of the intervertebral disc at L4-L5 segment showed significant changes, these observations might be explained by (Jensen 1980) who stated that the torsion stress in the spine comes from twisting or rotating on the long axis. Thus, combinations of movements, such as twisting, bending and bending with rotation, will result in increasing stresses and strains on the disc, especially with a superimposed load.

In the present study, the intervertebral disc at L4-L5 may be exposed to a high torsional stress movement due to its anatomical position, which may explain the appearance of degenerative changes at this level in comparison to L3-L4 and L5-S1 levels.

The decreasing in area and width of the intervertebral disc at L5-S1 levels might be explained by the findings of the study of (Pool-Goudzwaard et al. 2003; Sims and Moorman 1996) which indicated that the iliolumbar ligaments might restrict lower lumbar mobility. In addition, (Chadha et al. 2013; Kim et al. 2013) indicated that the facet orientation and tropism have an obvious effect in resisting torsion at L5-S1. (Kulak et al. 1976) indicated that the nucleus has a remarkable effect on sustaining the compressive axial loads. (Stokes 1988) confirmed that the major mechanical function of a facet joint of the lumbar spine is the restriction of axial rotation motion.

However, the decreasing in the width of the right side of the disc at L5-S1 level showed significant mean differences values. This could be explained by (Rousseau et al. 2006) findings who concluded that the obliquity of the sacral endplate caused the anterior intervertebral shear to be significant at the L5-S1 level.

In general, the left lower trunk rotation increased the posterior disc height of the right and left sides at L3-L4 lumbar segment, while reverse observations found at L5-S1 lumbar segment. Different observations showed by the intervertebral disc at L4-L5 level in which the posterior disc height of the right side decreased while the posterior height of the left side of the intervertebral disc increased. However, the mean differences values achieved significant P-values only during the second rotational position for the right side of the L4-L5 and L5-S.

These observations are associated with the height of the intervertebral foraminal height at L3-L4, L4-L5 and L5-S1 levels.

(Hasegawa et al. 1995) demonstrated that there were significant positive correlations between compression of the nerve root and the posterior disc height, the foraminal height, and the foraminal cross-sectional area for the four intervertebral levels between the second lumbar and first sacral vertebrae. The present study was in line with (Hasegawa et al. 1995) study.

(Orías et al. 2016) indicated that the height of the posterior and right zones of the disc increased significantly during right rotation at all lower lumbar segments except for the L5/S1 level, while the left and anterior zones decreased in height. However, these results are not totally in agreement with the findings of the current study because the current study used sagittal MRI images to obtain posterior disc height, while (Orías et al. 2016) obtained their results using axial an MRI.

The anterior disc height of the left side increased at all lower lumbar segments and left lower trunk rotational positions (R1 and R2). While, the anterior disc height of the right side showed reciprocal observations. However, the second rotational position caused the significant decreasing of the anterior disc height at all lower lumbar segments. This phenomenon can be explained by (Jensen 1980) finding that the nucleus serves as a gelatinous mass due to its water content. When a load is applied, this material produces a pressure within the nucleus that pushes the surrounding structures in all directions away from the centre of the nucleus.

In the present study, second lower trunk rotational position showed the significant effects on the area, width, and height of the right and left sides of the intervertebral disc, this might be explained by the that the lower trunk rotation which carried out by the third group (second rotation) could be coupled with flexion or lateral bending which may cause significant effects.

Therefore, the hypothesis that indicated that the intervertebral disc dimensions of each spinal segments will be affected more by applying the first active lower trunk rotational position (mean L5 angle: 88^0) was rejected. Meanwhile the hypothesis which stated that the intervertebral disc dimensions at L4-L5 level will be affected more by applying lower trunk rotation was confirmed.

This study was conceived to analyse the change in the intervertebral foramen dimensions during lower trunk rotation.

It has found that the left lower trunk rotation decreased left foramen areas and width, while the right foramen showed reciprocal observations. The mean differences for the second rotational position caused the significant mean differences. However, the right and left intervertebral foramen areas at L3-L4 level affected more by lower trunk rotation than L4-L5 and L5-S1 levels.

Lower trunk rotational positions caused the right and left foramen height to increase at the L3-L4 level. In contrast, the right and left foraminal height at the L5-S1 level decreased.

The height of the right and left foramen at L4-L5 followed different behaviour, in which, the right foraminal height decreased at L4-L5, while left foraminal height increased at L4-L5. However, the mean differences did not show significant values except of that at the left foramen at L3-L4 and L4-L5 for the second rotational position.

In a cadaveric study, (Fujiwara et al. 2001) reported that the axial rotation significantly decreased both width and area of the foramen on the rotation side while significantly increasing the height and area on the opposite side. However, the current study obtained its results from healthy volunteers.

(Panjabi et al. 1983) illustrated that left axial rotation enlarged the area of the right intervertebral foramen and right axial rotation decreased the area of the right foramen for the non-degenerative specimen. This study also showed that the right rotation caused a dramatic change in the foraminal width of the degenerated foramen. The current study confirms the in-vivo study.

(Chung et al. 2000) found that right rotation caused thickening of the right ligamentum flavum and left rotation increased the thickness of the left ligamentum flavum and resulted in a decrease in the spinal canal and dural sac size. In the current study, the ligamentum flavum might have influenced and reduced the width of the intervertebral foramen when it bulged because it constitutes part of the intervertebral foramen boundaries.

The foraminal heights at L3-L4, L4-L5, and L5-S1 levels followed different patterns corresponding to the lower trunk rotational positions. These patterns refer to the fact that the present study used different rotational techniques and the subjects performed maximum voluntary lower trunk rotational positions.

During data analysis, sagittal MRI images showed that the adjacent section of the vertebral body and vertebral endplates were the main factors that caused changes of the intervertebral foramen dimensions dramatically.

The current study showed that the neural foramen dimensions during second left lower trunk rotational position significantly changed, and this could give us an insight into the treatment benefits of manipulation therapy in spinal conditions (i.e., foraminal stenosis).

Accordingly, the hypothesis which stated that the intervertebral foraminal dimensions of each spinal segments will be affected more by applying the first active lower trunk rotational position (mean L5 angle: 88^0) was rejected. In addition, the hypothesis which indicated that the intervertebral foraminal dimensions at L4-L5 level will be affected more by applying lower trunk rotation was rejected.

6.3.3 The degree of lateral bending during lower trunk rotation

The degree of the lateral bending at all lower lumbar segments increased corresponding to the rotational positions of the lower trunk. The lateral bending angle at L4-L5 was the highest at all rotational positions. However, the mean differences values of the lateral bending angle were significant at the L4-L5 level only during the second rotational position. These results could be explained by (White and Panjabi 1990) who showed that the disc bulge occurs in the mid-disc plane when the spinal structures are subjected to simultaneous compression and the lateral bending. This disc bulge occurs most in the lateral and posterolateral direction on the concave side of the lateral bend. However, (Pearcy and Tibrewal 1984) showed different observation which showed that lateral bending at the upper three lumbar segments was about 10 degrees, while there were 6 and 3 degrees at L4-5 and L5-S1, respectively. In contrast, (Barnes et al. 2009) indicated that the primary lateral bending increased from three degrees at T12-L1 to 4.9 degrees at L4-L5, while reduced to 3.4 degrees at L5-S1. (Pearcy and Tibrewal 1984) indicated that there was no simple mechanical coupling of the spine rotations and the coordination between the shapes of the lumbar lordosis together with muscular actions are the main determining factors that may explain the relationship between the primary and accompanying rotations.

Therefore, the hypothesis which stated that the lateral bending angle will be the greatest with the first rotational position of the lower trunk (mean L5 angle: 88^0) was rejected.

6.3.4 The orientation angle of the left and right superior articular processes and the cross-sectional area of the gapping between the superior and inferior articular processes during lower trunk rotation.

The method in which the multiple MRI images were merged to fix reliable landmarks to measure the orientation of the superior lumbar articular processes was found to have high reliability (ICC ranged from 0.95 to 1). Therefore, this procedure can enable MRI users to diagnose or measure the orientation angle of the articular processe depending on the previously mentioned landmarks.

The orientation angle of the superior articular process in normal and pathological condition was previously mentioned in the literature review.

However, although (Boden et al. 1996) used this technique to compare the orientation of the facet of asymptomatic individuals with patients who had degenerative spondylolisthesis, the present study has adapted this technique for use with healthy individuals. Comparing the data from the present study with that of (Boden et al. 1996; Panjabi et al. 1993), the orientation angle of the superior articular facet in the neutral position at all examined lumbar levels showed approximately the same observations as that of the Boden technique with small variations.

In contrast, (Panjabi et al. 1993) method expressed large variation compared with the present method especially for the L4 articular facets (Table 6-1 and Table 6-2). These variations may be related to two reasons. The first reason is that (Panjabi et al. 1993) used a different technique to measure the rotational angle of the superior articular process as mention in the literature review. The second reason could be explained by (Bogduk 2005; Jaumard et al. 2011), who stated that the articular facets could vary both in the shape of their articular surfaces and in the general orientation that they faced. The complex mechanical performance of the facet joints may be dependent on the responsibilities imposed by the whole spine and on the other spine structures such as the intervertebral disc.

Table 6-1: Results of Boden et al. (1996)

Level	Side	No.	Mean and Standard Error of Mean
L5-S1			
	R	63	39 ± 1.3
	L	63	37 ± 1.2
L4-L5			
	R	66	42 ± 1.3
	L	66	40 ± 1.4
L3-L4			
	R	66	51 ± 1.1
	L	66	49 ± 1.3
L2-L3			
	R	16	59 ± 3.5
	L	16	56 ± 3.2

Table 6-2: Results of (Panjabi et al., 1993) (cited from Masharawi et al. 2004)

Vertebrae	Superior facet orientation angle	
	Left	Right
L2	50.1	45.6
L3	43.4	42.0
L4	34.0	31.0
L5	29.9	27.7

The current study indicated that the mean differences between the left and right superior articular processes according to their orientation angle and gapping distance at the L3-L4 level were higher than that of the other tested levels, while the L5 level recorded the lowest values. This observation could be explained by (Oxland et al. 1992), who concluded that the articular facets at the lumbosacral joint resisted the coupled axial

rotation when lateral bending was applied, whereas, a combination of motion such as lateral rotation under the applied axial torque were resisted most by the disc structure.

(Shin et al. 2013) showed that the dynamic axial rotation across individual motion level resulted in coupled contralateral bending towards the opposite side at L2-L3, and L3-L4 intervertebral levels, while L4-L5, and L5-S1 segments demonstrated coupling lateral bending towards the same side of rotation. In contrast, (Kozanek et al. 2009) stated that the lower range of torsion and bending in the upper lumbar segments along with the more sagittal orientation of the facet might better protect the annulus of the disc, which is most likely to fail in bending and torsion. The findings of (Kalichman et al. 2009; Toyone et al. 2009) may explain this phenomenon as they proposed that a more sagittal orientation of the facet joint promotes anterior gliding by reducing resistance to anterior shear forces.

In the present study, due to its position, the facet joint at L3 intervertebral level might introduce a maximum effort in order to overcome the excessive effect of torque on the adjacent intervertebral disc primarily for the second rotational position (R3). Similar findings were made by (Masharawi et al. 2004) who mentioned that regardless of the axes in which the lumbar segments motion is involved, a complex multiplanar movement can occur. This could explain the initiation of the rotational movement in the lumbar spine which depends on the more angulated left facet. These observations confirm the hypothesis that the degree of the facet orientation and the amount of the gapping between two articular processes of the normal facet during each lower trunk rotational position will help in a successful designing of the artificial facet.

Accordingly, the hypothesis which showed that the mean differences between the orientation angle of the right and the left superior articular processes and the cross-sectional area of the opening of the left articular at each individual lower lumbar segments will be the highest at the first rotational position of the lower trunk (mean L5 angle: 88^0) was rejected. In addition, the hypothesis which indicated that the mean difference between the orientation angle of the right and the left superior articular processes and the amount of the gapping between two articular processes of the normal facet will be the highest at L4-L5 level was rejected.

The observed data shows that the values of the mean differences between the left and right superior articular processes orientation angle and the gapping distance at L4-L5 and L5-S1 were the lowest values.

(Farfan and Sullivan 1967) concluded that the asymmetry of the facet joints correlated with the development of disc herniation, due to the fact that the coronal facing facet joint offers little resistance to intervertebral shear force. This means that the rotation occurs towards the side of the more coronal facing facet joint which possibly leads to additional torsional stress on the annulus fibrous and may cause disc injury at these intervertebral levels (L4-L5 and L5-S1).

Despite this fact, the mean difference between the orientation angle of right and left superior articular process showed minimum angle of orientation in the neutral position for the first tested group. These minimum degrees of orientation of the superior articular process did not cause any remarkable opening of the facet joints. This observation can be explained by the fact that when the adjacent intervertebral disc did not undergo a maximum applied load, the facets' gapping could apply with minimum effort, in another word, the degree of the mean difference between the orientation angle of the right and left superior articular facets can control the applied load on the disc by applying the required opening distance of the facet according to each involved lumbar segment. These observations of the mean differences and gapping distances between the left and right articular facets can be used to provide the necessary information to develop a successful designing of the artificial facet.

6.4 The efficacy of the MRI during lower trunk rotation

MRI proved to be the effective method to three dimensionally show the structures of the lumbar spine and sacroiliac joint. However, the images of certain anatomical regions in the human spine and sacroiliac joint appeared to have a poor contrast due to the presence of different soft tissue types, such as muscles, ligaments, joint capsules and cartilage. These limitations caused difficulty in the precise localisation of the anatomical landmarks of the selected parameters of the spine and the sacroiliac joint as mentioned in Chapter Four. These observations are in line with those of (Mendieta

2016; Rathnayaka Mudiyanselage 2011). In addition, long-term scanning caused motion artefacts, which may have resulted from breathing, blood flow in the vessels, respiration and heartbeat. Longer scanning times can cause random moving of the body parts, such as muscle contraction, which is initiated from nerve excitation and can be seen in the final image stack. Therefore, motion artefacts can occur as a result of the miss registration of pixels along the phase-encoding direction. These observations are in accordance with (Erasmus et al. 2004). In addition, these observations confirm the hypothesis that the MRI will be the effective method to show three dimensionally lumbar spine and sacroiliac joint structures, but the poor contrast and the motion artefacts resulted in causing some data to be excluded.

Chapter 7

Conclusions, Limitations, Contributions and Future Work

7.1 Introduction

The coordination between the shoulder and pelvis motions are crucial factors to continue a flexible dynamic trunk motion. Consequently, a better understanding of the normal lumbar spine biomechanical behaviour during each rotational position will enable us to obtain optimal functional performance of the spin during different movements and also provide valuable translational information to guide better physiotherapy in the future. It will also provide normal variant data that will help healthcare professionals and the specialist in the artificial spine implants to understand certain aspects of spinal pain. Consequently, the current study proposes an MRI study of the lumbar spine during different lower trunk rotational positions to investigate their effect on the normal spine structures with the consideration of the shoulder and pelvis girdles' motion.

7.2 Conclusions

- The right and left posterior boarders of the acromion processes were taken to measure the scapula positions during neutral and three lower trunk rotational positions. The distance between the right and left posterior borders of the acromion process and the table altered significantly in response to the different lower trunk rotational positions. These findings are an important reason for therapists to consider the pattern of motion and position of the scapula during spinal manipulation. In addition, the position of the right and left scapula can provide a baseline information about the degree of rotation of the lower trunk.
- To prove the accuracy of the modified goniometer and MRI holder to measure and control the pelvic angle of rotation during the first and second rotational positions of the lower trunk, the angle between the left and right posterior iliac spines and the horizon was measured using the modified goniometer. The goniometer measurements were then compared with the MRI measurement. The nonsignificant difference between the modified goniometer and MRI measurements demonstrate that the modified goniometer can provide a useful in vitro clinical means to control the pelvis angle of rotation depending on the

determined pelvic landmarks mainly when it is used in parallel with the MRI holder device.

- The mean differences between the angle of rotation of L5 and the rotational angle of the left and right posterior superior iliac spines in three tested sections were measured relative to the horizontal plane by using MRI and during three lower trunk rotational positions. The data showed there is no significant difference between the rotational angle of the L5 vertebrae and the rotational angle of the left and right posterior superior iliac spines according to the horizontal plane and different rotational positions of the lower trunk. Consequently, a manipulation therapy that targets the L5-S1 level would be futile.
- The angle of rotation of the three sections of the sacrum and ilium in three lower trunk rotational positions were measured relative to the horizontal plane using MRI. The results indicate that there is a nonsignificant difference between the rotational angles of two consecutive sections of the sacrum and between two consecutive sections of the ilium during all the selected anatomical sections and the rotational positions of the lower trunk. However, the results showed that the second lower trunk rotation (mean 66^0) caused the highest mean differences, while the third lower trunk rotation(mean 45^0) caused the lowest mean differences values in both sacroiliac joints and in all three sections of the sacrum and ilium. Although the findings of these measurements showed no significant effect, the results may explain the effects of manipulation therapy which is targeting the sacroiliac joint to provide a necessary information about the amount of the mobility of the different sections of the sacroiliac joint in each rotational position of the lower trunk to obtain better pain relive of the sacroiliac joint. As well as, this minimum mobility of the sacroiliac joint could be considered as a minimum relieve of the strain on the lumbar spine and it is therefore, clarify the effects of the manipulation therapy.
- The degree of vertebral rotation was calculated at two consecutive cuts of MRI to measure the relative vertebral motion at each individual lower lumbar segment and to quantify the rotational torque between L5 and L3 lumbar vertebral levels. The relative vertebral motion and the degree of the rotational torque in all examined vertebral levels and groups did not achieve statistical significances during all performed lower trunk rotational positions. However the

second rotational position (mean 66^0) caused the highest relative vertebral motions, while the first rotational position (mean 87.5^0) caused the highest rotational torque between the rotational degree of the L5 and L3 vertebrae. The vertebral level that showed the highest relative motion and the lowest degree of rotation was L3, while L5 vertebrae showed the adverse observation. This data may provide a new orientation in the treatment when using a manipulation therapy in spinal conditions. Each rotational position of the lower trunk has its unique effect on each vertebral level. Therefore, care should be taken to overcome the potential adverse effects of manipulation therapy. The difference in the spinal canal depth between two tested vertebral cuts at each vertebral level increased dramatically following the degree of the applied lower trunk rotational position. However, the data showed that the first (mean 87.5^0) and second (mean 66^0) rotational positions obtained the significant values at L3 and L5 intervertebral levels. In contrast, performing third lower trunk rotation position (45^0) caused the lowest and non-significant mean differences values at all examined lumbar levels. This observation may explain the rotational posture-dependent symptom of spinal stenosis.

- The current study used sagittal MRI to measure the area, width and height of the intervertebral disc and foramen of the lower lumbar vertebrae corresponding to three lower trunk rotational positions (87.5^0, 66^0, and 45^0). Low back rotation caused morphologic changes in the intervertebral discs and intervertebral foramens at L3-L4, L4-L5, and L5-S1 levels. At the rotation side, there was an increase in the area, width, and anterior height of the intervertebral disc at L3-L4 and L4-L5 levels. The opposite side to the rotation showed reciprocal changes. However, the area and width of the intervertebral disc at L4-L5 changed significantly during the second rotational position. In contrast, the intervertebral disc area and width at the L5-S1 level decreased at both sides. The left lower trunk rotation increased the posterior disc height of the right and left sides at L3-L4 lumbar segment, while reverse observations found at L5-S1 lumbar segment. Meanwhile, different observations showed the intervertebral disc at the L4-L5 level. In turn, left lower trunk rotation decreased left foramen areas and width, while the right foramen showed reciprocal observations. Furthermore, left lower trunk rotational positions caused the right and left foramen height to increase at the L3-L4 level. In contrast, the right and left

foraminal height at the L5-S1 level decreased. An anatomical relationship was indicated between the posterior height of the intervertebral disc at both sides and the foraminal height. The height of the right and left foramen at L4-L5 followed different behaviour. However, the second lower trunk rotational position caused the significant changes in the dimensions of the disc and foramen of the lower lumbar vertebrae. The current study showed that the neural foramen dimensions during second left lower trunk rotational position significantly changed. This could help explain the treatment benefits of manipulation therapy in the spinal conditions.

- The lateral bending angle of each two consecutive lower lumbar vertebrae for neutral and three rotational positions of the lower trunk was calculated using mid-sagittal MRI images. The degree of the lateral bending at all lower lumbar segments increased corresponding to the rotational positions of the lower trunk. The lateral bending angle at L4-L5 was the highest. However, the significant effect was only found during the second rotational position. Therefore, manipulative therapy may mainly focus on this level during treatment.
- The effect of three lower trunk rotational positions on the orientation of the superior articular process of the lower lumbar vertebrae and on the cross-sectional area of the gapping between the superior and inferior articular processes relative to the intervertebral disc rotational angle, were evaluated by using T2 Axial cuts 3D images. The current study indicated that the mean differences between the left and right superior articular processes according to their orientation angle at the L3-L4 level were higher than that of the other tested levels, while the L5 level recorded the lowest values. However, the mean differences values showed no significant effect for all performed lower trunk rotational positions. In contrast, the data showed that the mean differences of the cross-sectional area of the gapping distance of the left articular facets at all tested intervertebral levels significantly increased when subjects changed positions from neutral to the rotation positions. However, the second rotational position of the lower trunk (66^0) caused the highest mean differences values of the orientation angles and gapping distances of the right and left facet. These results indicated that the orientation and the gapping distance of the articular facet worked harmoniously with the amount of the applied load on the disc and did not depend on the degree of the disc rotational angle. These results may

provide baseline information to enable the development of the artificial implants of the right and left lumbar facet joints according to the changes in lower trunk rotational positions. In other words, the degree of the mean difference between the orientation angle of the right and left superior articular facets can control the applied load on the disc by applying the required opening distance of the facet according to each involved lumbar segment.

- MRI proved to be an effective method to three dimensionally show the lumbar spine and sacroiliac joint structures but the poor contrast and the motion artefacts resulted in the exclusion of some of the data.

7.3 Limitations

- Small sample size, which may not reflect the normal population.
- While the modified goniometer was proven to be an accurate method to measure the pelvis angle of rotation, this apparatus is limited to measuring of pelvis angle at 45^0 because there was difficulty to fit the measuring arm of the adaptive goniometer with the right and left posterior superior iliac spines.
- The physiological variations between individuals when they actively rotate their spines may explain the gap differences in rotation angles between subjects.
- It was difficult to diagnose the volunteer's spinal disorders as a result of the cost of MRI and difficulty of carrying out X-ray (i.e. risk of radiation exposure). For these reasons, much data was excluded because the scanned volunteers did not have well-hydrated discs.
- The anatomical variations in the lumbar facet orientations between individuals caused a considered high standard error in the measurements.
- The anatomical variations of the sacroiliac joint between individuals caused a considered a high standard error in the measurements.
- While MRI has proven to be an effective method to three dimensionally show lumbar spine and sacroiliac joint structures, the images of certain anatomical regions in the human spine and sacroiliac joint had a poor contrast. In addition, motion artefacts caused the exclusion of some of the data. In addition, motion artefacts may have resulted from breathing, blood flow in the vessels, respiration and heartbeat. Longer scanning times can cause random moving of the body

parts, such as muscle contraction, which is initiated from nerve excitation and can be seen in the final image stack. Therefore, motion artefacts can occur as a result of the miss registration of pixels along the phase-encoding direction (Erasmus et al., 2004). Thus, the protocol used and the length of movement of the scanned structure can determine the nature and the extent of the artefacts.

7.4 Contributions

To quantify the effect of three rotational positions of the lower trunk on the spine structures and on the shoulder and pelvis girdles, the following contributions were made:

- A novel MRI holder and a modified goniometer were used to measure and control the pelvis angle of rotation while maintaining the active rotational movement of the subject's pelvis. The method can help to prevent the motion artefacts during long term positioning.
- A new method was used to compare the goniometer measurements with MRI measurement to quantify the accuracy of the modified goniometer and MRI holder to measure and control the pelvic angle of rotation during lower trunk rotation.
- A novel method was used to compare the rotational angle of L5 vertebrae with the rotational angle of the left and right posterior superior iliac spines by selecting three anatomical sections of the posterior superior iliac spines.
- A new method was used to calculate the mean differences of the angle of rotation between two consecutive anatomical slices of the sacrum and ilium bones while using an unsharp mask filter to clarify the borders of the sacrum and ilium bones.
- A novel method was made to calculate the angle of vertebral rotation based on merging two selected cuts of T2 axial 3D acquisition. The angle of rotation at the first cut was made between the horizon and two points, the first point was made at the attachment of the left pedicle with the left superior articular processes while the second one was made at the opposite side. The second rotational angle was made between the horizon and the base of the left and right pedicles.

- A novel method was used to calculate the relative motion of each vertebral level by subtracting the angle of vertebral rotation at the first cut from the second cut.
- A novel method was obtained to quantify the difference in the spinal canal depth by using two selected cuts.
- A modified technique was defined to quantify the intervertebral disc and foramen depending on taking the average measurements of two consecutive sagittal slices that showed the obvious nerve root, pedicles, endplate of the upper vertebrae, and the obvious tip of the superior facet.
- A modified technique was used to measure the orientation angle of the superior articular processes depending on the rotational angle of the intervertebral disc and using three merging axial MRI cuts to distinguish the anterior and posterior borders of the superior articular processes from the adjacent soft tissues.

7.5 Future Work

This research has produced some original contributions and findings. However, the following recommendations have been made for future research in this topic:

- Quantify and compare the cross-sectional area of the gapping distance of the sacroiliac joints during different lower trunk positions by using the same three cuts of the right and left sacroiliac joints.
- Because quantifying the angle of vertebral rotation based on using two cuts of the same vertebrae, in which the first cut showed the first obvious point of the left transverse process and the second cut showed the last clear point of the right transverse process, the effect of each lower trunk rotational position on each side of dural sac can be qualified by obtaining the observation of the degree of compression on each side.
- Because the present study did not measure the bulging of the ligamentum flavum, mid- dis dimensions, flexion angle of the lower lumbar vertebrae. Consequently, further studies are needed to assess the effect of low trunk rotation on the morphological structure of the ligamentum flavum, mid-dis dimensions and flexion angle of the lower lumbar vertebrae.
- Because the current study used three cuts to quantify the orientation angle and the gapping distance of the facet, the gapping distance at the first selected cut

could be used to compare the differences between these cuts according to their gapping at each disc level (i.e., mid dis or at the borders of the disc). In addition, the orientation angle of the superior articular processes could be quantified at the endplate level instead of the disc level because the disc's biomechanical properties may vary between individuals.

References

Aaro, S. and Dahlborn, M. 1981. Estimation of vertebral rotation and the spinal and rib cage deformity in scoliosis by computer tomography. *Spine* 6(5), pp. 460–467.

Abbas, J., Hamoud, K., Masharawi, Y.M., May, H., Hay, O., Medlej, B., Peled, N. and Hershkovitz, I. 2010. Ligamentum flavum thickness in normal and stenotic lumbar spines. *Spine* 35(12), pp. 1225–1230.

Abitbol, M.M. 1989. Sacral curvature and supine posture. *American journal of physical anthropology* 80(3), pp. 379–389.

Adams, M.A. and Dolan, P. 1995. Recent advances in lumbar spinal mechanics and their significance for modelling. *Clinical biomechanics* 10(1), pp. 3–19.

Adams, M.A. and Hutton, W.C. 1981. The relevance of torsion to the mechanical derangement of the lumbar spine. *Spine* 6(3), pp. 241–248.

Adams, M.A. and Hutton, W.C. 1980. The effect of posture on the role of the apophysial joints in resisting intervertebral compressive forces. *The Journal of bone and joint surgery. British volume* 62(3), pp. 358–62.

Adhia, D.B., Milosavljevic, S., Tumilty, S. and Bussey, M.D. 2016. Innominate movement patterns, rotation trends and range of motion in individuals with low back pain of sacroiliac joint origin. *Manual Therapy* 21, pp. 100–108.

Ahmad, T., Goel, P. and Babu, C.R. 2011. A study of lumbar canal by MRI in clinically symptomatic and asymptomatic subjects. *J Anat Soc* 60(2), pp. 184–187.

Ahmed, A.M., Duncan, N.A. and Burke, D.L. 1990. The effect of facet geometry on the axial torque-rotation response of lumbar motion segments. *Spine* 15(5), pp. 391–401.

Al-Hadidi, M.T., Badran, D.H., Al-Hadidi, A.M. and Abu-Ghaida, J.H. 2001. Magnetic resonance imaging of normal lumbar intervertebral foraminal height. *Saudi medical journal* 22(11), pp. 1013–1018.

Allegri, M., Montella, S., Salici, F., Valente, A., Marchesini, M., Compagnone, C., Baciarello, M., Manferdini, M.E. and Fanelli, G. 2016. Mechanisms of low back pain: a guide for diagnosis and therapy. *F1000Research* 5, p. 1530. Available at: https://f1000research.com/articles/5-1530/v2.

Alqhtani, R.S., Jones, M.D., Theobald, P.S. and Williams, J.M. 2016. Investigating the contribution of the upper and lower lumbar spine, relative to hip motion, in everyday

tasks. *Manual Therapy* 21, pp. 268–273.

Alsancak, S., Sener, G., Erdemli, B. and Ogun, T. 1998. Three dimensional measurements of pelvic tilt in trans-tibial amputations: the effects of pelvic tilt on trunk muscles strength and characteristics of gait. *Prosthetics and orthotics international* 22(1), pp. 17–24.

Alyas, F., Connell, D. and Saifuddin, A. 2008. Upright positional MRI of the lumbar spine. *Clinical Radiology* 63(9), pp. 1035–1048.

Amadou, A., Sonhaye, L., James, Y.N., Assih, K., Agbangba, A.K. and Wattara, G. 2017. Normative dimensions of lumbar canal and dural sac by computer tomography in Togo. 5(3), pp. 1–4.

Argoubi, M. and Shirazi-Adl, A. 1996. Poroelastic creep response analysis of a lumbar motion segment in compression. *Journal of Biomechanics* 29(10), pp. 1331–1339.

Assendelft, W.J., Bouter, L.M. and Knipschild, P.G. 1996. Complications of spinal manipulation-a comprehensive review of the literature. *The Journal of Family Practice* 42(5), pp. 475–480.

Bailey, J.F., Miller, S.L., Khieu, K., O'Neill, C.W., Healey, R.M., Coughlin, D.G., Sayson, J.V., Chang, D.G., Hargens, A.R. and Lotz, J.C. 2018. From the international space station to the clinic: how prolonged unloading may disrupt lumbar spine stability. *Spine Journal* 18(1), pp. 7–14.

Bakland, O. and Hansen, J.H. 1984. The 'axial sacroiliac joint'. *Anatomia Clinica* 6(1), pp. 29–36.

Barakatt, E., Smidt, G.L., Dawson, J.D., Wei, S.H. and Heiss, D.G. 1996. Interinnominate Motion and Symmetry: Comparison Between Gymnasts and Nongymnasts. *Journal of Orthopaedic & Sports Physical Therapy* 23(5), pp. 309–319.

Barboriak, D.P., Padua, A.O., York, G.E. and MacFall, J.R. 2005. Creation of DICOM—Aware Applications Using ImageJ. *Journal of Digital Imaging* 18(2), pp. 91–99.

Barnes, D., Stemper, B.D., Yogananan, N., Baisden, J.L. and Pintar, F.A. 2009. Normal coupling behavior between axial rotation and lateral bending in the lumbar spine-biomed 2009. *Biomedical sciences instrumentation* 45, pp. 131–136.

Been, E., Li, L., Hunter, D.J. and Kalichman, L. 2011. Geometry of the vertebral bodies and the intervertebral discs in lumbar segments adjacent to spondylolysis and spondylolisthesis: Pilot study. *European Spine Journal* 20(7), pp. 1159–1165.

Berthonnaud, E., Herzberg, G., Zhao, K.D., An, K.N. and Dimnet, J. 2005. Three-dimensional in vivo displacements of the shoulder complex from biplanar radiography. *Surgical and Radiologic Anatomy* 27(3), pp. 214–222.

Birchall, D., Hughes, D.G., Hindle, J., Robinson, L. and Williamson, J.B. 1997. Measurement of vertebral rotation in adolescent idiopathic scoliosis using three-dimensional magnetic resonance imaging. *Spine* 22(20), pp. 2403–2407.

Boden, S.D., Riew, K.D., Yamaguchi, K., Branch, T.P., Schellinger, D. and Wiesel, S.W. 1996. Orientation of the Lumbar Facet Joints : Association with Degenerative Disc Disease. *Journal of Bone and Joint Surgery* 78(3), pp. 403–411.

Bogduk, N. 2005. *Clinical anatomy of the lumbar spine and sacrum*. 4th ed. pp.1-67. Churchill Livingstone.

Borich, M.R., Bright, J.M., Lorello, D.J., Cieminski, C.J., Buisman, T. and Ludewig, P.M. 2006. Scapular Angular Positioning at End Range Internal Rotation in Cases of Glenohumeral Internal Rotation Deficit. *Journal of Orthopaedic & Sports Physical Therapy* 36(12), pp. 926–934.

Bowen, V. and Cassidy, J.D. 1980. Macroscopic and microscopic anatomy of the sacroiliac joint from embryonic life until the eighth decadeNo Title. *Spine* 6(6), pp. 620–628.

Brinjikji, W., Luetmer, P.H., Comstock, B., Bresnahan, B.W., Chen, L.E., Deyo, R.A., Halabi, S., Turner, J.A., Avins, A.L., James, K. and Wald, J.T. 2015. Systematic Literature Review of Imaging Features of Spinal Degeneration in Asymptomatic Populations. *American Jounral of Neuroradiology* 36(4), pp. 811-816.

Cael C. 2010. *Functional anatomy musculoskeletal anatomy , kinesiology, and palpation for manual therapists*. 1st ed. Lippincott Williams& Wilkins.

Cerny, P., Marik, I. and Pallova, I. 2014. The radiographic method for evaluation of axial vertebral rotation - presentation of the new method. *Scoliosis* 9(1), pp. 1–9.

Chadha, M., Sharma, G., Arora, S.S. and Kochar, V. 2013. Association of facet tropism

with lumbar disc herniation. *European Spine Journal* 22(5), pp. 1045–1052.

Chen, H., Schlösser, T.P., Brink, R.C., Colo, D., Van Stralen, M., Shi, L., Chu, W.C., Heng, P.A., Castelein, R.M. and Cheng, J.C. 2017. The Height-Width-Depth Ratios of the Intervertebral Discs and Vertebral Bodies in Adolescent Idiopathic Scoliosis vs Controls in a Chinese Population. *Scientific Reports* 7, pp. 1–7.

Chi, W.M., Cheng, C.W., Yeh, W.C., Chuang, S.C., Chang, T.S. and Chen, J.H. 2006. Vertebral axial rotation measurement method. *Computer Methods and Programs in Biomedicine* 81(1), pp. 8–17.

Chung, S.S., Lee, C.S., Kim, S.H., Chung, M.W. and Ahn, J.M. 2000. Effect of low back posture on the morphology of the spinal canal. *Skeletal Radiology* 29(4), pp. 217–223.

Cinotti, G., De Santis, P., Nofroni, I. and Postacchini, F. 2002. Stenosis of Lumbar Intervertebral Foramen. *Spine* 27(3), pp. 223–229.

Cohen, S.P. 2005. Sacroiliac joint pain: A comprehensive review of anatomy, diagnosis and treatment. *Anesthesia and Analgesia* 101(5), pp. 1440–1453.

Collins, T.J. 2007. ImageJ for microscopy. *BioTechniques* 43(1 Suppl), pp. 25–30.

Coric, D. 2014. Spinal technologies not available in the United States: An editorial. *Neurosurgery* 61(1), pp. 26–29.

Costi, J.J., Stokes, I.A., Gardner-Morse, M., Laible, J.P., Scoffone, H.M. and Iatridis, J.C. 2007. Direct measurement of intervertebral disc maximum shear strain in six degrees of freedom : Motions that place disc tissue at risk of injury. *Journal of biomechanics* 40(11), pp. 2457–2466.

Cramer, G.D., Cantu, J.A., Dorsett, R.D., Greenstein, J.S., McGregor, M., Howe, J.E. and Glenn, W.V. 2003. Dimensions of the lumbar intervertebral foramina as determined from the sagittal plane magnetic resonance imaging scans of 95 normal subjects. *Journal of Manipulative and Physiological Therapeutics* 26(3), pp. 160–170.

Cramer, G.D., Tuck Jr, N.R., Knudsen, J.T., Fonda, S.D., Schliesser, J.S., Fournier, J.T. and Patel, P. 2000. Effects of side-posture positioning and side-posture adjusting on the lumbar zygapophysial joints as evaluated by magnetic resonance imaging: a before and after study with randomization. *Journal of Manipulative and Physiological*

Therapeutics 23(6), pp. 380–394.

Cramer, G.D. and Darby, S.A. 2005. *Basic and clinical anatomy of the spine, spinal cord, and ANS-E-Book*. 2nd ed. pp.308-331. Elsevier Health Sciences.

Criswell, A.J. 2013. Development of a lumbar facet joint replacement by. (Doctoral dissertation),University of Iowa.

Crommert, M.E., Halvorsen, K. and Ekblom, M.M. 2015. Trunk Muscle Activation at the Initiation and Braking of Bilateral Shoulder Flexion Movements of Different Amplitudes. *PloS one* 10(11), pp. 1–16.

Cuchanski, M., Cook, D., Whiting, D.M. and Cheng, B.C. 2011. Measurement of occlusion of the spinal canal and intervertebral foramen by intervertebral disc bulge. *SAS Journal* 5(1), pp. 9–15.

DeStefano L.A. 2017. *Greenmans principles of manual medicine*. 5th ed., pp.49-55. Wolters Kluwer.

Do, D.H., Taghavi, C.E., and Fong, W., Kong, M.H., Morishita, Y. and Wang, J.C. 2011. The relationship between degree of facet tropism and amount of dynamic disc bulge in lumbar spine of patients symptomatic for low back pain. *European Spine Journal*, 20(1), pp.71-78.

Dolan, P., Earley, M. and Adams, M.A. 1994. Bending and compressive stresses acting on the lumbar spine during lifting activities. *Journal of Biomechanics* 27(10), pp. 1237–1248.

Donatell, G.J., Meister, D.W., O'Brien, J.R., Thurlow, J.S., Webster, J.G. and Salvi, F.J. 2005. A simple device to monitor flexion and lateral bending of the lumbar spine. *IEEE Transactions on Neural Systems and Rehabilitation Engineering* 13(1), pp. 18-23.

Drerup, B. 1985. Improvements in measuring vertebral rotation from the projections of the pedicles. *Journal of Biomechanics* 18(5), pp. 369–378.

Ebert, R., Campbell, A., Kemp-Smith, K. and O'Sullivan, P. 2014. Lumbar spine side bending is reduced in end range extension compared to neutral and end range flexion postures. *Manual Therapy* 19(2), pp. 114–118.

Ebraheim, N., Sabry, F.F., Nadim, Y., Xu, R. and Yeasting, R.A. 2003. Internal

Architecture of the Sacrum in the Elderly: an anatomic and radiographic study. *Spine* 25(3), pp. 292–297.

Egund, N., Olsson, T.H., Schmid, H. and Selvik, G. 1978. Movements in the sacroiliac joints demonstrated with roentgen stereophotogrammetry. *Acta Radiologica* 19(5), pp. 833–846.

Ehara, S., El-Khoury, G.Y. and Bergman, R.A., 1988. The accessory sacroiliac joint: a common anatomic variant. *American Journal of Roentgenology* 150(4), pp. 857–859.

Von Eisenhart-Rothe, R.M., Jäger, A., Englmeier, K.H., Vogl, T.J. and Graichen, H. 2002. Relevance of Arm Position and Muscle Activity on Three-Dimensional Glenohumeral Translation in Patients with Traumatic and Atraumatic. *The American journal of sports medicine* 30(4), pp. 514–522.

Erasmus, L.J., Hurter, D., Naudé, M., Kritzinger, H.G. and Acho, S. 2004. A short overview of MRI artefacts. *SA Journal of Radiology* 8(2), pp. 13–17.

Ernst, E. and Assendelft, W.J.J. 1998. Chiropractic for low back pain: We don't know whether it does more good than harmo Title. *British medical journal* 317(7152), pp. 160–160.

Evans, D.W. 2010. Why do spinal manipulation techniques take the form they do? Towards a general model of spinal manipulation. *Manual Therapy* 15(3), pp. 212–219.

Farfan, H.F., Cossette, J.W., Robertson, G.H., Wells, R.V. and Kraus, H. 1970. The effects of torsion on the lumbar intervertebral joints: the role of torsion in the production of disc degeneration. *JBJS* 52(3), pp. 1115–1120.

Farfan, H.F. and Sullivan, J.D. 1967. The relation of facet orientation to intervertebral disc failure. *Canadian journal of surgery* 10(2), p. 179.

Fazey, P.J., Takasaki, H. and Singer, K.P. 2010. Nucleus pulposus deformation in response to lumbar spine lateral flexion: An in vivo MRI investigation. *European Spine Journal* 19(7), pp. 1115–1120.

Forthomme, B., Crielaard, J.M. and Croisier, J.L. 2008. Scapular positioning in athlete's shoulder: Particularities, clinical measurements and implications. *Sports Medicine* 38(5), pp. 369–386.

Fortin, M., Omidyeganeh, M., Battié, M.C., Ahmad, O. and Rivaz, H. 2017. Evaluation

of an automated thresholding algorithm for the quantification of paraspinal muscle composition from MRI images. *BioMedical Engineering OnLine* 16(1), p. 61.

Fredericson, M., Lee, S.U., Welsh, J., Butts, K., Norbash, A. and Carragee, E.J. 2001. Changes in posterior disc bulging and intervertebral foraminal size associated with flexion-extension movement: a comparison between L4–5 and L5–S1 levels in normal subjects. *The Spine Journal* 1(1), pp. 10–17.

Frigerio, N.A., Stowe, R.R. and Howe, J.W. 1974. Movement of the sacroiliac joint. *Clinical Orthopaedics and Related Research* 100, pp. 370–377.

Fujii, R., Sakaura, H., Mukai, Y., Hosono, N., Ishii, T., Iwasaki, M., Yoshikawa, H. and Sugamoto, K. 2007. Kinematics of the lumbar spine in trunk rotation: In vivo three-dimensional analysis using magnetic resonance imaging. *European Spine Journal* 16(11), pp. 1867–1874.

Fujiwara, A., An, H.S., Lim, T.H. and Haughton, V.M. 2001. Morphologic changes in the lumbar intervertebral foramen due to flexion-extension, lateral bending, and axial rotation: an in vitro anatomic and biomechanical study. *Spine* 26(8), pp. 876–882.

Ghasemi, A., Haddadi, K., Khoshakhlagh, M. and Ganjeh, H.R. 2016. The Relation between Sacral Angle and Vertical Angle of Sacral Curvature and Lumbar Disc Degeneration. *Medicine (United States)* 95(6), pp. 1–6.

Göçen, S., Havitçioğlu, H. and Alici, E. 1999. A new method to measure vertebral rotation from CT scans. *European Spine Journal* 8(4), pp. 261–265.

Van Goethem, J.W. 2010. *Magnetic resonance imaging of the spine. In Clinical MR Imaging*. Springer, Berlin, Heidelberg.

Goode, A., Hegedus, E.J., Sizer, P., Brismee, J.M., Linberg, A. and Cook, C.E. 2008. Three-dimensional movements of the sacroiliac joint: a systematic review of the literature and assessment of clinical utility. *The Journal of manual & manipulative therapy* 16(1), pp. 25–38.

Gouzien, P., Cazalbou, C., Boyer, B., de Tailly, P.D., Guenec, Y. and Sénécail, B. 1990. Measurements of the normal lumbar spinal canal by computed tomography. *Surgical and Radiologic Anatomy* 12(2), pp. 143–148.

Gracovetsky, S. and Farfan, H.F. 1986. The optimum spine. *Spine* 11(6), pp. 543–573.

Grassmann, S., Oxland, T.R., Gerich, U. and Nolte, L.P. 1998. Constrained testing conditions affect the axial rotation response of lumbar functional spinal units. *Spine* 23(10), pp. 1155–1162.

Griffith, J.F., Huang, J., Law, S.W., Xiao, F., Leung, J.C.S., Wang, D. and Shi, L. 2016. Population reference range for developmental lumbar spinal canal size. *Quantitative Imaging in Medicine and Surgery* 6(6), pp. 671–679.

Hall, T. and Robinson, K. 2004. The flexion-rotation test and active cervical mobility - A comparative measurement study in cervicogenic headache. *Manual Therapy* 9(4), pp. 197–202.

Hansson, T., Suzuki, N., Hebelka, H. and Gaulitz, A. 2009. The narrowing of the lumbar spinal canal during loaded MRI: The effects of the disc and ligamentum flavum. *European Spine Journal* 18(5), pp. 679–686.

Hasegawa, T., An, H.S., Haughton, V.M. and Nowicki, B.H. 1995. Lumbar Foramina1 Stenosis : Critical Heights of the Intervertebral Discs and Foramina. A cryomicrotome study in cadavera. *JBJS* 77(1), pp. 32–38.

Hashemi R.H, Bradley W.G., Lisanti J.C. 2010. *MRI: The Basics*. 3rd ed., pp.176. Lippincott Williams & Wilkins.

Haughton, V.M., Rogers, B., Meyerand, M.E. and Resnick, D.K. 2002. Measuring the axial rotation of lumbar vertebrae in vivo with MR imaging. *American Journal of Neuroradiology* 23(7), pp. 1110–1116.

Herzog, W. 2010. The biomechanics of spinal manipulation. *Journal of Bodywork and Movement Therapies* 14(3), pp. 280–286.

Hindle, R.J., Pearcy, M.J., Gill, J.M. and Johnson, G.R. 1989. Twisting of the human back in forward flexion. *Proceedings of the Institution of Mechanical Engineers, Part H: Journal of Engineering in Medicine* 203(2), pp. 83–89.

Ho, E.K., Upadhyay, S.S., Chan, F.L., Hsu, L.C. and Leong, J.C.Y. 1993. New methods of measuring vertebral rotation from computed tomographic scans. An intraobserver and interobserver study on girls with scoliosis. *Spine* 18(9), pp. 1173–1177.

Hoard, R.W., Janes, W.E., Brown, J.M., Stephens, C.L. and Engsberg, J.R. 2013. Measuring Scapular Movement Using Three-Dimensional Acromial Projection.

Shoulder & Elbow 5(2), pp. 93–99.

Hong, C.H., Park, J.S., Jung, K.J. and Kim, W.J. 2010. Measurement of the normal lumbar intervertebral disc space using magnetic resonance imaging. *Asian Spine Journal* 4(1), pp. 1-6.

Hughes, A., Makirov, S.K. and Osadchiy, V. 2015. Measuring spinal canal size in lumbar spinal stenosis: description of method and preliminary results. *International Journal of Spine Surgery* 9(3), pp. 1–9.

ke, H., Dorr, L.D., Trasolini, N., Stefl, M., McKnight, B. and Heckmann, N. 2018. Spine-Pelvis-Hip Relationship in the Functioning of a Total Hip Replacement. *The Journal of Bone and Joint Surgery* 100(18), pp. 1606–1615.

Inufusa, A., An, H.S., Lim, T.H., Hasegawa, T., Haughton, V.M. and Nowicki, B.H. 1996. Anatomic Changes of the Spinal Canal and Intervertebral Foramen Associated With Flexion-Extension Movemen. *Spine* 21(21), pp. 2412–2420.

Ishihara, H., Matsui, H., Osada, R., Ohshima, H. and Tsuji, H. 1997. Facet joint asymmetry as a radiologic feature of lumbar intervertebral disc herniation in children and adolescents. *Spine* 22(17), pp. 2001–2004.

Ishii, T., Mukai, Y., Hosono, N., Sakaura, H., Nakajima, Y., Sato, Y., Sugamoto, K. and Yoshikawa, H. 2004. Kinematics of the upper cervical spine in rotation: in vivo three-dimensional analysis. *Spine* 29(7), pp. E139–E144.

Iwahashi, H., Yoshimura, N., Hashizume, H., Yamada, H., Oka, H., Matsudaira, K., Shinto, K., Ishimoto, Y., Nagata, K., Teraguchi, M. and Kagotani, R. 2016. The association between the cross-sectional area of the dural sac and low back pain in a large population: The Wakayama Spine Study. *PLoS ONE* 11(8), p. 0160002.

Jacob, H.A.C. and Kissling, R.O. 1995. The mobility of the sacroiliac joints in healthy volunteers between 20 and 50 years of age. *Clinical Biomechanics* 10(7), pp. 352–361.

Janssen MM, Vincken KL, Kemp B, Obradov M, De Kleuver M, Viergever MA, Castelein RM, Bartels LW. 2010. Pre-existent vertebral rotation in the human spine is influenced by body position. *European Spine Journal* 19(10), pp. 1728–1734.

Jarvik, J.G. and Deyo, R.A. 2002. Diagnostic Evaluation of Low Back Pain with Emphasis on Imaging. *Annals of internal medicine*, 137(7), pp.586-597.

Jaumard, N.V., Welch, W.C. and Winkelstein, B.A. 2011. Spinal Facet Joint Biomechanics and Mechanotransduction in Normal, Injury and Degenerative Conditions. *Journal of Biomechanical Engineering* 133(7), p. 071010.

Jaumard, N.V., Udupa, J.K., Welch, W.C. and Winkelstein, B.A. 2014. Kinematic MRI to Define the Cervical Facet Joint Space for the Spine in Neutral & Torsion. *Spine* 39(8), pp. 664–672.

Jensen, G.M. 1980. Biomechanics of the lumbar intervertebral disk: a review. *Physical therapy* 60(6), pp. 765–773.

Kalichman, L., Suri, P., Guermazi, A., Li, L. and Hunter, D.J. 2009. Facet orientation and tropism: associations with facet joint osteoarthritis and degenerative spondylolisthesis. *International Society of Differentiation* 34(16), pp. E579–E585.

Kanno, H., Ozawa, H., Koizumi, Y., Morozumi, N., Aizawa, T. and Itoi, E. 2016. Increased Facet Fluid Predicts Dynamic Changes in the Dural Sac Size on Axial-Loaded MRI in Patients with Lumbar Spinal Canal Stenosis. *American Journal of Neuroradiology* 37(4), pp. 730-735.

Kapandji, I.A. 1974. *The Physiology of the Joints*. Churchill Livingstone, Edinburg, Scotland.

Karduna, A.R., McClure, P.W. and Michener, L.A. 2000. Scapular kinematics: Effects of altering the Euler angle sequence of rotations. *Journal of Biomechanics* 33(9), pp. 1063–1068.

Kelsey, J.L., Githens, P.B., White III, A.A., Holford, T.R., Walter, S.D., O'Connor, T., Ostfeld, A.M., Weil, U., Southwick, W.O. and Calogero, J.A. 1984. An epidemiologic study of lifting and twisting on the job and risk for acute prolapsed lumbar intervertebral disc. *Journal of orthopaedic research* 2(1), pp. 61–66.

Kendall, F.P., McCreary, E.K., Provance, P.G., Rodgers, M.M. and Romani, W.A. 2005. *Muscles: Testing and Function, with Posture and Pain (Kendall, Muscles)*. 5th ed., pp.58-67. Philadelphia: Lippincott Williams & Wilkins.

Kim, H.J., Chun, H.J., Lee, H.M., Kang, K.T., Lee, C.K., Chang, B.S. and Yeom, J.S. 2013. Changes in spinal canal diameter and vertebral body height with age. *Yonsei Medical Journal* 54(6), pp. 1498–1504.

Kim, H.J., Chun, H.J., Lee, H.M., Kang, K.T., Lee, C.K. 2013. The biomechanical influence of the facet joint orientation and the facet tropism in the lumbar spine. *The Spine Journal* 13(10), pp. 1301–1308.

Kimura, S., Steinbach, G.C., Watenpaugh, D.E. and Hargens, A.R. 2001. Lumbar spine disc height and curvature responses to an axial load generated by a compression device compatible with magnetic resonance imaging. *Spine* 26(23), pp. 2596–2600.

Knirsch, W., Kurtz, C., Häffner, N., Langer, M. and Kececioglu, D. 2005. Normal values of the sagittal diameter of the lumbar spine (vertebral body and dural sac) in children measured by MRI. *Pediatric Radiology* 35(4), pp. 419–424.

Ko, H.Y. and Park, B.K. 1997. Facet Tropism in Lumbar Motion Significance in Disc Herniation. *Archives of physical medicine and rehabilitation* 78(11), pp. 1211–1214.

Koes, B.W., Assendelft, W.J., Van der Heijden, G.J. and Bouter, L.M., 1996 1996. Spinal manipulation for low back pain: an updated systematic review of randomized clinical trials. *Spine* 21(24), pp. 2860–2871.

Kozanek, M., Wang, S., Passias, P.G., Xia, Q., Li, G., Bono, C.M., Wood, K.B. and Li, G. 2009. Range of motion and orientation of the lumbar facet joints in vivo. *Spine* 34(19), pp. E689–E696.

Krismer, M., Sterzinger, W., Haid, C., Frischhut, B. and Bauer, R. 1996. Axial rotation measurement of scoliotic vertebrae by means of computed tomography scans. *Spine* 21(5), pp. 576–581.

Krismer, M. 2002. Comment to "Sagittal morphology and equilibrium of pelvis and spine" by G. Vaz et al. *European Spine Journal* 11(1), pp. 88–88.

Krnrsi, C. and Lesur, E. 1985. Orientation of the articular processes at L4 , L5 , and S1 Possible role in pathology of the intervertebral disc. *Anatomia clinica* 7(1), pp. 43–47.

Kulak, R.F., Belytschko, T.B., Schultz, A.B. and Galante, J.O. 1976. Nonlinear behavior of the human intervertebral disc under axial load. *Journal of Biomechanics* 9(6), pp. 377–386.

LaFiandra, M., Holt, K.G., Wagenaar, R.C. and Obusek, J.P. 2002. Transverse plane kinetics during treadmill walking with and without a load. *Clinical Biomechanics* 17(2), pp. 116–122.

Lao, L., Daubs, M.D., Takahashi, S., Lord, E.L., Cohen, J.R., Zhong, G. and Wang, J.C. 2016. Kinetic magnetic resonance imaging analysis of lumbar segmental motion at levels adjacent to disc herniation. *European Spine Journal* 25(1), pp. 222–229.

Lavignolle, B., Vital, J.M., Senegas, J., Destandau, J., Toson, B., Bouyx, P., Morlier, P., Delorme, G. and Calabet, A. 1983. An approach to the functional anatomy of the sacroiliac joints in vivo. *Anatomia Clinica* 5(3), pp. 169–176.

Leboeuf-Yde, C., Klougart, N. and Lauritzen, T. 1996 1996. How common is low back pain in the Nordic population?: Data from a recent study on a middle-aged general Danish population and four surveys previously conducted in the Nordic countries. Spine, pp. 1518–1526.

Lee, D. 2004. *The pelvic girdle an approach to the examination and treatment of the lumbo pelvic-hip region*. 3rd ed., pp.15-17. Chrchill Livingstone.

Leone, A., Guglielmi, G., Cassar-Pullicino, V.N. and Bonomo, L. 2007. Lumbar intervertebral instability: a review. *Radiology* 245(1), pp. 62–77.

Lewis, S.E. and Fowler, N.E. 2009. Changes in Intervertebral Disk Dimensions After a Loading Task and the Relationship With Stature Change Measurements. *Archives of physical medicine and rehabilitation* 90(10), pp. 1795–1799.

Lewis, J., Green, A., Reichard, Z. and Wright, C. 2002. Scapular position: The validity of skin surface palpation. *Manual Therapy* 7(1), pp. 26–30.

Lim, Y.S., Mun, J.U., Seo, M.S., Sang, B.H., Bang, Y.S., Kang, K.N., Koh, J.W. and Kim, Y.U. 2017. Dural sac area is a more sensitive parameter for evaluating lumbar spinal stenosis than spinal canal area: A retrospective study. *Medicine (United States)* 96(49), p. e9087.

Liu, J., Ebraheim, N.A., Haman, S.P., Shafiq, Q., Karkare, N., Biyani, A., Goel, V.K. and Woldenberg, L. 2006. Effect of the increase in the height of lumbar disc space on facet joint articulation area in sagittal plane. *Spine* 31(7), pp. E198–E202.

Lovett, R.W. 1905. The mechanism of the normal spine and its relation to scoliosis. *The Boston Medical and Surgical Journal* 153(13), pp. 349–358.

Lu, Y.M., Hutton, W.C. and Gharpuray, V.M. 1996. Do bending, twisting, and diurnal fluid changes in the disc affect the propensity to prolapse? A viscoelastic finite element

model. *Spine* 21(22), pp. 2570–2579.

Mahato, N.K. 2011. Disc spaces, vertebral dimensions, and angle values at the lumbar region: a radioanatomical perspective in spines with L5–S1 transitions. *Journal of Neurosurgery: Spine* 15(4), pp. 371–379.

Maniadakis N. and Gray A. 2000. The Economic Burden of Dementia in the UK. *Pain* 84(1), pp. 95–103.

Mansfield P.J. and Neumann D.A. 2014. *Essentials of Kinesiology for the Physical Therapist Assistant-E-Book*. 2nd ed., pp.58-240. Elsevier Health Sciences.

Marawar, S.V., Ordway, N.R., Madom, I.A., Tallarico, R.A., Palumbo, M., Metkar, U., Wang, D., Huang, D. and Lavelle, W.F. 2016. Comparison of Surgeon Rating of Severity of Stenosis Using Magnetic Resonance Imaging, Dural Cross-Sectional Area, and Functional Outcome Scores. *World Neurosurgery* 96, pp. 165–170.

Marawar, S.V., Ordway, N.R., Madom, I.A., Tallarico, R.A., Palumbo, M., Metkar, U., Wang, D., Huang, D. and Lavelle, W.F. 2016. Comparison of Surgeon Rating of Severity of Stenosis Using Magnetic Resonance Imaging, Dural Cross-Sectional Area, and Functional Outcome Scores. *World Neurosurgery* 96, pp. 165–170.

Masharawi, Y., Rothschild, B., Dar, G., Peleg, S., Robinson, D., Been, E. and Hershkovitz, I. 2004. Facet Orientation in the Thoracolumbar Spine Three-dimensional Anatomic and Biomechanical Analysis. *Spine* 29(16), pp. 1755–1763.

Mawston, G.A. and Boocock, M.G. 2012. The effect of lumbar posture on spinal loading and the function of the erector spinae: implications for exercise and vocational rehabilitation. *New Zealand Journal of Physiotherapy* 40(3).

Mayoux-Benhamou, M.A., Revel, M., Aaron, C., Chomette, G. and Amor, B. 1989. A morphometric study of the lumbar foramen. *Surgical and Radiologic Anatomy* 11(2), pp. 97–102.

McGill, S.M. 1997. The biomechanics of low back injury: implications on current practice in industry and the clinic. *Journal of biomechanics* 30(5), pp. 465–475.

McRobbie D.W., Moor A. E., Graves M. J., P.M.R. 2003. *MRI from picture to proton*. pp.17. Cambridge University Press.

Meakin, J.R., Gregory, J.S., Smith, F.W., Gilbert, F.J. and Aspden, R.M. 2008.

Characterizing the Shape of the Lumbar Spine Using an Active Shape Model Reliability and Precision of the Method. 33(7), pp. 807–813.

Mendieta, J.B. 2016. An efficient and semiautomatic segmentation method for 3D surface reconstruction of the lumbar spine from Magnetic Resonance Imaging (MRI). (Doctoral dissertation, Queensland University of Technology.

Merkle, E.M. and Dale, B.M. 2006. Abdominal MRI at 3.0 T: The basic revisited. *American Journal of Roentgenology* 186(6), pp. 1524–1532.

Miao, J., Wang, S., Park, W.M., Xia, Q., Fang, X., Torriani, M.P., Wood, K.B. and Li, G. 2013. Segmental spinal canal volume in patients with degenerative spondylolisthesis. *The Spine Journal* 13(6), pp. 706–712.

Monier, A., Omoumi, P., Schizas, S., Becce, F. and Schizas, C. 2017. Dimensional changes of cervical and lumbar bony spinal canals in one generation in Western Switzerland: a computed tomography study. *European Spine Journal* 26(2), pp. 345-352.

Montgomery, T. 2016. The effects of sagittal plane postures on trunk rotation range of motion. (May).

Montgomery, T.C. 2008. The Effects of Sagittal Plane Postures on Trunk Rotation Range of Motion(Doctoral dissertation, Auckland University of Technology).

Moratal, D., Vallés-Luch, A., Martí-Bonmatí, L. and Brummer, M.E. 2008. k-Space tutorial: An MRI educational tool for a better understanding of k-space. *Biomedical Imaging and Intervention Journal* 4(1), pp. 1–8.

Myers, J.B., Laudner, K.G., Pasquale, M.R., Bradley, J.P. and Lephart, S.M. 2005. Scapular Position and Orientation in Throwing Athletes. *The American Journal of Sports Medicine* 33(2), pp. 263–271.

Nagai, K., Tateuchi, H., Takashima, S., Miyasaka, J., Hasegawa, S., Arai, R., Tsuboyama, T. and Ichihashi, N. 2013. Effects of trunk rotation on scapular kinematics and muscle activity during humeral elevation. *Journal of Electromyography and Kinesiology* 23(3), pp. 679–687.

Nash, C.L. and Moe, J.H. 1969. A study of vertebral rotation. *The Journal of bone and joint surgery. American volume* 51(2), pp. 223–229.

Natarajan, R.N., Lavender, S.A., An, H.A. and Andersson, G.B. 2008. Biomechanical Response of a Lumbar Intervertebral Disc to Manual Lifting Activities. *Spine* 33(18), pp. 1958–1965.

Nazari, J. 2007. The effects of different posture on lumbar spine loading. (Doctoral dissertation, UNIVERSITY OF ABERDEEN (UNITED KINGDOM)).

NICE NG59 National Institute for Health and Care Excellence. 2017. Available at:http://www.noebackpainprogramme.nhs.uk/wp-content/uploads/2015/05/National-Low-Back-and-Radicular-Pain-Pathway-2017_final.pdf [Accessed: 03-02-2018].

Nijs, J., Roussel, N., Struyf, F., Mottram, S. and Meeusen, R. 2007. Clinical Assessment of Scapular Positioning in Patients with Shoulder Pain: State of the Art. *Journal of Manipulative and Physiological Therapeutics* 30(1), pp. 69–75.

Noren, R., Trafimow, J., Andersson, G.B. and Huckman, M.S. 1991. The role of facet joint tropism and facet angle in disc degeneration. *Spine* 16(5), pp. 530–532.

Ogikubo, O., Forsberg, L. and Hansson, T. 2007. The relationship between the cross-sectional area of the cauda equina and the preoperative symptoms in central lumbar spinal stenosis. *Spine* 32(13), pp. 1423–1428.

Orías, A.A.E., Mammoser, N.M., Triano, J.J., An, H.S., Andersson, G.B. and Inoue, N. 2016. HHS Public Access. *Journal of manipulative and physiological therapeutics* 39(4), pp. 294–303.

Oxland, T.R., Panjabi, M.M. and Yamamoto, I. 1992. The effect of injury on rotational coupling at the lumbosacral joint. A biomechanical investigation. *Spine* 17(1), pp. 74–80.

Ozer, A.F., Suzer, T., Sasani, M., Oktenoglu, T., Cezayirli, P., Marandi, H.J. and Erbulut, D.U. 2015. Simple facet joint repair with dynamic pedicular system: Technical note and case series. *Journal of craniovertebral junction & spine* 6(2), pp. 65–68.

Paine, R. and Voight, M. 2013. Invited Clinical Commentary the Role of the Scapula. *International Journal of Sports Physical Therapy* 8(5), pp. 617–629.

Panjabi, M.M., Oxland, T., Takata, K., Goel, V., Duranceau, J. and Krag, M. 1993. Articular facets of the human spine. Quantitative three-dimensional anatomy. *Spine* 18(10), pp. 1298–1310.

Panjabi, M.M., Oxland, T.R., Yamamoto, I. and Crisco, J.J. 1994. Mechanical behaviour of the human lumbar and lumbosacral spine as shown by three-dimensional load-displacement curves. *JBJS* 76(3), pp. E492–E495.

Panjabi, M.M., Takata, K. and Goel, V.K. 1983. Kinematics of Lumbar Intervertebral Foramen. *Spine* 8(4), pp. 348–357.

Park, J.B., Chang, H., Kim, K.W. and Park, S.J. 2001. Facet Tropism A Comparison Between Far Lateral and Posterolateral Lumbar Disc Herniations. 26(6), pp. 677–679.

Park, W.H., Kim, Y.H., Lee, T.R. and Sung, P.S. 2012. Factors affecting shoulder-pelvic integration during axial trunk rotation in subjects with recurrent low back pain. *European Spine Journal* 21(7), pp. 1316–1323.

Parnianpour MO, Nordin M, Kahanovitz N, F. V. 1988. 1988 Volvo award in biomechanics. The triaxial coupling of torque generation of trunk muscles during isometric exertions and the effect of fatiguing isoinertial movements on the motor output and movement patterns. *Spine* 13(9), pp. 982–92.

Pearcy, M.J. and Tibrewal, S.B. 1984. Axial rotation and lateral bending in the normal lumbar spine measured by three-dimensional radiography. *Spine* 9(6), pp. 582–587.

Peretz, A.M., Hipp, J.A. and Heggeness, M.H. 1998. The internal bony architecture of the sacrum. *Spine* 23(9), pp. 971–974.

Pickar, J.G. 2002. Neurophysiological effects of spinal manipulation. *Spine Journal* 2(5), pp. 357–371.

Pool-Goudzwaard, A., van Dijke, G.H., Mulder, P., Spoor, C., Snijders, C. and Stoeckart, R. 2003. The iliolumbar ligament: its influence on stability of the sacroiliac joint. *Clinical Biomechanics* 18(2), pp. 99–105.

Preece, S.J., Willan, P., Nester, C.J., Graham-Smith, P., Herrington, L. and Bowker, P. 2008. Variation in pelvic morphology may prevent the identification of anterior pelvic tilt. *The Journal of manual & manipulative therapy* 16(2), pp. 113–7.

Prushansky, T., Ezra, N., Kurse, N., Man, L. and Schneiderman, Y. 2008. Reproducibility of sagittal pelvic tilt measurements in normal subjects using digital inclinometry. *Gait and Posture* 28(3), pp. 513–516.

Rasband, W. and Ferreira, T. 2012. ImageJ user guide. *ImageJ/Fiji*, 1, pp. 155–161.

Rathnayaka Mudiyanselage K. 2011. 3D Reconstruction of Long Bones Utilising Magnetic Resonance Imaging (MRI) (Doctoral dissertation, Queensland University of Technology).

Roaf, R. 1960. A study of the mechanics of spinal injuries. *The Journal of Bone and Joint Surgery* 42(4), pp. 810–823.

Roche, C.J., King, S.J., Dangerfield, P.H. and Carty, H.M. 2002. The Atlanto-axial Joint: Physiological Range of Rotation on MRI and CT. *Clinical Radiology* 57(2), pp. 103–108.

Rogers, B.P., Haughton, V.M., Arfanakis, K. and Meyerand, M.E. 2002. Application of image registration to measurement of intervertebral rotation in the lumbar spine. *Magnetic Resonance in Medicine* 48(6), pp. 1072–1075.

Rohrer, M., Bauer, H., Mintorovitch, J., Requardt, M. and Weinmann, H.J. 2005. Comparison of Magnetic Properties of MRI Contrast Media Solutions at Different Magnetic Field Strengths. *Investigative Radiology* 40(11), pp. 715–724.

Rousseau, M.A., Bradford, D.S., Hadi, T.M., Pedersen, K.L. and Lotz, J.C. 2006. The instant axis of rotation influences facet forces at L5/S1 during flexion/extension and lateral bending. *European Spine Journal* 15(3), pp. 299–307.

Saifuddin, A., Blease, S. and MacSweeney, E. 2003. Axial loaded MRI of the lumbar spine. *Clinical Radiology* 58(9), pp. 661–671.

Sashin, D. 1930. A critical analysis of the anatomy and the pathologic changes of the sacro-iliac joints. *JBJS* 12(4), pp. 891–910.

Saunders, F. 2013. CT measurement of the motion and inclination angles of the sacroiliac joint in German shepherd dogs with and without lumbosacral region pain, and in greyhounds.(Doctoral dissertation, Massey University).

Schafer, R.C. 1987. *Clinical biomechanics: musculoskeletal actions and reactions*. pp.465-469. Williams & Wilkins.

Van Schaik, J.P., van Pinxteren, B., Verbiest, H., Crowe, A. and Zuiderveld, K.J. 1997. The facet orientation circle: a new parameter for facet joint angulation in the lower lumbar spine. *Spine* 22(5), pp. 531–536.

Schmid, M.R., Stucki, G., Duewell, S., Wildermuth, S., Romanowski, B. and Hodler, J.

1999. Changes in cross-sectional measurements of the spinal canal and intervertebral foramina as a function of body position: in vivo studies on an open-configuration MR system. *AJR* 172(4), pp. 1095–1102.

Schneider, C.A., Rasband, W.S. and Eliceiri, K.W. 2012. NIH Image to ImageJ: 25 years of image analysis. *Nature methods* 9(7), pp. 671–5.

Scibek, J.S. and Carcia, C.R. 2014. Validation of a new method for assessing scapular anterior-posterior tilt. *International journal of sports physical therapy* 9(5), pp. 644–56.

Senoo, I., Orías, A.A.E., An, H.S., Andersson, G.B., Park, D.K., Triano, J.J. and Inoue, N. 2014. In Vivo Three-Dimensional Morphometric Analysis of the Lumbar Foramen in Healthy Subjects. *Spine* 39(16), pp. E929–E935.

Serhan, H.A., Varnavas, G., Dooris, A.P., Patwardhan, A. and Tzermiadianos, M. 2007. Biomechanics of the posterior lumbar articulating elements. *Neurosurgical Focus* 22(1), pp. 1–6.

Shekelle, P.G., Adams, A.H., Chassin, M.R., Hurwitz, E.L. and Brook, R.H. 2019. Spinal Manipulation for Low-Back Pain. *Annals of internal medicine*117(7).

Shin, J.H., Wang, S., Yao, Q., Wood, K.B. and Li, G. 2013. Investigation of coupled bending of the lumbar spine during dynamic axial rotation of the body. *European Spine Journal* 22(12), pp. 2671–2677.

Shirazi-Adl, A., Ahmed, A.M. and Shrivastava, S.C. 1986. Mechanical response of a lumbar motion segment in axial torque alone and combined with compression. *Spine* 11(9), pp. 914–927.

Shirazi-Adl, A. 1989. On the fibre composite material models of disc annulus—comparison of predicted stresses. *Biomechanics* 22(4), pp. 357–365.

Shirazi-Adl, A. 1991. Finite-element evaluation of contact loads on facets of an L2-L3 lumbar segment in complex loads. *Spine* 16(5), pp. 533–541.

Shirazi-Adl, A. 1994. Nonlinear stress analysis of the whole lumbar spine in torsion-Mechanics of facet articulation. *Journal of Biomechanics* 27(3), pp. 289–299.

Sims, J.A. and Moorman, S.J. 1996. The role of the iliolumbar ligament in low back pain. *Medical Hypotheses* 46(6), pp. 511–515.

Smidt, G.L., Wei, S.H., McQuade, K., Barakatt, E., Sun, T. and Stanford, W. 1997.

Sacroiliac motion for extreme hip positions: a fresh cadaver study. *Spine* 22(18), pp. 2073–2082.

Smidt, G.L., McQuade, K. and Wei, S.H. 1995. Sacroiliac kinematics for reciprocal straddle positions. *Spine* 20(9), pp. 1047–54.

Smith, L.J. and Fazzalari, N.L. 2009. The elastic fibre network of the human lumbar anulus fibrosus: Architecture, mechanical function and potential role in the progression of intervertebral disc degeneration. *European Spine Journal* 18(4), pp. 439–448.

Sprigle, S., Flinn, N., Wootten, M. and McCorry, S. 2003. Development and testing of a pelvic goniometer designed to measure pelvic tilt and hip flexion. *Clinical Biomechanics* 18(5), pp. 462–465.

Stokes, I. A. 1988. Mechanical function of facet joints in the lumbar spine. *Clinical Biomechanics* 3(2), pp. 101–105.

Stokes, I.A.F. and Iatridis, J.C. 2004. Mechanical Conditions That Accelerate Intervertebral Disc Degeneration : Overload Versus Immobilization. 29(23), pp. 2724–2732.

Storm, P.B., Chou, D. & Tamargo, R.J. 2002. Lumbar spinal stenosis, cauda equina syndrome, and multiple lumbosacral radiculopathies. *Physical Medicine and Rehabilitation Clinics of North America* 13(3), pp. 713–733.

Struyf, F., Nijs, J., Mottram, S., Roussel, N.A., Cools, A.M. and Meeusen, R. 2014. Clinical assessment of the scapula: A review of the literature. *British Journal of Sports Medicine* 48(11), pp. 883–890.

Sturesson, B., Uden, A. and Onsten, I. 1999. Can an external frame fixation reduce the movements in the sacroiliac joint?: A radiostereometric analysis of 10 patients. *Acta Orthopaedica Scandinavica* 70(1), pp. 42–46.

Sturesson, B., Uden, A. and Vleeming, A. 2000. A radiostereometric analysis of movements of the sacroiliac joints during the standing hip flexion test. *Spine* 25(3), pp. 364–368.

Suzuki, S.H.I.G.E.O., Yamamuro, T.A.K.A.O., Shikata, J.I.T.S.U.H.I.K.O., Shimizu, K.A.T.S.U.J.I. and Iida, H.I.R.O.K.A.Z.U. 1989. Ultrasound measurement of vertebral rotation in idiopathic scoliosis. The Journal of bone and joint surgery 71(2), pp. 252–

255.

Tacar, O., DemÄrant, A., Nas, K. and AltindaÄŸ, O. 2003. Morphology of the lumbar spinal canal in normal adult Turks. *Yonsei medical journal* 44(4), pp. 679–685.

Takashima, H., Takebayashi, T., Shishido, H., Yoshimoto, M., Imamura, R., Akatsuka, Y., Terashima, Y., Fujiwara, H., Nagae, M., Kubo, T. and Yamashita, T. 2016. Comparison with magnetic resonance three-dimensional sequence for lumbar nerve root with intervertebral foramen. *Asian spine journal* 10(1), pp. 59–64.

Tardieu, C., Hasegawa, K. and Haeusler, M. 2017. How Did the Pelvis and Vertebral Column Become a Functional Unit during the Transition from Occasional to Permanent Bipedalism? *Anatomical Record* 300(5), pp. 912–931.

Torun, F., Dolgun, H., Tuna, H., Attar, A., Uz, A. and Erdem, A. 2006. Morphometric analysis of the roots and neural foramina of the lumbar vertebrae. *Surgical Neurology* 66(2), pp. 148–151.

Toyone, T., Ozawa, T., Kamikawa, K., Watanabe, A., Matsuki, K., Yamashita, T. and Wada, Y. 2009. Facet Joint Orientation Difference Between Cephalad and Caudad Portions A Possible Cause of Degenerative Spondylolisthesis. *Spine* 34(21), pp. 2259-2262.

Tulsi, R.S. and Hermanis, G.M. 1993. A study of the angle of inclination and facet curvature of superior lumbar zygapophyseal facets. *Spine* 18(10), pp. 1311–1317.

Tunset, A., Kjaer, P., Chreiteh, S.S. and Jensen, T.S. 2013. A method for quantitative measurement of lumbar intervertebral disc structures: an intra-and inter-rater agreement and reliability study. *Chiropractic & manual therapies* 21(1), p. 26.

Ueno, K. and Liu, Y.K. 1987. A Three-Dimenstional Nonlinear Finite Element Model of Lumbar Intervertebral Joint in Torsion. *Journal of Biomechanical Engineering* 109(3), pp. 200–209.

University of Nottingham (2018). Available at:

https://www.nottingham.ac.uk/research/groups/spmic/facilities/1.5-tesla.aspx
[Accessed: 30 June 2018]

Videman, T. and Nurminen, M. 2004. The occurrence of anular tears and their relation to lifetime back pain history: A cadaveric study using barium sulfate discography. *Spine*

29(23), pp. 2668–2676.

Wang, H., Zhang, Z. and Zhou, Y. 2015. Irregular alteration of facet orientation in lumbar segments: possible role in pathology of lumbar disc herniation in adolescents. *World Neurosurgery* 86, pp. 321–327.

Weiser, W.M., Lee, T.Q., McMaster, W.C. and McMahon, P.J. 1999. Effects of Simulated Scapular Protraction on Anterior Glenohumeral Stability. *The American Journal of Sports Medicine* 27(6), pp. 801–805.

Weishaupt, D., Schmid, M.R., Zanetti, M., Boos, N., Romanowski, B., Kissling, R.O., Dvorak, J. and Hodler, J. 2000. Positional MR Imaging of the Lumbar Spine: Does It Demonstrate Nerve Root Compromise Not Visible at Conventional MR Imaging? *Radiology* 215(1), pp. 247–253.

Weiss, H. 1995. Measurement of vertebral rotation: Perdriolle versus Raimondi. *Eur Spine J* 4, pp. 34–38.

White, A .A. and Panjabi, M.M. 1990. *Clinical biomechanics of the spine*. 2nd ed., pp.2-87. Philadelphia: JB Lippincott Company.

Wilder, D.G., Pope, M.H. and Frymoyer, J.W. 1980. The functional topography of the sacroiliac joint. *Spine* 5(6), pp. 575–579.

Willén J, Danielson B, Gaulitz A, Niklason T, Schönström N, H.T. 1997. Dynamic effects on the lumbar spinal canal: axially loaded CT-myelography and MRI in patients with sciatica and/or neurogenic claudication. *Spine* 22(24), pp. 2968–76.

Wong, A.Y., Karppinen, J. and Samartzis, D. 2017. Low back pain in older adults: risk factors, management options and future directions. *Scoliosis and spinal disorders* 12(1), p. 4.

Yamaguchi, T., Bae, W., Inoue, N., Gregory, D., Cory, E., Sah, R. and Masuda, K. 2011. Intervertebral disc height measurement: Comparison of two-dimensional and three-dimensional methods. *Trans Orthop Res Soc* 36, p. 173.

Yuan, S., Zou, Y., Li, Y., Chen, M. and Yue, Y. 2016. A clinically relevant MRI grading system for lumbar central canal stenosis. *Clinical Imaging* 40(6), pp. 1140–1145.

Zhong, W. et al. 2015. In vivo dynamic changes of dimensions in the lumbar intervertebral foramen. *The Spine Journal* 15(7), pp. 1653–1659.

Zhou, S.H., McCarthy, I.D., McGregor, A.H., Coombs, R.R.H. and Hughes, S.P.F. 2000. Geometrical dimensions of the lower lumbar vertebrae–analysis of data from digitised CT images. *European Spine Journal* 9(3), pp. 242–248.

APPENDIX A

Mr M J H McCarthy

Consultant Spinal Surgeon

Affix Patient Label

Rotation MRI Questionnaire

This document contains a series of standard assessments that are very useful in helping us assess patients with spinal problems. As you are a healthy volunteer it is anticipated that the assessments will return “normal” scores / normative data.

Today’s Date:

Where is your pain located? Please shade the problem areas on the diagram and mark the worst affected area.

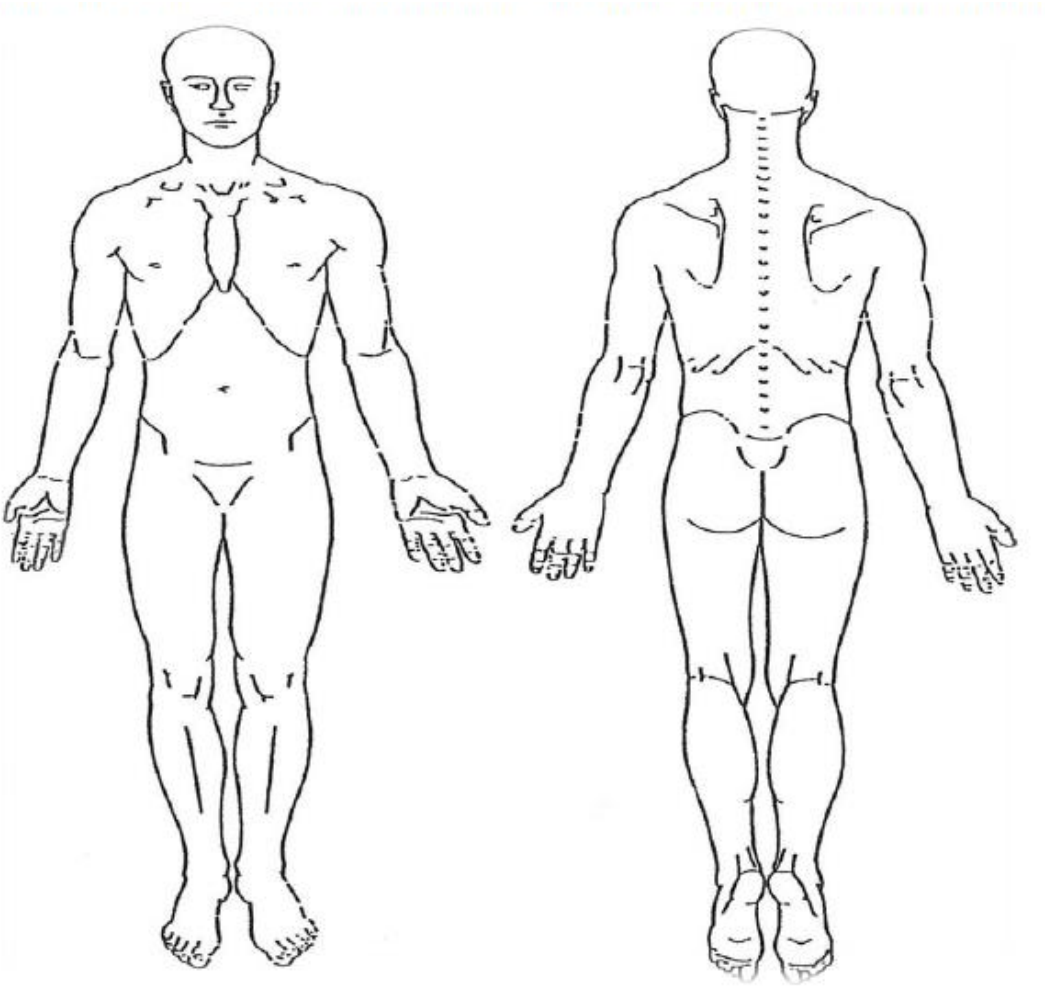

Please mark a point on the line between the faces to indicate how much **BACK / NECK PAIN** you have felt **OVER THE LAST MONTH**.

Figure 50(1)

No pain **Worst pain ever**

Please mark a point on the line between the faces to indicate how much **ARM / LEG PAIN** you have felt **OVER THE LAST MONTH.**

No pain **Worst pain ever**

PLEASE ANSWER BY CIRCLING THE WORDS THAT BEST FIT YOUR PROBLEM.

Which of these problems is the worst for you?

Back / Neck pain Arm / Leg / buttock pain Sensory disturbances None of these

How far can you walk before you have to stop because of your problem?

100 yards 200 yards 400 yards 800 yards 1 mile or more

During the past week, how much did your problem interfere with your normal work (including housework)?

Not at all Little bit Moderately Quite a bit Extremely

If you had to spend the rest of your life with the symptoms you have right now, how would you feel about it?

Very satisfied Somewhat satisfied Ambivalent Dissatisfied Very dissatisfied

Please reflect on your last week. How would you rate your quality of life?

Very good Good Moderate Bad Very bad

During the past 4 weeks, how many days did you cut down on the things you usually do (work, housework, recreational activities) because of your problem?

None 1-7 days 8-14 days 15-21 days >21 days

During the past 4 weeks, how many days did your problem keep you from going to work (job, school, housework)?

None 1-7 days 8-14 days 15-21 days >21 days

Have you had previous spine surgery?

Yes No

Does the problem affect your sleep?

Yes No

What is your current status? E.g. Student, housewife, working, retired, disabled

……

How much time have you lost from work in the last year?

None less than a week one to three weeks

three to six weeks six to twelve weeks three to six months

six to twelve months more than one year

Are you receiving disability benefit?

Yes No

Is there any personal injury claim pending regarding your back pain?

Yes No

Have you had to retire because of your back?

Yes No

EQ5D

We would like to know how good or bad your health is **TODAY**.

The scale is numbered from 0 to 100.

100 means the best health you can imagine.

0 means the worst health you can imagine.

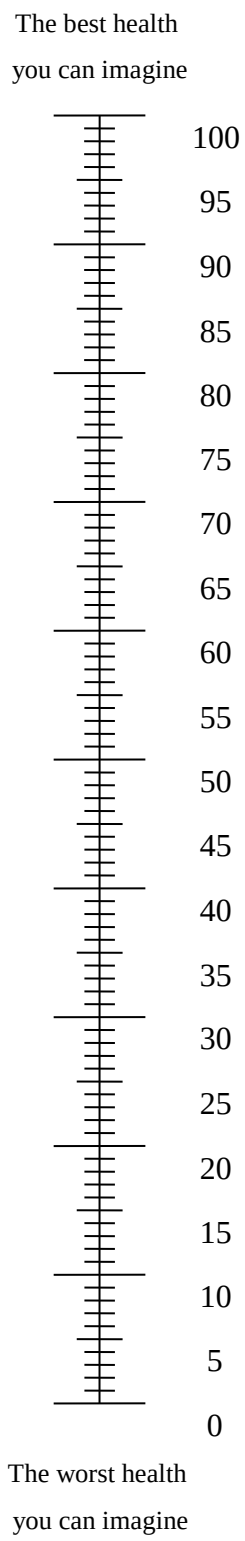

Under each heading, please tick the ONE box that best describes your health **TODAY**:

MOBILITY

I have no problems in walking about ❑

I have slight problems in walking about ❑

I have moderate problems in walking about ❑

I have severe problems in walking about ❑

I am unable to walk about ❑

SELF-CARE

I have no problems washing or dressing myself ❑
I have slight problems washing or dressing myself ❑
I have moderate problems washing or dressing myself ❑
I have severe problems washing or dressing myself ❑
I am unable to wash or dress myself ❑

USUAL ACTIVITIES *(e.g. work, study, housework, family or leisure activities)*

I have no problems doing my usual activities ❑
I have slight problems doing my usual activities ❑
I have moderate problems doing my usual activities ❑
I have severe problems doing my usual activities ❑
I am unable to do my usual activities ❑

PAIN / DISCOMFORT

I have no pain or discomfort ❑
I have slight pain or discomfort ❑
I have moderate pain or discomfort ❑
I have severe pain or discomfort ❑
I have extreme pain or discomfort ❑

ANXIETY / DEPRESSION

I am not anxious or depressed ❑
I am slightly anxious or depressed ❑
I am moderately anxious or depressed ❑
I am severely anxious or depressed ❑
I am extremely anxious or depressed ❑

Oswestry Disability Index (ODI) v2

Could you please complete this questionnaire? It is designed to give us information as to how your back (or leg) trouble has affected your **ability to manage in everyday life**. Please answer as much as possible. Mark **ONE** box only in each section that **most closely describes you over the last month**.

Section 1 – Pain Intensity
- ☐ I have no pain at the moment.
- ☐ The pain is very mild at the moment.
- ☐ The pain is moderate at the moment.
- ☐ The pain is fairly severe at the moment.
- ☐ The pain is very severe at the moment.
- ☐ The pain is the worst imaginable at the moment.

Section 2 – Personal Care (washing, dressing, etc.)
- ☐ I can look after myself without causing extra pain.
- ☐ I can look after myself normally but it is very painful.
- ☐ It is painful to look after myself and I am slow and careful.
- ☐ I need some help but manage most of my personal care.
- ☐ I need help everyday in most aspects of self-care.
- ☐ I do not get dressed, wash with difficulty and stay in bed.

Section 3 – Lifting
- ☐ I can lift heavy weights without extra pain.
- ☐ I can lift heavy weights but it gives extra pain.
- ☐ Pain prevents me from lifting heavy weights off the floor, but I can manage if they are conveniently positioned, e.g. on a table.
- ☐ Pain prevents me from lifting heavy weights, but I can manage light to medium weights if they are conveniently positioned.
- ☐ I can lift only very light weights.
- ☐ I cannot lift or carry anything at all.

Section 4 – Walking
- ☐ Pain does not prevent me from walking any distance.
- ☐ Pain prevents me walking more than 1 mile.
- ☐ Pain prevents me walking more than ½ mile.
- ☐ Pain prevents me walking more than 100 yards.
- ☐ I can walk only with a stick or crutches.
- ☐ I am in bed most of the time and have to crawl to the toilet.

Section 5 – Sitting
- ☐ I can sit in any chair as long as I like.
- ☐ I can sit in my favorite chair as long as I like.
- ☐ Pain prevents me from sitting for more than 1 hour.
- ☐ Pain prevents me from sitting for more than ½ hour.
- ☐ Pain prevents me from sitting for more than 10 minutes.
- ☐ Pain prevents me from sitting at all.

Section 6 – Standing
- ☐ I can stand as long as I want without extra pain.
- ☐ I can stand as long as I want but it gives me extra pain.
- ☐ Pain prevents me from standing for more than 1 hour.
- ☐ Pain prevents me from standing for more than ½ hour.
- ☐ Pain prevents me from standing for more than 10 minutes.
- ☐ Pain prevents me from standing at all.

Section 7 – Sleeping
- ☐ My sleep is never disturbed by pain.
- ☐ My sleep is occasionally disturbed by pain.
- ☐ Because of pain I have less than 6 hours of sleep.
- ☐ Because of pain I have less than 4 hours of sleep.
- ☐ Because of pain I have less than 2 hours of sleep.
- ☐ Pain prevents me from sleeping at all.

Section 8 – Sex Life (if applicable)
- ☐ My sex life is normal and causes no extra pain.
- ☐ My sex life is normal but causes some extra pain.
- ☐ My sex life is nearly normal but is very painful.
- ☐ My sex life is severely restricted by pain.
- ☐ My sex life is nearly absent because of pain.
- ☐ Pain prevents any sex life at all.

Section 9 – Social Life
- ☐ My social life is normal and gives me no extra pain.
- ☐ My social life is normal but increases the degree of pain.
- ☐ Pain has no significant effect on my social life apart from limiting my more energetic interests, e.g. sports, etc.
- ☐ Pain has restricted my social life and I do not go out as often.
- ☐ Pain has restricted my social life to my home.
- ☐ I have no social life because of pain.

Section 10 – Traveling
- ☐ I can travel anywhere without pain.
- ☐ I can travel anywhere but it gives extra pain.
- ☐ Pain is bad but I manage journeys over two hours.
- ☐ Pain restricts me to journeys of less than one hour.
- ☐ Pain restricts me to short necessary journeys under 30 minutes.
- ☐ Pain prevents me from traveling except to receive treatment.

PHQ-9

Over the last 2 weeks, how often have you been bothered by any of the following problems? *(Use "✔" to indicate your answer)*	**Not at all**	**Several days**	**More than half the days**	**Nearly every day**
1. Little interest or pleasure in doing things.....	0	1	2	3
2. Feeling down, depressed, or hopeless.....	0	1	2	3
3. Trouble falling or staying asleep, or sleeping too much.....	0	1	2	3
4. Feeling tired or having little energy.....	0	1	2	3
5. Poor appetite or overeating.....	0	1	2	3
6. Feeling bad about yourself — or that you are a failure or have let yourself or your family down.....	0	1	2	3
7. Trouble concentrating on things, such as reading the newspaper or watching television.....	0	1	2	3
8. Moving or speaking so slowly that other people could have noticed? Or the opposite — being so fidgety or restless that you have been moving .around a lot more than usual.....	0	1	2	3
9. Thoughts that you would be better off dead or of hurting yourself in some way.....	0	1	2	3

(***For office coding: Total Score*** _____ = ___ + ___ + ___)

If you checked off any problems, how difficult have these problems made it for you to do your work, take care of things at home, or get along with other people?

Not difficult at all	**Somewhat difficult**	**Very difficult**	**Extremely difficult**
☐	☐	☐	☐

GAD-7

Over the last 2 weeks, how often have you been bothered by the following problems? *(Use "✔" to indicate your answer)*	Not at all	Several days	More than half the days	Nearly every day
1. Feeling nervous, anxious or on edge	0	1	2	3
2. Not being able to stop or control worrying	0	1	2	3
3. Worrying too much about different things	0	1	2	3
4. Trouble relaxing	0	1	2	3
5. Being so restless that it is hard to sit still	0	1	2	3
6. Becoming easily annoyed or irritable	0	1	2	3
7. Feeling afraid as if something awful might happen	0	1	2	3

Sport activities

A gymnastic ❑

Weightlifting ❑

Football ❑

Rugby ❑

Holder test

Comfort ❑

Discomfort ❑

Cramp pain:

At the lower trunk ❑

At the buttock ❑

At the thigh ❑

At the leg ❑

Reference

Spine Dragon (2018). Available at: http://www.spinedragon.com/questionnaires.php [Accessed:1 June 2018]

SHOULDER PAIN AND DISABILITY INDEX (SPADI)

Please place a mark on the line that best represents your experience during the last week attributable to your shoulder problem.

Pain scale

How severe is your pain?
Circle the number that best describes your pain where: 0 = no pain and 10 = the worst pain imaginable.

At its worst? 0 1 2 3 4 5 6 7 8 9 10

When lying on the involved side? 0 1 2 3 4 5 6 7 8 9 10

Reaching for something on a high shelf? 0 1 2 3 4 5 6 7 8 9 10

Touching the back of your neck? 0 1 2 3 4 5 6 7 8 9 10

Pushing with the involved arm? 0 1 2 3 4 5 6 7 8 9 10

Total pain score /50 x 100 = %

(Note: If a person does not answer all questions divide by the total possible score, eg. if 1 question missed divide by 40)

Disability scale

How much difficulty do you have?

Circle the number that best describes your experience where: 0 = no difficulty and 10 = so difficult it requires help

Washing your hair? 0 1 2 3 4 5 6 7 8 9 10

Washing your back? 0 1 2 3 4 5 6 7 8 9 10

Putting on an undershirt or jumper? 0 1 2 3 4 5 6 7 8 9 10

Putting on a shirt that buttons down the front? 0 1 2 3 4 5 6 7 8 9 10

Putting on your pants? 0 1 2 3 4 5 6 7 8 9 10

Placing an object on a high shelf? 0 1 2 3 4 5 6 7 8 9 10

Carrying a heavy object of 10 pounds (4.5kilograms)

0 1 2 3 4 5 6 7 8 9 10

Removing something from your back pocket? 0 1 2 3 4 5 6 7 8 9 10

Total disability score: _____/ 80 x 100 = %

(Note: If a person does not answer all questions divide by the total possible score. For example, if one question missed divide by 70).

Total SPADI score: _____ 130 x 100 = %

(Note: If a person does not answer all questions divide by the total possible score. For example, if one question missed divide by 120) .

Reference

Shoulder Pain and Disability Index (2018).

Available at: https://www.tac.vic.gov.au/files-to-move/media/upload/spi.pdf

[Accessed: 20 June 2018]

APPENDIX B

Table B-1: Comparison between goniometer and MRI measurements of the pelvis rotational angle using right and left posterior superior iliac spines

Group	Position	Pelvis rotation measurements(^{0})using Goniometer		Pelvis rotation measurements using MRI(^{0})					
		PSISS (M±SE)	ICC	PSISS1 (M±SE)	ICC	PSISS2 (M±SE)	ICC	PSISS3 (M±SE)	ICC
2	2 (R1) n=4	90.7± .47	85(.87-.93)	90.2± 2.3	1(.99-1)	90.9±2.2	.99(.97-1)	90.4±2.4	.99(.99-1)
3	3 (R2) n=4	65.5±1.6	82(.80-.90)	68.6±2.5	.99(.98-1)	67.7±2.4	.99(.98-1)	68±2.7	.99(.99-1)

R1: first rotational position, R2: second rotational position, PSISS: posterior superior iliac spines, M: mean, SE: standard error, ICC: intra-class correlation coefficient, PSISS1: the angle between the left and right posterior iliac spines and the horizontal plane at the level of the ala of the sacrum , PSISS2: the angle between the left and right posterior iliac spines and the horizontal plane at the level of the S1-S2, PSISS3: the angle between the posterior iliac spines and the horizontal plane at the level of the S2-S3.

Table B-2: The relation between the rotational angle of L5 and the right and left posterior superior iliac spines at three tested anatomical sections(PSISS1, PSISS2, PSISS3)relative to the horizontal plane according to four lower trunk positions (N, R2, R3, R4)

Groups	Position	The rotational angle of the L5 level and the rotational angle of the posterior iliac spines in three sections							
		L5A		PSISS1		PSISS2		PSISS3	
		(M ± SE)	ICC	(M ± SE)	ICC	(M ± SE)	ICC	(M ± SE)	ICC
2	1(N) n=4	1.6±.9	1(.99-1)	1.5±.9	1(1-1)	1.40±.81	.99(.99-1)	1.6±.8	.99(.99-1)
	2(R1) n=4	89.5±2.3	.99(.98-1)	90.2±2.3	1(.99-1)	90.9±2.2	.99(.97-1)	90.4±2.4	.99(.99-1)
3	1(N) n=4	1.4±.7	.99(.97-1)	1.125±.76	.99(.99-1)	1.075±.41	.99(.98-1.)	1.275±.413	.99(.97-1)
	3(R2) n=4	67.475±2.5	.99(.97-1)	68.6±2.5	.99(.98-1)	67.7±2.4	.99(.98-1)	68±2.7	.99(.99-1)
4	1(N) n=3	.65±.07	1(1-1)	.9±.1	1(.99-1)	.6±.08	1(1-1)	0.4±0.07	1(1-1)
	4(R3) n=3	42.8±.94	.99(.97-1)	43.3±.95	.99(.98-1)	43.2±.95	.99(.97-1)	42.7±1.1	.99(.97-1)

L5A: The angle between the intervertebral disc at L5-S1 level and the horizon, PSISS1: the angle between the left and right posterior iliac spines and the horizontal plane at the level of the ala of the sacrum , PSISS2: the angle between the left and right posterior iliac spines and the horizontal plane at the level of the S1-S2, PSISS3: the angle between the posterior iliac spines and the horizontal plane at the level of the S2-S3,N: neutral position, R1: first rotation, R2: second rotation, R3: third rotation , M: mean, SE: standard error, MD1: the mean difference between the rotational angle of L5 angle and PSIS1, MD2: the mean difference between rotational angle of PSISS1 and PSISS2, MD3: the mean difference between the rotational angle of PSISS2 and PSISS3.

Table B-3: The angle between the left sacrum, ilium and the horizontal plane at three different anatomical sections according to four positions(N, R1,R2,R3) of the lower trunk

Groups	Position	Angle between the left sacroiliac joint and the horizontal plane					
		LSAS1		LSAS2			LSAS3
		(M ±SEM)	ICC	(M ±SEM)	ICC	(M ± SEM)	ICC
1	1(N) n=4	38.5±1.2	.96(.81-.99)	44.5±.1.5	.97(.87-.99)	52.9±2.8	.96(.84-.99)
	2(R1) n=4	130.4±3.3	.97(.88-.99)	134.2±2.4	.96(.81-.99)	139.2±3.4	.98(.89-.99)
2	1(N) n=4	40.2±.7	1(1-1)	47±.71	.99(.98-1)	52.8±1.6	.97(.88-.99)
	3(R2) n=4	107±4.3	.98(.93-.99)	117.2±3.1	.97(.87-.99)	116.5±1.7	.95(.79-.99)
3	1(N) n=3	37±1.4	.96(.84-.99)	41.2±2.2	.96(.82-.99)	52.3±2	.95(.79-.99)
	4(R3) n=3	81.7±2	.95(.79-.99)	85±1.6	.95(.78-.99)	82.7±1.8	.96(.82-.99)
		LIAS1		LIAS2			LIAS3
		(M ± SEM)	ICC	(M ± SEM)	ICC	(M ± SEM)	ICC
1	1(N) n=4	53.5±1.3	.96(.82-.99)	51.4±1.1	1(.99-1)	56±1.31	.99(.98-1)
	2(R1) n=4	143.5±2.9	.97(.85-.99)	136.6±4	.98(.92-.99)	133.5±3.6	.99(.99-1)
2	1(N) n=4	51.2±2.2	.96(.82-.99)	53.1±1.8	.96(.81-.99)	58±2.8	.99(.98-1)
	3(R2) n=4	120.5±4	.98(.92-.99)	115.2±3.3	.97(.88-.99)	125.8±4.2	.99(.99-1)
3	1(N) n=3	51.1±.9	10(1-1)	52.8±1.4	.96(.84-.99)	57.75±1.1	.99(.97-1)
	4(R3) n=3	97.7±.2.1	.96(.81-.99)	93.2±.2.6	.96(.83-.99)	96±2	.99(.99-1)

LSAS1: the angle between the left sacrum and the horizontal plane at the level of the ala of the sacrum , LSAS2: the angle between left sacrum and the horizontal plane at the level of the S1-S2, LSAS 3: the angle between the left sacrum and the horizontal plane at the level of the S2-S3, LIAS1: the angle between the left ilium and the horizontal plane at the level of the ala of the sacrum , LIAS2: the angle between left ilium and the horizontal plane at the level of the S1-S2, LIAS 3: the angle between the left ilium and the horizontal plane at the level of the S2- S2, MD: the mean differences, ICC: intra-class correlation coefficient

Table B-4: The angle between the right sacrum, ilium and the horizontal plane at three different anatomical sections according to four different positions (N, R1,R2,R3) of the lower trunk

Groups	Position	Angle between the right sacroiliac joint and the horizontal plane					
		RSAS1		RSAS2			RSAS3
		(M ±SEM)	ICC	(M ± SEM)	ICC	(M ± SEM)	ICC
2	1(N) n=4	39.6±1.8	.99(.97-1)	47.2±2.8	.99(.99-1)	57.7±2.2	.99(.99-1)
	2(R1) n=4	49.2±2.6	.99(.99-1)	42.2±3.5	.99(.97-1)	37.8±2.6	.99(.98-1)
3	1(N) n=4	38.9± .7	.99(.97-1)	47 ±.7	.99(.98-1)	53.6± 1.4	.99(.98-1)
	3(R2) n=4	30.3± 3.9	1(.99-1)	22.3±4	.99(.97-1)	15.4±2.4	.99(.99-1)
4	1(N) n=3	37.7±1.2	.99(.98-1)	45±1.9	.99(.99-1)	54.5±2.5	.99(.99-1)
	4(R3) n=3	8.8±2.1	.99(.97-1)	5.1±.6	.99(.97-1)	7.3±1.3	.99(.97-1)
		RIAS1		RIAS2			RIAS3
		(M ± SEM)	ICC	(M ± SEM)	ICC	(M ± SEM)	ICC
1	1(N) n=4	53±2	.99(.99-1)	50.7±4.6	1(.99-1)	55.7±3.7	.99(.97-1)
	2(R1) n=4	39.2±2.3	.99(.98-1)	40.3±2.4	.99(.97-1)	37.2±1.8	.99(.99-1)
2	1(N) n=4	51.7± 1.4	.99(.97-1)	53± 1.7	.99(.99-1)	56± 1.4	.99(.96-1)
	3(R2) n=4	21.4±4.8	.99(.99-1)	15.5 ±3.9	.99(.97-1)	9.9±3.5	.99(.97-1)
3	1(N) n=3	48±.9	.99(.97-1)	45.7±2.8	.99(.98-1)	54±2.4	.99(.98-1)
	4(R3) n=3	8.3±1.8	.99(.97-1)	6±1.5	.99(.97-1)	7.6±1.6	.99(.97-1)

RSAS1: the angle between the right sacrum and the horizontal plane at the level of the ala of the sacrum , RSAS2: the angle between right sacrum and the horizontal plane at the level of the S1-S2, RSAS 3: the angle between the right sacrum and the horizontal plane at the level of the S2-S3, RIAS1: the angle between the right ilium and the horizontal plane at the level of the ala of the sacrum , RIAS2: the angle between right ilium and the horizontal plane at the level of the S1-S2, RIAS 3: the angle between the right ilium and the horizontal plane at the level of the S2-S3, ICC: intra-class correlation coefficient.

Table B-5: The degree of rotation of the lower lumbar segments during the first rotational position of the lower trunk for the first and second groups

Group	Position	IVL	RA1 (M&SE)	ICC	RA2 (M&SE)	ICC	MD (RA1-RA2)	SCDD (M&SE)	ICC
1(without MRIH)	1(N) n=7	L3	3.9±.9	.98(.94-.99)	4.3±1	.99(.99-1.0)	-.4	4.6±.3	.99(.99-1)
		L4	3.7±1	.96(.89-.99)	4.5±1	.94(.81-.98)	-0.8	2.5±.2	.98(.94-.99)
		L5	3.6±1	.98(.96-.99)	3.8±1	.99(.98-.99)	-0.2	1.1±.0	.95(.86-.99)
	2(R1) n=7	L3	79.9±1.4	.96(.86-.99)	80.9±1.4	.98(.94-.99)	-1	5.8±.3	1.0(1.0-1)
		L4	84.8±1.4	.93(.79-.98)	85.3±1.4	.94(.82-.98)	-.5	3.5±.6	.95(.83-.99)
		L5	87.7±1.5	.98(.94-.99)	88.1±1.5	.99(.96-.99)	-.4	1.8±1.1	.96(.89-.99)
2(with MRIH)	1(N) n=5	L3	1.8±.5	.93(.74-.99)	2.1±.6	.99(.98-1.0)	-0.3	3.3±.5	.99(.99-1)
		L4	2.0±.7	.99(.99-1.0)	2.2±.7	.99(.98-1.0)	-0.2	1.8±.8	1.0(1.0-1)
		L5	2.2±1	.97(.88-.99)	2.3±1	.98(.93-.99)	-0.1	.8±.1	.96(.86-.99)
	3(R1) n=5	L3	77.4±1.6	.93(.75-.99)	78.6±1.5	.96(.84-.99)	-1.2	5.6±.5	.99(.99-1.0)
		L4	82.6±1.9	.94(.79-.99)	83.3±1.9	.97(.90-.99)	-.7	3.2±.2	.98(.92-.99)
		L5	87.0±2	.99(.95-.99)	87.5±1.9	.99(.96-.99)	-.5	1.8±.2	.97(.88-.99)

IVL: intervertebral level, N: neutral position, R1: the first rotation position, M: mean (°), SE: standards error, ICC: intra-class correlation coefficient, SCD: spinal canal depth, MRIH; MRI holder, RA1: the vertebral rotation in the first tested cut, RA2: the vertebral rotation in the second tested cut.

Table B-6: The degree of rotation of the lower lumbar segments during the second and third rotational positions of the lower trunk for the third and fourth groups

Group	Position	IVL	RA1(M&SE)	ICC	RA2(M&SE)	ICC	MD(RA1-RA2)	SCD (M&SE)	ICC
3(with MRIH)	1(N) n=5	L3	1.8±.5	.97(.88-.99)	2.1±.6	.99(.99-1)	-.3	2.9±.4	.99(.99-1)
		L4	2.2±.6	.99(.99-1)	2.3±.7	.97(.90-.99)	-.1	1.6±.1	.98(.93-.99)
		L5	2.3±1	.97(.88-.99)	2.4±1	.98(.91-.99)	-.1	.8±.1	.95(.81-.99)
	4(R2) n=5	L3	57.8±1.7	.95(.81-.99)	59.8±2	.98(.93-.99)	-2	4.2±.5	.99(.98-1)
		L4	62.1±1.9	.94(.79-.99)	63.2±1.9	.94(.78-.99)	-1.1	2.5±.2	.98(.92-.99)
		L5	65.2±1.9	.98(.95-.99)	66±2	.99(.97-.99)	-.8	1.5±.0	1(1-1)
4(with MRIH)	1(N) n=4	L3	1.6±.4	.99(.95-.99)	1.9±.4	.99(.98-1)	-.3	3.1±.5	.99(.98-1)
		L4	1.4±.3	.99(.96-1)	1.6±.3	.98(.90-.99)	-.2	2±.2	.98(.93-.99)
		L5	1.2±.2	1(1-1)	1.3±.2	1(1-1)	-.1	1±.0	1(1-1)
	5(R3) n=4	L3	38.6±.8	.99(.98-1)	39.4±.9	.99(.99-1)	-.8	3.8±.4	.99(.96-.99)
		L4	41.7±1.4	.97(.84-.99)	42.2±1.4	.96(.84-.99)	-.5	2.4±.2	.97(.85-.99)
		L5	44.5±.1.2	1(.99-1)	44.9±.1.1	.98(.89-.99)	-.4	1.2±.0	1(1-1)

IVL: intervertebral level, N: neutral position, R3: the second rotation position, R4: the fourth rotation position, M: mean (°), SE: standards error, ICC: intra-class correlation coefficient, SCD: spinal canal depth, MRIH; MRI holder, RA1: the angle of vertebral rotation in the first tested cut, RA2: the angle of vertebral rotation in the second tested cut of each vertebral level.

Table B-7: The area, width, anterior and posterior disc height of the intervertebral disc (IVD) in neutral and first rotational positions of the lower trunk for the first group without using MRI holder

IVL (Right Side)	Area		Width		Posterior disc height		Anterior disc height	
	M(mm2)±ER	ICC [95%CI]	M(mm)±ER	ICC[95%CI]	M(mm)±ER)	ICC[95%CI]	M(mm)±ER	ICC[95%CI]
L3-L4 RSD(N)	319±17	1(.99-1)	35.4±1	.98(.93-.99)	6.9±.5	.99(.98-.99)	13.2±.3	.98(.95-.99)
L3-L4 RSD(R1)	294.8±15	.99(.99-1)	32.4±1	.97(.91-.99)	7.2±.5	.99(.99-1)	12.3±.4	.99(.98-.99)
L4-L5 RSD(N)	321.5±12	.99(.99-1)	33.2±1	.96(.89-.99)	6.6±.4	.99(.98-.99)	13.3±.4	.99(.98-.99)
L4-L5 RSD (R1)	290.8±10	.99(.99-1)	29.7±1	.98(.93-.99)	5.9±.2	.98(.94-.99)	12.7±.4	.99(.99-1)
L5-S1 RSD (N)	165.2±11	.99(.99-1)	25.6±1	.97(.89-.99)	4.3±.2	.99(.97-.99)	10.7±.8	.96(.89-.99)
L5-S1 RSD (R1)	138.8±14	.99(.99-1)	22.8±1	.99(.97-.99)	3.7±.1	.97(.91-.99)	9.8±.7	.96(.87-.99)
IVL (Right Side)	Area		Width		Posterior disc height		Anterior disc height	
	M(mm2)±ER	ICC[95%CI]	M(mm)±ER	ICC[95%CI]	M(mm)±ER	ICC[95%CI]	M(mm)±ER	ICC[95%CI]
L3-L4 LSD (N)	307.8±18	1(.99-1)	33.2±1	.98(.94-.99)	6.7±.6	.94(.83-.99)	12.3±.5	.99(.98-.99)
L3-L4 LSD (R1)	322.8±17	1(.99-1)	32.2±1	.99(.99-1)	7.2±.5	.99(.99-.99)	12.7±.4	.99(.98-.99)
L4-L5 LSD (N)	269.8±12	.99(.99-1)	31.7±1	.98(.94-.99)	6.1±.5	.99(.98-.99)	12.8±.4	.99(.98-.99)
L4-L5 LSD (R1)	300.8±12	.99(.99-1)	32.1±1	.98(.94-.99)	6.4±.5	.99(.98-.99)	13.4±.4	.99(.99-1)
L5-S1 LSD (N)	144.5±12	.99(.99-1)	24.2±1	.97(.90-.99)	4.3±.3	.98(.96-.99)	10.9±.8	.96(.89-.99)
L5-S1 LSD (R1)	121.4±9	.99(.99-1)	23.1±1	.98(.93-.99)	3.5±.2	.97(.92-.99)	11.5±.6	.99(.99-1)

IVL=intervertebral level, N= neutral position, R1: first rotational position, RSD = right sagittal disc, LSD = left sagittal disc, M=mean, SE=standard error, MD=mean difference, ICC=intra class correlation coefficient.

Table B-8: The area, width, anterior and posterior height of the intervertebral disc (IVD) in neutral and first rotational positions of the lower trunk for the second group with using MRI holder

IVL (Right Side)	Area		Width		Posterior disc height		Anterior disc height	
	M(mm2)±ER	ICC[95%CI]	M(mm)±ER	ICC[95%CI]	M(mm)±ER	ICC[95%CI]	M(mm)±ER	ICC[95%CI]
L3-L4 RSD(N)	397±22	.99(.97-1)	37.6±1	.99(.98-1)	8.6±.4	.99(.97-1)	15.9±.9	.99(.97-1)
L3-L4 RSD(R2)	367.2±22	1(1-1)	34.3±1	.99(.98-1)	9.3±.6	.99(.97-1)	14.9±.9	.99(.97-1)
L4-L5 RSD(N)	327.5±37	.99(.98-1)	35.1±.6	.99(.97-1)	8.9±.5	.99(.98-1)	14.9±.8	.99(.97-1)
L4-L5 RSD (R2)	292.5±24	1(1-1)	31.3±2	.99(.98-1)	7.9±.5	.99(.97-1)	14.2±.4	.99(.97-1)
L5-S1 RSD (N)	206.5±27	.99(.98-1)	27.1±1	.99(.97-1)	5.4±.4	.99(.97-1)	14.5±1	.99(.97-1)
L5-S1 RSD (R2)	172.5±31	1(.99-1)	24.1±2	.99(.99-1)	4.8±.6	.99(.97-1)	14.1±1	.99(.99-1)
IVL (Left Side)	Area		Width		Posterior disc height		Anterior disc height	
	M(mm2)±ER	ICC[95%CI]	M(mm)±ER	ICC[95%CI]	M(mm)±ER	ICC[95%CI]	M(mm)±ER	ICC[95%CI]
L3-L4 LSD (N)	367.2±20	.99(.99-1)	38.1±1	.99(.97-1)	6.4±.3	.99(.97-1)	13.5±.6	.99(.97-1)
L3-L4 LSD (R2)	403.7±19	1(1-1)	37.3±1	.99(.97-1)	7±.4	.99(.97-1)	14.5±.9	.99(.97-1)
L4-L5 LSD (N)	354.5±34	1(.99-1)	36.2±.9	.99(.97-1)	6.8±.7	.99(.97-1)	16.3±1	.99(.99-1)
L4-L5 LSD (R2)	420.5±34	1(1-1)	36.4±1	.99(.99-1)	7.5±1	.99(.99-1)	17.5±.9	.99(.97-1)
L5-S1 LSD (N)	190.5±30	1(.99-1)	27.2±1	.99(.97-1)	4.4±1	.99(.97-1)	13.8±1	.99(.99-1)
L5-S1 LSD (R2)	170.2±27	1(1-1)	26.2±1	.99(.99-1)	4±.5	.99(.97-1)	14.5±1	.99(.99-1)

IVL=intervertebral level, N= neutral position, R2=- second rotational position, RSD = right sagittal disc, LSD = left sagittal disc, M=mean, SE=standard error, MD=mean difference, ICC=intra class correlation coefficient.

Table B-9: The area, width, anterior and posterior height of the intervertebral disc (IVD) in the neutral and second rotational position of the lower trunk for the third group with using MRI holder

IVL (Right Side)	Area		Width		Posterior disc height		Anterior disc height	
	M(mm2)±ER)	ICC[95%CI]	M(mm)±ER)	ICC [95%CI]	M(mm)±ER)	ICC[95%CI]	M(mm)±ER)	ICC[95%CI]
L3-L4 RSD(N)	360.2±22	1(.99-1)	37.3±2	.98(.92-.99)	8.4±.3	.99(.97-1)	14.0±.8	.99(.98-1)
L3-L4 RSD(R3)	310.0±25	1(.99-1)	32.5±1	.97(.88-.99)	9.5±.3	.99(.98-1)	13.3±.5	.99(.97-1)
L4-L5 RSD(N)	314.7±33	.99(.96-1)	36.8±1	.97(.89-.99)	7.9±.5	.99(.96-1)	14.4±.1	1(1-1)
L4-L5 RSD (R3)	253.2±38	1(.99-1)	29.1±3	.98(.94-.99)	6.7±.4	.99(.97-1)	14.2±.6	.99(.98-1)
L5-S1 RSD (N)	172.2±10	.99(.98-1)	26.6±.9	.99(.99-1)	4.8±.2	.98(.90-.99)	13.0±.2	.98(.92-.99)
L5-S1 RSD (R3)	102.2±8	.99(.98-1)	19.8±.5	.99(.98-1)	3.8±.1	.99(.97-1)	11.8±.2	.99(.97-1)
IVL (Left Side)	Area		Width		Posterior disc height		Anterior disc height	
	M(mm2) ±ER)	ICC[95%CI]	M(mm) ±ER)	ICC[95%CI]	M(mm) ±ER)	ICC[95%CI]	M(mm) ±ER)	ICC[95%CI]
L3-L4 LSD (N)	333.0±22	1(.99-1)	37.1±1	.99(.99-1)	6.1±.4	.99(.96-1)	12.8±.4	.99(.98-1)
L3-L4 LSD (R3)	379.7±32	1(1-1)	37.3±1	.99(.99-1)	7.0±.4	.99(.97-1)	14.7±.4	.99(.98-1)
L4-L5 LSD (N)	326.5±15	.99(.99-1)	36.3±1	.98(.91-.99)	5.7±.1	.96(.82-.99)	14.8±.5	.99(.98-1)
L4-L5 LSD (R3)	400.5±11	1(1-1)	37.6±1	.99(.99-1)	6.7±.3	.99(.97-1)	17.1±.3	.99(.97-1)
L5-S1 LSD (N)	152.5±27	1(.99-1)	26.2±1	.98(.91-.99)	3.5±.3	.98(.93-.99)	11.1±.3	.98(.92-.99)
L5-S1 LSD (R3)	137.±26	1(1-1)	26±.8	.99(.97-1)	2.7±.4	.99(.98-1)	12.9±.4	.99(.97-1)

IVL=intervertebral level, N= neutral position, R3=- third rotational position, RSD = right sagittal disc, LSD = left sagittal disc, M=mean, SE=standard error, MD=mean difference, ICC=intra class correlation coefficient.

Table B-10: The area, width and height of the right and left intervertebral foramen in neutral and first rotational positions of the lower trunk for the first group without using MRI holder

IVL (Right Side)	Area		Width		Height	
	M(mm^2)±ER	ICC [95%CI]	M(mm)±ER	ICC [95%CI]	M(mm)±ER	ICC [95%CI]
L3-L4 RF(N)	167.4±1	.97(.93-.99)	9.3±.4	.99(.98-.99)	21.6±.2	.98(.95-.99)
L3-L4 RF(R1)	181.4±2	.97(.90-.99)	10.3±.5	.99(.98-.99)	22.2±.3	.99(.96-.99)
L4-L5 RF(N)	137±3	.99(.97-.99)	7.1±.4	.99(.98-.99)	21±.5	.93(.80-.98)
L4-L5 RF (R1)	146.7±2	.98(.94-.99)	7.8±.4	.99(.98-.99)	20.4±.5	.99(.98-.99)
L5-S1 RF(N)	141.2±7	.99(.99-.99)	8.5±.5	.99(.98-.99)	17±.8	.94(.82-.98)
L5-S1 RF (R1)	147±7	.99(.99-.99)	9.5±.7	.99(.99-1)	16±.7	.99(.99-1)
IVL (Left Side)	Area		Width			Height
	M(mm2) ±ER	ICC [95%CI]	M(mm) ±ER	ICC [95%CI]	M(mm) ±ER	ICC [95%CI]
L3-L4 LF(N)	165.1±3	.98(.96-.99)	9±.2	.97(.90-.99)	21.7±.4	.99(.99-1)
L3-L4 LF(R1)	151.8±3	.99(.96-.99)	7.9±.2	.99(.96-.99)	21.9±.5	.99(.98-.99)
L4-L5 LF(N)	133.4±5	.99(.98-.99)	7.3±.4	.99(.98-.99)	19.1±.9	.97(.91-.99)
L4-L5 LF(R1)	123.2±4	.99(.97-.99)	6.3±.3	.99(.97-.99)	20.1±.6	.99(.99-1)
L5-S1 LF(N)	133.5±7	.99(.99-1)	8.2±.5	.99(.98-.99)	16.2±.5	.99(.98-.99)
L5-S1 LF (R1)	126.1±7	.99(.99-1)	7.2±.5	.99(.98-.99)	15.5±.5	.99(.98-.99)

IVL=intervertebral level, N= neutral position, R1: first rotational position, RF= right foramen, LF=left foramen, M=mean, SE=standard error, MD=mean difference, ICC=intra class correlation coefficient.

Table B-11: The area, width and height of the right and left intervertebral foramen (IVF) neutral and first rotational positions of the lower trunk for the second group with using MRI holder

IVL (Right Side)	Area		Width		Height	
	M(mm2)±ER	ICC[95%CI]	M(mm)±ER	ICC[95%CI]	M(mm)±ER	ICC[95%CI]
L3-L4 RF(N)	173.2±3	.99(.97-1)	8.6±.4	.99(.97-1)	21.2±.7	.99(.98-1)
L3-L4 RF(R2)	191.2±2	.99(.99-1)	10.3±.4	.99(.97-1)	22.3±.7	.99(.97-1)
L4-L5 RF(N)	142.5±3	.99(.97-1)	6.9±.7	.99(.98-1)	20.4±1	.99(.97-1)
L4-L5 RF (R2)	158.7±2	.99(.99-1)	7.9±.6	.99(.97-1)	19.6±.6	.99(.97-1)
L5-S1 RF(N)	168±7	.99(.98-1)	9.8±.8	.99(.97-1)	18±.8	.99(.98-1)
L5-S1 RF (R2)	175.7±5	1(.99-1)	11.3±.8	.99(.97-1)	16.9±.8	.99(.97-1)
IVL (Left Side)	Area		Width		Height	
	M(mm2)±ER	ICC[95%CI]	M(mm)±ER	ICC[95%CI]	M(mm)±ER	ICC[95%CI]
L3-L4 LF(N)	175±3	.99(.99-1)	9±.5	.99(.98-1)	21.8±.4	.99(.97-1)
L3-L4 LF(R2)	153.5±5	1(.99-1)	7.1±.2	.99(.97-1)	22±.4	.99(.98-1)
L4-L5 LF(N)	141.6±4	1(.99-1)	7.2±.2	.99(.98-1)	19.4±1	.99(.99-1)
L4-L5 LF(R2)	126.1±3	.99(.99-1)	6±.3	.99(.97-1)	20.8±.4	.99(.97-1)
L5-S1 LF(N)	168.7±7	1(.99-1)	9.5±.7	.99(.97-1)	18.8±1	.99(.99-1)
L5-S1 LF (R2)	161.5±7	1(.99-1)	8.3±.4	.99(.97-1)	17.6±.3	.99(.97-1)

IVL=intervertebral level, N= neutral position, R2: second rotational position, RF= right foramen, LF=left foramen, M=mean, SE=standard error, MD=mean difference, ICC=intra class correlation coefficient.

Table B-12: The area, width and height of the right and left intervertebral foramen (IVF) in neutral and second rotational positions of the lower trunk for the third group with using MRI holder

IVL (Right Side)	Area		Width		Height	
	M(mm2)±ER)	ICC[95%CI]	M(mm)±ER)	ICC[95%CI]	M(mm)±ER	ICC[95%CI]
L3-L4 RF(N)	177.5±2	.98(.92-.99)	8.2±.9	.99(.98-1)	21.5±.7	.99(.98-1)
L3-L4 RF(R3)	220.7±5	.99(.96-1)	11.5±.3	.99(.94-.99)	23.0±.6	.99(.97-1)
L4-L5 RF(N)	146.7±1	.96(.84-.99)	7.8±.1	1(1-1)	20.8±.6	.99(.98-1)
L4-L5 RF (R3)	174.0±4	.98(.93-.99)	10.1±.5	.99(.96-1)	18.1±1	.99(.97-1)
L5-S1 RF(N)	177.2±4	.99(.96-1)	9.8±.4	.99(.95-.99)	18.5±1	.99(.99-1)
L5-S1 RF (R3)	188.5±4	.98(.93-.99)	11.8±.2	.99(.95-.99)	16.8±1	.99(.99-1)
IVL (Left Side)	Area		Width		Height	
	M(mm2)±ER)	ICC[95%CI]	M(mm)±ER	ICC[95%CI]	M(mm)±ER	ICC[95%CI]
L3-L4 LF(N)	175.7±5	.99(.95-.99)	9.5±.5	.99(.97-1)	21.2±.1	1(1-1)
L3-L4 LF(R3)	144.5±5	.99(.96-1)	6.3±.6	.99(.99-1)	21.9±.2	.99(.99-1)
L4-L5 LF(N)	141.2±4	.98(.94-.99)	7.0±.4	.99(.97-1)	19.5±.6	.99(.98-1)
L4-L5 LF(R3)	113.5±3	.99(.98-1)	4.7±.4	.99(.97-1)	21.3±.2	.99(.97-1)
L5-S1 LF(N)	175.5±7	.99(.97-1)	9.8±.1	.97(.89-.99)	18.5±1	.99(.99-1)
L5-S1 LF (R3)	157.5±4	.98(.93-.99)	7.7±.4	.99(.97-1)	17.0±1	.99(.98-1)

IVL=intervertebral level, N= neutral position, R3: first rotational position, RF= right foramen, LF=left foramen, M=mean, SE=standard error, MD=mean difference, ICC=intra class correlation coefficient

Table B-13: The orientation angle of the lumbar superior articular processes and the cross-sectional area of the gapping distance between the superior and inferior articular processes during the first lower trunk position for the first and second tested groups (Descriptive table)

Groups	Position	IVL	RAADL (M & SE)	ICC	LSAPOA (M & SE)	ICC	RSAPOA (M & SE)	ICC	CSALF (M & SE)	ICC	CSARF (M & SE)	ICC
1 (without MRIH)	1(N) n=5	L2-L3	3.8±1.1	.96(.86-.99)	55.4±2.7	.97(.88-.99)	54.6±2.2	.96(.83-.99)	.0±.0	0.(0.0-0.0)	0±0	0.0(0.0-0.0)
		L3-L4	3.8±1	.96(.85-.99)	51.9±3.8	.98(.94-.99)	53.7±3.7	.98(.94-.99)	0±0	0.0(0.0-0.0)	0±0	0.0(0.0-0.0)
		L4-L5	3.7±1.1	.97(.87-.99)	42.7±2.2	.97(.89-.99)	43.6±3.6	.98(.93-.99)	.0±.0	0.0(0.0-0.0)	0±0	0.0(0.0-0.0)
		L5-S1	4.3±.1	.96(.85-.99)	36.7±2.7	.97(.89-.99)	37.1±3.6	.98(.93-.99)	0±0	0.0(0.0-0.0)	0±0	0.0(0.0-0.0)
	2(R1) n=5	L2-L3	81±1.6	.95(.82-.99)	54.7±2.1	.96(.83-.99)	56.1±2.2	.96(.83-.99)	1.4±.9	.95(.82-.99)	0±0	0.0(0.0-0.0)
		L3-L4	83.6±1.7	.97(.89-.99)	46.8±3.9	.98(.94-.99)	49.2±3.4	.98(.92-.99)	10.4±4	.99(.95-.99)	0±0	0.0(0.0-0.0)
		L4-L5	86.4±1.7	.96(.83-.99)	44.1±3.5	.98(.93-.99)	45.5±3.5	.98(.93-.99)	1.3±.7	.99(.99-1)	0±0	0.0(0.0-0.0)
		L5-S1	88±1.7	.96(.84-.99)	39.5±4.3	.98(.94-.99)	40.8±3.7	.98(.93-.99)	0±0	0.0(0.0-0.0)	0±0	0.0(0.0-0.0)
2 (with MRIH)	1(N) n=3	L2-L3	1.3±.1	1(1-1)	59.4±2.6	.98(.88-1)	60.2±2.2	.97(.85-.99)	0±0	0.0(0.0-0.0)	0±0	0.0(0.0-0.0)
		L3-L4	1.5±.5	.99(.93-1)	47.8±3	.97(.84-.99)	47±2.9	.97(.83-.99)	0±0	0.0(0.0-0.0)	0±0	0.0(0.0-0.0)
		L4-L5	.7±.2	.98(.89-1)	41.3±.6	.99(.98-1)	41.9±.9	.99(.98-1)	0±0	0.0(0.0-0.0)	0±0	0.0(0.0-0.0)
		L5-S1	.4±.2	1(1-1)	34.3±2.3	.97(.86-.99)	35.1±2.4	.98(.87-1)	0±0	0.0(0.0-0.0)	0±0	0.0(0.0-0.0)
	3(R1) n=3	L2-L3	80.3±3.8	.97(.85-.99)	56.7±2.7	.97(.80-.99)	59.1±2.5	.98(.88-1)	10.1±5.3	.99(.94-1)	0±0	0.0(0.0-0.0)
		L3-L4	85.3±2.9	.97(.83-.99)	43±1.8	.99(.99-1)	46±1.7	1(.99-1)	19.8±5.2	.98(.91-1)	0±0	0.0(0.0-0.0)
		L4-L5	86.9±2.8	.97(.82-.99)	38.5±.7	.99(.98-1)	40.6±.8	1(1-1)	5.7±2.8	.97(.81-.99)	0±0	0.0(0.0-0.0)
		L5-S1	88.3±2.8	.97(.82-.99)	33.4±2.3	.98(.86-.99)	35.4±2.6	.96(.79-.99)	0±0	0.0(0.0-0.0)	0±0	0.0(0.0-0.0)

IVL: intervertebral level, N: neutral position, R1: the first rotation position , R2: the second rotation position, M: mean , SE: standards error, ICC: intra-class correlation coefficient, MRIH; MRI holder, RAADL: rotational angle at disc level , LSAPOA: left superior articular process orientation angle , RSAPOA: right superior articular process orientation angle, MD: mean difference , CSALF: cross-sectional area of the gaping distance between the superior and inferior articular processes of the left facet, CSARF: cross-sectional area of the gaping distance between the superior and inferior articular processes of the right facet, . ICC: intra-class correlation coefficient

Table B-14: The orientation angle of the lumbar superior articular processes and the cross-sectional area of the gapping distance between the superior and inferior articular processes during the second and third lower trunk positions for the third and fourth tested groups (Descriptive table).

Groups	Position	IVL	RAADL	ICC	LSAPOA (M & SE)	ICC	RSAPOA (M & SE)	ICC	CSALF (M & SE)	ICC	CSARF (M & SE)	ICC
3(with MRH)	1(N) n=4	L2-L3	1.9± .4	.99(.96-.99)	59.6±2.4	.97(.85-.99)	60.6±2.4	.99(.94-.99)	0±0	0.0(0.0-0.0)	0±0	0.0(0.0-0.0)
		L3-L4	2.6±.4	.99(.96-.99)	47.91±2.3	.96(.83-.99)	47.2±2.7	.97(.86-.99)	0±0	0.0(0.0-0.0)	0±0	0.0(0.0-0.0)
		L4-L5	1.4±.7	.99(.98-1)	42.3±1	.99(.99-1)	42.1±1.3	.99(.98-1)	0±0	0.0(0.0-0.0)	0±0	0.0(0.00-0.0)
		L5-S1	1.3±.8	.99(.99-1)	31±1.1	.99(.98-1)	32.8±.1.1	.94(.76-.99)	0±0	0.0(0.0-0.0)	0±0	0.0(0.0-0.0)
	4(R2) n=4	L2-L3	56.4±2.1	.96(.80-.997)	54.9±3.4	.97(.89-.99)	58.7±3.2	.98(.93-.99)	17.1±4.8	.98(.94-.99)	0±0	0.0(0.0-0.0)
		L3-L4	61.5±1.7	.96(.81-.99)	42.8±.9	.99(.98-1)	48±1.2	.95(.80-.99)	34.4±3.9	.98(.91-.99)	0±0	0.0(0.0-0.0)
		L4-L5	65.3±2.6	.99(.95-.99)	39.3± 1.2	.96(.81-.99)	43±1	.99(.99-1)	10±4.2	.98(.92-.99)	0±0	0.0(0.0-0.0)
		L5-S1	67.4±2.5	.98(.89-.99)	30.8±1.1	.95(.79-.99)	33.6±1.6	.97(.88-.99)	7±4.9	.99(.97-1)	0±0	0.0(0.0-0.0)
4(with MRIH)	1(N) n=3	L2-L3	1.3±.1	1(1-1)	60±3	.97(.84-.99)	60.7±2.7	.97(.80-.99)	0±0	0.0(0.0-0.0)	0±0	0.0(0.0-0.0)
		L3-L4	1.3±.6	.99(.97-1)	47.7±2.9	.97(.83-.99)	47.9±4.1	.98(.87-1)	0±0	0.0(0.0-0.0)	0±0	0.0(0.0-0.0)
		L4-L5	.925±.1	1(1-1)	42.4±.35	.98(.88-1)	42± 1.3	.99(.99-1)	0±0	0.0(0.0-0.0)	0±0	0.0(0.0-0.0)
		L5-S1	.65±.07	1(1-1)	36.3±3	.97(.84-.99)	37.5±3.3	.97(.81-.99)	0±0	0.0(0.0-0.0)	0±0	0.0(0.0-0.0)
	5(R3) n=3	L2-L3	39.3± .6	.99(.95-1)	57.8±3	.97(.84-.99)	58.8±3.0	.97(.84-.99)	0	0.0(0.0-0.0)	0±0	0.0(0.0-0.0)
		L3-L4	40.9±.7	.99(.96-1)	44.5±2.7	.97(.80-.99)	47.1±2.7	.98(.90-1)	16.8±1	.99(.99-1)	0±0	0.0(0.0-0.0)
		L4-L5	42.2± .9	.99(.97-1)	40.1±.1.3	.99(.99-1)	42±.1.31	.99(.98-1)	4.7±2.8	.97(.83-.99)	0±0	0.0(0.0-0.0)
		L5-S1	42.8±.9	.99(.99-1)	35.8±3	.97(.84-.99)	37.5±2.1	.97(.80-.99)	0±0	0.0(0.0-0.0)	0±0	0.0(0.0-0.0)

IVL: intervertebral level, N: neutral position, R3: the first rotation position , R4: the second rotation position, M: mean , SE: standards error, ICC: intra-class correlation coefficient, MRIH: MRI holder, RAADL: rotational angle at disc level , LSAPOA: left superior articular process orientation angle , RSAPOA: right superior articular process orientation angle, MD: mean difference , CSALF: cross-sectional area of the gaping distance between the superior and inferior articular processes of the left facet, CSARF: cross-sectional area of the gaping distance between the superior and inferior articular processes of the right facet.